ASSESSMENT OF IMPACT OF ROADSIDE FRICTIONS ON PASSENGER CAR UNIT VALUES AND CAPACITY OF URBAN ROADS IN DISORDERED TRAFFIC USING MICROSCOPIC SIMULATION MODEL

Thesis

Submitted in partial fulfilment of the requirements for the degree of

DOCTOR OF PHILOSOPHY

by

POOJA RAJ

DEPARTMENT OF CIVIL ENGINEERING

NATIONAL INSTITUTE OF TECHNOLOGY KARNATAKA,

SURATHKAL, MANGALORE - 575025

AUGUST, 2021

ASSESSMENT OF IMPACT OF ROADSIDE FRICTIONS ON PASSENGER CAR UNIT VALUES AND CAPACITY OF URBAN ROADS IN DISORDERED TRAFFIC USING MICROSCOPIC SIMULATION MODEL

Thesis

Submitted in partial fulfilment of the requirements for the degree of

DOCTOR OF PHILOSOPHY

by

POOJA RAJ

(Register No. 165114CV16F15)

Under the Guidance of

Dr. A. U. Ravi Shankar

and

Dr. A. Gowri (External Guide)

DEPARTMENT OF CIVIL ENGINEERING

NATIONAL INSTITUTE OF TECHNOLOGY KARNATAKA

SURATHKAL, MANGALORE - 575 025

AUGUST, 2021

DECLARATION

I hereby *declare* that the Research Thesis entitled "**Assessment of Impact of Roadside Frictions on Passenger Car Unit Values and Capacity of Urban Roads in Disordered Traffic using Microscopic Simulation Model**" which is being submitted to the **National Institute of Technology Karnataka, Surathkal** in partial fulfilment of the requirements for the award of the Degree of **Doctor of Philosophy** in **Department of Civil Engineering** is a *bonafide report of the research work carried out by me*. The material contained in this Research Thesis has not been submitted to any University or Institution for the award of any degree.

Pooja

Pooja Raj
Register Number: 165114CV16FI5
Department of Civil Engineering

Place: NITK Surathkal
Date: 03.08.2021

CERTIFICATE

This is to *certify* that the Research Thesis entitled "**Assessment of Impact of Roadside Frictions on Passenger Car Unit Values and Capacity of Urban Roads in Disordered Traffic using Microscopic Simulation Model**" submitted by **Mrs. Pooja Raj** (Register Number: **165114CV16F15**) as the record of the research work carried out by her, is *accepted as the Research Thesis submission* in partial fulfilment of the requirements for the award of degree of Doctor of Philosophy.

03.08.2021

Dr. A.U. Ravi Shankar
(Research Guide)
Professor
Department of Civil Engineering
NITK Surathkal

Date: 03.08.2021

Dr. Gowri Asaithambi
(Research Guide - External)
Assistant Professor
Department of Civil and Environmental Eng.
IIT Tirupati

06/09/2021

Dr. B. R. Jayalekshmi
(Chairman-DRPC)
Head of the Department
Department of Civil Engineering
NITK Surathkal

NATIONAL INSTITUTE OF TECHNOLOGY KARNATAKA, SURATHKAL
DEPT. OF CIVIL ENGG.

Chairman (DRPC)
Department of Civil Engineering
National Institute of Technology Karnataka, Surathkal
Mangalore - 575 025, Karnataka, INDIA

ACKNOWLEDGEMENTS

It is my pride and privilege to express my heartfelt gratitude to my research supervisors, **Dr. A. Gowri,** Assistant Professor, Department of Civil and Environmental Engineering, IIT Tirupati and **Prof. A.U. Ravi Shankar**, Professor, Department of Civil Engineering, NITK Surathkal for their valuable guidance, total involvement, committed supervision, sustained encouragement and inspiration to carry out this research work smoothly. Their keen engineering and scientific insight have helped me tremendously in improving the technical content and practical relevance of the thesis. Working with them has been a great learning experience for me. This research would not have been possible without their support and guidance. To accomplish my doctorate thesis under their supervision has been both a great privilege and honour for me.

I wish to thank **Prof. B. R. Jayalekshmi,** Professor and Head of Civil Engineering, NITK, Surathkal for providing all the departmental facilities to carry out my study successfully. I also take this opportunity to thank former Department Heads namely, **Prof. K. Swaminathan**, **Prof. Varghese George** and **Prof. Venkat Reddy (Ret.)** for their timely help during my entire research period.

I express my sincere gratitude and thanks to my RPAC members, **Dr. Raviraj H. M**, Assistant Professor, Department of Civil Engineering, NITK, and **Dr. A. Senthil Thilak,** Assistant Professor, Department of Mathematical and Computational Sciences, NITK, for their valuable comments and suggestions in completing the thesis.

I am deeply grateful to former post-graduate students of NITK, **Mr. Pranav Dhikale, Mr. Swapnil Biyani** and **Mr. Kanak** for their timely help during data extraction. Special thanks to **Mrs. Shahana A.,** former M.Tech. student**,** NITK, **Mr. Kalaanidhi S.,** Research Scholar, Faculty of Civil and Environmental Engineering, Technion Israel Institute of Technology, Israel, **Ms. Madhuri Kashyap**, Research Scholar, Department of Civil and Environmental Engineering, IIT Tirupati, **Dr. Punith B. Kotagi**, former Research Scholar, Department of Civil Engineering, NITK for extending all the possible help and suggestions.

I sincerely thank faculty members of Department of Civil Engineering, NITK, for their valuable guidance and encouragement during my Ph.D. research work. I also like to extend my gratitude to the office and supporting staff of Department of Civil Engineering, for their encouragement, help and support provided during the research work.

I would also like to express my sincere gratitude to the authorities of NITK Surathkal, for providing me excellent facilities and comfortable stay in the campus.

Very special thanks go to my friends, **Mrs. Adhirashree, Mr. Panditharadhya, Ms. Deeptha M. S, Mrs. Nithya R., Mrs. Anusree Anand, Mrs. Ranchana M. P, Mrs. Chandana, Ms. Spoorthi S. K., Mrs. Vibhoosha M. P, Mrs. Nayana Devaraj, Mrs. Aswathy Annie Varghese, Mr. Abhay Nair, Mr. Athul Krishnan** and **Mr. Vishnu Rajmohan** who encouraged me to keep going through those good and not so good times. I really miss my dear brother, Late **Mr. Manu O. Kuttan,** former Research Scholar, NITK at this phase of my life. I thank all my friends in my life who were always co-operative to me.

I am greatly indebted to my mother, **Mrs. Anitha Das K. M**., my uncle, **Mr. Rajdas K. M.** and other beloved family members for their blessings, sacrifice, affection, encouragement, and support that meant a lot to me throughout my life.

I am especially thankful to my husband, **Mr. L. J. Dileep;** my brother-in-law, **Mr. L. J. Basant** and my in-laws for their understanding, encouragement and moral support to successfully complete this work.

Last but not the least, I am very much thankful to The Almighty, who granted me the wisdom and strength to learn and finish this research work successfully.

POOJA RAJ
(165114CV16FI5)

ABSTRACT

Representation of traffic in terms of its car equivalences (Passenger Car Unit) is more appropriate to estimate capacity in disordered traffic due to the presence of several vehicle types with varying static and dynamic characteristics following poor lane discipline. Many attempts have been made to overcome the complexities involved in accurate estimation of Passenger Car Unit (PCU) in disordered traffic. The widely used method for PCU estimation considers the relative speed and projected area (length × width) of vehicles. However, as a vehicle will be influenced by a larger area than its projected area, which is proportionate to the surrounding vehicle types (effective area of a vehicle); this study aims to deal with the influence of surrounding vehicles while estimating its PCU value under disordered traffic condition. PCU values are influenced by various factors such as traffic conditions, geometric conditions, road side frictions, etc. Among these factors, roadside frictions (e.g., curbside bus stops, undesignated pedestrian crossings, roadside parking) cause significant deterioration in the quality of urban traffic flow and thus, considerably influence road capacity which in turn affects the PCU values. Many research works have been carried out to investigate the impacts of some of the influencing factors (e.g., vehicular composition, traffic volume, road width) on traffic characteristics as well as PCU values. However, the sensitivity of PCU values and capacity due to the presence of roadside frictions are not adequately studied. Furthermore, PCU values and capacity for urban roads recommended by the existing manuals (e.g., IRC 106 1990) are applicable only for the ideal/base sections i.e., the section devoid of any side frictions. The recently published highway capacity manual (Indo-HCM 2017) suggests adjustment factors for capacity estimation of roads with the presence of a few side frictions (e.g., parking, access points, bus stops), however, the adjustment factors for estimating PCU values are not suggested. To address these gaps, this research study aims to estimate PCU values for vehicles under the influence of curbside bus stop and undesignated pedestrian crossings which are the most common roadside frictions being observed in developing countries. As the change in PCU values will have an influence on capacity as well, it is essential to study the impact of curbside bus stop and undesignated pedestrian crossings on capacity. Lack of space for providing

exclusive bus bays and higher demand for public transport buses in urban roads justify the need for investigating the influence of curbside bus stop. The non-compliant behaviour of pedestrians at undesignated pedestrian crossings creates complex vehicle-pedestrian interactions which affect the capacity of roads and thus, this justifies the need for studying the influence of pedestrians. Furthermore, the influence of side frictions on PCU values and capacity are not considered in the existing studies which used simulation tools. Hence, this study mainly aims at development of a simulation model to examine the influence of these side frictions on PCU values as well as capacity.

Methodology of this study involves development and validation of a microscopic simulation model for ideal section (base model) using the data collected from Bangalore city, India. To study the impact of side frictions on PCU values and capacity, two different urban divided arterials are selected; one with the presence of curbside bus stop and an ideal section near it (Ideal_bus), and another with undesignated pedestrian crossings and an ideal section near it (Ideal_ped). Logics involved in base model development are formulated and implemented in MATLAB using object-oriented programming concepts. To estimate the PCU values for different vehicles, a new methodology considering the influence of surrounding vehicles is proposed and incorporated in the validated model. The base validated model is then modified to simulate the traffic manoeuvers on urban roads in the presence of curbside bus stop (bus stop model). To study the vehicle-pedestrian interactions in disordered traffic, the base model is modified in such a way that the movement logics of vehicles and pedestrians consider vehicle-pedestrian interactions (vehicle-pedestrian interaction model). The relative influences of various parameters such as traffic volume, vehicular composition, bus proportion (applicable only for bus stop section), proportion of stopping buses (applicable only for bus stop section), and pedestrian volume (applicable only for pedestrian section) in the presence of side frictions are investigated by carrying out sensitivity analysis. With simulated results from sensitivity analysis, regression models are developed to predict PCU values for different types of vehicles and capacity of road sections, with and without curbside bus stop, and with and without undesignated pedestrian crossings.

The simulated results of sensitivity analysis indicate the significant differences in PCU values due to the presence of curbside bus stops when vehicular composition, bus proportion, proportion of stopping buses, and traffic volume are varied. For observed vehicular composition and traffic volume, simulated PCU values for bus showed a drastic increment of 28% in bus stop section when compared to that of ideal section. As curbside bus stops create temporal pseudo bottlenecks, capacity of bus stop section significantly gets reduced by 18% from that of ideal section for observed vehicular composition. Due to the impact of undesignated pedestrian crossings, the capacity reduction in pedestrian section when compared to that of ideal section is found to be 19.1% for observed vehicular composition and pedestrian volume. PCU values for vehicles are also found to have significant variations with change in vehicular composition, traffic volume and pedestrian volume. The study findings and results can be used by traffic engineers and planners to predict realistic PCU and capacity values for planning and designing of new facilities with side frictions instead of directly adopting the values available in the existing manuals.

The study results find interesting implications in updating standards related to PCU and capacity estimation considering the influence of curbside bus stops and undesignated pedestrian crossings. In future, this research can be extended to study the impact of curbside bus stops, undesignated pedestrian crossings and other roadside frictions (e.g., parking, encroachments) on PCU values and capacity of different facility types (e.g., urban undivided roads, rural roads, intersections) by modifying the logics in the simulation model. The bus stop model can be further modified to simulate the traffic manoeuvers in sections with bus bays and exclusive bus lanes. The model describing the vehicle-pedestrian interactions can be modified to determine surrogate safety measures (e.g., time-to-collision between vehicles and pedestrians) that reflect the safety of urban roads (where the presence of pedestrians is significant).

Keywords: Passenger Car Unit; Capacity; Curbside Bus Stop; Undesignated Pedestrian Crossing; Vehicle-Pedestrian Interactions; Urban Divided Roads; Disordered Traffic; Microscopic Simulation.

CONTENTS

LIST OF FIGURES

LIST OF TABLES

ABBREVIATIONS

MORTH	Ministry of Road Transport and Highways
CAGR	Compound Annual Growth Rate
CSE	Centre for Science and Environment
PCU	Passenger Car Unit
HCM	Highway Capacity Manual
TRRL	Transport and Road Research Laboratory
IRC	Indian Roads Congress
Indo-HCM	Indian Highway Capacity Manual
I-HCM	Indonesian Highway Capacity Manual
PCE	Passenger Car Equivalent
OOP	Object-Oriented Programming
ANOVA	Analysis of Variance
SD	Standard Deviation
Min.	Minimum
Max.	Maximum
Ideal_bus	Ideal Section near Bus Stop Section
Ideal_ped	Ideal Section near Pedestrian Section
TW	Two-wheelers
THW	Three-wheelers
HV	Heavy Vehicles
MAPE	Mean Absolute Percentage Error
LCV	Light Commercial Vehicles
MC	Median to Curb
CM	Curb to Median
PD_MC	Perpendicular Pattern from Median to Curb
OD_MC	Oblique Pattern from Median to Curb
PD_CM	Perpendicular Pattern from Curb to Median
OD_CM	Oblique Pattern from Curb to Median
VTG	Vehicular Time Gap

VCTG	Vehicle’s Cumulative Time Gap
PTG	Pedestrian Time Gap
PCTG	Pedestrian’s Cumulative Time Gap
T	Simulation Clock Time
P	Precision Time
SI	Scan Interval
SRT	Simulation Run Time
SV	Subject Vehicle
LV	Leader Vehicle
AV	Adjacent Vehicle
MATLAB	Matrix Laboratory
MLR	Multiple Linear Regression
SFM	Social Force Model
LOS	Level of Service
TLTW	Two-Lane Two-Way
DBL	Dedicated Bus Lanes
VISSIM	Verkehr In Städten SIMulation Model
MCU	Motor Cycle Unit
MEU	Motorcycle Equivalent Unit
FFS	Free-flow Speed
MLC	Mandatory Lane Changing
DLC	Discretionary Lane Changing
XBLs	Exclusive Bus Lanes
SB	Stopping Bus
DP	Deceleration Position of Stopping Bus
DT	Dwell Time of Stopping Bus
CPSB	Current Position of Stopping Bus
BST	Bus Stopped Time

NOTATIONS

m	Meter
veh/h	Vehicles per hour
ped/h	Pedestrian per hour
m/s	Meter per second
s	Second
m/s^2	Meter per second square
R^2	Goodness of fit
F_{obs}	F observed value
F_{crit}	F critical value
σ	Standard deviation
μ	Mean
r	Random number
λ	Mean arrival rate of vehicles
Z	Standard normal deviate
τ	Reaction time
v_k	Speed of subject vehicle type '*k*'
v_k^a	Subject vehicle speed based on acceleration phase
v_k^b	Subject vehicle speed based on deceleration phase
V_k	Subject vehicle free-flow/desired speed
a_k	Acceleration rate
b_{ik}	Deceleration rate of SV '*k*' with respect to leader vehicle '*i*'
X_i	Position of leader vehicle '*i*'
X_k	Subject vehicle position
s_i	Effective size of leader vehicle '*i*'
α_{ik}	Sensitivity factor
v_i	Leader vehicle speed
$b_{ik}^{\wedge}$	Deceleration of LV as judged by SV
v_{km}	Mean speed of subject vehicle type '*k*'
v_{carm}	Mean speed of passenger car '*car*'

A_{km}	Mean effective area of subject vehicle type '*k*'
A_{carm}	Mean effective area of passenger car '*car*'
A_k	Effective area of subject vehicle type '*k*'
l_k	Length of the subject vehicle
w_k	Width of the subject vehicle
L	Longitudinal gap between SV and LV
W	Lateral gap between SV and AV
E_k	Effective lateral distance of the subject vehicle
F_k	Effective longitudinal distance of the subject vehicle
Z_k	Physical size of SV
Z_{adj}	Physical size of AV
D_k	Lateral distance of SV
D_{adj}	Lateral distance of AV
n_c	Number of samples of case '*c*'
NC	Total number of cases present
PCU_c	PCU value for case '*c*'
PCU_k	Weighted PCU value for vehicle type '*k*'
PCU/h	PCU per hour
t_{veh}	Approaching vehicle's passing time
t_j	Pedestrian's crossing time
D_j	Distance (road width) travelled by the pedestrian, '*j*'
t_a	Reaction time of pedestrian when vehicle approaches
t_b	Safe time for pedestrians considering the next approaching vehicle
v_{veh}	Approaching vehicle's current speed
d_{j_veh}	Distance between pedestrian and approaching vehicle
$\boldsymbol{f}_j^0$	Destination force of pedestrian
$\boldsymbol{f}_j^m$	Pedestrian-pedestrian interaction force
$\boldsymbol{f}_j^{obs}$	Repulsive force of pedestrian from an obstacle
$\boldsymbol{f}_j^a$	Attractive force of pedestrian
T_j	Relaxation time of pedestrian
v_j^0	Preferred speed of pedestrian

$\boldsymbol{v}_j$	Walking speed of pedestrian
$\boldsymbol{d}_j$	Destination position of pedestrian
$\boldsymbol{p}_j$	Current position of pedestrian
$\boldsymbol{e}_{d;j}$	Directional vector from pedestrian to destination
$\boldsymbol{e}_{m;j}$	Directional vector from pedestrian *'j'* to pedestrian *'m'*
$U_{m:j}$	Interaction strength
B_{mj}	Range of interaction
d_{mj}	Distance between the centers of pedestrians, '*j*' and '*m*'
R_{mj}	Sum of the radii of pedestrians, '*j*' and '*m*'
K	Constant value
I_p	Intensity of a position stressor
$\boldsymbol{n}_j^{veh}$	Two-dimensional unit vector directing from approaching vehicle to pedestrian *'j'*
p_{veh}	Approaching vehicle's position
v_{veh}	Approaching vehicle's speed
v_{gipps}	Approaching vehicle's speed obtained from original Gipps' model
PCU_{TW}	PCU of TW
PCU_{THW}	PCU of THW
PCU_{BUS}	PCU of bus
PCU_{HV}	PCU of HV
P_{Car}	Percentage of cars
P_{THW}	Percentage of three-wheelers
P_{Bus}	Percentage of buses
$P_{S_{Bus}}$	Percentage of stopping buses
$P_{nS_{Bus}}$	Percentage of non-stopping buses
P_{HV}	Percentage of heavy vehicles
TV	Traffic volume
ped_vol	Pedestrian Volume

CHAPTER 1

INTRODUCTION

1.1 GENERAL

Road transport is the primary mode of transport which plays a vital role in conveyance of goods and passengers and linking the centres of production, consumption and distribution. It has a great advantage over other modes of transport for its flexible service. It plays a significant role in influencing the pattern of distribution of economic activity and improving productivity. The rapid growth of urbanization in both developed and developing nations caused severe impact on road transportation sector especially because of the urban vehicular growth. However, this impact on road transportation sector is quite major in case of developing countries as the behaviour of road traffic, roadway system and traffic stream characteristics in developing countries (e.g., India, China) fundamentally varies from that of developed nations. Most of the developed countries have traffic which is homogeneous in nature comprising large proportion of vehicles with not same but similar dimensions, predominantly cars and a small proportion of trucks and other vehicles that follow lane discipline. In contrast, disordered traffic which is mostly observed in developing countries, is encompassed with vehicles having a wide range of dynamic and static characteristics occupying any available position on the road space without complying to any lane discipline.

In developing countries like India, the urban population has gone up from 17% in 1951 to 29% in 2001 and is expected to increase up to around 37% in terms of percentage of total population by the year 2021 (Statistical Year Book India 2018). The rapidly expanding population attracts a variety of economic activities in flourishing cities, which in turn encounters fast escalations in urban travel demand. Transport demand in most of the Indian cities has increased substantially due to an increase in population as a result of both natural birth rates and migration from rural areas and smaller towns. To meet the demand for urban road transport, variety of transport modes such as cars, motorized two-wheelers, buses, heavy vehicles, etc. are used. According to the statistics provided by the Ministry of Road Transport and Highways (Annual Report, MORTH, 2019-2020), the total registered vehicles in the country grew at a Compound Annual Growth Rate (CAGR) of 10.11 % between 2007 and 2017. It is observed that total number of registered motor vehicles in India increased from about 0.3 million in 1951 to 253 million in 2017 (Annual Report, MORTH, 2019-2020) as shown in Figure 1.1. The class-wise composition of registered motor vehicles in India during the year 1951-2017 is depicted in Figure 1.2. The share of two wheelers in total registered motor vehicles increased from 8.8 % to 73.86 % from the year 1951-2017. The share of cars, jeeps and taxis is observed to have a steep decline from 52% to 13.3 % from the year 1951-2017. The shares of buses and goods vehicles also reduced from 11.1 % to 0.74 % and 26.8 % to 4.84 %, respectively by the end of year 2017 (Annual Report, MORTH, 2019-2020). The basic problem is not the number of vehicles in the entire country but their over-concentration in urban areas or a few selected cities, particularly in metropolitan cities like Bangalore, Delhi, Chennai, etc.

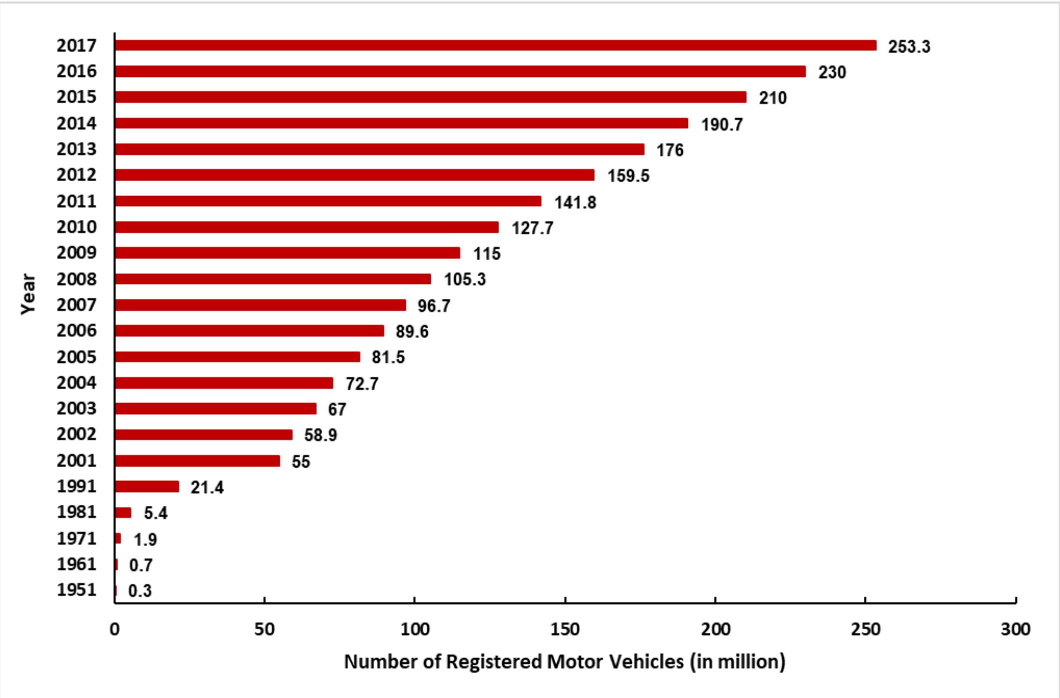

Figure 1. 1 Total Number of Registered Motor Vehicles in India (1951-2017)

Source: Annual Report, MORTH, 2019-2020

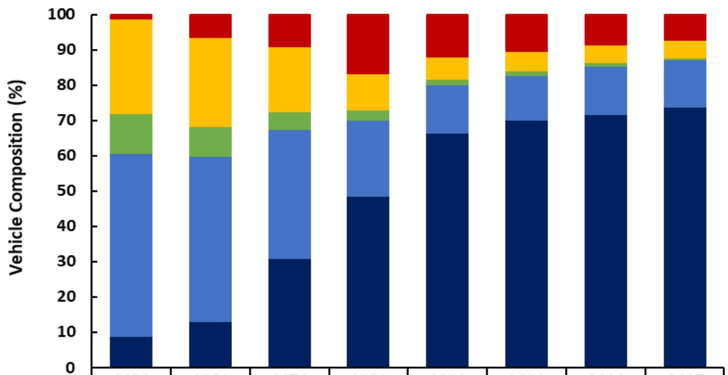

	1951	1961	1971	1981	1991	2001	2011	2017
Other Vehicles	1.3	6.3	9.1	16.6	11.9	10.5	8.5	7.27
Goods Vehicle	26.8	25.3	18.4	10.3	6.3	5.4	5	4.84
Buses	11.1	8.6	5	3	1.5	1.2	1.1	0.74
Cars, Jeeps and Taxis	52	46.6	36.6	21.5	13.8	12.8	13.6	13.3
Two-wheelers	8.8	13.2	30.9	48.6	66.4	70.1	71.8	73.86

Figure 1. 2 Class-wise Composition of Registered Motor Vehicles (1951-2017)

Source: Annual Report, MORTH, 2019-2020

Furthermore, India is having the second largest road network in the world with the total road length over 62,04,426 kilometres (38,55,251.58 miles) as on 31st March 2018 (Annual Report, MORTH, 2019-2020). India is the country where more than 15% of the world's human population lives, constituting just 5% of the world's motor vehicle population. Although, India is having high volume of road length and lower number of vehicles per capita than in developed countries, the disorderliness in traffic with wide variety of vehicle types and weak lane discipline especially in urban areas resulting in higher volume to capacity ratio during peak hours makes them suffer from worse congestion, delay, pollution and accidents. Congestion in both passenger and commercial traffic are widespread in Indian cities and indicate the seriousness of their transport problems. Traffic congestion in urban roads of developing countries creates significant challenges to transport planners. Road traffic congestion restricts the continuous vehicular flow causing delay of travel and reduction in speed, which in turn affect the reliability of road network.

Prevalent traffic congestion particularly during peak hour not only increases the delay but also increases the pollution level. The average peak hour speed of vehicles in Indian cities is far less than the optimum one. According to Centre for Science and Environment (CSE), the emission of all the three major air pollutants namely carbon monoxide, hydrocarbons and nitrogen oxides drastically increases with a reduction in motor vehicle speeds. Thus, the growing air pollution caused by vehicular emissions that depend on vehicle speed, age of vehicle and emission rate leads to serious environmental problems. On the other hand, due to inadequate transport infrastructure and its improper use, and lack of effective road-safety policies, accident rates are also increasing which is considered as a serious problem concerning the safety of road users in Indian urban roads. The nature of road accident problem in Indian cities is different in many ways from that in their counterparts in the developed countries. Pedestrians, bicyclists, motorcyclists, and non-motorized vehicle occupants are often the most vulnerable in Indian cities, unlike cities from developed world where car and public transport users are the most vulnerable. The analysis of road accident data 2018 reveals that about 1,280 accidents and 415 deaths take place every day on Indian roads which further translates into 53 accidents and loss of 17 lives on an average every hour in our country. During 2018, a total of 4,67,044 road accidents are reported. Of these 29.5 per cent are fatal accidents. The number of persons killed in road accidents are 1,51,417 (Annual Report, MORTH, 2019-2020).

Thus, to overcome the different levels of difficulties faced by many developing countries like India due to the disordered nature of traffic, efficient designing of roads and providing effective traffic operations is imperative. Capacity being the fundamental input recommended for road systems operation and planning, many organisations in several countries have introduced guidelines to estimate capacity. However, as there are several types of vehicles sharing and operating on same carriageway width without any physical segregation between motorized and non-motorized vehicles, and without proper lane discipline; studying the interactions between moving vehicles under disordered traffic condition is highly complex. Also expressing traffic volume as number of vehicles passing a given section of road or traffic lane per unit time is inappropriate. Thus, the problem of measuring volume of such disordered traffic can be addressed by converting the different types of vehicles into a uniform measure of vehicles known as Passenger Car Unit (PCU) and expressing the volume in terms of Passenger Car Unit (PCU) per hour.

1.2 PASSENGER CAR UNIT (PCU) AND CAPACITY OF URBAN ROADS

Passenger Car Unit (PCU) is the universally adopted unit of measure for representing traffic volume or capacity. PCU is a factor used to convert a traffic stream composed of different vehicle types into an equivalent traffic stream composed exclusively of passenger cars. Highway Capacity Manual (HCM 2010) defined PCU as "the number of passenger cars displaced in the traffic flow by truck or a bus under the prevailing roadway and traffic condition." However, the definition of PCU by Transport and Road Research Laboratory (TRRL) 1965, London, UK is given as "on any particular section of road under particular traffic condition, if the addition of one vehicle of a particular type per hour will reduce the average speed of the remaining vehicles by the same amount as the addition of, say x cars of average size per hour, then one vehicle of this type is equivalent to x PCU". But all these definitions are stated with respect to the homogeneous traffic. The concept of PCUs was introduced for accounting the trucks or buses in homogeneous traffic as these vehicles are affecting the speeds of the cars. Over the decades, the estimation of PCU for trucks and buses were studied in detail for homogeneous traffic conditions (Huber, 1982; Benekohal and Zhao, 1999). In homogeneous traffic conditions, the PCU values for trucks, buses and recreational vehicles varies from 1.5-4.5, 1.25-3.2 and 1-4, respectively for different facility types (HCM, 2010; Transport for London, 2010; Pajecki *et al.*, 2019). PCU of each type of vehicle is found to have primary importance in disordered traffic studies particularly on capacity analysis, signal design, traffic management, etc. For disordered traffic, the PCUs are estimated to convert different vehicle types equivalent to passenger car (Chandra and Sikdar, 2000; Tiwari *et al.,* 2000; Chandra and Kumar, 2003; Bains *et al.,* 2012; Dhamaniya and Chandra, 2013; Mohan and Chandra, 2016). Indian Roads Congress (IRC 106 1990) defines static PCU values for different types of vehicles in India based on vehicular composition. Recently, Indian Highway Capacity Manual (Indo-HCM 2017) defined PCU as "the amount of impedance caused to flow of traffic by other vehicle types in comparison with that of passenger cars." This converted factor, PCU provides an estimated homogeneous traffic so that it can be used in studying road density, traffic flow models and capacity analysis. Table 1.1 gives the PCU values suggested for Indian traffic conditions (Indo-HCM, 2017).

Traffic capacity is defined in Highway Capacity Manual (HCM 2010) as "the maximum number of vehicles that can pass through a point or uniform section of carriageway lane in one direction per hour under prevailing roadway, traffic, or ambient conditions." Indian Road Congress (IRC 106 1990) outlines capacity of urban roads as a function of the roadside fringe conditions. Recently, Indian Highway Capacity Manual (Indo-HCM 2017) defined capacity of urban roads as "the maximum number of vehicles that can pass a given point or section of road on a lane or roadway, during one hour under the most nearly ideal roadway and traffic conditions which can possibly be attained."

It may be noted that capacity values and design service volume provided in IRC (1990) is obsolete due to the fact that capacity recommended in IRC: 106 (1990) is evolved based on static PCU values and also, might be due to rapid progress witnessed during last decade in road engineering and vehicle technology on the urban roads of India. The above radical changes can be attributed as the primary reasons for change in PCU values and capacity in Indo-HCM (2017) as compared to values reported in IRC: 106. Furthermore, influence of a vehicle type on a traffic stream is not same across the different traffic states and facilities. It is understood from many literature (Chandra and Sikdar, 2000; Chandra and Kumar, 2003; Bains *et al.*, 2012; Dhamaniya and Chandra, 2013) that the PCU values vary with the change in traffic, road geometric and other circumstances and thus, the application of dynamic PCUs is widely used in disordered traffic. That means, each vehicle type will have a set of PCU values for different traffic conditions, geometric conditions, etc. But, gathering field data for the different traffic mix corresponding to the different volume levels is a tedious and practically difficult endeavour (Arasan and Arkatkar, 2010). However, in disordered traffic, there is a much need for considering all the factors such as traffic conditions, vehicle compositions, vehicle conditions etc. to derive the appropriate PCU values (dynamic PCU values) which can be estimated using simulation tools. In Indo-HCM (2017), dynamic PCU values for varying widths of urban carriageways are presented (Table 1.1). The evolved design service volumes and capacity values for the base sections covering varying widths of urban carriageways (Indo-HCM 2017) are presented in Table 1.2.

Table 1.1 Suggested PCU Values for Different Vehicle Types for Varying Widths of Urban Roads in Indian Traffic Condition

Vehicle Type	Two-Lane Undivided		Four-Lane Divided		Six-Lane Divided	
	Range	Median	Range	Median	Range	Median
Two-Wheeler	0.10-0.31	0.2	0.11-0.33	0.20	0.10-0.71	0.21
Three-Wheeler	0.33-2.65	0.73	0.39-1.66	0.80	0.36-2.68	0.83
Car	1.00	1.00	1.00	1.00	1.00	1.00
Bus	1.79-6.50	3.77	1.62-5.90	4.58	1.58-5.90	4.60
HV	2.70-4.81	3.70	2.70-5.68	3.80	2.70-7.58	3.90

Source: Indo-HCM, 2017

Table 1.2 Capacity and Recommended Design Service Volume of Base Sections of Urban Roads

S.No.	Typology of the Road	Capacity (PCUs/h)	Lane Capacity (PCUs/h)	Design Service Volume (PCUs/h)
1	Two Lane Undivided	2400	1200	1680
2	Four Lane Divided	5400 (2700)	1350	3780 (1890)
3	Six Lane Divided	8400 (4200)	1400	5880 (2940)
4	Eight Lane Divided	13600 (6800)	1700	9520 (4760)
5	Ten Lane Divided	20000 (10000)	2000	14000 (7000)

*Note: The values in brackets represent PCUs per hour per direction**

Source: Indo-HCM, 2017

As mentioned above, PCU and capacity values vary with several factors associated with it such as traffic conditions, geometric conditions, environmental conditions, driver behaviour, roadside frictions, etc. However, in urban roads of developing countries, roadside frictions such as curbside bus stops, undesignated pedestrian crossings, roadside parking, street vendors, etc. cause significant deterioration in the quality of traffic flow. Therefore, side frictions considerably influence the capacity of roads which in turn affects the PCU values of vehicles.

1.3 SIDE FRICTIONS

The activities that prevail on the sides of roads and also, within the road which can lead to conflict and affect the movement of the traffic flow reducing the function of road performance are side frictions. Side frictions are defined as the physical features that are likely to impede the traffic flow in Indian Highway Capacity Manual (Indo-HCM 2017). Indonesian Highway Capacity Manual (I-HCM 1997) defines side friction as the interaction between traffic flow and roadside activities causing a reduction of capacity and speed, especially for urban roads. Activities likely to disrupt traffic flow include the following;

• Blockage of the travelled way i.e., reduction of effective width which includes:

(a) Public transport vehicles which may stop anywhere to pick up and set down passengers

(b) Pedestrians crossing or moving along the travelled way

(c) Non-motorized vehicles and slow-moving motor vehicles

• Shoulder activities:

(a) Parking and un-parking activities

(b) Pedestrians and non-motorized vehicles moving along shoulders

• Roadside activities:

(a) Roadside accessibility including vehicles entering and leaving roadside premises via gates and driveways

(b) Trading activities (i.e., food stalls, vendors), movement of vehicles and pedestrians depending on land use type.

Figure 1.3 shows the various roadside frictions in India. Out of all the existing side frictions in developing countries, curbside bus stops (Figure 1.3 (b)) and undesignated pedestrian crossings (Figure 1.3 (c)) are commonly observed side frictions in urban areas and have significant influence on traffic flow and PCU values. This is because, the demand for public transport buses in urban areas are relatively high. Also, most of the bus stops observed under disordered traffic conditions are curbside bus stops as the roads in most developing countries lack enough space for constructing exclusive bus-lanes or bus bays, which is commonly seen in developed nations. Similarly, pedestrians are one of the important entities in traffic environment and the most vulnerable among road users in urban areas. Every person necessarily starts or ends their journey as a walking trip and it is found to be the most efficient and effective mode of transportation for short trips. Unlike in developed countries where the pedestrians cross the road at designated pedestrian crossings, pedestrians in developing countries cross the road for several reasons at their own will from anywhere disrupting the traffic besides the possibility of accidents. Due to the value of time or their urgency, pedestrians also follow non-compliant behaviour while crossing the road. Crossing of pedestrians at undesignated locations, especially at mid-block sections on urban roads of developing countries is thus a very common scenario.

(a) Roadside Parking

(b) Curbside Bus Stop

(c) Undesignated Pedestrian Crossings

(d) Street Vendors

Figure 1. 3 Road Side Frictions Observed on Urban Roads in India

When mobility becomes a priority, road links are usually described in terms of speed-flow relationships, which describe their functionality in terms of the main operational characteristics namely, free-flow speed/ desired speed and capacity. Side friction on a roadway restricts the continuous or smooth vehicular flow movement, thereby affecting capacity and level of service. Curbside bus stops obstruct traffic flow when the buses stop in the same lane of travel that reduce the effective width of road available for the movement of other vehicles in the traffic stream creating a temporary bottleneck condition. The stream speed gets reduced due to deceleration of buses that tend to stop near bus stop and subsequent acceleration of buses that attempt to re-enter the traffic especially during peak hour, resulting in reduction in capacity and change in PCU values. On the other hand, undesignated pedestrian crossings which create complex vehicle-pedestrian interactions have two-fold effects. One, the pedestrians set themselves in danger and the next, vehicle speeds and traffic capacity also adversely get affected which in turn influence the PCU values. Hence, accurate analysis and modelling of traffic flow is required to study the impact of these roadside frictions on PCU values for different vehicle types and capacity of roads.

1.4 TRAFFIC FLOW MODELLING

On Indian urban roads, as the traffic is highly disordered in nature comprising vehicles of wide-ranging static and dynamic characteristics occupying positions on any part of the road based on the space availability, analysing and modelling the complex vehicular interactions through a mathematical method is more complicated. Hence, an appropriate modelling technique needs to be developed. Computer simulation modelling is better suited for studying various traffic characteristics, as they are more efficient, economic, and flexible. Simulation can be used for experimental studies to study detailed relations and to produce attractive visual demonstrations of present and future scenarios which would be too complicated for analytical or numerical treatment. In simulation, various experiments can be carried out by developing a model without disturbing the real-world system.

Traffic simulation is the mathematical modelling of transportation systems such as freeway junctions, arterial routes, roundabouts, etc. through the application of computer software to better help plan, design and operate transportation systems. Depending on the level of detailing, simulation models are classified into macroscopic, mesoscopic and microscopic models. Out of these models, microscopic simulation models have enhanced area of application with availability of greater computing power. A microscopic simulation model provides a description of movements of individual vehicles that are considered to be a result of the interactions between driver-vehicle elements; the interactions between driver-vehicle elements and the road characteristics, external conditions, and the traffic regulations and control. Most microscopic simulation models assume that a driver will only respond to one vehicle that is driving in the same lane directly in front of him. These models are effective in evaluating heavily congested conditions, complex geometric configurations and system-level impacts of proposed transportation improvements that are beyond the limitations of other tool types. Thus, development of a microscopic traffic simulation model to study the complex traffic manoeuvers observed due to the presence of side frictions in urban roads of disordered traffic is necessary.

1.5 NEED FOR THE STUDY

In disordered traffic conditions, expressing capacity as the maximum number of vehicles passing a given section of road per unit time will be inappropriate due to the presence of several vehicle types with varying static and dynamic characteristics following poor lane discipline. To overcome this, traffic flow is analysed by converting different vehicle types into a uniform measure of vehicles called Passenger Car Unit (PCU). PCU values are different for different vehicle types and they are influenced by various factors such as traffic conditions, geometric conditions, environmental conditions, driver behaviour, roadside frictions, etc. However, in urban roads of developing countries, roadside frictions such as curbside bus stops, undesignated pedestrian crossings, roadside parking, street vendors, stopped vehicles, entry and exit of the vehicles from side roads, slow-moving vehicles, etc. cause significant deterioration in the quality of traffic flow. Thus, they considerably influence capacity which in turn affects the PCU values. Out of all the existing roadside frictions, curbside bus stops and undesignated pedestrian crossings are commonly observed in urban areas and have a significant influence on the PCU values as well as capacity of roads. Higher demand for public transport buses and lack of space for providing exclusive bus bays in urban areas are the major reasons for the presence of curbside bus stops. Curbside bus stops obstruct the traffic flow when buses stop in the same travel lane thereby reducing the effective road width creating a temporary bottleneck condition in the traffic stream. Pedestrians are another most important entities in traffic environment and the most vulnerable among road users. Unlike in developed countries where the pedestrians cross the road sections at designated pedestrian crossings with adequate facilities, pedestrians in developing countries cross the road at their own will from anywhere disrupting the traffic besides the possibility of accidents. The non-compliant behaviour of pedestrians at undesignated pedestrian crossings creates complex vehicle-pedestrian interactions. Here, the pedestrians set themselves in danger and also, the vehicle speeds and road capacity adversely get affected which in turn influence the PCU values. Moreover, PCU values and capacity for urban roads recommended by the existing manuals (e.g., IRC 106 1990) are applicable only for the ideal/base sections i.e., the section devoid of any side frictions. The recently published highway capacity manual (Indo-HCM 2017) suggests adjustment factors for capacity estimation of roads with side frictions, however, the adjustment factors for estimating PCU values are not suggested. Hence, it is essential to estimate PCU and capacity values of roads with side frictions in disordered traffic. To analyse and model the impact of side frictions on PCU values for different vehicle types and capacity, analytical methods can be used. But, due to the disorderliness in traffic of developing countries, it is extremely difficult to model the behaviour of traffic through analytical methods. Simulation modelling technique is found to be more robust than empirical methods to examine the complex vehicular interactions in disordered traffic, as they are more efficient, economic, and flexible. Hence, development of a traffic simulation model to simulate the traffic behaviour in the presence of side frictions and to investigate the influence of these side frictions on PCU values and capacity is necessary. The above aspects thus justify the need for the study.

1.6 OBJECTIVES OF THE RESEARCH WORK

This research work aims to investigate the impact of side frictions on PCU values and capacity of urban roads under disordered traffic conditions using microscopic traffic simulation model with following specific objectives:

- To develop a microscopic traffic simulation model (base model) for an ideal mid-block section of urban divided roads in disordered traffic.
- To propose a methodology to determine dynamic Passenger Car Unit (PCU) values for different types of vehicles from the model.
- To develop bus stop simulation model and vehicle-pedestrian simulation model by modifying the base model.
- To develop regression models to predict PCU values and road capacity with and without the presence of side frictions by performing sensitivity analysis using simulation model.

1.7 NOVELTY OF THE WORK

Initially, the study focuses on proposing a new methodology considering the influence of surrounding vehicles to estimate the PCU values for different vehicle types. The logics involved in estimating PCU values using the proposed methodology are incorporated in a simulation model developed in the present study. Although the developed simulation model for ideal section (base model) is similar to those models developed in past studies, the validated model is modified to simulate the traffic manoeuvers on roads with side frictions such as curbside bus stops (bus stop model) and undesignated pedestrian crossings (vehicle-pedestrian simulation model). Researchers carried out limited attempts to simulate vehicle-pedestrian interactions in disordered traffic. In vehicle-pedestrian interaction model developed in the study, in order to explain the approaching vehicle's influence on the pedestrian, a new term is added to the Social Force Model (SFM). Moreover, the sensitivity of PCU values as well as capacity due to the relative influences of various parameters such as traffic volume, vehicular composition, bus proportion (applicable only for bus stop section), proportion of stopping buses (applicable only for bus stop section), and pedestrian volume (applicable only for pedestrian section) in the presence of side frictions are investigated by carrying out sensitivity analysis. With the simulated results from sensitivity analysis, regression models are developed to predict PCU values for different types of vehicles and capacity of road sections, with and without curbside bus stop, and with and without undesignated pedestrian crossings.

1.8 ORGANIZATION OF THE THESIS

The thesis consists of ten chapters. Chapter 1 gives introduction, need and objectives of the research work. Chapter 2 focuses on the relevant literature review on studies on PCU, capacity, side frictions and simulation modelling on homogeneous and disordered traffic conditions, and gaps in the literature. Chapter 3 describes the methodology adopted for the study. Chapter 4 explains the detailed process of data collection and extraction. Chapter 5 focuses on development of a simulation model through a computer program, model calibration and validation. Chapter 6 describes the methodology adopted for estimating PCU in the developed simulation model. Chapter 7 describes how the developed simulation model is modified to incorporate a curbside bus stop and undesignated pedestrian crossings. Chapter 8 and 9 focuses on the assessment of influence of curbside bus stop and undesignated pedestrian crossings, respectively on PCU values and capacity of urban roads. Summary and conclusions of the study are presented in Chapter 10.

CHAPTER 2

LITERATURE REVIEW

2.1 GENERAL

A comprehensive review of literature has been carried out on the studies related to Passenger Car Unit (PCU), capacity, side frictions and traffic simulation models for homogeneous and disordered traffic conditions. These studies are organized in separate sections of this chapter. The effort taken in studying the literature systematically has resulted in the identification of certain gaps which are elaborated at the end of this chapter.

2.2 STUDIES ON HOMOGENEOUS TRAFFIC CONDITIONS

2.2.1 Estimation of Passenger Car Unit (PCU) and Capacity

2.2.1.1 Estimation of Passenger Car Unit (PCU)

Parameters used for the estimation of PCU for various types of road facility are different under homogeneous and mixed traffic conditions. For homogeneous traffic, researchers have used several parameters such as speed (e.g., Aerde and Yagar 1984), headway (e.g., Krammes and Crowley 1986), density (e.g., Huber 1982), delay (e.g., Craus *et al.* 1980), travel time (e.g., Keller and Saklas 1984) and queue discharge flow (QDF) (e.g., Al-Kaisy *et al.* 2002). Table 2.1 presents the summary of the study approaches and the parameters used for PCU estimation in homogeneous traffic conditions.

Cunagin and Messer (1983) estimated PCU values for 14 vehicle types under specified typical conditions for two-lane and four-lane rural highways using the delay experienced by a passenger car due to non-passenger vehicles and the delay experienced by a passenger car due to other passenger cars.

$$PCE_{ij} = (D_{ij} - D_{base})/D_{base} \tag{2.1}$$

where, PCE_{ij} = Passenger Car Equivalent (PCE) of vehicle type i under flow condition j; D_{ij} = delay to standard passenger cars due to vehicle type i under flow condition j; and D_{base} = delay to standard passenger cars due to slower passenger cars. An analytical model was developed to estimate PCE values based on speed distributions, traffic volumes, and vehicle types. Aerde and Yagar (1984) estimated PCU values based on relative rates of speed for each type of vehicle traveling in the main direction and for all vehicles combined traveling in the opposing direction. PCU for a vehicle type n (E_n) is determined using following equation:

$$E_n = C_n / C_1 \tag{2.2}$$

where, C_n = coefficient of speed reduction for vehicle type n; C_1 = coefficient of speed reduction for passenger cars. They also determined platooning PCEs in terms of both platoon leadership and follower creation. Keller and Saklas (1984) calculated PCU values for heavy vehicles using TRANSYT (TRAffic Network StudY Tool) as a function of traffic volume, vehicle classification, and signal settings on an urban arterial road. Passenger Car Unit (PCU) is calculated as follows:

$$PCU = \frac{TT_i}{TT_o} \tag{2.3}$$

where, TT_i = total travel time of vehicle type 'i' in hours and TT_o = total travel time of the base vehicle 'o' in hours.

Fan (1989) studied PCU values for congested conditions on expressway segments in Singapore using volume-to-capacity (V/C) ratio instead of density or level of service because these freeways operate at level of service (LOS) E. Elefteriadou *et al.* (1997) developed PCE values for different types of trucks using NETSIM (NETwork SIMulation) model for freeways, two-lane highways and arterials. Benekohal and Zhao (1999) recommended a delay-based method for estimating PCU of heavy vehicles at signalized intersections. Mathematically, PCE for a heavy vehicle type i based on delay is expressed by the following equation:

$$D\_PCE_i = 1 + \frac{\Delta d_i}{d_0} \tag{2.4}$$

where, D_PCE_i = PCE for a heavy vehicle type i based on delay, Δd_i = additional delay caused by a vehicle type i and d_0 = average vehicle delay when the traffic is composed of passenger cars only.

Al-Kaisy *et al.* (2002) developed a new approach by deriving PCE using Queue Discharge Flow (QDF) capacity as equivalency criterion. Rahman *et al.* (2003) developed a new method for estimating PCEs for large vehicles at signalized intersections based on the increased delay caused by the large vehicle. Demarchi and Setti (2003) derived the PCEs for each truck type on multilane divided highways of

USA. Al-Kaisy *et al.* (2005) utilizes microscopic traffic simulation model, INTEGRATION to develop PCU factors for heavy vehicles on level terrain and specific upgrades during congestion. Ahmed (2010) identified and quantified the characteristics of heavy vehicles that have an impact on freeway at different levels of congestion, with an emphasis on operations at level of service. Passenger Car Equivalent (*PCE*) factor was calculated using the headway ratio method based on following equation:

$$PCE = \frac{HV_{headway}}{PC_{headway}} \tag{2.5}$$

where, $HV_{headway}$ = Heavy vehicle (*HV*) headway; $PC_{headway}$ = Passenger car (*PC*) headway. Sarraj and Jadili (2012) estimated PCUs for different vehicle types at signalized intersections in Gaza using headway method. Obiri-Yeboah *et al.* (2014) evaluated passenger car equivalents for three vehicle categories; cars, medium vehicles, and trucks at signalized intersections within the Kumasi Metropolis, Ghana using headway ratio method. Lee (2015) developed PCEs for heavy vehicles at roundabouts of USA using flow rate. The PCE was developed such that the variation in the entry capacity in various mixes of cars and heavy vehicles was minimized. The PCE was also applied to the prediction of the entry capacity using a roundabout capacity model. Al-zerjawi (2016) used the ratio of density of passenger cars (K_{car}) to density of trucks (K_{truck}) on multi-lane highways under homogeneous traffic conditions to determine the PCUs for trucks.

$$PCU = \frac{K_{car}}{K_{truck}} \tag{2.6}$$

The models were developed for estimating average free-flow speed and for identifying the distribution of individual free-flow speeds. The headway method was used by Dayyabu *et al.* (2019) to estimate PCU values for trucks and three-wheelers at signalized intersections in Abuja, Nigeria. Macioszek *et al.* (2019) determined the numerical values of passenger car equivalent factors for heavy vehicles (trucks, buses, trucks with trailers, articulated buses) on turbo roundabouts. Lu *et al*. (2020) identified PCE values for two-lane two-way (TLTW) highway at various traffic volume with an emphasis on congestion conditions. This study introduced an analytical model, combining a headway-based and a delay-based algorithm, for estimating PCEs of HV on a TLTW highway.

Table 2.1 Summary of the Study Approaches and the Parameters used for PCU Estimation in Homogeneous Traffic Conditions

Approach	Parameters							Remarks		
	SP	TH	SH	FRD	DL	QD	TT	Authors (Year)	Country	Facility Type
Speed Modelling	✓							Aerde & Yagar (1984)	Australia & USA	H
Flow rate and Density				✓				Huber (1982)	USA	H
				✓				Demarchi & Setti (2003)	USA	H
				✓				Lee (2015)		RO
				✓				Al-zerjawi (2016)	Iraq	H
Delay					✓			Craus et al. (1980)	Israel	H
					✓			Cunagin & Messer (1983)	USA	H
					✓			Benekohal & Zhao (1999)		SI
					✓			Rahman et al. (2003)	Japan	SI
					✓			Lu et al. (2020)	USA	H
Headway Method			✓					Krammes & Crowley (1986)	USA	F
		✓						Ahmed (2010)	USA	F
		✓						Sarraj & Jadili (2012)	USA	SI
		✓						Dayyabu et al. (2019)	Nigeria	SI
		✓						Lu et al. (2020)	USA	H
Queue Discharge						✓		Al-Kaisy et al. (2002)	USA	F
Simulation							✓	Keller & Saklas (1984)	USA	SI
	✓							Elefteriadou et al. (1997)		F & H
						✓		Al-Kaisy et al. (2005)		F & H

Note: SP = Speed; TH= Time Headway; SH = Space Headway; FRD = Flow Rate and Density; DL = Delay; QD = Queue Discharge; TT = Travel Time; H = Highway; F= Freeway; SI = Signalized Intersection; RO = Roundabout.

2.2.1.2 Estimation of Capacity

Akcelik and Besley (2001) discussed two methods for measuring capacity at intersections, such as measuring departure flow rates under saturated conditions, and measuring departure flow rates during saturated portions of individual stop-go cycles (traffic signal or gap acceptance cycles). The authors identified a maximum queue discharge (saturation) speed that corresponds to the maximum queue discharge flow rate (s) observed at the signal stop line. Hagring *et al.* (2003) evaluated the need for more complex capacity models than currently exist in order to properly represent driver gap-acceptance behaviour at multilane roundabouts. The complexity arises when drivers are assumed to simultaneously accept pairs of critical gaps in the outer and inner circulating lanes before they enter the roundabout. Chodur (2005) developed a capacity model for un-signalized intersections in Poland. The paper presents the results and recommends how to adapt the HCM 2000 method to the Polish conditions. A stochastic concept for highway capacity analysis is presented by Brilon *et al.* (2007). A method for the estimation of capacity distribution functions from empirical data based on statistical methods for lifetime data analysis is introduced. This method is derived for the analysis of freeway capacity. Regression analysis was employed to estimate the capacity of each kind of urban roads by Cao *et al.* (2010). Dahl and Lee (2012) identified the limitations of the existing roundabout capacity estimation methods with respect to truck traffic. The capacity was estimated with the existing capacity models with the adjusted gap-acceptance parameters. Xue *et al.* (2014) considered lane-changing process and time headway loss to estimate capacity of on-ramp merging section of Shanghai urban expressway using dynamics and gap acceptance theory. Lee (2015) developed PCEs such that the variation in the entry capacity in various mixes of cars and heavy vehicles was minimized. Zhao *et al.* (2016) presented a theoretical model to estimate the lane group capacity at signalized intersections with the consideration of the effects of access points. Two scenarios of access point locations, upstream or downstream of the signalized intersection, and impacts of six types of access traffic flow are taken into account. The proposed capacity model was validated based on VISSIM simulation. Results of extensive numerical analysis reveal the substantial impact of access point on the capacity, which has an inverse correlation with both the number of major street lanes and the distance between the intersection and access point. Loder *et al.* (2019) developed a sublinear relationship between network size and critical accumulation to understand the traffic capacity of urban networks.

2.2.2 Various Factors affecting PCU and Capacity

Cunagin and Messer (1983) found that PCE values for specific grades on two-lane rural highways are overly conservative for both moderate and steep grade conditions. Fan (1989) found that buses, light and heavy trucks and trailers generally have higher PCU factors compared with the PCU used in US and UK for the level terrain. Elefteriadou *et al.* (1997) examined the impact of variables such as grade, length of grade, truck percentage, and level of traffic flow on PCEs. For freeway sections, it was found that PCEs remain mostly unchanged or even decrease with increase in traffic flow. For arterials and two-lane highways, there is no noticeable trend between PCEs and level of traffic flow. Also, for freeway sections, PCEs remain mostly unchanged, and sometimes they increase with increasing percentage of trucks in the traffic stream. For arterials, however, PCEs mostly decrease with an increase in percentage of trucks. Benekohal and Zhao (1999) found that delay based PCU values depend on traffic volume, type and percentage of trucks. The field data indicated that the passenger car equivalents increase as the traffic volume and the percentage of heavy vehicles increase. Al. Kaisy (2002) quantified the effect of heavy vehicles on traffic which is great during congestion than during under-saturated conditions. Rahman *et al.* (2003) studied the effects of a large vehicle's position in the queue to estimate the PCE value. Demarchi and Setti (2003) studied the impact of heavy vehicles on traffic streams, particularly on grades by deriving the PCEs for each truck type on multilane divided highways of USA. Al-Kaisy *et al.* (2005) modelled the performance of heavy vehicles on grades and studied their effect on traffic stream on level terrain and upgrades of freeways and multilane highways during congestion.

Ahmed (2010) found that PCE value is higher than the HCM 2000 recommended value of 1.5 for level freeway sections under congested conditions and with the presence of more than 9% heavy vehicles. Dahl and Lee (2012) examined the effect of heavy vehicles (trucks) on the entry capacity of roundabouts. The capacity was compared with the observed capacity at three roundabouts. It was found that the rate of reduction in the observed capacity with an increase in the circulating flow was lower at the roundabouts with a higher truck percentage. Obiri-Yeboah *et al.* (2014) studied the influence of the prevailing traffic mix, flow conditions and the effect of roadside friction on PCEs at the intersections. Lu *et al*. (2020) identified PCE values for two-lane two-way (TLTW) highway at various traffic volume with an emphasis on congestion conditions. This study also contributed to the literature by providing relationships among PCE, the traffic volume level (TVL) of both lanes, and the TVL duration on a TLTW highway.

2.2.3 Impact of Roadside Frictions on Traffic Flow Characteristics

2.2.3.1 Empirical Methods

Bang (1995) studied the impact of side friction on speed-flow relationships for rural and urban highways. It is observed that side frictions may reduce free-flow speed on two-lane two-way interurban roads up to 16 km/h and capacity up to 20 per cent in comparison with roads having very low friction conditions. Rahman *et al.* (2003) analysed the effects of non-motorized vehicles on urban road traffic characteristics. Aronsson and Bang (2005) developed speed prediction models by analysing factors that affect speed on urban roads in Sweden. They found that side friction factors including parked vehicles, roadside premises, and unprotected road users negatively impacts traffic stream speed. Chiguma (2007) developed simplified procedures to study the effect of side friction on capacity (macroscopic analysis) and to study the effect of individual side friction components on speed (microscopic analysis). The study was conducted in two parts, of which each involved a distinctive approach. Part one involved a macroscopic approach where traffic and friction data were collected and analysed at an aggregated level, whereas part two involved a microscopic approach where data of individual frictional elements were collected and analysed individually. The individual friction factors through regression analysis were weighted and combined into one unit of measure of friction called ‘FRIC’. The effect of ‘FRIC’ on speed-flow curves was analysed. The results showed significant impact on speed for both road types.

Roundabout entry capacity is estimated using empirical approach in the presence of significant levels of pedestrian crossings by Meneguzzer and Rossia (2011). Lee *et al.* (2014) conducted a study on undivided three lane roadways in Virginia. They found that the probability of lane-changing violations increases at curb side bus stops. Yang *et al.* (2015) estimated the impacts of pedestrians on capacity and average control delay for the major street through traffic at two-way stop-controlled (TWSC) intersections. The variation in capacity due to side friction, presence of non-motorized traffic and effective utilization of lane width is compared. Gayah *et al.* (2016) examined the capacity of an isolated signalised intersection when a nearby roadway obstruction is present in either the upstream or downstream direction. To quantify the loss of capacity caused by an obstruction, the authors applied the variational theory of kinematic waves in a moving-time coordinate system. Zheng *et al.* (2016) constructed an empirical mathematical model to study the influence of pedestrians crossing the roads on the capacity of urban roads in three pedestrian crossing approaches including freely crossing the street, uncontrolled crossing of the pedestrian crosswalk, and controlled crossing of the pedestrian crosswalk. Castrillon and Laval (2018) proposed a modification of the method of cuts to estimate the effect of bus operations on the macroscopic fundamental diagram of long arterial corridors with uniform signal parameters and block lengths. Amini and Tilg (2018) analysed the effects of the duration of temporary bottlenecks on arterials with the macroscopic fundamental diagram (MFD) and modelled it analytically.

2.2.3.2 Simulation Methods

Fitzpatrick and Nowlin (1997) analysed the influence of bus stop design on the operation of suburban arterial roads using simulation. The results indicated that the bus bay design provide the greatest benefit when compared to curbside stops at traffic volumes of approximately 350 vehicles per hour per lane (vphpl) and above. Silva (2000) developed a simulation software to represent buses and their interactions with other traffic flow on urban roads. Galatioto and Bell (2007) studied the effects of illegal parking in an urban area of Palermo, Italy. A micro-simulation model was set-up, calibrated and validated using measured traffic parameters. In the study, a set of different illegal double-parking situations were designed, modelled and from the simulated outputs the environmental and traffic impacts were analysed. Bergman *et al*. (2011) evaluated the roundabout level-of-service in the presence of pedestrian crossings using both analytical models and simulation models. Widanapathiranage *et al.* (2013)

used microscopic traffic simulation modelling to treat the BRT station operation and to analyse the relationship between station bus capacity and BRT line bus capacity. Ben-Dor *et al.* (2018) presented MATSim (Multi-Agent Transport Simulation) that assess the impact of Dedicated Bus Lanes (DBL) on urban road traffic, focusing on the transportation network of the city of Sioux Falls and comparing the effects of adding a DBL vs. converting one of the lanes into a DBL, for each link that is exploited by public transport.

2.2.4 Traffic Simulation Models

Chandler *et al.* (1958) proposed a linear model using stimulus-response concept. According to the concept, a driver's response is proportional to the stimulus he perceives.

$$Response_n\ (t) = Sensitivity_n\ (t) \times Stimulus_n\ (t - \tau_n) \tag{2.7}$$

where, t = observation time, τ_n = reaction time for driver 'n'. Various investigations were made on this model by researchers associated with General Motor (GM) laboratory and they incorporated speed and spacing into the sensitivity term giving the model a non-linear form. Gazis *et al.* (1961) established the non-linear model named as generalized General Motor (GM) model. The GM model assumes that the leader relative speed is the car following stimulus.

Gipps (1981) proposed a modified car following model calibrated using assumptions about driving behaviour such as acceleration, deceleration, maximum speed, etc. for traffic simulation. Leutzbach *et al.* (1986) suggested a model considering psychophysical aspects of driving behaviour. Response time and desired spacing are the two parameters to be optimised. According to this model, acceleration of the vehicle ahead is considered as a stimulus for the following vehicle. Fritzsche (1994) developed a microscopic single-lane car following model for one-way two-lane highways by considering the characteristic properties of the driver and the vehicle. He assumed that, any vehicle in the stream interacted with four vehicles; nearest leader and follower in the same lane and in the other lane. When a driver changes his lane from left to right, in one-way flow environment, he need not revert to the left lane again and he may continue to move through the same lane. But in a two-way two-lane road, once the driver changes his lane to the right, he will continuously try to get to the left lane, immediately after overtaking a vehicle in the left lane.

A Microscopic Traffic SIMulator (MITSIM) has been developed by Yang and Koutsopoulos (1996) for modelling traffic networks with advanced traffic control, route guidance and surveillance systems. MITSIM represents networks in detail and simulates individual vehicle movements using car following, lane changing, and traffic signal responding logic. This simulator models integrated traffic networks in detail and uses car following, lane changing, signal and event responding logic in modelling vehicle movements. Kruass (1997) recommended a model which is different from Gipps model. Response time, braking rate and maximum desired speed are the parameters to be optimised. Hidas (1998) has described a car-following model specifically developed for urban interrupted traffic situations. The model is based on a desired spacing criterion which is assumed to be a linear function of the speed. He derived equations for acceleration for conditions: (*a*) when following close to the desired distance and (*b*) approaching from a large distance. This microscopic model has found to be a good representation of the vehicle movements in a simple form. But this model describes only the above two conditions: one for approaching of a vehicle moving at slower speed and the other for describing the motion while following that vehicle. So, the applicability of this model is limited to one-way single lane road.

Brackstone *et al.* (1999) described about the range of options available in the choice of car-following models. The study reported that the study of car-following models has been extensive, with conceptual basis supported by empirical data, but generally limited by the lack of time-series following behaviour. In many cases, work has also been accomplished in investigation of model stability and the implications of each of the relationships to macroscopic flow characteristics. Also, it was reported that the evolution of car-following models is slow, and many would argue that they are sufficiently valid for the purposes for which these models are required. A new microscopic simulation model for the analysis of vehicular flow at a toll plaza system is presented by Astarita *et al.* (2001). Aycin and Benekohal (2001) studied the stability and performance of the car following models such as NETSIM, INTRAS, FRESIM, CARSIM and INTELSIM under congested traffic conditions. It was found that the headways of car following vehicles are assumed as approximately equal to their reaction times in case of NETSIM and CARSIM models. They also observed certain unrealistic acceleration fluctuations and a large number of maximum decelerations in INTRAS and FRESIM. Toledo (2002) developed a model in which drivers try to accelerate in order to facilitate lane changing. The model assumes that drivers who try to change lanes select a target gap in traffic so that they plan to merge into the traffic within a few seconds. Different acceleration models are applied depending on the target gap choice. The Lighthill-Whitham-Richards kinematic wave traffic flow model was extended by Zhang and Jin (2002) to describe traffic with different types of vehicles, in which all types of vehicles are completely mixed and travel at the same group velocity. A study of such a model with two vehicle classes (e.g., passenger cars and trucks) showed that when both classes of traffic have identical free-flow speeds, the model (*a*) satisfies the first-in-first-out rule, (*b*) is anisotropic, and (*c*) has the usual shock and expansion waves and a family of contact waves.

Gunay (2007) developed a car following model considering weak discipline based on the discomfort caused by lateral friction between vehicles. Casas *et al.* (2010) focused on Aimsun transport simulation software, with particular emphasis on its dynamic simulation capabilities. Zhenga *et al.* (2012) evaluated several typical car-following models by using trajectory data from real traffic conditions and genetic-algorithm-based calibration method. The models with calibrated parameters were validated not only under uncongested traffic conditions but also under congested traffic conditions. Xiong *et al.* (2015) developed a 24-hour large-scale microscopic traffic simulation model for the before-and-after study of a new tolled freeway in Washington, D.C. The EPA's Motor Vehicle Emission Simulator is linked with the microscopic simulation model for the estimation of environmental impacts. The calibrated model system has been used to comprehensively evaluate a newly built toll road in Maryland, U.S. The case study demonstrates the feasibility and capability of large-scale microscopic simulation in transportation applications. Bowman and Miller (2016) created models for vehicle arrivals, turning behaviour, and traffic flow and used them to drive microscopic traffic simulations built upon real world data. Lint and Calvert (2018) presented a generic multi-level microscopic traffic modelling and simulation framework for modelling driver distraction.

2.3 STUDIES ON DISORDERED TRAFFIC CONDITIONS

2.3.1 Estimation of Passenger Car Unit (PCU) and Capacity

2.3.1.1 Estimation of Passenger Car Unit (PCU)

For mixed traffic, Chandra *et al.* (1995) developed an equation considering speed- area ratio to estimate PCUs for different vehicle types. Other parameters such as density (e.g., Tiwari *et al.* 2000), queue discharge (e.g., Mohan and Chandra 2017), headway (e.g., Saha *et al.* 2009), area occupancy (e.g., Kumar *et al.* 2017), time occupancy (e.g., Mohan and Chandra 2016), influence area (e.g., Paul and Sarkar 2013) and travel time (e.g., Mahidadiya and Juremalani 2016) are also used under mixed traffic conditions. Table 2.2 presents the summary of the study approaches and the parameters used for PCU estimation in disordered traffic conditions.

Chandra *et al.* (1995) proposed a new concept using speed and projected area to estimate dynamic PCU values for mixed traffic conditions. In speed-area ratio method or Chandra's method, PCU is directly proportional to speed ratio and inversely proportional to projected area ratio with respect to the standard vehicle as given below:

$$PCU = \frac{V_c / V_i}{A_c / A_i} \tag{2.8}$$

where, V_c and V_i = mean speeds of car and vehicle type i, respectively; and A_c and A_i = their respective projected rectangular areas on the road. They mentioned that out of existing methods for PCU estimation in mixed traffic conditions, speed-area ratio method is most appropriate due to the availability of required data. Chandra and Sikdar (2000) considered the same concept of Chandra *et al.* (1995) to determine dynamic PCU values of different types of vehicles on two-lane roads in different parts of India. Satyanarayana *et al.* (2012), Khanorkar *et al.* (2014), Shalkamy *et al.* (2015), Mondal *et al.* (2017) also determined PCU values of different types of vehicles using Chandra's method (Chandra *et al*. 1995).

Area occupancy concept was first proposed for heterogeneous traffic by Mallikarjuna and Rao (2006). They modified CA based simulation model to model the mixed traffic for estimating the PCE values. Since density does not represent the mixed traffic characteristics appropriately, area occupancy or areal density is used as a performance measure in estimating the PCE values. Areal density is defined as sum of the total vehicle area projected on the ground per unit area of road way. Tiwari *et al.*

(2000) and Tiwari *et al.* (2007) estimated PCU values for mixed traffic conditions using modified density method. PCU is calculated using density and 85th percentile width which is given as follows:

$$(PCU_{Xi})_j = [\frac{k_{car}/W_{85car}}{(q_{Xi}/u_{Xi})/W_{85Xi}}]_j \quad (2.9)$$

where, for the highway type *j*, PCU_{Xi} = Passenger Car Unit for traffic entity group *Xi*, W_{85Xi} = 85th percentile distribution width (m) for traffic entity group *Xi* in heterogeneous traffic, q_{Xi} = flow of traffic entity group *Xi* in heterogeneous traffic (entities/hour) and u_{Xi} = space mean speed of traffic entity group *Xi* (km/h). They used 85th percentile distribution width used by passenger cars in mixed traffic conditions to reflect density over a highway area instead of just length. Arasan and Arkatkar (2010) obtained PCU values for different types of vehicles using microscopic simulation, HETEROSIM (HETEROgeneous SIMulation model).

Bains *et al.* (2012) modelled traffic flow on Indian expressways by determining Passenger Car Unit (PCU) of different vehicle categories on a level terrain using the micro-simulation model, VISSIM (Verkehr In Städten SIMulation model). Paul and Sarkar (2013) developed a conceptual model by modifying Chandra's method for determining dynamic PCU values as shown in Figure 2.1. The passenger car equivalency of a vehicle type is inversely proportional to the ratio of speed and directly proportional to the space requirement of a vehicle with respect to car.

$$PCU = (A_i \times V_c) / (V_i \times A_c) \quad (2.10)$$

where V_c and V_i = speeds of car and vehicle type *i*, respectively and A_c and A_i = their influence area.

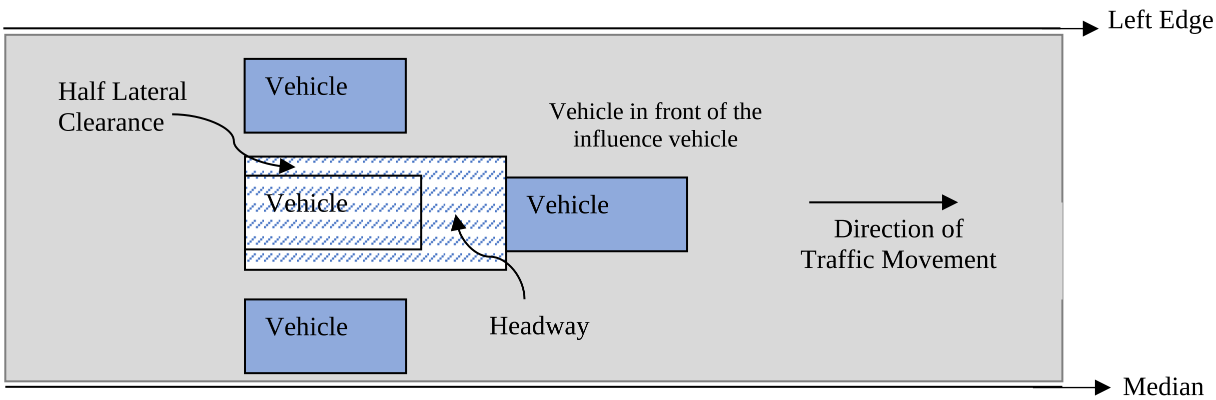

Figure 2. 1 Conceptual Model for Determining Dynamic PCU Values

Source: Paul and Sarkar, 2013

Giuffre *et al.* (2015) estimated passenger car equivalents for heavy vehicles on freeway using a simulation model, AIMSUN. Swamy *et al.* (2016) estimated PCU based on influence area considering surrounding vehicles for different flow conditions. The PCU of the vehicle moving at a particular speed was calculated by finding the influence area of the vehicle using the relationship between the clearance, width and length of that vehicle. Sonu *et al.* (2016) estimated PCU values of different vehicle categories at a typical four-legged roundabout based on the concept of time occupancy. A stream equivalency factor (*k*) has also been developed based on the estimated PCU to convert the heterogeneous traffic flow into a homogenous stream equivalent without making use of PCU factors.

Mohan and Chandra (2017) used queue clearance rate method for estimating PCE at signalized intersections. The results obtained from this technique were compared with other existing methods. Queue clearance rate method does not need values of saturation flow and yielded good estimates of PCE throughout the simulation runs. Method based on saturation flow delivered the best result, but its use was limited to traffic composed only of two types of vehicles. Queue clearance rate method did not require value of saturation flow and yielded good estimates of PCE throughout the simulation runs. Kumar *et al.* (2017) estimated Passenger Car Unit (PCU) using different methods on an eight-lane divided carriageway multi-lane urban road in Delhi. Three methods, which are examined for its accuracy, are: (i) TRRL (Transport Road Research Laboratory, UK) definition (ii) speed-area ratio concept (iii) a proposed methodology in this study. The results show that the PCU values suggested by speed-area ratio, generally overestimates the flows, at different traffic volumes. However, the values obtained using TRRL definition (considering speed or area occupancy as measure of base) and optimized PCU values using area occupancy concept are found to be consistent with the traffic flow in cars-only traffic situation at different flow conditions. Asaithambi *et al.* (2017) estimated PCU values using a microscopic simulation model developed specifically for a signalized intersection located in Chennai city, India. Sugiarto *et al.* (2018) measured the values of Passenger Car Unit (PCU) at a four-legged roundabout in Aceh province, Indonesia based on the time occupancy data in complex traffic operation. The method used was the vehicle's time occupancy, in which calculated from the average time required by each vehicle to pass through the roundabout area. Patel and Dhamaniya (2019) proposed a technique to estimate saturation flow by converting mixed traffic flow from vehicle per hour to PCU per hour by estimating the PCU values using time occupancy method during the saturated green time with different level of traffic interaction. Regression based stream equivalency models are developed for quick and easy estimation of saturation flow. Deshmukh *et al*. (2019) demonstrated the Passenger Car Unit (PCU) at various volume levels, ranging from moderately low to congested conditions. Krishna *et al*. (2019) develop PCU values for heterogeneous traffic conditions on urban roads using speed and projected area. Ballari (2020) estimated passenger car equivalents for heterogeneous traffic stream. The method given by Chandra and Kumar (2003) is used for estimating PCUs for various types of roads with different roadway and traffic conditions by Gaur and Sachdeva (2020).

Other than estimation of PCU, a few studies were carried out on estimation of Motorcycle Unit (MCU) in those economies where motorcycles are found to be dominant. Minh *et al.* (2005) used the same formula developed by Chandra considering motorcycles instead of passenger cars. The modified formula used for MCU conversion is given as:

$$MCU_i = \frac{V_{mc}/V_i}{A_{mc}/A_i} \tag{2.11}$$

where, MCU_i is Motorcycle Unit of vehicle type i; V_{mc}, V_i are mean speed of motorcycles and vehicle type i, respectively; A_{mc}, A_i are the respective projected rectangular area (length × width) of motorcycles and vehicle type i on the road. Cao *et al.* (2010) modified Chandra's method for estimation of MCU. They considered effective space instead of projected area. The modified formula for estimation of MCU is given as:

$$MCU_k = \frac{V_{mc}/V_k}{S_{mc}/S_k} \tag{2.12}$$

where, MCU_k = MCU of vehicle type k, V_{mc}, V_k = mean speed of motorcycles and vehicle type k, respectively and S_{mc}, S_k = mean effective space for motorcycles and vehicle type k, respectively. Cao and Sano (2012) also used the same concept of effective space for the estimation of MCU. An attempt was made by Asaithambi and Mahesh (2016) to estimate the MCU values for different categories of vehicles considering motorcycle as a standard vehicle in Indian traffic conditions. Tan *et al.* (2018) developed a model for Motorcycle Equivalent Unit (MEU) estimation considering a relationship between MEU values and significant parameters such as trajectory, velocity and safety distance. Tu *et al.* (2020) estimated the value of Motorcycle Equivalent Unit (MEU) of container trucks in motorcycle dominated traffic flow by observing the actual traffic flow, identifying the effective space and analysing the relationship between the effective space and velocity.

2.3.1.2 Estimation of Capacity

Chandra and Kumar (2003) analysed the effect of lane width on capacity of two-lane road under mixed traffic conditions. Chandra (2004) estimated capacity for two-lane roads under mixed traffic conditions. Prasetijo (2005) a new method, conflict technique which is based on pragmatically simplified concept for capacity analysis at unsignalized intersections under mixed traffic flow. A number of simulation runs were performed to determine the capacity of a two-lane road by Dey *et al*. (2008). Velmurugan *et al*. (2010) evaluated roadway capacity of multi-lane high speed corridors under heterogeneous traffic conditions through traditional and microscopic simulation models. Madhu and Velmurugan (2011) estimated roadway capacity of eight-lane divided urban expressways under heterogeneous traffic through microscopic simulation models. Puvvala *et al*. (2013) modelled traffic flow on Indian urban expressways with specific reference to Delhi–Gurgaon expressway and estimate its capacity using the micro-simulation model, VISSIM. Mehar *et al.* (2013) examined the application of microscopic traffic simulation model, VISSIM to determine capacity of multilane highways and to calibrate two major parameters of the model to suit mixed traffic conditions. Traffic flow data collected on a section of four-lane divided highway are used to develop the speed-flow curve. It was found that VISSIM in its original form overestimates both speed and capacity of the highway. Mehar *et al.* (2014) estimated capacity for interurban multilane highways in India at different levels of service (LOS). Important VISSIM parameters are first calibrated to reflect mixed traffic flow behaviour and then, the software is used to draw the speed-volume relationships for cars and one of the remaining four categories of vehicles in the traffic stream.

Jabeena *et al.* (2015) studied the flow characteristics of an expressway in Ahmedabad. The developed model showed linear and exponential speed-density relationships and also, parabolic speed-flow and flow-density relationships. In this study, the obtained capacity from simulation model was found to be about 4600 PCE / hour/direction. Chandra *et al.* (2015) investigated the effect of traffic mix on capacity of highways. The VISSIM software is calibrated and used to generate the traffic operations based on field data using capacity as the measure of performance. Speed-flow curves are developed to find simulated capacity values for different combinations of standard car and one of the remaining four types of vehicles in the traffic stream. Naidu *et al.* (2015) presented important aspects of capacity evaluation for road designing using PCE. Mathematical model is developed which uses Indian Road Congress (IRC) specifications on which regression analysis is performed for capacity values provided for urban roads, which are used for developing standard capacity functions. Capacity is derived on the basis of PCE and road geometric factors, which results in realistic prevailing road capacities in Indian roads. Shah and Raval (2016) estimated capacity of C. G. Road of Ahmedabad city. The capacity is determined and compared with suggested value by IRC. The observed capacity is much higher than the suggested value of capacity by IRC. Mankar and Khode (2016) analysed the capacity of urban roads by means of Greenshields's model and result is compared with microscopic model, and significant of width of lane is explored. Patnaik *et al*. (2017) develop a roundabout entry capacity model by employing Influence Area for Gap Acceptance (INAGA) method under heterogeneous traffic flow conditions. Deshmukh *et al*. (2019) calculated the capacity of roadway using the Greenshields's model and this capacity was further utilised to find the level of service offered by the roadway to the users. Patnaik *et al*. (2020) developed two signalized-based roundabouts entry capacity model by employing regression-based multiple non-linear regression model (MNLR) and artificial intelligence-based age-layered population structure genetic programming (ALPS GP) model under heterogeneous traffic conditions. Gaur and Sachdeva (2020) developed speed-flow relationships and estimated capacity of a four-lane intercity road.

Table 2.2 Summary of the Study Approaches and the Parameters used for PCU Estimation in Disordered Traffic Conditions

Approach	Parameters										Remarks		
	SP	TH	SH	FRD	QD	PA	IA	AO	TO	TT	Authors (Year)	Country	Facility Type
Chandra's Method	✓					✓					Chandra et al. (1995)	India	H
	✓					✓					Chandra & Sikdar (2000)		H
	✓					✓					Khanorkar et al. (2014)		H
	✓					✓					Shalkamy et al. (2015)	Egypt	RM
	✓					✓					Mondal et al. (2017)	India	UM
	✓					✓					Krishna et al. (2019)		
	✓					✓					Gaur and Sachdeva (2020)		
Flow rate and Density				✓							Tiwari et al. (2000)	India	RM
Headway Method		✓									Saha et al. (2009)	Bangladesh	SI
Queue Discharge					✓						Mohan & Chandra (2017)	India	SI
Space Occupancy	✓						✓				Paul & Sarkar (2013)	India	UM
								✓			Mallikarjuna & Rao (2006)		RM
	✓						✓				Swamy et al. (2016)		E
								✓			Kumar et al. (2017)		UM
Time Occupancy									✓		Mohan & Chandra (2016)	India	USI
									✓		Sonu et al. (2016)		RO
									✓		Patel and Dhamaniya (2019)		SI
Travel Time										✓	Mahidadiya & Juremalani (2016)	India	SI
Simulation	✓										Arasan & Arkatkar (2010)	India	H
	✓					✓					Bains et al. (2012)		E
				✓							Giuffre et al. (2015)	Italy	F
		✓									Asaithambi et al. (2017)		SI

Note: SP = Speed; TH= Time Headway; SH = Space Headway; FRD = Flow Rate and Density; QD = Queue Discharge; PA = Projected Area; IA = Influence Area; AO = Area Occupancy; TO = Time Occupancy; TT = Travel Time; UM = Urban Mid-block; RM = Rural Mid-block; H = Highway; E = Expressway; SI = Signalized Intersection; USI = Un-signalized Intersection; RO = Roundabout.

2.3.2 Various Factors affecting PCU and Capacity

Chandra and Kumar (2003) studied the effect of lane width on PCU values for different categories of vehicles and also, on the capacity of a two-lane road. It was found that the PCU for a vehicle type increases linearly with the width of carriageway. The capacity of a two-lane road also increases with total width of the carriageway and the relationship between the two follows a second-degree curve. Chandra (2004) has shown that the capacity of a two-lane rural road is affected by the road roughness. Chandra (2004) evaluated the effect of influencing parameters like gradient, lane width, shoulder width, vehicular composition, directional split, slow moving vehicles and pavement surface conditions, on capacity of two-lane roads under mixed traffic conditions. Arasan and Krishnamurthy (2008) found that the PCU value of a vehicle type varies significantly with variation in traffic volume. Dey *et al*. (2008) studied the effect of traffic mix on capacity and speed. Arkatkar and Arasan (2010) applied a simulation model of heterogeneous traffic flow, named HETEROSIM, to quantify the vehicular interaction, in terms of PCU, for the different categories of vehicles, by considering the traffic flow of representative composition, on up-grades of different magnitudes for intercity roads in India. Velmurugan *et al*. (2010) based on traditional and microscopic simulation models. Arasan and Arkatkar (2010) obtained PCU values for different types of vehicles for a wide range of traffic volume and roadway conditions using microscopic simulation, HETEROSIM. The PCU values obtained for different types of vehicles and for a wide range of traffic volume and roadway conditions indicate that the PCU value of a vehicle significantly changes with change in traffic volume and width of roadway. Bains *et al.* (2012) modelled traffic flow on Indian expressways by determining Passenger Car Unit (PCU) of different vehicle categories for different volume levels on a level terrain using the micro-simulation model, VISSIM. It has been found that PCU decreases with increase in volume-capacity ratio irrespective of vehicle category. The study also revealed that at a given volume level, the PCU of a given vehicle category decreases when its own proportion increases in the stream. Praveen and Arasan (2013) used micro-simulation technique to derive equivalency values (PCU factors) on a purely homogeneous (cars-only) traffic stream as well as on a heterogeneous traffic stream for different categories of road vehicles over a wide range of traffic flow and compositions on four-lane divided urban roads in India. Khanorkar *et al*. (2014) studied the impact of lane width of road on Passenger Car Unit and capacity under mix traffic condition in cities on congested highways. PCU values for different type of vehicles are suggested by Mehar *et al*. (2014) at different level of service (LOS) and for different traffic composition on four-lane and six-lane divided highways.

Giuffre *et al*. (2015) studied the effect of heavy vehicles on PCU values based on operational characteristics of a turbo-roundabout. PCE estimations are found to be small at low flow rates and increase with increased flow rates because at low flow rates, there are only few passenger cars that can be influenced by heavy vehicles. Chandra *et al*. (2015) investigated the effect of traffic mix on capacity of four-lane and six-lane divided highways in India. Arun *et al*. (2016) studied the effect of various roadway and operational factors on capacity. They estimated the effect of road geometrics and pavement roughness on free-flow speeds (FFS) and capacities of multi-lane interurban highway segments. For both the types of highways, the types of variables affecting capacity are found to be different. Non-standard widths of medians were found to be significantly affecting the capacity of four-lane divided highways, but not of six-lane divided highways probably. Shah and Raval (2016) found that traffic composition has a higher influence on the capacity of roads. Mankar and Khode (2016) checked the sudden increase in width of lane on the road and result shows that with the increase in road width, capacity of road also increases. Asaithambi *et al.* (2017) examined the influence of traffic volume, traffic composition and road width on PCU values. It was observed that presence of heavy vehicles and increase in road width affects the PCU values. The PCU estimates obtained for different types of vehicles of mixed traffic and wide range of traffic volume levels indicate that the PCU value of a vehicle significantly changes with change in traffic volume. Bharadwaj *et al.* (2018) investigated the effect of traffic composition and the use of a paved emergency lane on capacity. Deshmukh *et al*. (2019) demonstrated the Passenger Car Unit (PCU) at various volume levels, ranging from moderately low to congested conditions. Krishna *et al*. (2019) found that PCU values vary with speed, land use pattern and vehicles dimensions. Ballari (2020) observed that PCE values of different types of vehicles have been found to be different at different ranges of volume and composition. Gaur and Sachdeva (2020) determined capacity of a four-lane intercity road with varying shoulders. The shoulder conditions considered in the study are surfaced shoulder, good shoulder, average shoulder and poor shoulder.

2.3.3 Impact of Roadside Frictions on Traffic Flow Characteristics

2.3.3.1 Empirical Methods

The impact of bus stops which are set near unsignalized intersections on capacity of the intersections are analysed by Pei and Wu (2004). Jianrong and Hua (2007) analysed the influence of the normal public transit bus stopping on the traffic flow. Mei *et al*. (2009) developed a model of road traffic delay caused by curb parking to analyse the effect on road traffic after setting curb parking in road. Laxman *et al*. (2010) analysed the pedestrian flow characteristics when interacted with vehicles under mixed traffic conditions. Munawar (2011) studied the effect of side friction factors on capacity and speed at urban arterial roads in Indonesia. He found that there are significant differences between the actual speed/capacity and the predicted speed/capacity. Hidayati *et al.* (2012) focused on heterogeneous traffic flows and roadside activity levels in urban streets as they relate to the safety management scheme's School Safety Zone (ZoSS). They quantified the effects of roadside activities such as vehicles in and outside the side area, vehicles parking on the street, vendors, pedestrians, and buses stopped in and around the area and the ZoSS facility on speed behaviour in Indonesia. The results indicate that the percentage of motorcycles reached more than 70% on all locations and the implementation of the ZoSS was not effective in reducing the speed of vehicles. Cherry *et al.* (2012) focused on factors influencing mid-block crossing and gap acceptance. They remotely observed illegal mid-block crossing of a six-lane urban arterial in Kunming, China, tracking 522 accepted gaps and 152 rejected gaps in a two-stage crossing (roadside to median and median to roadside). They also fit a probit discrete outcome model to the data to estimate environmental determinants of gap acceptance (and rejection) behaviour, including gap size, vehicle speed, time waiting and gap lane position. Chand *et al.* (2014) investigated the capacity drop on seven sections of six-lane-divided urban arterial road due to a curbside bus stop. Three sections were without any side friction and the remaining four sections were with curbside bus stop. The average mid-block capacity of a six–lane divided urban road without side friction was found to be 6314 PCU/h which was termed as base capacity.

This base capacity was used to compare the capacity of a section with curbside bus stop. The reduction in capacity due to a bus stop was found to be in the range of 8 to 13 percent. Patel and Joshi (2014) carried out a study on six lane divided urban arterial road in Patna and Pune city of India. The variation in capacity due to side friction, presence of non-motorized traffic and effective utilization of lane width is compared. Based on the study, it is observed that the capacity of the urban arterial road is greatly affected by effect of lane width, presence of NMV and effect of side friction. Patna city having the carriageway width of 10.5 m but due to side parking the effective utilization of the lane is only 7.0 m which result into 57% reduction in the capacity. Also due to the side friction and presence of the NMV the 14% reduction in speed is observed in Patna city compared to Pune city. Bansal *et al.* (2014) presented a methodology to quantify the impact of bus-stops on the speed of other motorized vehicles (the total motorized vehicle fleet minus the buses) under heterogeneous traffic conditions. Dhamaniya and Chandra (2014) carried out a study to find the pedestrian influence on capacity of six lane urban roads. 15% reduction in capacity was observed for a pedestrian cross-flow of 508 peds/h. Kadali *et al.* (2015) conducted a study to check whether any significant difference in the speed of the vehicular traffic when pedestrians were crossing. Rao and Rao (2015) evaluated side friction impact on free-flow speed in India. They reported a reduction in FFS of 57% and 67% at bus stop locations and at on street parking locations respectively.

Salini *et al.* (2016) analysed the impact of road side frictions on traffic characteristics of urban roads in India. Multiple linear regression analysis was chosen to relate the factors contributing to reduction in speed caused by side friction factors such as bus stops, pedestrians and on- street parking. Reduction in speed was studied for stretches with individual side frictions as well as stretches under the combined effect of all the factors. The result showed that there was significant impact of side friction on vehicular speed on urban roads and could also bring about the extent of impact of individual factors on speed. Pallavi *et al.* (2016) estimated the effect of side friction events on traffic flow variables and analysed the maximum flow of multilane divided urban road at mid-block sections. The observation showed that the maximum flow was reduced on Section II due to higher side friction compared to section I which is having medium side friction. The presence of shops, parking manoeuvers and more pedestrian movements may be the main reason for maximum flow reduction on section II. Pal and Roy (2016) quantified the impact of roadside friction on travel speed and LOS of Indian rural highways. Based on data collected from three study sections, speed-flow curves were developed for various side friction levels and five threshold values for LOS are suggested considering operational speed and freedom of manoeuver as measure of effectiveness. Parmar *et al.* (2016) analysed the effect of side friction factors on traffic performance measures on urban roads. This study involved a macroscopic approach in which we calculate the combined friction factor and also, used SPSS software for finding the friction (FRIC). The results show that on two-lane two-way roads, all studied factors exhibited statistically significant impact on speed. Harison *et al.* (2016) studied the impact of side friction on speed and capacity of urban road links and to analyse the results of side friction impacts and speed flow rate. They concluded that the side friction for the developing countries may become the severe problem because it is directly affecting the speed of the vehicles.

Pal and Roy (2016) developed a Road Side Friction Index (RSFI) to quantify the impact of side friction generated from road side markets on performance of two-lane rural roads in India. In another study, Pal and Roy (2017) proposed a methodology to quantify the effect of side friction factors generated in road side markets. Five levels of service (LOS) were recommended, the threshold values were based on operational speed and freedom to manoeuver as measures of effectiveness. Rao *et al.* (2017) evaluated the influence of roadside frictions on the capacity of roads in Delhi. Stream speed reduced to 49-57% because of bus stops and bus-bays whereas on-street parking caused 45-67% stream speed reduction. It is observed that presence of a friction points eventually reduces the roadway capacity and an attempt has been made to quantify the amount of speed reduction due to friction points. Percentage reduction in capacity due to the presence of bus bay is more than kerb-side bus stops as number of buses operating in later case is less and moreover, building entry and exit of bus bay exaggerated the capacity reduction. Asaithambi *et al.* (2016) investigated the changes in pedestrian road crossing behaviour of an intersection under mixed traffic conditions before and after signal installation. For this purpose, traffic and pedestrian data were collected from an intersection located in Mangalore city. Kuttan *et al.* (2017) studied the impact of pedestrian road crossing behaviour on the capacity and level of service of urban undivided roads. Golakiya and Dhamaniya (2019) attempted to quantify the reduction in capacity of six-lane and four-lane divided urban arterial roads due to such crossing manoeuver by pedestrians. A mathematical equation has been developed showing the relationship among pedestrian cross-flow and capacity drop. Three kerb side bus stops in Addis Ababa city of varying traffic volume, bus frequency, bus dwell time and effective road widths are considered by Dea *et al.* (2019) to evaluate the reduction in speed due to kerb side bus stop under variable roadway and traffic conditions. Jin *et al.* (2019) developed an extended link-node structured two-lane cell transmission model (CTM) that is capable of dynamically capturing the effect of lane blockage at bus stops and comprehensively modelling mandatory and discretionary lane changing (MLC and DLC) manoeuvers along a bus route under various traffic demand levels. Patkar and Dhamaniya (2020) studied influence of nonmotorized vehicles on speed characteristics and capacity of mixed motorized traffic of urban arterial mid-block sections. The interaction between vehicle and pedestrian crossing at the undesignated mid-block location is assessed by Golakiya *et al.* (2020). The speed reduction in individual category of vehicles due to pedestrian crossings has been determined. Considering the fact that speed is linearly related to density, speed models are generated for sections without side friction (base section) and with pedestrian crossing (side friction section) for six-lane urban arterials. Biswas *et al*. (2020) analysed the influence of side friction on the capacity of undivided urban streets. Three elements of side friction were considered in their study viz. on-street parking, pedestrian movements and non-motorized vehicles. Gaur and Sachdeva (2020) studied the effect of slow-moving vehicles on capacity of the road and found that they reduce the capacity.

2.3.3.2 Simulation Methods

Koshy and Arasan (2005) investigated the impact of bus dwell time on traffic flow and speed using a microscopic traffic simulation model. Arasan and Vedagiri (2008) used a traffic simulation model to examine the effect of exclusive bus lanes on urban arterials for a wide range of traffic volume levels. Chen *et al.* (2010) presented a microscopic traffic simulation approach to the capacity impact analysis of weaving sections caused by the installation of exclusive bus lanes (XBLs) on urban expressways. Arasan and Vedagiri (2010) modified and validated a developed microsimulation model of heterogeneous traffic flow and applied the model to study the impact of provision of reserved bus lanes on urban roads. Wang *et al.* (2012) studied the pedestrian-vehicle interaction behaviour in urban street environment by micro-simulation modelling. Iin (2015) used VISSIM, microscopic simulation software, to study the delay caused by side friction under heterogeneous traffic conditions in Indonesia. He found that side friction increased delay per vehicle by 34%. Chao *et al.* (2015) captured the realistic process of vehicle–pedestrian interaction for mixed traffic simulation. Irawati (2015) focuses on delay evaluation as the impact of side friction that takes place on one of traditional market in Central Java, Indonesia, using microscopic simulation model, VISSIM. From simulation results and Lilliefors method test to figure out the significance, they concluded that there is significant difference between the delays of road segment with side friction than the delay of road segment without side friction. Taking data from the Beijing southwest third ring expressway, a simulation model was built by Chen *et al.* (2016) using Paramics. The simulation model was pre-evaluated before and after the bus lanes set, and the model was post-evaluated to verify the validity of the model after the bus lanes were implemented. Lu *et al.* (2016) established a reliable simulation model to represent the vehicle yielding and pedestrian crossing behaviours at unsignalized crosswalks in a realistic way. Liu *et al.* (2017) developed a microscopic pedestrian behaviour model considering various interactions on pedestrian dynamics at crosswalks. Ningbo *et al.* (2017) established a modified social force model for interactions between pedestrians and vehicles at unmarked roadways. Wang *et al.* (2018) developed a cellular automata (CA) model to simulate the interactions between pedestrian crossings and motorized vehicles in a residential area. Chauhan *et al*. (2020) measured the impact of on-street parking and non-motorized vehicles on the performance of an urban road using VISSIM.

2.3.4 Traffic Simulation Models

Palaniswamy (l983) developed a generalized simulation model for vehicular behaviour under heterogeneous traffic conditions. The different situations considered by him in his study are single lane, intermediate lane and two-lane roads. The study concentrated on the impact of geometry and vehicular characteristics on the traffic flow. Also, considered the fuel consumption due to gradient, wind resistance, etc. Arasan and

Koshy (2005) developed a simulation model suitable for replicating heterogeneous traffic flow, based on the interval scanning technique with fixed increment time advance. It has been found that the method of treating the entire road space as a single unit, for the purpose of simulation, and representing the different types of vehicles as rectangular blocks on the surface, is more appropriate for simulating highly heterogeneous traffic flow. Gipps model was used for car-following logic to update the positions of vehicles. Mathew *et al.* (2006) made an attempt to simulate heterogeneous traffic using the principles of cellular automata. Dey *et al*. (2008) studied the speed, placement, arrival, acceleration, and overtaking characteristics of different types of vehicles, and a computer program is developed to simulate the traffic flow on a two-lane highway incorporating all these characteristics. Venkatesan *et al.* (2008) used object-oriented programming (OOP) approach to develop a simulation model for replicating heterogeneous traffic. OOP approach was implemented in C++ language. In vehicle movement logic, overtaking and car-following behaviour of vehicles were incorporated and Gipps model was used for car-following logic to update the positions of vehicles. An object-oriented methodology (OOM) for heterogeneous traffic simulation is proposed by Gowri *et al.* (2009) with focus on mid-block and intersection flow modelling. A dynamic stochastic type discrete event simulation model is modelled by Arasan and Dhivya (2010). Mathew and Radhakrishnan (2010) presented a methodology for representing non lane-based driving behaviour and calibrating a micro-simulation model for highly heterogeneous traffic at signalized intersection. Calibration parameters were identified using sensitivity analysis, and the optimum values for these parameters were obtained by minimizing the error between the simulated and field delay using genetic algorithm (GA). The proposed methodology was demonstrated using Verkehr in Staedten simulation (VISSIM), a widely used psychophysical car-following model-based microsimulation software. Parameters of both car-following models Wiedemann 74 and Wiedemann 99 were considered in this study.

Mathew and Ravishankar (2011) studied the performance of major car-following models such as General Motors (GM), Modified GM (MGM), Leutzbach, Gipps, Krauss, Intelligent driver model (IDM), Microscopic Traffic SIMulator (MITSIM) model and Bando model. Analysis of car-following data indicates the existence of distinct behaviour for each vehicle-type combination. Ravishankar and Mathew (2011) tried to modify the widely used Gipps's car-following model to incorporate vehicle-type dependent parameters. Bains *et al.* (2012) modelled traffic flow on Indian Expressways by evaluating Passenger Car Unit (PCU) or Passenger Car Equivalents (PCE) of different vehicle categories at different volume levels in a level terrain using the micro-simulation model, VISSIM. Asaithambi *et al.* (2012) studied the effect of intra-class variability, lane discipline, and composition on traffic flow characteristics under mixed traffic conditions. A microscopic traffic simulation model was calibrated and validated using the data from a four-lane divided urban arterial road. Gipps model was used for car-following logic. Based on the simulation results, speed–flow and speed–density relationships were established. Kanagaraj *et al.* (2013) focused on the evaluation of different car following models namely Gipps Model, Intelligent Driver Model (IDM), Krauss Model and Das and Asundi Model under mixed traffic conditions. Metkari *et al.* (2013) made an attempt to quantify the unaccounted parameters of heterogeneity for Indian traffic into the existing car-following models to form a modified car-following model. A simulation model was developed as a software program to study the performance of the modified car-following model replicating Indian traffic conditions. The model was also used to simulate the traffic stream and some preliminary results were obtained. Validation of the model was done with field data collected from a major road in Delhi. Budhkar and Maurya (2014) modelled bidirectional mixed traffic stream with weak lane discipline. Luo *et al.* (2014) investigated the operational characteristics of the mixed traffic flow and developed a cellular automaton model to replicate the traffic behaviours on a bi-directional road with respect to the physical and mechanical features of different vehicle types. Asaithambi *et al.* (2016) focuses on evaluation of different vehicle-following models such as Gipps, Intelligent Driver Model (IDM), Krauss Model, and Das and Asundi under mixed traffic conditions. Kanagaraj and Treiber (2018) proposed a general multi particle model for disordered self-driven high-speed particles and the results showed that it reproduces the observed characteristics of mixed traffic. The main idea is to generalize a conventional acceleration-based car-following model to a two-dimensional force field. Cellular automata (CA) being a simple and powerful analytical tool has been used for modelling heterogeneous traffic by Das *et al.* (2020). Mondal and Gupta

(2020) presented a methodology for model development and a unique calibration process for mixed traffic streams using the widely used simulation software Vissim.

2.4 SUMMARY

A detailed review on various studies related to PCU and capacity of roads, factors affecting PCU and capacity values, impact of roadside frictions and traffic flow modelling using simulation tools have been carried out.

Representation of traffic in terms of its car equivalences (PCU) is imperative to estimate capacity in disordered traffic. Based on the literature survey on PCU estimation methods, it is observed that researchers used different approaches for estimating the PCU values for different vehicle types in homogeneous and disordered traffic conditions. The approaches used for estimating PCU in homogeneous traffic conditions (e.g., Aerde and Yagar 1984; Krammes and Crowley 1986; Huber 1982; Craus *et al.* 1980; Keller and Saklas 1984; Al-Kaisy *et al.* 2002) cannot be applied to disordered traffic conditions that are characterized by weak lane discipline and presence of wide variety of vehicles. Continuous research works have been carried out to overcome the complexities involved in accurate estimation of PCU in disordered traffic (Chandra and Kumar 2003; Paul and Sarkar 2013; Kumar *et al.* 2017; Patel and Dhamaniya 2019; Krishna *et al.* 2019; Praveen and Ashalatha 2019). The widely used method for PCU estimation (Chandra and Kumar 2003) considers the relative speed and projected area (length × width) of the vehicles. As the vehicles are influenced by a larger area than its projected area, proportionate to the surrounding vehicle types (effective area of a vehicle); it is necessary to deal with the influence of surrounding vehicles while estimating PCU values. In the study conducted by Paul and Sarkar (2013), vehicle’s influence area is the parameter used along with its speed to estimate the PCU value of the vehicle, but the equation for calculating influence area includes the projected area of the vehicle, the longitudinal gap or space headway between the vehicle and its leader, and half the lateral gap between the vehicle and its adjacent vehicle. They failed to focus on determining the proportions between physical sizes of the vehicle and its adjacent vehicle which will provide more realistic estimate of PCU under disordered traffic conditions. A few researchers used the concept of effective area approach considering the influence of surrounding vehicles to estimate the MCU values

(Minh *et al*. 2005; Cao *et al.* 2010; Cao and Sano 2012; Asaithambi and Mahesh 2016), but they did not focus on estimation of PCU values. Moreover, no comprehensive literature is available on PCU estimation using the concept of effective area approach with the help of a simulation model under disordered traffic conditions. A few studies conducted by Praveen and Arasan (2013); Mishra *et al.* (2017); Deshmukh *et al.* (2019) used various other parameters such as speed, area occupancy, etc. in their simulation models to estimate PCU.

PCU values vary with several factors associated with it such as vehicular composition, traffic volume, geometric conditions, side frictions, etc. However, due to the limitation of collecting the large amount of field data, studying the effects of these factors on PCU values has become difficult. Still a few researchers examined the effect of some of these factors like vehicular composition, traffic volume, road width etc. on PCU in homogeneous and disordered traffic (Arasan and Arkatkar 2010; Khanorkar *et al.* 2014; Parmar *et al*. 2018). However, the relative influence of these factors in the presence of side frictions on PCU has received less attention. Although researchers have not focused on investigating the effect of side frictions on PCU, they examined the side friction impact on traffic flow characteristics like speed using empirical methods in homogeneous and disordered traffic conditions (Pei and Wu 2004; Reddy *et al.* 2008; Bansal *et al.* 2014; Chand *et al*. 2014; Yang *et al.* 2015; Salini *et al*. 2016; Rao *et al*. 2017; Jin *et al.* 2019; Dea *et al.* 2019, Patkar and Dhamaniya 2020). Simulation methods are also used to study the impact of side frictions such as curbside bus stops and undesignated pedestrian crossings on traffic flow characteristics (Koshy and Arasan 2005; Arasan and Vedagiri 2008; Chen *et al.* 2010; Widanapathiranage *et al.* 2013; Iin 2015; Chen *et al*. 2016; Ben-Dor *et al.* 2018). But the studies on assessment of impact of curbside bus stops and undesignated pedestrian crossings on PCU values for several vehicle types using simulation models are limited especially in case of disordered traffic. Simulation tools are found to be more potent than the mathematical models to examine the relative impact of various influencing factors in the presence of side frictions on PCU values for different vehicle types.

A comprehensive review on studies related to development of traffic simulation models is performed. Various simulation models (Yang and Koutsopoulo 1996; Astarita *et al.* 2001; Toledo 2002; Xiong *et al.* 2015) and commercial software (e.g.,

VISSIM, AIMSUN, CORSIM, MITSIM, NETSIM, INTRAS, FRESIM, CARSIM, INTELSIM) have been developed for modelling homogeneous traffic conditions. But, the scope of applicability of these models and software to mixed traffic has not been clearly verified due to the presence of various types of vehicles travelling without lane discipline. In developed software, off-the-shelf software has certain drawbacks and hence, to overcome these issues, the researcher has to rely on the programming interface of the software. On the other hand, few researchers developed simulation models for various facility types including mid-block sections under disordered traffic conditions (Arasan and Koshy 2005; Venkatesan *et al.* 2008; Asaithambi *et al.* 2012; Metkari *et al.* 2013; Asaithambi *et al.* 2018; Kanagaraj and Treiber 2018; Sun *et al.* 2019). However, these models did not focus on estimating PCU values and investigating the effect of side frictions on PCU values. Koshy and Arasan (2005) incorporated bus stop in their simulation model to study the influence of bus stops on speed, but they failed to mention about the bus decelerating position and position at which bus attains its normal speed. It is necessary to incorporate these positions of bus as the stream speed gets reduced due to deceleration of buses that tend to stop near bus stop and subsequent acceleration of buses that re-enter the traffic, which in turn affect the PCU values. Similarly, in recent decade, many studies have been conducted to analyse the interaction between vehicles and crossing pedestrians in disordered traffic empirically (Laxman *et al.* 2010; Cherry *et al.* 2012; Dhamaniya and Chandra 2014; Kadali *et al.* 2015; Asaithambi *et al.* 2016; Patel *et al.* 2018; Golakiya and Dhamaniya 2019; Golakiya *et al.* 2020). However, simulating the real-world vehicle-pedestrian interactions still remain a less explored research topic under disordered traffic conditions. Various traffic simulation tools (such as VISSIM) are used to simulate vehicle–pedestrian interaction. However, their approach specifies the pedestrian's moving preference to only one conflicting side, which is less practical. Moreover, a few attempts are carried out to analyse the vehicle-pedestrian interaction in disordered traffic by developing simulation models (Wang *et al.* 2012; Chao *et al.* 2015; Lu *et al.* 2016; Liu *et al.* 2017; Ningbo *et al.* 2017; Wang *et al.* 2018). Although, these studies are performed to study the vehicle-pedestrian interactions, they focused only on behaviour of crossing pedestrians but not the behaviour of vehicles. However, in vehicle-pedestrian interaction model developed by Chao *et al.* 2015, behaviour of both vehicles and pedestrians during their interaction are explained, but the logics involved in the generation and placement of vehicles and pedestrians are not reported. They have not discussed about non-lane disciplined traffic and the pedestrian crossing patterns observed in disordered traffic conditions. Thus, a detailed study on how a simulation model for vehicle-pedestrian interaction in disordered traffic can be developed is also necessary to understand their interactions and investigate the influence of undesignated pedestrian crossings on PCU values.

Furthermore, as the PCU values are used for capacity analysis of roads with side frictions, investigating the effects of side frictions on capacity is imperative. Moreover, PCU values and capacity for urban roads recommended by the existing manuals (e.g., IRC 106 1990) are applicable only for the ideal/base sections i.e., the section devoid of any side frictions. The recently published highway capacity manual (Indo-HCM 2017) suggests adjustment factors for capacity estimation of roads with the presence of a few side frictions (e.g., parking, access points, bus stops), however, the adjustment factors for estimating PCU values are not suggested. As the change in PCU values will have an influence on capacity as well, it is essential to study the impact of curbside bus stop and undesignated pedestrian crossings on capacity. Hence, it is essential to develop generalized models to develop and update standards related to PCU and capacity estimation in the presence of side frictions.

2.5 GAPS IN THE LITERATURE

Based on the summary of literature, following research gaps are observed.

(1) Many attempts have been made to overcome the complexities involved in accurate estimation of PCU in disordered traffic. The widely used method for PCU estimation considers the relative speed and projected area (length × width) of vehicles. However, as a vehicle will be influenced by a larger area than its projected area, which is proportionate to the surrounding vehicle types (effective area of a vehicle); it is necessary to deal with the influence of surrounding vehicles while estimating its PCU value under disordered traffic condition.

(2) Researchers examined the effect of various factors like traffic volume, traffic composition, road width, etc. on PCU values as well as capacity of urban roads. However, the sensitivity of PCU values and capacity due to the presence of roadside

frictions (e.g., curbside bus stops, undesignated pedestrian crossings) are not adequately studied. Moreover, PCU values and capacity for urban roads recommended by the existing manuals (e.g., IRC 106, 1990) are applicable only for the ideal/base sections i.e., the section devoid of any side frictions. The recently published highway capacity manual (Indo-HCM 2017) suggests adjustment factors for capacity estimation of roads with the presence of a few side frictions (e.g., parking, access points, bus stops), however, the adjustment factors for estimating PCU values are not suggested. To address these gaps, this research study aims to estimate PCU values for vehicles under the influence of curbside bus stop and undesignated pedestrian crossings in disordered traffic. As the change in PCU values will have an influence on capacity as well, it is essential to study the impact of curbside bus stop and undesignated pedestrian crossings on capacity.

(3) The use of effective area approach to estimate PCU values, and studying the influence of commonly observed side frictions such as curbside bus stops and undesignated pedestrian crossings on PCU values are not considered in the existing studies which used simulation tools. Moreover, simulating the real-world vehicle-pedestrian interactions still remain a less explored research topic under disordered traffic conditions. Hence, development of a simulation model is essential to simulate the vehicle-pedestrian interactions and the traffic manoeuvers linked with a curbside bus stop to examine the influence of these side frictions on PCU values and capacity, and also to estimate PCU values using effective area approach.

CHAPTER 3

METHODOLOGY AND DATA COLLECTION

3.1 GENERAL

This chapter discusses the overview of detailed methodology adopted in this research work to achieve the specific objectives. Methodology of the study includes several steps which are illustrated in Figure 3.1.

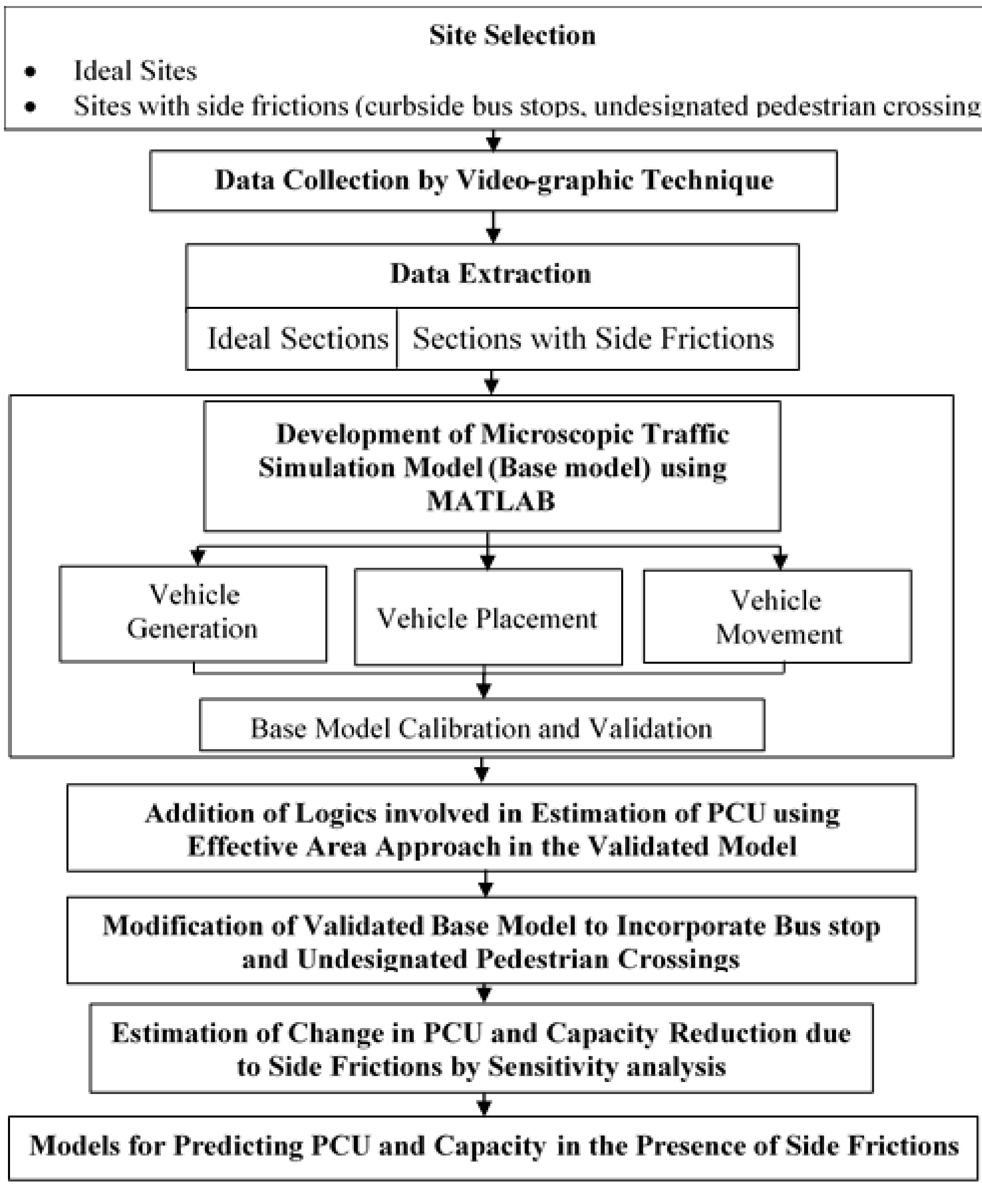

Figure 3. 1 Overview of Study Methodology

In this chapter, the process of data collection and extraction from the ideal road sections and sections with side frictions such as curbside bus stop and undesignated pedestrian crossings have also been described in detail.

3.2 SITE SELECTION, DATA COLLECTION AND EXTRACTION

3.2.1 Site Selection

Reconnaissance and preliminary surveys are conducted to identify the suitable divided mid-block sections in urban areas for this study. The mid-block sections are selected considering the geometric and traffic flow characteristics, and also the availability of vantage points for mounting the video cameras. Identifying an urban road with ideal section and only one side friction on the same stretch was also a difficult task. To study the impact of side frictions on PCU values and capacity, level and straight road sections in two different urban divided arterials are selected; one with the presence of only curbside bus stop and an ideal section (devoid of any side frictions) near it (Ideal_bus), and another with only undesignated pedestrian crossings and an ideal section near it (Ideal_ped). Table 3.1 shows the checklist for selection of suitable ideal sections for the proposed study.

Table 3.1 Checklist for Selection of Ideal Sections

Sl. No.	Required Conditions
1	Level and straight road section
2	Availability of vantage points for mounting the video cameras
3	The section should be 100 m away from the intersections and bus stops
4	Free from any side interference
5	Absence of roadside parking
6	No side roads or cross roads present near the study section
7	Pedestrian road crossing activities should be less

Moreover, a suitable straight road section with a curbside bus stop is selected in such a way that the section is 100 m away from intersections and also free from all other side frictions with availability of vantage points for mounting the video cameras. Similarly, a straight road section with pedestrians crossing the road at undesignated locations is selected in such a way that the section is free from all other side interferences with availability of vantage points for mounting the video cameras, and is also 100 m away from intersections and bus stops.

3.2.2 Data Collection

The traffic data required for this study are collected from two different four-lane divided urban arterial roads in Bangalore city, which is the third most populous city and fifth most populous urban agglomeration in India. The traffic on the roads of Bangalore city is highly disordered in nature with widely varying static and dynamic characteristics of vehicles. Five different types of vehicles considered in the study are motorized two-wheelers (TW), cars, three-wheelers (THW), buses and heavy vehicles (HV) (includes Light Commercial Vehicles (LCV) and trucks). Due to the limitation of man power and financial support, more amount of data could not be collected.

3.2.2.1 Data Collection from a Section with Curbside Bus Stop and Ideal Section (Ideal_bus)

To study the influence of curbside bus stops on PCU and capacity values, data are collected from four-lane divided mid-block sections located in HAL old airport road, Bangalore city. The data for this study are collected based on the understanding that a curbside bus stop creates temporary bottlenecks causing a considerable reduction in speeds of approaching vehicles only at a particular region/length termed as influence region of the bus stop (Bansal *et al.*, 2014; Rao *et al.*, 2017). Thus, data collection is performed on two sections (clear distance of 250 m between each section on the same straight road) where one section consists of a curbside bus stop (bus stop section) and another is an ideal section (Ideal_bus). Figure 3.2 shows the photographs and layout of ideal_bus and bus stop section. In this study, due to limited field of view of cameras, the length of the bus stop section is considered as 70 m. This 70 m section is thus treated as the influence region of the bus stop considering the effect of bus entering (upstream of the bus stop) and leaving (downstream of the bus stop) the section. Data are collected only from one direction of the selected road (7 m wide) using video-graphic technique on a weekday during peak and off-peak periods of traffic. Data are collected from both the sections simultaneously by mounting the cameras on elevated points near the sections.

(a)

(b)

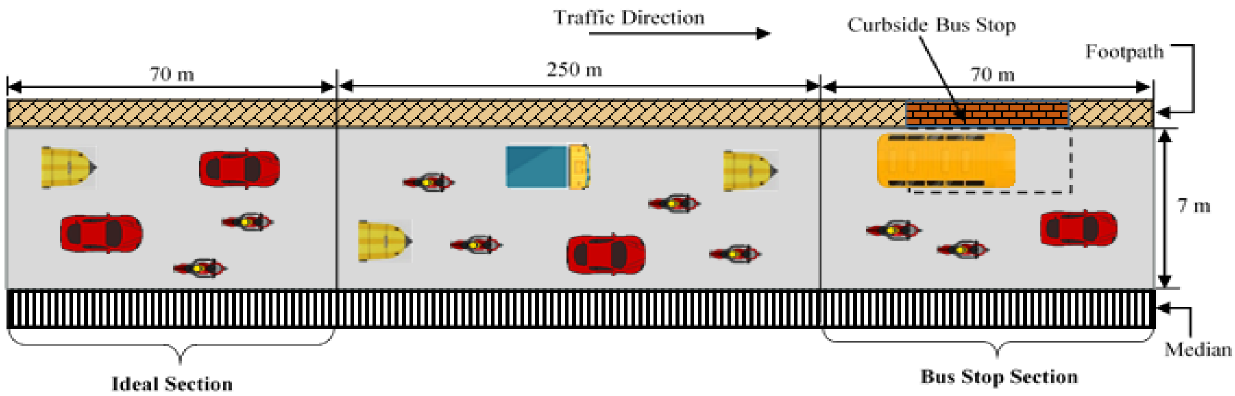

(c)

Figure 3.2 Photographs of (a) Ideal Section (Ideal_bus) and (b) Bus Stop Section, and (c) Layout of Study Sections located on HAL Old Airport Road, Bangalore city

3.2.2.2 Data Collection from a Section with Undesignated Pedestrian Crossings and Ideal Section (Ideal_ped)

The traffic data collected from divided mid-block sections located in Hosur road, Bangalore city are used to investigate the impact of undesignated pedestrian crossings on PCU and capacity values. Data are collected from a section with undesignated pedestrian crossings (pedestrian section) and from an ideal section (Ideal_ped) on the same straight road where there is a clear distance of 200 m between each section. Similar to the bus stop section, the influence of pedestrians on vehicles occurs only at a particular region/length of the road where the pedestrians are observed crossing. Due to limited field of view of cameras, the length of the pedestrian section is considered as 70 m. Also, from the field, as the pedestrian crossings were observed only within this section, 70 m is considered as the influence region of pedestrians. Data collection is performed only from one direction of selected road (7 m wide). Video cameras are used for collecting the data on a weekday during peak and off-peak periods of traffic. Data are collected from both the sections simultaneously by mounting the cameras on elevated points near the sections. Figure 3.3 shows the photographs and layouts of ideal_ped and pedestrian section.

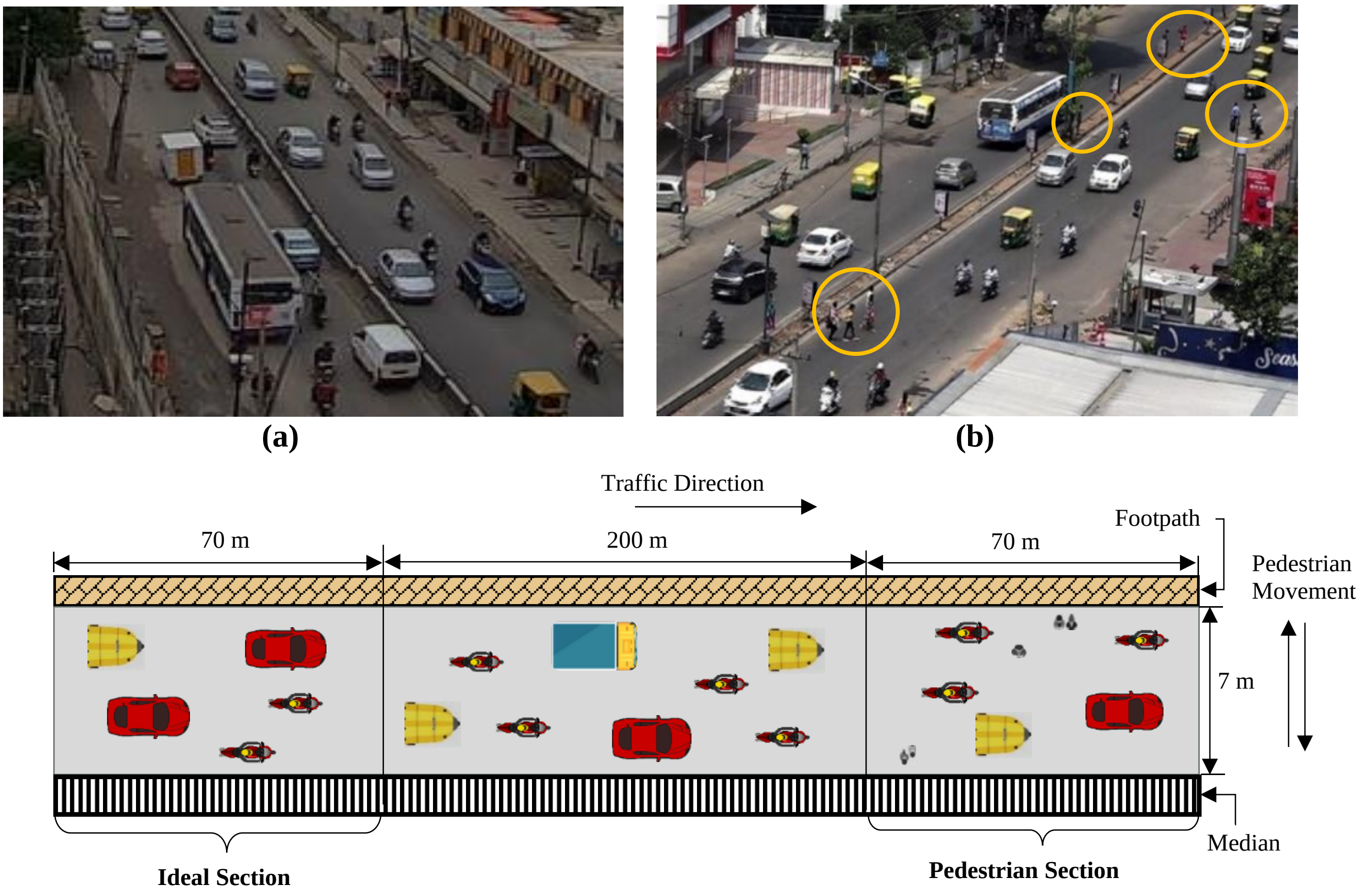

(a) **(b)** **(c)**

Figure 3.3 Photographs of (a) Ideal Section (Ideal_ped) and (b) Pedestrian Section, and (c) Layout of Study Sections located on Hosur Road, Bangalore City

3.2.3 Data Extraction

The peak and off-peak hour videos collected from study sections are processed further in image processing software, Irfanview to extract the required disaggregate data from video at the rate of 30 frames per second (Gowri, 2011). Irfanview (Irfanview 4.38) is an image viewer that can view, edit and convert an ordinary image file or video file into a graphical image, which makes it possible to obtain the coordinates (X, Y) of all the points in terms of pixels on the image. Gridlines with sufficient scale are plotted in AUTOCAD with obtained (X, Y) image coordinates. The gridlines are divided into lateral blocks of 1 m each and longitudinal blocks of 5 m each in case of bus stop section and ideal_bus section. The gridlines overlaid in case of pedestrian section and ideal_ped section, are divided into lateral blocks of 1 m each and longitudinal blocks of 2 m each. These gridlines are overlaid on videos using Ulead Video Studio 10.0 editor. The overlaid gridline videos are then converted to frames using irfanview to extract the required data. Figure 3.4 shows a sample image of gridlines drawn for ideal_bus section.

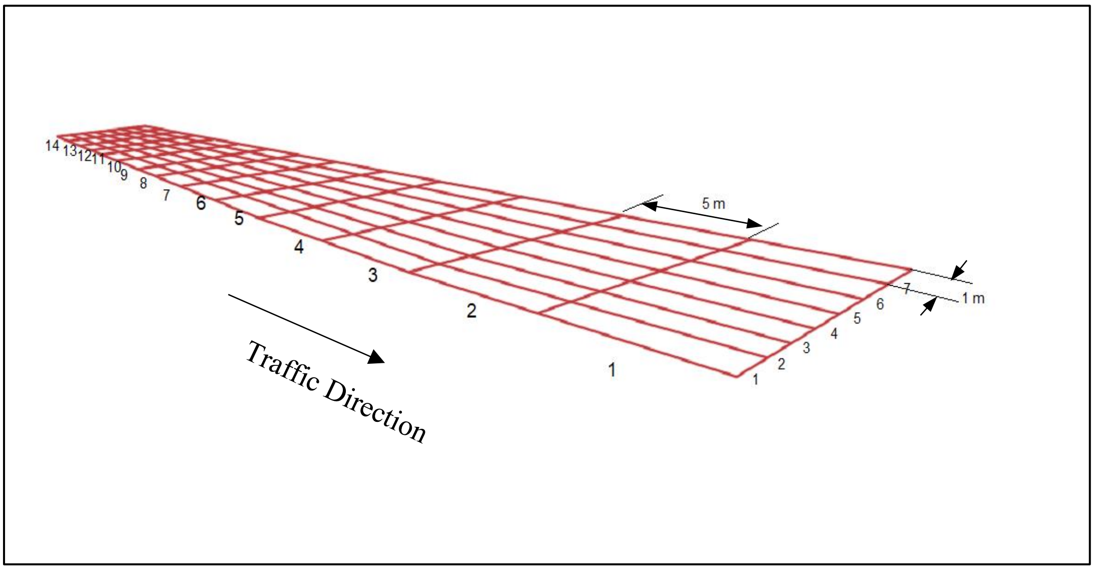

Figure 3.4 Sample Picture of Gridline Image of Ideal section located on HAL Old Airport Road, Bangalore City

Knowing distances on the ground and corresponding coordinates on the screen, correction factors (screen to ground) are applied to the obtained coordinates to reduce the parallax effect due to camera height and angle change (Gowri, 2011). The procedure for calculating the correction factors for longitudinal and lateral blocks is explained in Appendix I. The sample of correction factors for longitudinal and lateral blocks of gridline image of ideal_bus section, are calculated and is presented in Table I.1. Image coordinates in pixels are converted into real coordinates by multiplying the image coordinates with respective longitudinal and lateral correction factors. Figure I.1 shows the gridline image of ideal section located on HAL Road, Bangalore City.

3.2.3.1 Data Extraction from Bus Stop Section and Ideal_bus Section

Class-wise traffic flow is extracted for each five minutes from 4.5 hours data collected each during morning (6.30-11.00 am) and evening (2.30-7.00 pm) hours for both ideal and bus-stop sections. The hour having maximum flow is identified as the peak hour. The peak hour is between 8.40 am-9.40 am with traffic flow of 3970 vehicles per hour (veh/h) and 3354 veh/h for ideal_bus and bus stop sections, respectively. Both the sections have similar vehicular composition since they are on the same straight road. In both these sections, TW accounted for the largest share of vehicular composition with approximately 53% and HV with the least share of approximately 1% (Figure 3.5). In section with curbside bus stop, bus category is further classified into stopping (1.7%) and non-stopping buses (0.3%). Off-peak traffic data between 5.00 am to 6.00 am are collected for both the sections to extract free-flow speeds of vehicles and they are given as inputs to the simulation model.

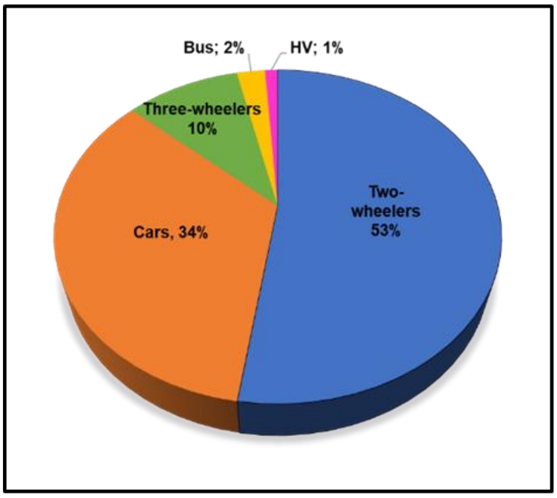

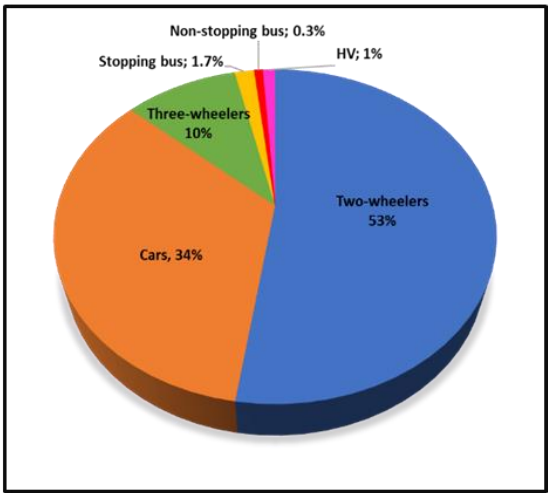

(a) **(b)**

Figure 3.5 Vehicular Composition of (a) Ideal_bus Section and (b) Bus Stop Section

The data extracted from ideal_bus section are vehicular time gaps, free-flow speeds, vehicular speeds during peak hour, acceleration and deceleration rates of vehicles, lateral positions at entry, longitudinal and lateral gaps of different vehicle types. These parameters are given as inputs in the base simulation model and are also used for calibration and internal validation of the base model. The additional data extracted from bus stop section are frequency of stopping and non-stopping buses, position at which bus stops, dwelling time of stopping bus, position at which stopping bus starts decelerating, position at which stopping bus attains its normal speed, deceleration and acceleration rate of stopping buses. These parameters are given as inputs to modify the base model to simulate the traffic manoeuvres in a section with curbside bus stop.

3.2.3.2 Data Extraction from Section with Undesignated Pedestrian Crossings and Ideal_ped Section

Classified count of traffic flow is carried out for each five-minute interval by playing the recorded videos collected from section with undesignated pedestrian crossings and ideal_ped section for four hours each during morning (7.00-11.00 am) and evening (3.00-7.00 pm) hours to identify the peak hour. The peak hour is between 8.45 am - 9.45 am with a traffic flow of 3664 veh/h and 3276 veh/h for ideal_ped and pedestrian sections, respectively; where TW accounted for the largest share of approximately 51% and HV with the least share of approximately 2% (Figure 3.6). The off-peak flow is taken from 5.00 am to 6.00 am for both the sections to extract free-flow speeds of vehicles and they are given as inputs to the simulation model. As data collection is performed for unidirectional traffic, pedestrian crossings in pedestrian section are also considered for unidirectional traffic. Pedestrians are classified as pedestrians moving from “median to curb (MC)” and from “curb to median (CM)” according to their direction of movement. A pedestrian flow of 404 pedestrians per hour (ped/h) is observed, where 296 ped/h travel from median to curb, and 108 ped/h travel from curb to median. Figure 3.7 shows the cross flow of pedestrians from median to curb and curb to median in pedestrian section.

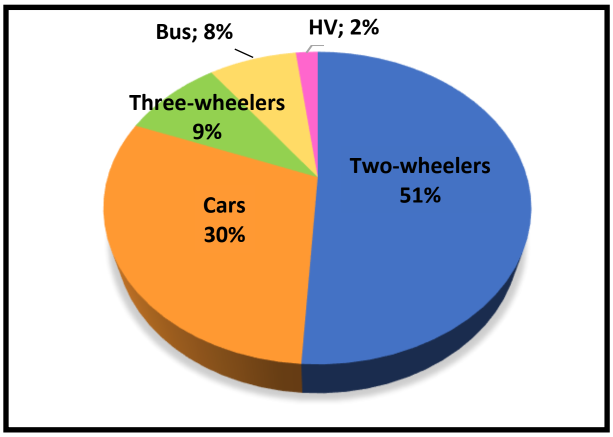

Figure 3.6 Vehicular Composition of Ideal_ped Section and Pedestrian Section

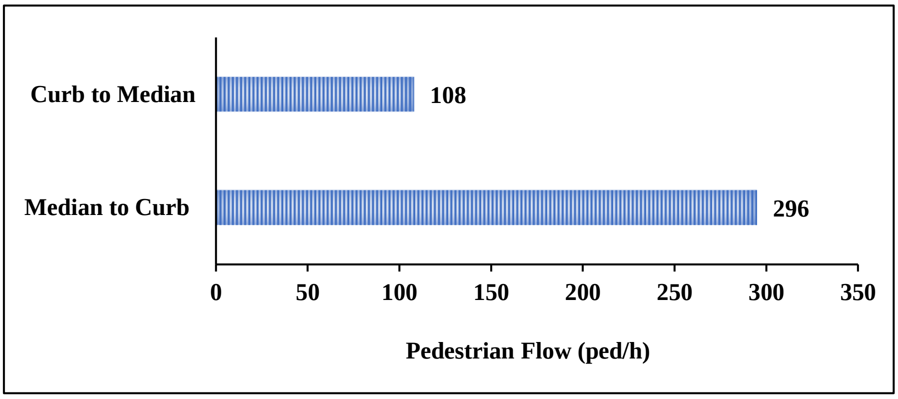

Figure 3.7 Pedestrian Cross Flow in the Pedestrian Section

The vehicular data extracted from ideal_ped are vehicular time gaps, free-flow speeds and speed of vehicles during peak hour as the selected ideal section is used for external validation of the base simulation model. These parameters are given as inputs to the model to simulate the traffic behaviour in ideal_ped section. In addition to the vehicular data, pedestrian characteristics such as pedestrian cross flow, pedestrian time gap, entry and exit positions of pedestrians, pedestrian waiting time and pedestrian crossing/walking speed are extracted from pedestrian section, to provide them as inputs to modify the base model for simulating vehicle-pedestrian interactions.

3.3 DATA ANALYSIS

The extracted data required to study the influence of roadside frictions on PCU and capacity values are analysed before providing them as inputs to the simulation model. Analysis of the extracted data from the ideal sections and the sections with side frictions are discussed as follows.

3.3.1 Analysis of Ideal Section (Ideal_bus) Data

Initially, the data extracted from ideal_bus section are analysed as they are used for base model calibration and internal validation. Free-flow speeds (desired speeds) of vehicles are obtained from the traffic data collected during off-peak hour (5 am – 6 am). Vehicular time gaps, speeds and acceleration/deceleration of each type of vehicles, lateral positions of vehicles at entry, lateral and longitudinal gaps between the vehicles are obtained from the peak hour data. Lateral positions of vehicles at entry, lateral and longitudinal gaps between the vehicles are calculated from the image coordinates using correction factors.

3.3.1.1 Free-flow Speed

Free-flow speeds of different types of vehicles are necessary for developing a traffic simulation model. Free-flow speed is defined as the maximum speed that can be achieved by any given vehicle type when there are no interruptions of other vehicle types in the traffic for the given road width and terrain conditions (Indo-HCM 2017). Time taken by the vehicles to travel a trap length of 70 m during off-peak period of traffic is obtained and free-flow speeds are calculated (Table II.1).

The one-way Analysis of Variance (ANOVA) test indicates that the free-flow speeds of different vehicle types are significantly different (F_{obs}= 29.8, F_{crit}=2.38) from each other at 5% level of significance. Descriptive statistics for free-flow speeds of different types of vehicles is given in Table 3.2. In the table, aggregate speed refers to the speed of the traffic stream. The mean free-flow speed of two-wheelers (TW) is higher (16.2 m/s) because of their smaller sizes and higher manoeuverability followed by cars (16.1 m/s) due to their higher operating capabilities whereas heavy vehicles (HV) travel with a minimum mean free-flow speed (11.2 m/s) due to their larger size and lower manoeuverability. Different probability distribution functions are fitted to class-wise data of free-flow speeds and goodness-of-fit test for each probability density function is conducted by K-S test at 5% significance level. Table 3.3 shows the best fit distribution for free-flow speeds of class-wise vehicle data. The results indicate that all vehicle types follow normal distribution.

Table 3.2 Descriptive Statistics for Free-flow speed of Different Types of Vehicles

Vehicle Type	Free-Flow Speed (m/s)				Sample size
	Mean	SD	Min.	Max.	
Aggregate	14.4	3.4	6.7	25.0	829
Two-wheelers	16.2	3.5	10.0	25.0	238
Three-wheelers	12.8	2.6	6.7	16.7	35
Cars	16.1	2.9	8.3	25.0	456
Buses	12.2	1.0	10.0	14.3	64
Heavy vehicles	11.2	1.3	8.3	13.5	36

Note: SD = Standard Deviation; Min. = Minimum value; Max. = Maximum value

Table 3.3 Best Fit Distribution and Parameters for Free-flow Speeds of Vehicle Types

Vehicle Type	Best Fit Distribution	Parameters	K-S value
Two-wheelers	Normal	σ=3.5, μ=16.2	0.03
Three-wheelers	Normal	σ=2.6, μ=12.8	0.03
Cars	Normal	σ=2.9, μ=16.1	0.05
Bus	Normal	σ=1.0, μ=12.2	0.04
Heavy Vehicles	Normal	σ=1.3, μ=11.2	0.08

Note: μ = Mean; σ = Standard Deviation

3.3.1.2 Vehicular Time Gap

Time gap is defined as the time elapsed between the passage of successive vehicles crossing a reference line along the road width. Distribution models for time gaps developed for homogenous traffic conditions cannot be applied directly to disordered traffic conditions. This is due to the fact that the occurrences of zero-time gap are nearly impossible for homogenous traffic conditions as the observations are made based on lane; whereas, under disordered traffic conditions, smaller vehicles like TW move parallelly along the entire width of the road, which create significant number of zero-time gaps. Hence, time gap observations are made on entire width of road in disordered traffic conditions instead of lane–wise, which is more appropriate due to the absence of lane discipline (Table II.2).

The one-way ANOVA test indicates that the time gaps of different vehicle types are significantly different (F_{obs} = 9.33, F_{crit} = 2.37) from each other at 5% level of significance. Descriptive statistics for time gap of different types of vehicles is given in Table 3.4. Due to the smaller sizes and higher manoeuverability and to maintain higher speeds, the mean time gap of two-wheelers is found to be lesser (0.8 s) whereas larger sized vehicles like HV have a mean time gap of 1.5 s as they travel at a lower speed. Different probability distribution functions are fitted to aggregate data of time gaps and goodness-of-fit test for each probability density function is conducted by K-S test at 5% significance level. The data follow negative exponential distribution for a level of significance of 0.05. The parameter (λ) obtained from the distribution of time gap is 1.1095, which is used as inputs in simulation model for generation of vehicles.

Table 3.4 Descriptive Statistics for Time Gap of Different Types of Vehicles

Vehicle Type	Time Gap (s)				Sample size
	Mean	SD	Min.	Max.	
Aggregate	0.9	2.0	0	7.0	3970
Two-wheelers	0.8	2.0	0	6.9	2080
Three-wheelers	1.0	2.1	0	6.9	391
Cars	0.9	1.8	0	6.8	1359
Buses	1.4	1.3	0	7.0	97
Heavy vehicles	1.5	1.5	0	6.8	43

3.3.1.3 Vehicular Speeds

Speed of a vehicle is defined as the distance it travels per unit of time. Velocity or speed is the rate of movement of traffic usually expressed in kilometre per hour (km/h) or metre per second (m/s). It is one of the important factors directly influencing mobility. The arithmetic mean of speeds of the vehicles occupying a given length of road at a given instant is the space mean speed. Space mean speed is obtained by sampling the vehicles over an area or a section. Speed of different types of vehicles is thus calculated by dividing the trap length (70 m) travelled by the vehicle by the time taken by the vehicle to cross this trap length (Table II.2).

The one-way ANOVA test indicates that the speeds of vehicle types are significantly different (F_{obs} = 82.5, F_{crit} = 2.37) from each other at 5% level of significance. Descriptive statistics for speeds of different types of vehicles is given in Table 3.5.

Table 3.5 Descriptive Statistics for Speed of Different Types of Vehicles

Vehicle Type	Speed (m/s)				Sample size
	Mean	SD	Min.	Max.	
Aggregate	12.7	2.2	4.6	19.4	3970
Two-wheelers	13.2	2.2	5.9	19.4	2080
Three-wheelers	11.5	1.7	4.8	16.4	391
Cars	12.4	1.9	6.4	19.4	1359
Buses	11.8	1.8	4.6	15.8	97
Heavy vehicles	10.6	1.8	4.9	14.4	43

Smaller sizes and higher manoeuverability of two-wheelers keep their mean speed higher (13.2 m/s) followed by cars (12.4 m/s) due to their higher operating capabilities whereas HV travel with a minimum mean speed (10.6 m/s) due to their larger sizes. During the survey period, state of traffic varies from continuous flow condition to a congested condition, and vice versa. This is the reason for obtaining a wide range of speed values for vehicle types.

3.3.1.4 Vehicle Acceleration and Deceleration Rates

Acceleration and deceleration rates are the rate of change of speed of a vehicle, expressed in m/s^2. Acceleration rate is a positive value whereas deceleration rate is a negative value. Acceleration and deceleration capability of vehicles varies with their dimension, power to weight ratio and type of gear transmission mechanism. In disordered traffic, acceleration and deceleration rates vary according to various speeds for different types of vehicles and also, it depends on prevailing traffic conditions. As the gridlines on the frames are divided into longitudinal blocks of 5 m each, two 10 m stretches one after the entry point and other before the exit point are considered. The speed of the first stretch is obtained by considering the time taken by the vehicle to cross this stretch. Similarly, the speed of second stretch is obtained. The acceleration or deceleration rate is obtained by calculating the speed difference at these two stretches and time taken by the vehicle to cross these stretches (Table II.2).

The one-way ANOVA test indicates that the acceleration rates of different vehicle types are significantly different ($F_{obs} = 2.53$, $F_{crit} = 2.37$) from each other at 5% level of significance. Descriptive statistics for acceleration of different types of vehicles is obtained and shown in Table 3.6. The mean acceleration capability of cars is higher (1.7 m/s^2) as they have higher operating characteristics whereas HV have lesser mean acceleration rate (1.2 m/s^2).

Table 3.6 Descriptive Statistics for Acceleration of Different Types of Vehicles

Vehicle Type	Acceleration Rate (m/s^2)				Sample Size
	Mean	SD	Min.	Max.	
Aggregate	1.4	0.5	0.4	5.5	1900
Two-wheelers	1.6	0.6	0.4	5.4	790
Three-wheelers	1.3	0.3	0.4	1.9	205
Cars	1.7	0.4	0.5	5.5	811
Buses	1.4	0.2	0.4	1.9	65
Heavy vehicles	1.2	0.2	0.4	1.6	29

The one-way ANOVA test indicates that the deceleration rates of vehicle types are significantly different (F_{obs} = 2.64, F_{crit} =2.37) from each other at 5% level of significance. Descriptive statistics for deceleration of different types of vehicles is shown in Table 3.7. The mean deceleration rate of cars is higher (1.6 m/s^2) since they have the capability to decelerate immediately whereas HV travel at a lower speed and they gradually decelerate due to their larger size and lower manoeuverability and hence, their mean rate of deceleration is minimum (1.3 m/s^2).

Table 3.7 Descriptive Statistics for Deceleration of Different Types of Vehicles

Vehicle Type	Deceleration Rate (m/s^2)				Sample Size
	Mean	SD	Min.	Max.	
Aggregate	1.4	0.6	0.5	5.9	1488
Two-wheelers	1.5	0.6	0.6	5.9	963
Three-wheelers	1.4	0.3	0.5	1.9	120
Cars	1.6	0.6	0.5	4.7	378
Buses	1.4	0.4	0.5	2.0	18
Heavy vehicles	1.3	0.2	0.5	1.8	9

3.3.1.5 Lateral Gap

Lateral gap is an important parameter for passing manoeuver. Lateral gap is defined as the lateral distance between two vehicles with their length overlapping with each other. Lateral gap for each subject vehicle with respect to the adjacent vehicles is extracted (Table II.3). Knowing the image coordinates of subject vehicle and adjacent vehicle in pixels, real coordinates are obtained by applying the correction factors calculated for each grid block.

The one-way ANOVA test indicates that the lateral gaps of different vehicle types are significantly different (F_{obs} = 4.99, F_{crit} = 2.37) from each other at 5% level of significance. Descriptive statistics for lateral gaps of different types of vehicles is shown in Table 3.8. The mean lateral gap for two-wheelers with smaller sizes is lesser (1.3 m) whereas HV and buses due to their larger sizes maintain a higher lateral gap with adjacent vehicles (1.5 m).

Table 3.8 Descriptive Statistics for Lateral Gaps of Different Types of Subject Vehicles

Vehicle Type	Lateral Gaps (m)				Sample Size
	Mean	SD	Min.	Max.	
Aggregate	1.5	0.8	0.1	3.4	1405
Two-wheelers	1.3	0.7	0.1	2.5	691
Three-wheelers	1.4	0.7	0.1	3.0	151
Cars	1.4	0.7	0.1	3.0	475
Buses	1.5	0.8	0.2	3.4	31
Heavy vehicles	1.5	0.8	0.4	3.3	20

Lateral gaps also depend upon speeds of the subject vehicles and their corresponding types. In the simulation model, lateral gaps are given as input to the model based on the speed of subject vehicles. Figure 3.8 shows relationship between observed lateral gaps and speeds of subject vehicles. Relationship between lateral gaps and speeds of different types of subject vehicles are plotted and it is found that second-degree polynomial relationship gives a better R^2 value. Coefficient of correlation (R^2) is used to determine the goodness of fit of the models. The results indicate that lateral gap increases with increase in speed of subject vehicle. It is observed that there is a significant variation in the lateral gaps and found to have non-linear relationship with speed of vehicles. TW due to their smaller sizes even at a higher speed squeeze in between the vehicles and hence, they maintain a maximum lateral gap of only 2.5 m with the adjacent vehicles. But, if buses and heavy vehicle are travelling at higher speeds, the adjacent vehicles considering their safety try to maintain a larger maximum lateral gap with buses (3.4 m) and HV (3.3 m).

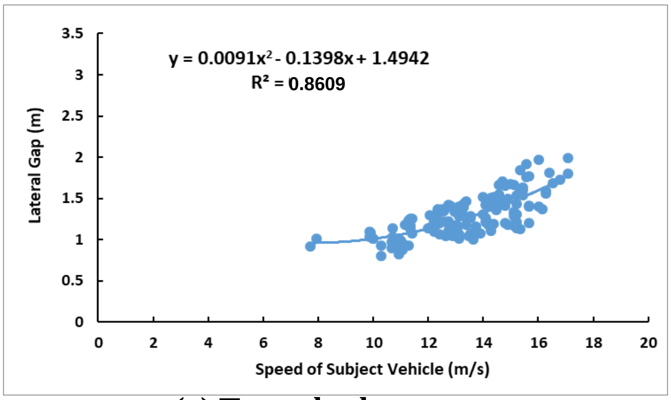

(a) Two-wheelers

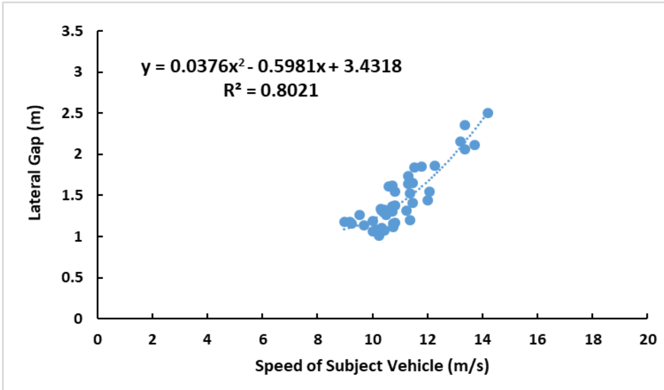

(b) Three-wheelers

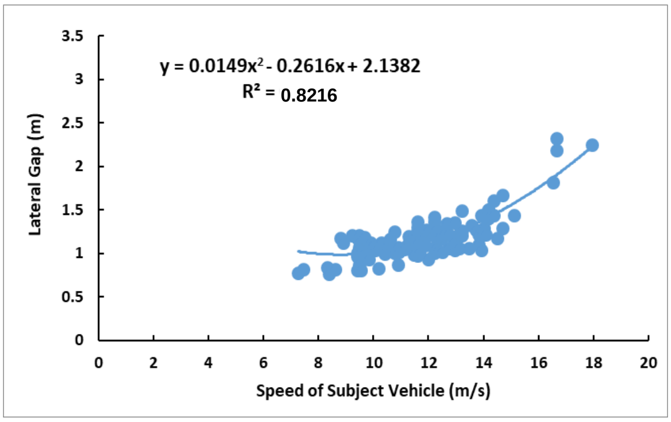

(c) Cars

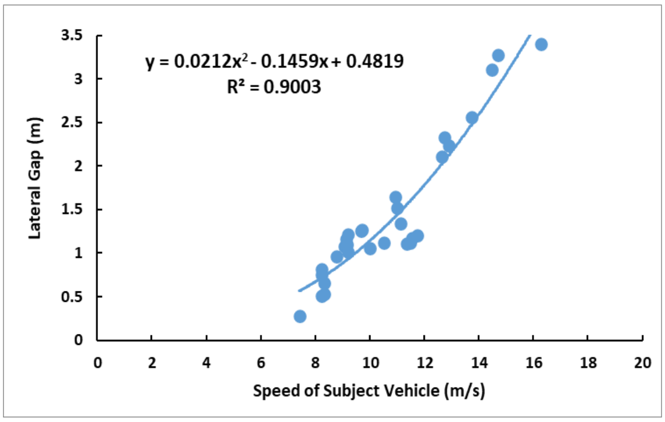

(d) Buses

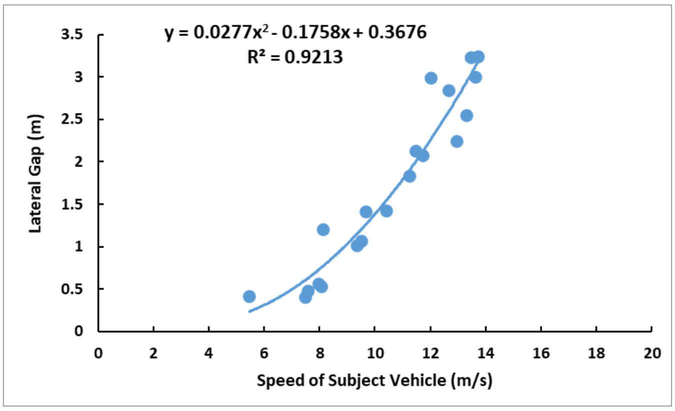

(d) Heavy Vehicles

Figure 3.8 Relationship Between Lateral Gap and Speed of Subject Vehicle

3.3.1.6 Longitudinal Gap

Drivers of different types of vehicles will always tend to maintain sufficient longitudinal clearances in the front and back with respect to other vehicles to avoid collision. Longitudinal gap is defined as the clear distance between the back bumper of the leader vehicle and front bumper of the subject vehicle with their width overlapping with each other. With reference to VISSIM software (PTV VISSIM), influence of leader vehicle on subject vehicle takes place within a look ahead distance of 20-30 m. For each type of subject vehicle, the longitudinal gaps are obtained (Table II.4).

The one-way ANOVA test indicates that the longitudinal gaps of vehicle types are significantly different (F_{obs} = 10.25, F_{crit}=2.38) from each other at 5% level of significance. Descriptive statistics for longitudinal gaps of different types of vehicles is obtained and shown in Table 3.9. Smaller sized vehicle like two-wheelers maintain lesser gap with the leader since they move at higher speeds due to their higher manoeuverability, and hence, the mean longitudinal gap for two-wheelers is found to be minimum (14.2 m). HV maintain larger gaps (19.8 m) as they move at lower speeds due to their larger sizes.

Table 3.9 Descriptive Statistics for Longitudinal Gaps of Vehicle Types

Vehicle Type	Longitudinal Gap (m)				Sample Size
	Mean	SD	Min.	Max.	
Aggregate	15.5	7.5	1.3	29.8	1235
Two-wheelers	14.2	7.4	1.3	29.4	472
Three-wheelers	13.7	7.7	2.1	29.5	79
Cars	16.6	7.3	2.1	29.4	644
Buses	17.8	8.8	4.3	29.5	20
Heavy vehicles	19.8	8.7	5.4	29.8	11

Longitudinal gap also depends upon speed of the subject vehicle and their respective types. Longitudinal gaps are also given as inputs to the simulation model based on the speeds of subject vehicles. Figure 3.9 shows relationship between longitudinal gap and speed of subject vehicle.

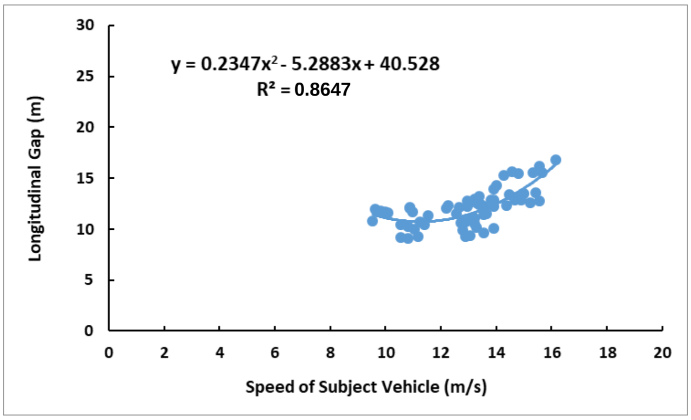

(a) Two-wheelers

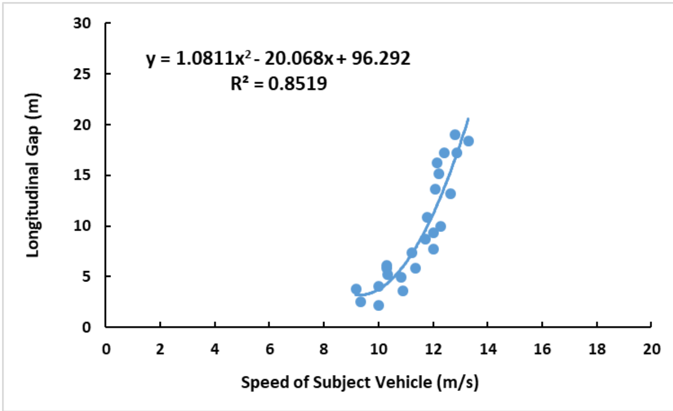

(b) Three-wheelers

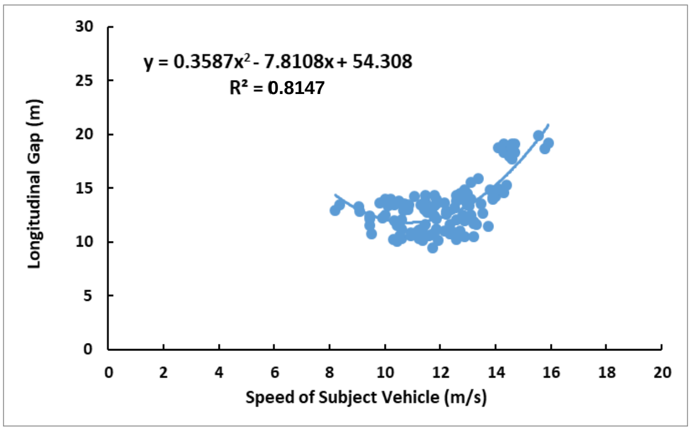

(c) Cars

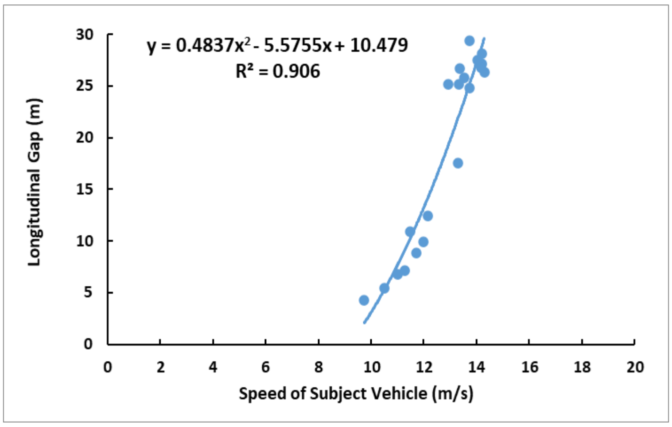

(d) Buses

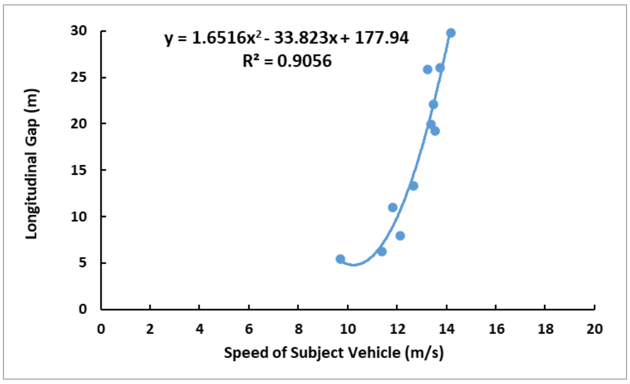

(e) Heavy Vehicles

Figure 3.9 Relationship between Longitudinal Gap and Speed of Subject Vehicle

Relationship between longitudinal gaps and speed of different types of subject vehicles shows that second degree polynomial relationship gives a better R^2 value. The results indicate that the longitudinal gap increases with increase in speed of subject vehicle.

3.3.1.7 Lateral Placement of Vehicles

Lateral placement of a vehicle is defined as the closest lateral position of the vehicle from the median of the road when the vehicle is in motion. Lateral positions of vehicle types are extracted when the front bumper of the subject vehicle touches the entry line (Table II.5). It is necessary to analyse the lateral placement of the vehicles to incorporate it in the vehicle placement logic of simulation model.

Frequency distribution for lateral position of vehicles on the entire width of the road is shown in Figure 3.10. It is found that majority of the vehicles (66.4%) are preferred to travel near the median of the road (0-3.5 m). Two-wheelers (median lane: 58.2%; shoulder lane: 41.9%) and three-wheelers (median lane: 54.5%; shoulder lane: 45.5%) occupy almost the entire width of the road as they tend to occupy every lateral gap available on the road due to their smaller sizes and higher manoeuverability. Most of the cars (81.3 %) prefer to travel near the median of the road so as to maintain higher speeds. Buses (76.3%) and HV (79.1%) are concentrated near the median of the road so as to avoid side interferences from other vehicles.

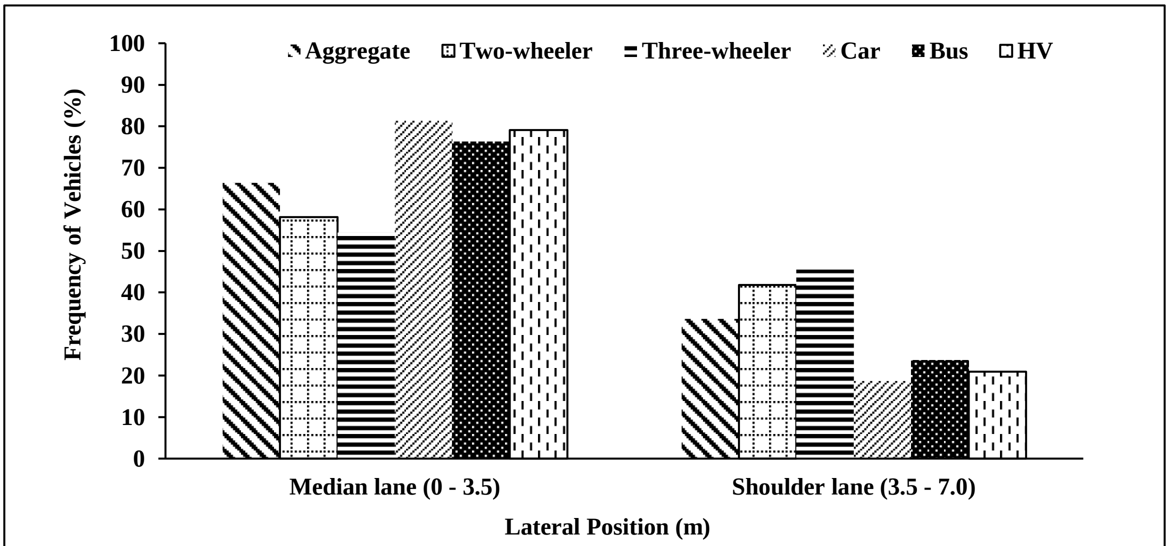

Figure 3.10 Frequency Distribution for Lateral Position of Different Vehicle Types

3.3.2 Analysis of Bus Stop Section Data

For the investigation of impact of curbside bus stops on PCU and capacity values, analysis of data collected from curbside bus stop is necessary. The curbside bus stop section consists of buses classified as stopping (1.7%) and non-stopping (0.3%) buses along with other vehicles. Non- stopping buses are those buses such as tourist buses, school buses, etc. which do not stop at the bus stop. The stopping buses in bus stop section have different characteristics compared to non-stopping buses and other vehicles, as these buses stop at the curbside bus stop for a particular time (i.e., bus dwelling time).

3.3.2.1 Characteristics of Stopping Bus

Various parameters of stopping buses extracted from the curbside bus stop section are bus dwelling time, position at which bus stops (bus stopping position) observed with respect to the entry line of the stretch, bus deceleration rate before stopping and acceleration rate while moving from the stopped position, position at which bus starts decelerating (bus decelerating position) and position at which bus attains its normal speed (Table 3.10 and Table II.6). The mean position at which bus starts decelerating (bus decelerating position) is 30 m before the mean bus stopping position and bus attains its normal speed after traveling 20 m from the mean bus stopping position.

Table 3.10 Characteristics of Stopping Bus at Bus Stop Section

Parameters	Descriptive statistics				Sample size
	Mean	SD	Min.	Max.	
Bus Dwelling Time (s)	5	3.2	1.2	9.2	57
Bus Stopping Position from entry line (m)	41.02	5.5	32.9	49.9	57
Stopping Bus Deceleration Rate (m/s^2)	1.3	0.2	0.2	1.7	57
Stopping Bus Acceleration Rate (m/s^2)	1.2	0.4	0.2	1.6	57

3.3.2.2 Vehicular Speed in the Presence of Curbside Bus Stop

To understand the variations in speeds of vehicles due to the presence of curbside bus stop, aggregate and class-wise speeds of vehicles are extracted. Vehicular speed is calculated for each vehicle type considering the time taken to travel the selected trap length (70 m) with curbside bus stop. Descriptive statistics for vehicular speeds due to the influence of curbside bus stop are given in Table 3.11. The mean speed of two-wheelers is higher (10.7 m/s) whereas buses travel with a minimum mean speed of 6.2 m/s as a few buses stop at the bus stop which reduces the bus speed to zero m/s.

Table 3.11 Descriptive Statistics for Speeds of Different Types of Vehicles

Vehicle Type	Speed of Vehicles (m/s)				Sample size
	Mean	SD	Min.	Max.	
Aggregate	10.0	2.1	3.9	15.5	3354
Two-wheelers	10.7	1.7	3.9	15.5	1778
Three-wheelers	9.2	1.4	4.0	12.7	335
Cars	9.5	1.4	4.2	13.4	1140
Buses	6.2	2.2	0	10.3	67
Heavy vehicles	8.7	1.1	4.5	10.4	34

3.3.3 Analysis of Ideal Section (Ideal_ped) Data

As ideal_ped section is used for external validation of the base simulation model, parameters such as free-flow speed and time gaps are only used as input to the model. Speeds of each vehicle type are estimated from the field data to compare with simulated speeds obtained as output from the model. Vehicular free-flow speeds are obtained from the traffic data collected from Hosur road, Bangalore city during off-peak hour (5.00 – 6.00 am). Vehicular time gaps and speeds of each type of vehicle are obtained from the peak hour data.

3.3.3.1 Free-flow Speed

The one-way ANOVA test indicates that the free-flow speeds of different vehicle types are significantly different (F_{obs} = 30.2, F_{crit}=2.42) from each other at 5% level of significance. Descriptive statistics for free-flow speed of different types of vehicles is given in Table 3.12. Two-wheelers having smaller sizes and higher manoeuverability travel at a higher free-flow speed (19.1 m/s) followed by cars (18.5 m/s) due to their higher operating characteristics whereas HV travel with a minimum mean free-flow speed (11.5 m/s) due to their larger sizes and lower manoeuverability. Different probability distribution functions are fitted to class-wise data of free-flow speeds and goodness-of-fit test for each probability density function is conducted by K-S test at 5% significance level. Table 3.13 shows the best fit distribution for free-flow speeds of class-wise data. The results indicate that all vehicle types follow normal distribution.

Table 3.12 Descriptive Statistics for Free-flow Speed of Different Types of Vehicles

Vehicle Type	Free-flow Speed (m/s)				Sample size
	Mean	SD	Min.	Max.	
Aggregate	18.4	4.5	7.0	23.3	603
Two-wheelers	19.1	4.4	8.7	23.3	241
Three-wheelers	13.5	2.6	7.7	18.0	58
Cars	18.5	4.3	8.7	23.3	123
Buses	12.6	1.6	7.0	15.7	120
Heavy vehicles	11.5	1.7	7.0	15.0	61

Table 3.13 Best Fit Distribution and Parameters for Free-flow Speeds of Vehicle Types

Vehicle Type	Best Fit Distribution	Parameters	K-S value
Two-wheelers	Normal	σ=4.3, μ=18.5	0.03
Three-wheelers	Normal	σ=2.6, μ=13.5	0.04
Cars	Normal	σ=4.4, μ=19.1	0.05
Bus	Normal	σ=1.6, μ=12.6	0.04
Heavy Vehicles	Normal	σ=1.7, μ=11.5	0.06

3.3.3.2 Vehicular Time Gap

The one-way ANOVA test indicates that the time gaps of different vehicle types are significantly different (F_{obs} = 10.55, F_{crit} =2.41) from each other at 5% level of significance. Descriptive statistics for time gap of different types of vehicles is given in Table 3.14. The mean time gap of two-wheelers is lesser (0.85 s) because they try to maintain higher speeds whereas HV have mean time gap of 2.08 s.

Table 3.14 Descriptive Statistics for Time Gap of Different Types of Vehicles

Vehicle Type	Time Gap (s)				Sample size
	Mean	SD	Min.	Max.	
Aggregate	0.96	2.0	0	7.2	3664
Two-wheelers	0.85	1.9	0	6.6	1869
Three-wheelers	1.09	1.7	0	6.8	330
Cars	0.95	1.8	0	6.8	1099
Buses	1.90	2.2	0	7.2	293
Heavy vehicles	2.08	2.0	0	6.9	73

Different probability distribution functions are fitted to aggregate data of time gaps and goodness-of-fit test for each probability density function is conducted by K-S test at 5% significance level. It is observed that data follow negative exponential distribution for a level of significance of 0.05. The parameter (λ) obtained from the distribution of time gap is 1.04, which is used as an input in the simulation model.

3.3.3.3 Vehicular Speed

The one-way ANOVA test indicates that the speeds of vehicle types are significantly different (F_{obs} = 52.6, F_{crit}=2.41) from each other at 5% level of significance. Descriptive statistics for speeds of different types of vehicles is given in Table 3.15. Smaller sizes and higher manoeuverability of two-wheelers keep their mean speed higher (13.5 m/s) followed by cars (13.1 m/s) due to their higher operating capabilities whereas HV travel with a minimum mean speed (9.1 m/s) due to their larger sizes and lower manoeuverability.

Table 3.15 Descriptive Statistics for Speeds of Different Types of Vehicles

Vehicle Type	Speed (m/s)				Sample size
	Mean	SD	Min.	Max.	
Aggregate	12.7	2.5	5.4	19.4	3664
Two-wheelers	13.5	2.0	7.4	18.7	1869
Three-wheelers	10.3	1.6	6.7	12.7	330
Cars	13.1	1.9	7.5	19.4	1099
Buses	9.7	1.4	6.6	12.5	293
Heavy vehicles	9.1	1.3	5.4	12.0	73

3.3.4 Analysis of Pedestrian Section Data

The data extracted from the section with undesignated pedestrian crossings are analysed to assess the influence of undesignated pedestrian crossings on PCU and capacity values. Based on the direction of movement of pedestrians from curb to median (CM) and from median to curb (MC), the parameters required for simulating pedestrians are analysed.

3.3.4.1 Pedestrian Crossing Pattern

Due to the disorderliness in traffic, the pedestrians cross the road whenever safe gaps are available between the vehicles, either in perpendicular or in oblique pattern (Asaithambi *et al.*, 2016). Hence, they are sub-divided as pedestrians moving in, "perpendicular pattern from median to curb (PD_MC)", "oblique pattern from median to curb (OD_MC)", "perpendicular pattern from curb to median (PD_CM)" and "oblique pattern from curb to median (OD_CM)" based on their crossing pattern. Those pedestrians moving in oblique pattern are further classified as "oblique right" and "oblique left" to know which side they travel. Crossing patterns of pedestrians are shown in Figure 3.11. The proportion of pedestrians with different crossing patterns for the study section are shown in Figure 3.12.

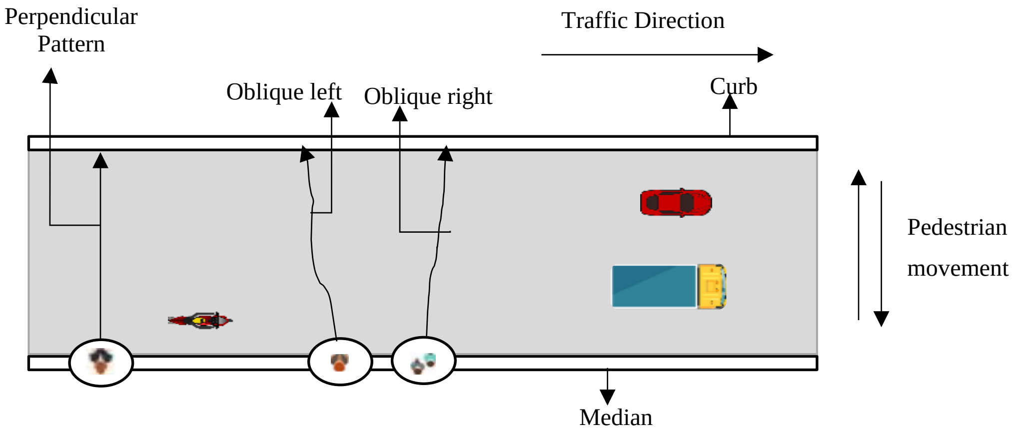

(a) Pedestrians Moving from Median to Curb

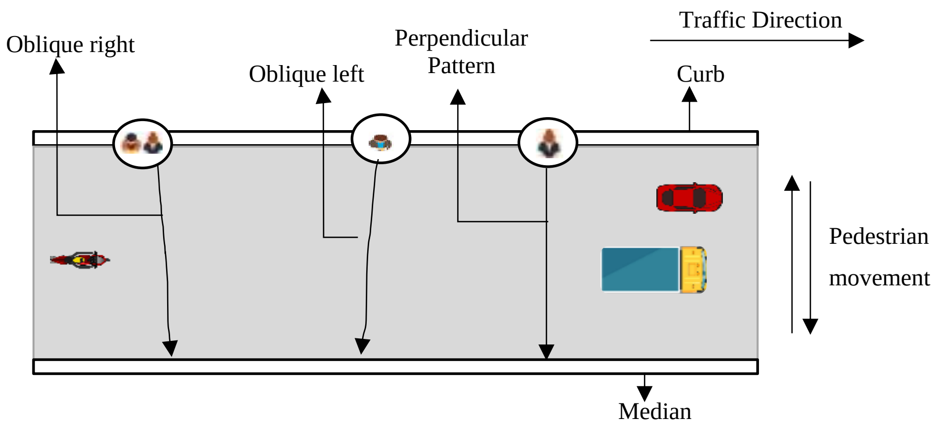

(b) Pedestrians Moving from Curb to Median

Figure 3.11 Crossing Patterns of Pedestrians from (a) Median to Curb and (b) Curb to Median

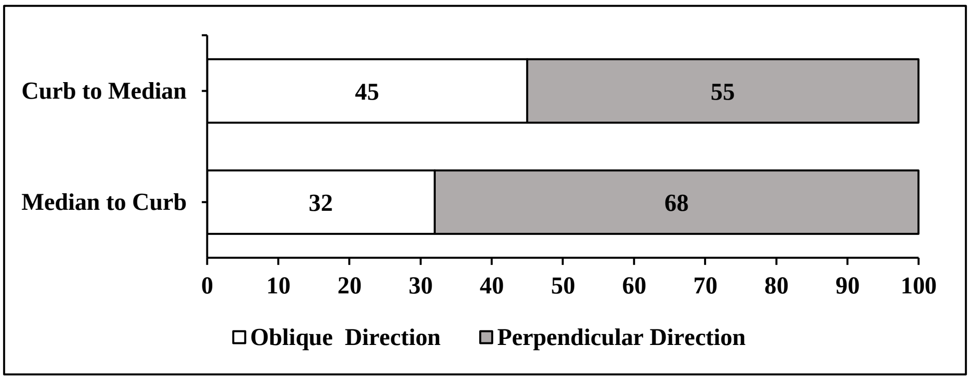

Figure 3.12 Proportion of Pedestrians with Different Crossing Patterns

3.3.4.2 Pedestrian Time Gap

In this study, pedestrian time gap is defined as the elapsed time between the passage of successive pedestrians crossing a reference line along the road length. Pedestrian time gap is extracted by considering the time at which each pedestrian reaches the median or curb to cross the road (Table II.7). Descriptive statistics for pedestrian time gap is given in Table 3.16.

Table 3.16 Descriptive Statistics for Pedestrian Time Gap

Pedestrian Type	**Pedestrian Time Gap (s)**				**Sample size**
	Mean	**SD**	**Min.**	**Max.**	
Aggregate	8.6	12.1	0	50.2	404
Median to Curb	8.5	12.2	0	50.2	296
Curb to Median	8.8	11.7	0	44.2	108

Different probability distribution functions are fitted to aggregate data of pedestrian time gaps and goodness-of-fit test for each probability density function is conducted by K-S test at 5% significance level. It is observed that data follows negative exponential distribution for a level of significance of 0.05. The parameter (λ) obtained from the distribution of pedestrian time gap is 0.116, which is used for generation of pedestrians in the developed model.

3.3.4.3 Pedestrian Walking Speed

Crossing time of pedestrians, i.e., the time taken by the pedestrians to cross the entire road width is the major factor which determines the walking speed of pedestrians. Pedestrian walking or crossing speed is calculated by dividing the width of the road with the crossing time of pedestrians (Table II.7). Pedestrian speeds for oblique pattern was calculated by assuming that those pedestrians will be travelling a distance negligibly larger than road width. This is because the oblique paths of most of the pedestrians were found to be acute. Descriptive statistics for pedestrian speeds are given in Table 3.17. Pedestrian walking speeds obtained from the field are used to compare with the speeds obtained from the simulation model.

Table 3.17 Descriptive Statistics for Pedestrian Speed

Pedestrian Type	Pedestrian Speed (m/s)				Sample size
	Mean	SD	Min.	Max.	
Aggregate	0.95	0.3	0.2	2.0	404
Median to Curb	0.94	0.3	0.2	2.0	296
Curb to Median	0.97	0.4	0.3	1.7	108

3.3.4.4 Pedestrian Waiting Time

Pedestrians, arriving at the curb or median for crossing the road, look for acceptable gaps between vehicles in the traffic stream. They either accept or reject such gaps. Rejection of prevailing gaps leads to longer waiting time at the curbside. Pedestrian waiting time is the amount of time pedestrians wait near the curb or median to cross the road safely. Waiting time of pedestrians is estimated by determining the difference in time taken by pedestrians to reach the curb or median to the time at which pedestrians start to cross the road (Table II.7). Descriptive statistics for pedestrian waiting time is given in Table 3.18. The mean waiting time of pedestrians at median is higher (7.3 s) as the pedestrians already travelled half way of the divided road and by waiting at the median, they try to find a larger gap between the approaching vehicles in the remaining half way of the road.

Table 3.18 Descriptive Statistics for Pedestrian Waiting Time

Pedestrian Type	Pedestrian Waiting Time (s)				Sample size
	Mean	SD	Min.	Max.	
Aggregate	6.3	8.7	0	30.8	404
Median to Curb	7.3	9.1	0	30.8	296
Curb to Median	3.6	6.7	0	26.0	108

3.3.4.5 Position of Pedestrians

Position of a pedestrian is defined as the closest lateral position of the pedestrian from the entry of the selected road section. Pedestrian positions are extracted when the foot of the pedestrian touches the entry line of undesignated pedestrian crossing (Table II.7). Entry line of undesignated pedestrian crossing can be anywhere either at the curb or at the median based on the direction pedestrian movement. Figure 3.13 represents the pedestrian position. Descriptive statistics for pedestrian position are given in Table 3.19.

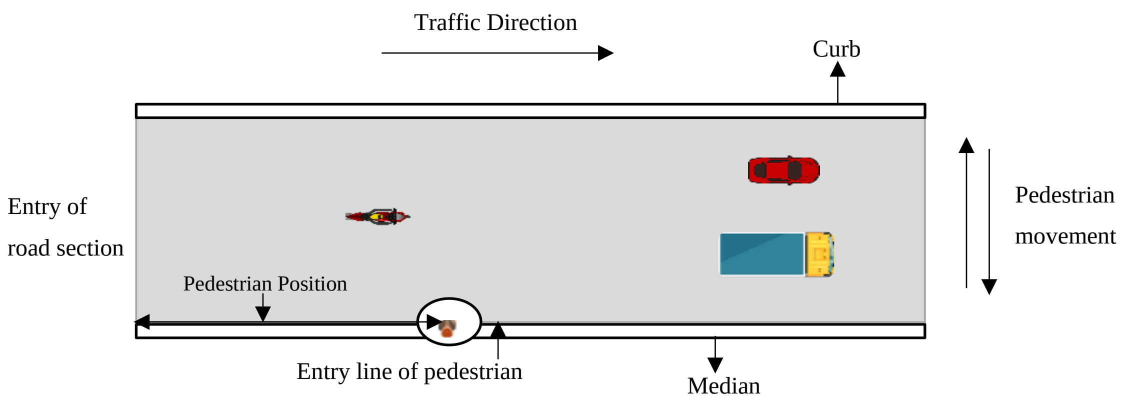

Figure 3.13 Position of Pedestrian

Table 3.19 Descriptive Statistics for Pedestrian Position

Pedestrian Type	Pedestrian Position (m)				Sample size
	Mean	SD	Min.	Max.	
Aggregate	41.7	20.7	4.3	69.3	404
Median to Curb	40.1	20.5	4.3	64.2	296
Curb to Median	45.8	20.8	5.8	69.3	108

Different probability distribution functions are fitted to aggregate data of pedestrian position and goodness-of-fit test for each probability density function is conducted by K-S test at 5% significance level. Table 3.20 shows the best fit distribution for pedestrian positions. It is observed that data follow uniform distribution for a level of significance of 0.05. The positions of pedestrians are incorporated in the logic of pedestrian placement in the vehicle-pedestrian simulation model based on the obtained distribution.

Table 3.20 Best Fit Distribution and Parameters for Pedestrian Position

Vehicle Type	Best Fit Distribution	Parameters	K-S value
Median to Curb	Uniform	σ=20.5, μ=40.1	0.04
Curb to Median	Uniform	σ=20.8, μ=45.8	0.05

3.3.4.6 Vehicular Speed in the Presence of Undesignated Pedestrian Crossings

Other than pedestrian data, aggregate and class-wise data of speeds of vehicles are also extracted to understand the variations in vehicular speeds due to the presence of pedestrians. Vehicular speed is calculated for each of the vehicle type considering the time taken to travel the selected trap length (70 m) with pedestrian crossings. As a vehicle travelling through the 70 m section will have contact with many crossing pedestrians on the stretch, the change in speed when it approaches each pedestrian will be reflected in the overall speed extracted considering the 70 m length. Descriptive statistics for vehicular speeds due to the impact of undesignated pedestrian crossings are given in Table 3.21. The mean speed of TW is higher (9.2 m/s) whereas HV travel with a minimum mean speed of 8.0 m/s.

Table 3.21 Descriptive Statistics for Speeds of Different Types of Vehicles

Vehicle Type	Vehicular Speed (m/s)				Sample size
	Mean	SD	Min.	Max.	
Aggregate	8.9	2.2	3.2	16.4	3276
Two-wheelers	9.2	2.0	3.8	16.4	1671
Three-wheelers	8.1	1.8	3.3	12.2	294
Cars	9.0	2.0	3.4	16.0	984
Buses	8.1	1.3	3.2	11.7	262
Heavy vehicles	8.0	1.9	3.5	11.3	65

3.4 DEVELOPMENT OF A MICROSCOPIC TRAFFIC SIMULATION MODEL (BASE MODEL)

A traffic simulation model specifically for an ideal mid-block section of urban divided road (base model) is developed based on microscopic approach and the logics involved are implemented in MATLAB programming language using object-oriented programming concepts. The framework of the model consists of mainly three processes: vehicle generation, vehicle placement and vehicle movement. Vehicle generation is the primary step involved in traffic simulation where vehicles are generated randomly. Any generated vehicle is placed at the beginning of the simulation stretch considering the safe longitudinal gap, width of the vehicle and available lateral gap. The positions and speeds of all vehicles placed are updated sequentially from the exit to the entry of the simulation stretch at each time step using the logics of vehicle movement. After the development of base model, the model is revised by making modifications to the inbuilt parameters, until the model accurately represents the real traffic system. The model results are then compared with the corresponding field observed values to perform model validation. Validation of the model is performed using internal and external data sets.

3.5 ESTIMATION OF PASSENGER CAR UNIT (PCU) VALUES FROM THE BASE MODEL

In order to obtain PCU values for different vehicle types as output from the validated base model, the logics involved in estimation of PCU values using a new methodology proposed considering the influence of surrounding vehicles (effective area approach) are incorporated in the simulation model.

3.6 MODIFICATION OF DEVELOPED BASE MODEL TO INCORPORATE BUS STOP AND UNDESIGNATED PEDESTRIAN CROSSINGS

The validated base model is then modified to simulate the traffic manoeuvers in the section with a curbside bus stop and the section with undesignated pedestrian crossings to study their impact on PCU values and capacity of urban mid-block sections.

3.7 ESTIMATION OF CHANGE IN PCU AND CAPACITY REDUCTION DUE TO SIDE FRICTIONS

The developed and modified simulation models are then applied to assess the influence of curbside bus stop and crossing pedestrians on PCU values as well as capacity by performing sensitivity analysis. The relative influences of various parameters such as traffic volume, vehicular composition, bus proportion (applicable only for bus stop section), proportion of stopping buses (applicable only for bus stop section), and pedestrian volume (applicable only for pedestrian section) in the presence of side frictions are investigated by carrying out sensitivity analysis.

3.8 MODELS FOR PREDICTING PCU AND CAPACITY IN THE PRESENCE OF SIDE FRICTIONS

With simulated results of PCU and capacity values from sensitivity analysis, regression models are developed to predict PCU values (for different types of vehicles) and capacity of sections, with and without curbside bus stop, and with and without undesignated pedestrian crossings. These models can be applied in updating standards for PCU and capacity estimation in the presence of side frictions in disordered traffic conditions. Using the regression models, traffic engineers and planners can predict realistic PCU and capacity values during planning and designing of new facilities with side frictions instead of directly adopting the values available in the existing manuals.

3.9 SUMMARY

The detailed explanation of each step in the overall methodology of the research work is provided in this chapter. Video-graphic traffic data are collected on mid-block sections without and with side frictions located on urban divided roads in Bangalore city, India. The parameters required for this study are extracted from the collected video data using image processing software. The details of data collected from the sections with side frictions such as curbside bus stop and undesignated pedestrian crossings, and ideal sections near them. Detailed methodology for extraction of the required traffic data from the collected videos has been discussed and presented. The extracted data from all the sections are then analysed before providing those parameters as input to the simulation model. Descriptive statistics of each parameter are obtained and presented in tables. In order to develop a microscopic traffic simulation model for an ideal section (base model), the logics involved are formulated and implemented in MATLAB programming language using object-oriented programming concepts. The developed base model is calibrated and validated with the field data collected from urban roads in Bangalore city. To estimate the PCU values for different vehicles, the effective area approach is incorporated in the model. The base model is then modified to simulate the traffic manoeuvers in the section with a curbside bus stop and the section with undesignated pedestrian crossings, and the corresponding PCU and capacity values are obtained. Sensitivity analysis is carried out using the developed and modified models to investigate the influence of curbside bus stop and undesignated pedestrian crossings on PCU and capacity values. With the simulated results of PCU and capacity values for varying influencing factors, regression models are developed to predict PCU values for different vehicle types, and capacity of roads with and without side frictions.

CHAPTER 4

DEVELOPMENT OF MICROSCOPIC TRAFFIC SIMULATION MODEL

4.1 GENERAL

A traffic simulation model specifically for an ideal mid-block section (ideal_bus) of urban divided road (base model) is developed based on microscopic approach and implemented in MATLAB using object-oriented programming concepts. The simulation model developed for ideal section is similar to those models developed for midblock sections under disordered traffic conditions in past studies (Arasan and Vedagiri, 2010; Arasan and Arkatkar, 2010; Metkari *et al.,* 2013; Asaithambi *et al.,* 2018; Kotagi *et al.,* 2018). However, these simulation tools are not open access tools. In the study, the model is developed in such a way that it can be used to estimate PCU values for different vehicle types using the proposed methodology and also, to study the effect of side frictions on PCU and capacity values. The concepts of object-oriented programming and logics involved in developing simulation model is different for different facility types. This chapter discusses about the object-oriented programming concepts, logics and supporting algorithms used in the development of a simulation model for an urban divided mid-block section which is free from the effect of bus stops, pedestrians, parked vehicles, intersections and other interferences, referred as base model in the thesis. To make simulation models look real, model calibration and validation are necessary. Validation of the model includes internal and external validation. This chapter also describes the process of calibration and validation of the developed simulation model.

4.2 FRAMEWORK AND LOGICS OF SIMULATION MODEL

The framework of a model simulated for a mid-block section consists of mainly three major logics: vehicle generation, vehicle placement and vehicle movement. Each of these major logics have sub-modules, where vehicle generation includes 1) generation of vehicular time gap, 2) identifying the vehicle type, 3) assignment of free-flow speed to the generated vehicles; vehicle placement includes 1) placement of the vehicles at the entry; vehicle movement includes 1) updation of positions and speeds of the vehicles at each time step. The flow diagram illustrating the general structure of a mid-block simulation model is shown in Figure 4.1.

The algorithm used for model development consists of major steps involved in generating, placing and moving vehicles (Table 4.1). The first step is to initialize the simulation after providing the necessary inputs. The parameters extracted from ideal section are given as inputs to the model. After the initialization, the main simulation loop is activated. The first step in the main loop is to compute the vehicle time gap using time gap distribution. Based on the time gap distribution, each vehicle is generated. When a vehicle is generated, its vehicle type is identified and free-flow speed is assigned. The generated vehicle is placed along the road width based on the available lateral and longitudinal gaps, when the simulation clock time becomes equal to its cumulative time gap. A time scan procedure is adopted for the simulation so that all aspects related to individual vehicles in the study traffic stream will be scanned and recorded according to the simulation framework at chosen intervals of time (Arasan and Kashani, 2003). The interval scanning technique with fixed increment of time (scan interval as 1 s) is used to update the position and speed of the vehicle placed sequentially from exit to entry of the road stretch (Arasan and Koshy 2005; Arasan and Vedagiri, 2010; Kanagaraj *et al.*, 2008; Arasan and Arkatkar, 2010; Metkari *et al.*, 2013; Asaithambi *et al.*, 2018; Kotagi *et al.*, 2018). When each vehicle is moved, the outputs such as their number ids, their time gaps, their types, their updated speeds and updated positions at each time step are saved. The last step in the main loop is updating the current time step to the next time step. The entire process of simulation is continued until the total simulation run time is over. Warm-up time and warm-up zones are included to eliminate the transient state of the system.

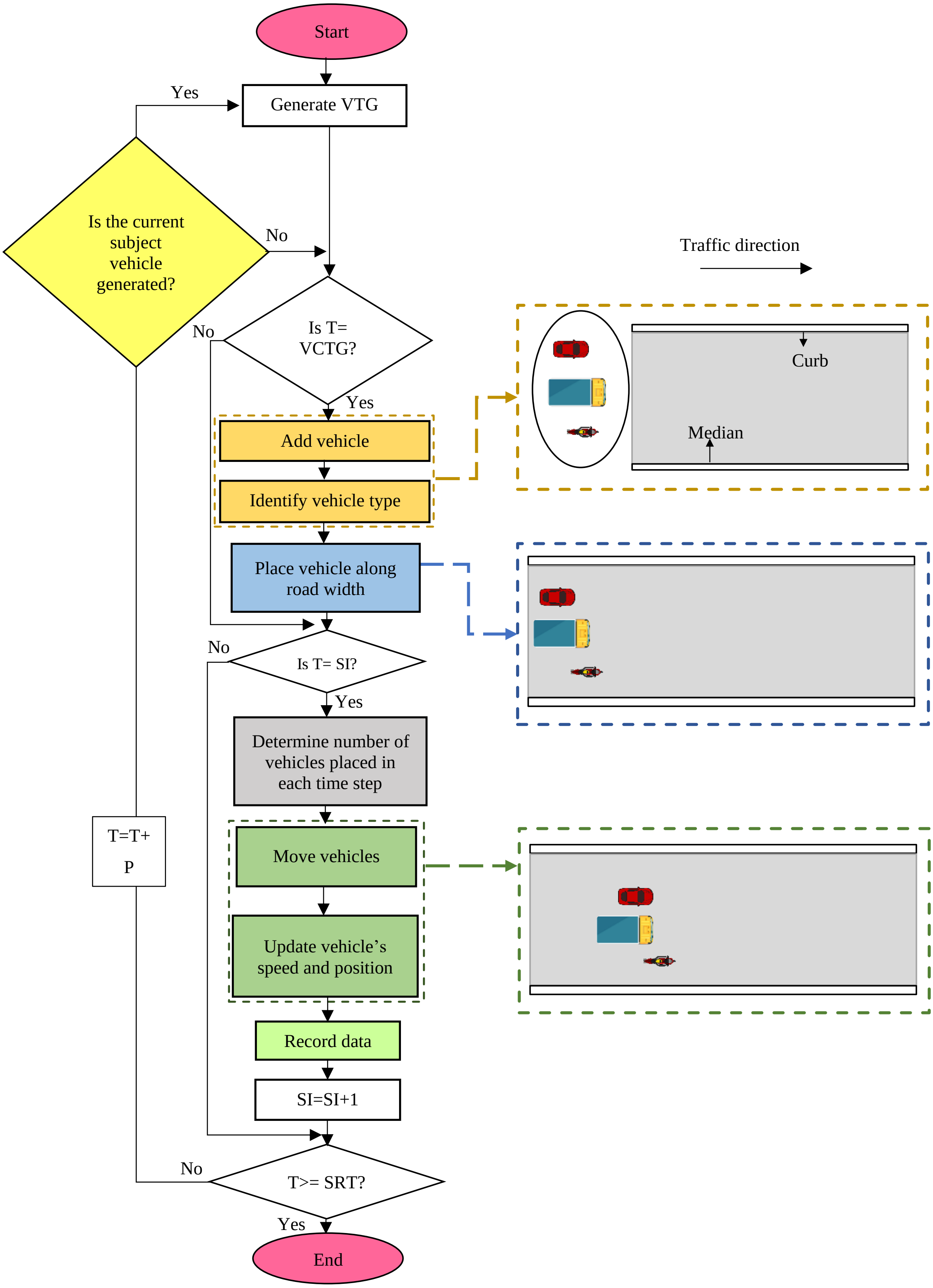

Note: T= Simulation Clock Time; P = Precision Time; SI = Scan Interval; SRT =Simulation Run time; VTG = Vehicular Time Gap; VCTG = Vehicle's Cumulative Time Gap.

Figure 4.1 Framework for Mid-block Simulation Model

Table 4.1. **Algorithm for Development of Simulation Model**

(1) Initialize the simulation based on the given inputs
(2) Compute vehicular time gap (VTG) using time gap distribution and generate a new vehicle
(3) Identify the vehicle type based on vehicular composition
(4) Assign desired speed to the vehicle along with its static and dynamic characteristics
(5) When simulation clock time (T) becomes equal to vehicle's cumulative time gap (VCTG), place the vehicle based on available lateral and longitudinal gaps
(6) Update speed and position of the vehicle (move the vehicle)
(7) Save the results/output
(8) Increment to the next time step
(9) Repeat steps 2-8 until the simulation run time (3600 s) is over

4.2.1 Vehicle Generation

Vehicle generation is the primary step involved in model development. Traffic variables are stochastic in nature as the vehicles arrive randomly and hence, simulation models require randomness to be incorporated to take care of stochasticity. This is easily done by generating a sequence of random numbers. Random numbers are used for generation of vehicle arrivals, identifying the vehicle type and assignment of free speed of vehicles in the model.

4.2.1.1 Generation of Vehicular Time Gap

The traffic data on time gaps of vehicles collected from the selected section are examined and the results showed that the vehicles arrive randomly. Time gaps are observed from entire road width in disordered traffic due to non-lane discipline. The logic for generation of vehicles is shown in Figure 4.2. For generation of vehicles, the model uses random number streams, which are generated by specifying seed values. Vehicle generation process is performed based on time gap distribution. Based on the field data on time gaps, the best fit distribution obtained is negative exponential distribution. The vehicular time gap is obtained using equation (4.1).

$$VTG = -\left(\frac{1}{\lambda}\right) \ln r_1 \tag{4.1}$$

where, VTG = Vehicular time gap (s), λ = mean arrival rate of vehicles (veh/s), and r_1 = random number (0 to 1). The range of time gap observed in the field is from 0 to 7 s.

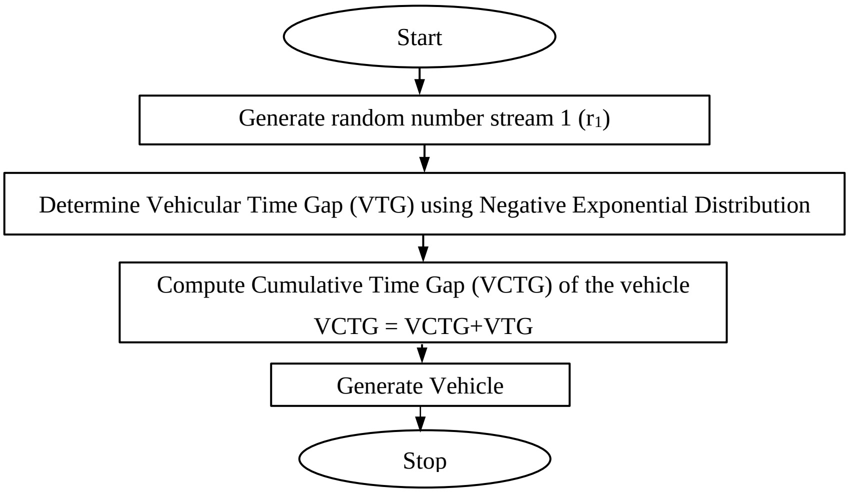

Figure 4.2 Logic for Generation of Vehicles

4.2.1.2 Identifying Vehicle Type

Once a vehicle is generated, the vehicle type is identified based on the percentage composition of traffic. For this purpose, a set of random number is generated and those random numbers are compared with the cumulative composition of each type of vehicle obtained from the field. Accordingly, the vehicle type is decided. Figure 4.3 illustrates the logic for vehicle type identification considering the cumulative composition of ideal_bus section.

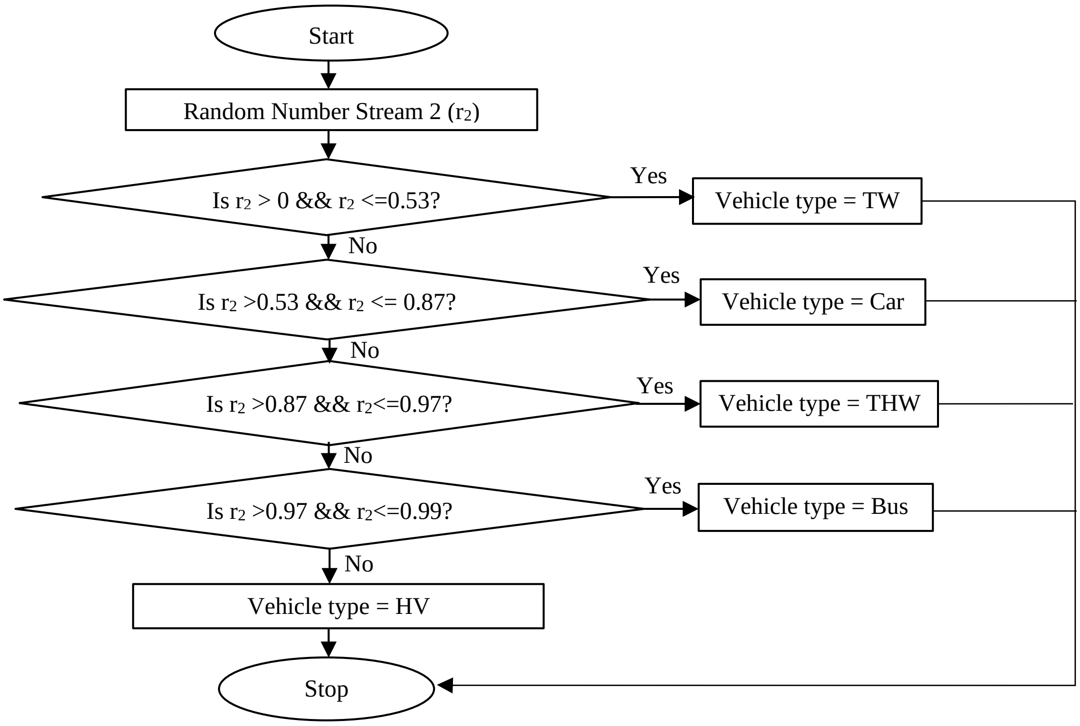

Figure 4.3 Logic for Identification of Vehicle Type in Ideal_bus Section

4.2.1.3 Assignment of Free-flow Speed

Whenever a vehicle is generated, it is assigned with a free-flow speed along with its static (length and width) and dynamic (acceleration, deceleration, etc.) characteristics. It is assumed that all vehicles enter the simulation road stretch with their free-flow speed, and during the simulation process the vehicles are not allowed to exceed their assigned free-flow speeds. Figure 4.4 illustrates the logic for assignment of free-flow speeds to the vehicles. The free-flow speeds of vehicles follow normal distribution based on the field data. Hence, Box-Muller transformation method is used to generate the standard normal deviate used for estimating the free-flow speed by using the following equation.

$$Z = (-2\ln r_3)^{1/2} \text{ x } \cos(2\Pi r_4) \tag{4.2}$$

where, Z = standard normal deviate; r_3, r_4 = random numbers from random number streams 3 and 4. Random number streams vary depending upon the vehicle type.

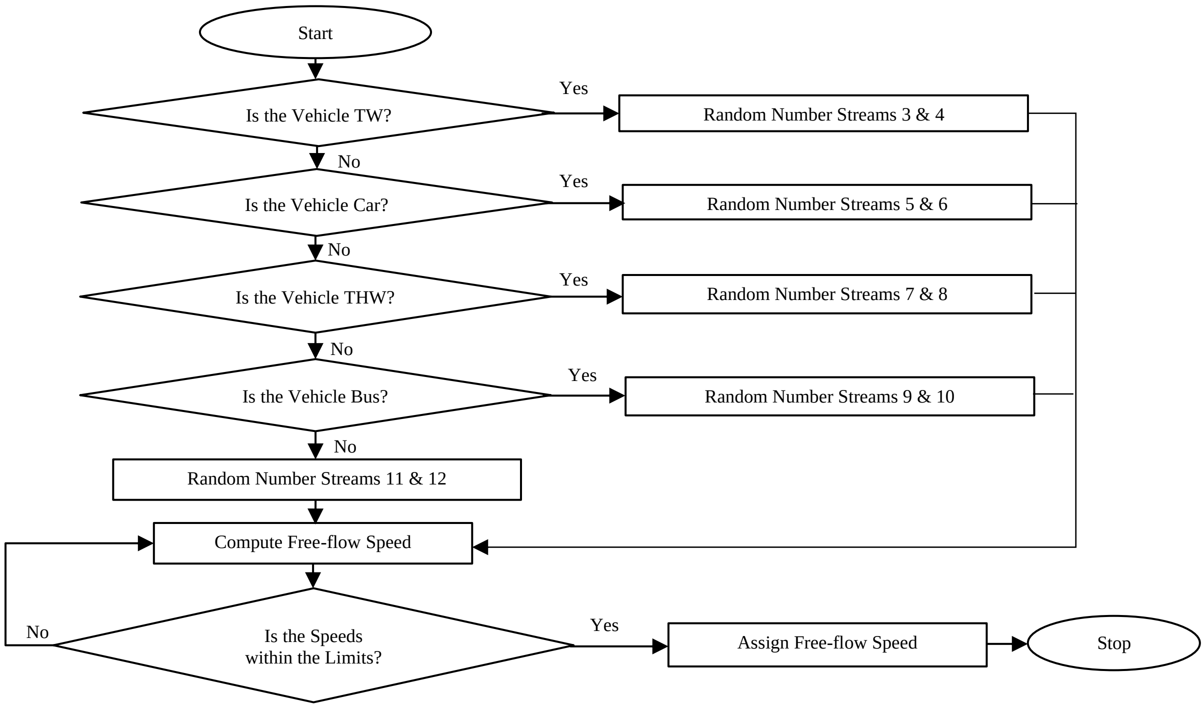

Figure 4.4 Logic for Assignment of Free-flow Speed

The free-flow speed of each vehicle type is obtained using the following equation.

$$V_k = \mu_k + \sigma_k Z \tag{4.3}$$

where,

V_k = free-flow speed of subject vehicle type '*k'*; μ_k = mean speed of vehicle type '*k'*; σ_k = standard deviation of speed of vehicle type '*k'*; *Z* = standard normal deviate. A check is also made to find out whether the computed free-flow speeds are within the minimum and maximum limits of free-flow speeds obtained from the field.

4.2.1.4 Algorithm for Vehicle Generation

The algorithm used for vehicle generation consists of steps involved in generating vehicular time gaps, identifying the vehicle type and assignment of free-flow speed to the generated vehicles (Table 4.2). In vehicle generation process, different random number streams with different seed values are generated. As can be seen in the table, the first step is to initialize the simulation after providing the inputs followed by generation of random number streams. The information regarding all aspects of simulation like road width and length, simulation run time, precision time, scan interval, the initial values for time gap, cumulative time gap, etc. are defined in the input file which is loaded during the initialization step.

Table 4.2 Vehicle Generation Algorithm

1) Initialize the simulation based on the given inputs
2) Generate random number streams
3) Compute time gap using time gap distribution
4) Add a new vehicle
5) Identify vehicle type based on vehicular composition
6) Define static and dynamic characteristics
7) Calculate free-flow speed
8) Check if the free-flow speed obtained is within the minimum and maximum limits
9) If free-flow speed is within limits, assign the free-flow speed to the vehicle generated
10) Otherwise, use the next random number generated and compute free-flow speed
11) Repeat steps 8-10 until the free-flow speed comes within the limits
12) Save the results
13) Increment to next time step
14) Determine the number of vehicles generated in each time step
15) Repeat the entire process until the end of simulation run time

After the initialization, the main simulation loop is activated, which runs till it reaches the end of the simulation run time. The first step in the main loop is to compute time gaps and add new vehicles to the simulated area. After the addition of new vehicles, the vehicle type is identified based on the vehicular composition. In the next step, its static and dynamic properties are assigned, and then the free-flow speed is computed and assigned. The vehicle id, time gap, vehicle type, vehicle length and width, and free-flow speed of each newly added vehicle are saved. The last step in the main loop is updating the time step to the next time step/ scan interval. The number of vehicles generated in each time step are determined.

4.2.2 Vehicle Placement

Vehicle placement implies positioning of vehicles at the start of simulation stretch in a suitable location across the road width based on the longitudinal and lateral gaps. In India, vehicles occupy the entire road space without any confinements for manoeuvring due to the absence of lane discipline. Hence, vehicles are placed in a suitable position across the width of the road based on available longitudinal and lateral gaps. When the clock time (T) becomes equal to cumulative time gap of the vehicle (VCTG) generated, vehicle placement logic is invoked. Any vehicle generated is placed at the beginning of the simulation road stretch considering the safe longitudinal gap, width of the vehicle and available lateral gap. Figure 4.5 shows the logics for placement of vehicles. The lateral and longitudinal gaps available for each type of vehicle are determined based on their speeds. For this purpose, a second-degree polynomial relationship between gaps and speeds of vehicles are obtained from field data to calculate the lateral and longitudinal gaps of each vehicle corresponding to their speeds.

From the field data, it is noticed that mostly vehicles travel near the median of the road as they can maintain higher speeds. Hence, lateral and longitudinal gaps available for vehicle placement are checked consecutively starting from median to the curb (right to left edge). Here, the first vehicle in the list is placed directly leaving a specified lateral gap from the right edge (lateral gap from median) without checking for gaps as it is not influenced by any adjacent and leader vehicles. Moreover, all the vehicles in the first scan interval or time step are not influenced by leader vehicles and thus, these vehicles check only for the available lateral gaps. From the next scan interval onwards, vehicles start checking for longitudinal gaps along with lateral gaps as the vehicles placed start moving. For this purpose, the closest vehicle in front overlapping with the width of subject vehicle within the look ahead distance of 30 m (PTV VISSIM; Asaithambi and Joseph 2018; Anand *et al.,* 2019) is identified as leader and the longitudinal gap between these vehicles is determined. If there are more than one vehicle in front of the SV with the same longitudinal distance, then the vehicle in front with maximum width overlapped with the subject vehicle is considered as leader. So, if the available longitudinal (L) and lateral (D) gaps are adequate for the vehicle to get placed (Figure 4.6), it is placed leaving a lateral gap from median. If the gaps are deficient, vehicle tries to shift laterally according to its alignment and then gaps are checked for placement in the next position. Still if the gaps are inadequate, that particular vehicle is kept in queue and it is checked for placement in next scan interval. During each scan interval, vehicles in queue are given preference over a newly generated vehicle for placement.

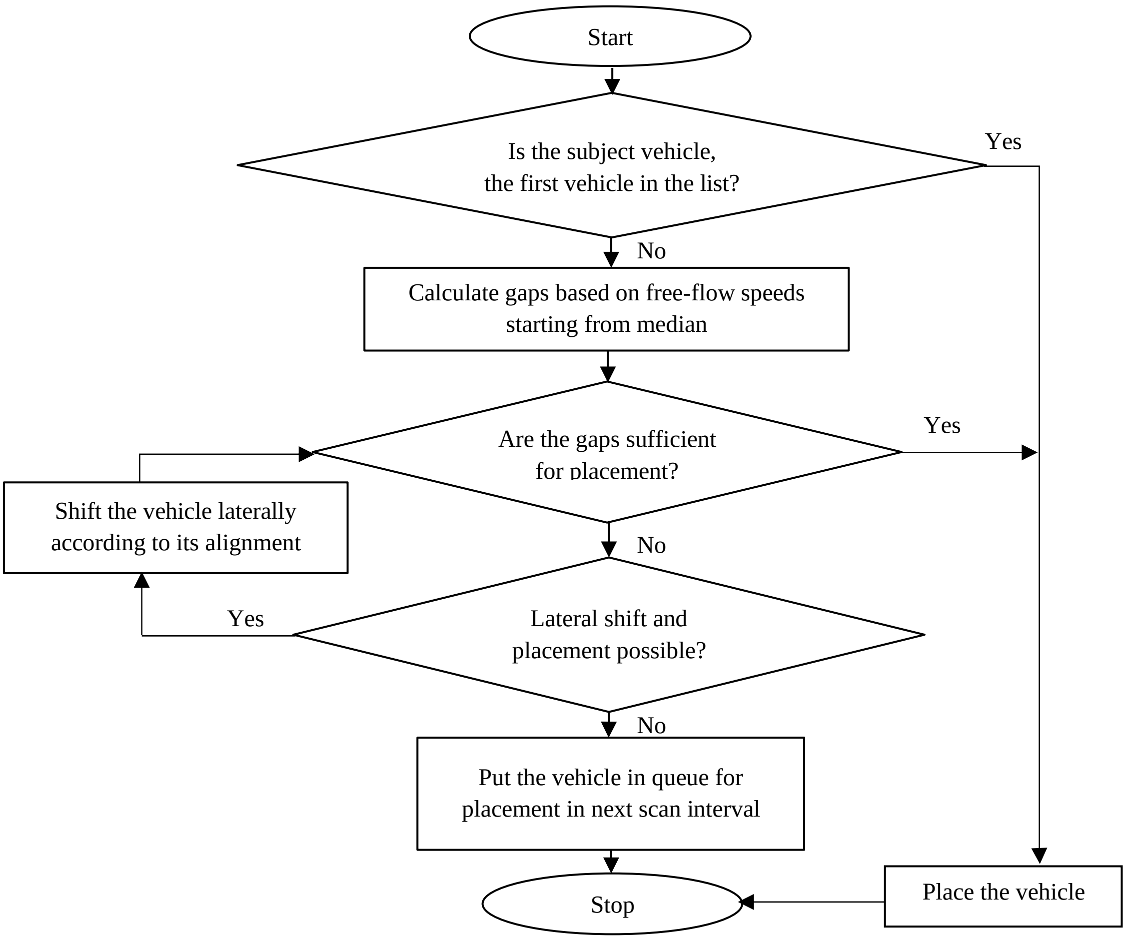

Figure 4.5 Logic for Placement of Vehicles

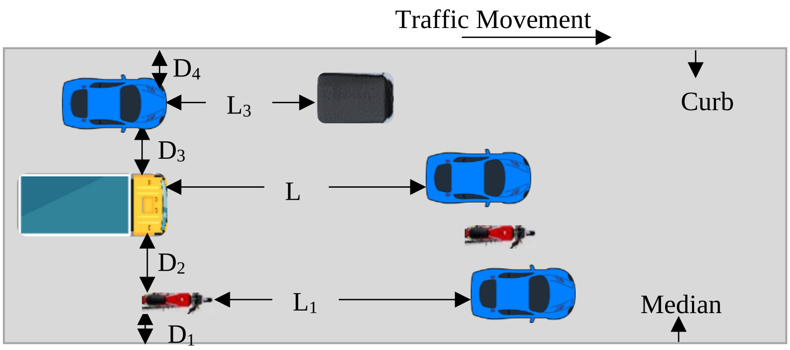

Figure 4.6. Longitudinal and Lateral Gaps for Vehicle Placement

4.2.2.1 Algorithm for Vehicle Placement

The algorithm used for vehicle placement consists of steps involved in placing the vehicle after identifying the vehicle type and assigning the free-flow speed (Table 4.3).

Table 4.3. Vehicle Placement Algorithm

1) Initialize the simulation based on the given inputs
2) Check if the subject vehicle is the first generated vehicle
3) If yes, place the vehicle near median leaving a lateral gap from median
4) If no, check if the simulation clock time is less than or equal to 1 s and check if there are any more vehicles to be placed within 1 s
5) If yes, place the next vehicle leaving a lateral gap from the first vehicle
6) If no, check if there is a vehicle in front (leader) overlapping with the subject vehicle
7) If there is no leader, check if the lateral gap is sufficient (in each time step, check for available lateral gap is done from right edge to left edge.)
8) If lateral gap is sufficient, place the vehicle
9) Else shift the vehicle to next position laterally
10) If there is a leader, check if longitudinal and lateral gaps are sufficient to place the subject vehicle
11) If gaps are sufficient, place the vehicle
12) Else shift the vehicle to next position laterally
13) In steps 8, 9, 11 and 12, when the vehicle tries to shift laterally check if the gaps are sufficient in its new position
14) If yes, place the vehicle
15) If no, put the vehicle in queue
16) Save the results
17) Set the time index to the next time step
18) In next time step (t = t+1), give preference to the vehicles in queue
19) Continue the entire process until the end of simulation run time

The first step is to initialize the simulation after providing the inputs. After the initialization, the main simulation loop is activated, which runs till the end of the simulation run time. The first step in the main loop is to check whether the vehicle to be placed is the first vehicle generated and if yes, the vehicle is placed near the median. After the placement of first vehicle, the lateral and longitudinal gaps available for the next vehicles to get placed is checked. If gaps are available, the vehicle is placed laterally otherwise vehicle is moved to the queue. When each vehicle is placed, the outputs such as its lateral and longitudinal positions, and its leader are saved. The last step in the main loop is updating the time step to the next time step. In each scan interval, check is done to find whether there is any vehicle in queue, if yes, then that vehicle in queue is given preference over the regular vehicle to be placed.

4.2.3 Vehicle Movement

Vehicle movement logic involves updating vehicular positions and speeds at every scan interval (1 s). The positions and speeds of the vehicles placed are updated sequentially from the exit to entry end of the simulation stretch at each scan interval using the logics of vehicle movement. Each vehicle performs their longitudinal and lateral movements according to vehicle following and lane changing logics. Vehicle following models better describe longitudinal behaviour of the vehicle. In disordered traffic, roads in urban areas remain congested and hence, subject vehicle (SV) follows its leader closely and choose its speed and safe longitudinal gap so as to avoid rear-end collision (Kanagaraj *et al.* 2013). Thus, Gipps model (Gipps 1981), which is a safety distance car following model, is considered reasonable and ideal for this study. The model is derived based on assumptions such as keeping safe distance from the leading vehicle, driving at a desired speed and producing accelerations within a comfortable range. The movable distance of each subject vehicle in each scan interval is calculated and the possibility of free movement is checked. If free movement is not possible, then the subject vehicle will either change its lateral position (lateral shift) or decelerate and follow the leader vehicle based on the available gaps. Rule-based lateral movement model along with longitudinal model is used to describe the lateral shifts carried out by the vehicle.

Gipps car-following model with vehicle dependent parameters is formulated on the basis of different conditions (Ravishankar and Mathew 2011). Figure 4.7 shows the vehicle movement logic using Gipps car following model. In Gipps car-following model, the formula for calculating speed of the vehicle comprises of two phases: accelerating and decelerating phases. The first phase ensures that the vehicle does not exceed its free-flow speed and the vehicle accelerates to its desired speed with an acceleration rate that initially increases with speed and then decreases to zero as the vehicle approaches its free-flow speed. Each vehicle is assumed to accelerate to its free-flow speed or to the maximum peak hour speed, whichever is minimum. Thus, when the subject vehicle (SV) is not influenced by any other surrounding vehicles, the vehicle is free to move at its free-flow speed. If the movement of the subject vehicle is not impeded by preceding vehicle, the updated speed of SV '*k*' at time $(t+\tau)$ is given as:

$$v_k^a\,(t+\tau) = v_k\,(t) + 2.5a_k\,\tau\,(1-\frac{v_k(t)}{V_k})\,(0.025\,\frac{v_k\,(t)}{V_k})^{½} \tag{4.4}$$

where, $v_k(t)$ = SV speed at time t (m/s), a_k = acceleration rate of SV (m/s^2), τ = reaction time (s), V_k = desired speed/free-flow speed of SV (m/s). If the movement of the subject vehicle is impeded by that of the preceding vehicle i.e., if width of SV overlaps with that of a leader vehicle (LV), then its speed depends on the properties of the leader vehicle. When the SV speed is greater than LV speed, SV tries to initiate lateral shift by checking the gaps on both sides and ensures that the SV is able to accelerate in its new position. If it is possible, then SV tries to shift either to its right or left side and then accelerates, otherwise the SV remains in its present position, decelerates and follows its LV. When the SV decelerates, the updated speed of SV type '*k*' at time $(t + \tau)$ is given as:

$$v_k^b(t + \tau) = b_{ik}\,\tau+(b_{ik}^2\,\tau^2-b_{ik}\,(2\,(X_i\,(t)-\,\alpha_{ik}\,s_i - X_k(t))-v_k(t)\tau-(\frac{v_i\,(t)^2}{b_{ik}^{\wedge}})))^{1/2} \tag{4.5}$$

where, b_{ik} = deceleration rate of SV '*k*' with respect to LV '*i*' (m/s^2), $X_i(t)$ = position of LV '*i*' at time t (m), $X_k\,(t)$ = position of SV '*k*' at time t (m), τ = SV's reaction time (s), s_i = effective size of LV '*i*' (m), i.e., length of LV plus a safe gap into which SV is not willing to encroach, α_{ik} = sensitivity factor, $v_k(t)$ = speed of SV '*k*' at time t (m/s), $v_i(t)$ = speed of LV '*i*' at time t (m/s) and $b_{ik}^{\wedge}$ = deceleration of LV '*i*' as judged by SV '*k*' (m/s^2). When the SV speed is less than LV speed, SV accelerates or decelerates depending upon the safe longitudinal gap between SV and its LV. Hence, the updated speed is the minimum of speeds obtained from acceleration (v_k^a) and deceleration phases (v_k^b). Position of SV 'k' at time ($t + \tau$) is updated using the following equation.

$$X_k(t + \tau) = X_k\ (t) + 0.5(v_k\ (t) + v_k\ (t + \tau))\ \tau \qquad (4.6)$$

where, $X_k\ (t)$ = position of SV 'k' at time t (m), $v_k(t)$ = speed of SV 'k' at time t (m/s), $v_k\ (t+\tau)$ = speed of SV 'k' at time $(t+\tau)$ (m/s), and τ = reaction time (s).

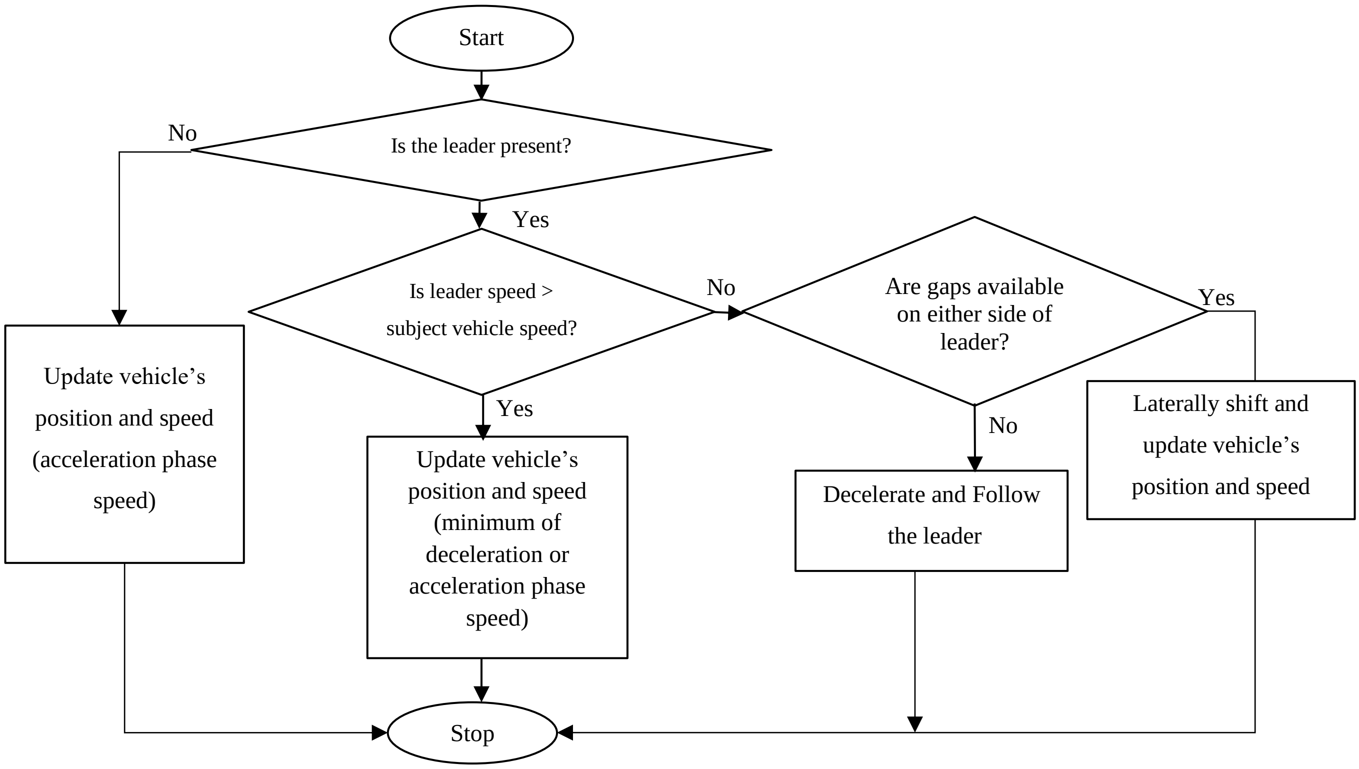

Figure 4.7 Logic for Vehicle Movement using Gipps model

4.2.3.1 Algorithm for Vehicle Movement

The algorithm used for vehicle movement consists of steps involved in making decisions by the vehicles to either accelerate or decelerate or shift laterally, and update the speeds and positions of the vehicles (Table 4.4). After providing inputs and initializing them, the first step in the main loop is to check whether the vehicle has a leader. If there is no leader, the vehicle accelerates and update its speed and position. If the subject vehicle is influenced by a leader, check is done to find out whether the speed of the subject vehicle is less than that of leader. If speed of subject vehicle is greater than its leader, vehicle checks for the gaps on its right and left side so that it can accelerate and move at higher speed. If gap is present on either of the sides and if the vehicle can accelerate its new position, vehicle laterally shifts otherwise vehicle remains in the same position and decelerates. If the speed of subject vehicle is less than its leader, vehicle accelerates or decelerates depending upon the safe longitudinal gap between SV and its LV. The speeds are updated by calculating the minimum of speeds obtained from acceleration and deceleration phases. When each vehicle is moved, the outputs such as its updated speed, updated position and updated leader at each time step are saved. The last step in the main loop is updating the time step to the next time step. The entire process is continued till simulation run time is over.

Table 4.4 Vehicle Movement Algorithm

1) Initialize the simulation based on the given inputs
2) Consider all vehicles placed in previous time step
3) Check if the subject vehicle has a leader
4) If no, compute speed based on acceleration phase and update its position
5) If yes, check if speed of the subject vehicle is less than its leader
6) If speed of SV is less than the that of leader, update vehicle's position and speed by calculating minimum of deceleration or acceleration phase speed based on safe longitudinal gap
7) If speed of SV is greater than speed of leader, check for gaps on right and left side of the vehicle
8) If gap is available, check whether the vehicle can accelerate in the new position
9) If yes, shift the vehicle laterally either to left or right side based on the available gap
10) Update position and speed of subject vehicle, and find the new leader for all the vehicles
11) If no gap is available and if the vehicle cannot accelerate in its new position, the vehicle decelerates and follow the previous leader
12) Update the position and speed of subject vehicles based on deceleration phase
13) Save the trajectory data and speeds of each vehicle
14) Increment to the next time step
15) Repeat the entire process until the end of simulation run time

4.3 COMPUTER PROGRAM FOR MID-BLOCK SIMULATION

The above-mentioned logics for developing a basic unidirectional traffic simulation model for urban divided mid-block sections are implemented in MATLAB programming language using object-oriented programming (OOP) concepts. The elements of object-oriented programming such as objects, classes, inheritance, encapsulation and polymorphism help the programmer to develop more intelligible, maintainable and expandable codes (Venkatesan *et al.* 2008; Gowri *et al*. 2009). In OOP, objects are the fundamental run-time components. A class is represented as a group of similar objects. Classes are user defined data types. In the class, properties and methods are defined. The methods consist of several virtual functions which perform the major tasks in the program. In this study, the program is divided into different virtual functions. The entire process remains to be object-oriented with three super-classes.

4.3.1 Class Relationships

A class diagram to explain the various classes and their relationship for developing the model using microscopic simulation is presented in Figure 4.8. "The symbols used for representing the object relationship follow the Unified Modelling Language (UML)" (Booch 1994; Bahrami 1999). In the developed model, objects such as *TW, Car, THW, Bus* and *HV* represent different vehicle types in this study. These objects *TW, Car, THW, Bus* and *HV* are the sub-classes derived from the superclass *Vehicle* class. Hence, their properties are inherited from the *Vehicle* class. Superclass *Vehicle* is associated with another superclass *Link*. Finally, the objects and virtual functions of class *Link*, where all the logics are performed are associated with *Main Simulator* class.

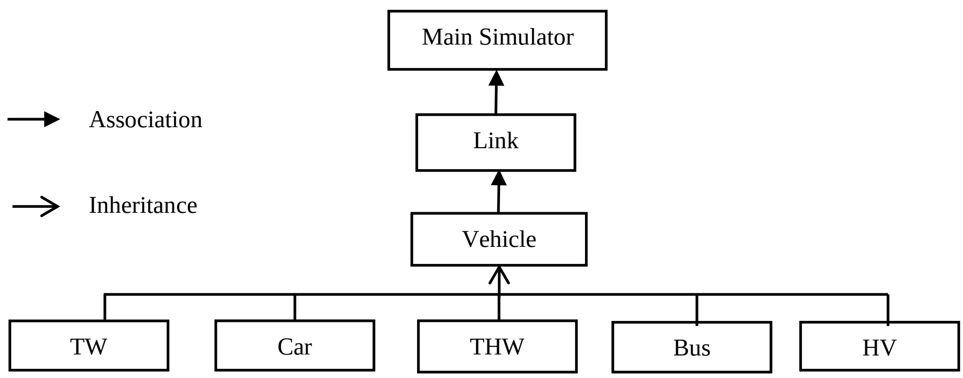

Figure 4.8 Class Diagram for Unidirectional Disordered Traffic Simulation

4.3.2 *Vehicle* Class

The superclass *Vehicle* encapsulates a vehicle's characteristics with already defined series of values for each type of vehicle. Subclasses like *TW, Car, THW, Bus and HV* are derived from superclass *Vehicle*. This class is characterized by various properties which build the vehicle structure. *Vehicle* class consists of vehicle properties such as vehicle type, vehicle length, vehicle width, acceleration, deceleration, desired speed, longitudinal gap, lateral gap, minimum and maximum speed, coordinates of subject vehicle at each time step, speed of each subject vehicle during the simulation run. Figure 4.9 shows the properties of *Vehicle* class.

```
classdef Vehicle
    % VEHICLE Summary of this class goes here
    % Detailed explanation goes here

    properties
          veht % vehicle type
          w % vehicle width
          l % vehicle length
          acc % acceleration
          dec % deceleration
          max_v % maximum speed
          V % desired speed
          min_v % minimum speed
          longgap % longitudinal gap
          latgap % lateral gap
          x   % x coordinate
          y   % y coordinate
          v   % vehicle speed
    end
```

Figure 4.9 Properties of *Vehicle* Class

4.3.3 *Link* Class

The *Link* class encapsulates the performance of traffic flow. The major task of *Link* class is to implement the logics of the model, i.e., vehicle generation, vehicle placement and vehicle movement. The vehicular manoeuvers such as longitudinal and lateral movement are composed in this class. This class also updates the position and speed of vehicles at every time step. The *Link* class comprises of several virtual functions such as *VehGeneration (), Placeveh (), UpdateVeh ()*. These functions execute the required operations such as generation, placement, and updation of speeds and positions of vehicles, and simulate the vehicular flow. The required input to simulate traffic flow includes various parameters such as length and width of the road, scan interval, total simulation run time, simulation clock time, precision time, reaction time of drivers and traffic flow. The class *Link ()* takes care of the initialization process based on these user inputs. The various user-defined properties in this class are shown in Figure 4.10.

```
classdef Link
    % LINK Summary of this class goes here
    % Detailed explanation goes here

    properties
          rw = 7; % road width
          rl = 1000; % road length
          simtime = 3600; % simulation run time
          precision = 0.01; % precision time
          SI = 1; % scan interval
          flow; % traffic flow
          RT = 1; % reaction time
          T; % simulation clock time
          tn; % number of vehicles generated in each time step
    end
```

Figure 4.10. Properties of *Link* Class

4.3.4 *Main Simulator* Class

The *Main Simulator* class defines various attributes responsible for flow of various modules of simulation. The virtual function, *link* declared in the *Main Simulator* class process the attributes such as length and width of the simulation stretch, traffic flow, and simulation run time. Declaration of virtual function, *link* in *Main Simulator* class is given in figure 4.11. The main function is used to create objects of class *Link* and perform the functions in it. It initiates the simulation run and operates the different steps of the entire simulation process.

```
function link = Link (rl, rw, flow, simtime)
% Simulator class parameters
    If (nargin~=0)
          link.rw = rw; % road width
          link.rl = rl; % road length
          link.simtime = simtime; % simulation run time
          link.flow = flow; % traffic flow
    end
```

Figure 4.11. Declaration of Virtual Function, *link* in *Main Simulator* Class

4.4 INPUTS TO THE SIMULATION MODEL

The following are the variables observed from the field given as input to the simulation model.

- Length and width of the road used for simulation
- Total simulation time
- Precision time
- Scan interval
- Reaction time of drivers
- Type of distribution for time gaps of vehicles
- Vehicular composition (percentage of each type of vehicle)
- Free-flow speeds for each type of vehicle
- Dimensions of each type of vehicle
- Acceleration and deceleration rate for each type of vehicles

Table 4.5 gives the values used for the input variables in the simulation model. Depending upon the vehicular composition, vehicle types are identified. Five different types of vehicles such as two-wheelers (TW), three-wheelers (THW), cars, buses and heavy vehicles (HV) are considered in the study. Their dimensions considered in the study (Venkatesan *et al.* 2008) are presented in Table 4.6. The type of distribution for vehicular time gaps, free-flow speeds for each type of vehicle, acceleration rate and deceleration rate for each type of vehicle, lateral and longitudinal gaps based on speed of each vehicle type are given as input based on the field data. The tables presenting the descripting statistics of free-flow speeds, acceleration and deceleration rates for different vehicle types are given in Chapter 3.

Table 4.5 Values of Input Variables in the Simulation model

Input Variable	**Value**
Simulation length of the road	1000 m
Width of the road	7 m
Total simulation time	3600 s
Precision time	0.01 s
Scan interval	1 s
Reaction time of drivers	1 s

Table 4.6 Vehicle Categories and their Dimensions

Category	Average dimension		Projected rectangular area on ground (m^2)
	Length (m)	Width (m)	
Car	3.72	1.44	5.39
Bus	10.10	2.43	24.74
HV	7.50	2.35	17.62
Three-wheeler	3.20	1.40	4.48
Two-wheeler	1.87	0.64	1.20

4.5 OUTPUTS FROM THE MODEL

Numerical results and animation of traffic flow are the outputs of the simulation model. The following numerical results are obtained at the end of simulation run:

- Traffic flow
- Average traffic stream speed
- Average class-wise speeds
- Time gap of each vehicle
- Vehicular trajectories at each time step
- Road capacity
- Animated Output

The traffic flow obtained from the model for ideal_bus section is 3985 veh/h. The average stream speed obtained from the simulation model is 13.4 m/s. Speeds of TW, cars, THW, buses and HV are 14.3 m/s, 12.7 m/s, 11.8 m/s, 11.8 m/s and 11.2 m/s, respectively. The traffic flow, mean traffic stream speed and mean class-wise speeds obtained as outputs are used to validate the simulation model. Time gap of each vehicle obtained from the simulation model is shown in Table IV.1. The trajectory and speed values of vehicles obtained from the base simulation model at each step are presented in Table IV.2. The flow levels are incremented from lower to higher level in the simulation model until a maximum traffic flow is obtained. This maximum traffic flow obtained is considered as the capacity (veh/h). The obtained capacity value from the model is 4208 veh/h. The animation module of the simulation model displays the model's operational behaviour graphically during the simulation runs. It is a useful tool for validation of the model, and also, helpful in studying the changes in the behaviour of the system when various input parameters are changed. In animated output, to represent non-lane disciplined traffic, the entire road space is treated as a single component (rectangular in shape) instead of individual lanes. Vehicles moving on the road are depicted as rectangular blocks with appropriate dimensions (Venkatesan *et al.* 2008) and different colours based on vehicle types (Figure 4.12).

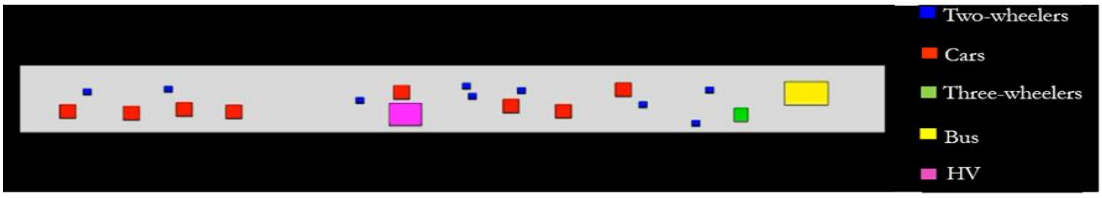

Figure 4.12. Snapshot of Animation of Simulated Disordered Traffic Flow in Ideal Section

4.6 MODEL CALIBRATION

Calibration of a model is an iterative process of comparing the model with a real system and revising the model by making modifications to the inbuilt parameters, if necessary, until the model accurately represents the real system. Trial-and-error process is adopted to estimate the model parameters, compare the model to actual traffic behaviour and calculate the error between results obtained from the model and field until the accuracy is judged to be acceptable. The general parameters such as reaction time (τ), sensitivity factor (α_{ik}), deceleration of leader vehicle as judged by subject vehicle ($b_{ik}^{\wedge}$) are used to calibrate the model. Along with the general parameters, a few vehicle-specific parameters are also calibrated. Table 4.7 shows calibrated parameters used in this study.

4.6.1 General Calibrated Parameters for the Model

4.6.1.1 Reaction Time (τ)

Reaction time (τ) is defined as the time taken by the subject vehicle to adjust its speed based on variations in the speed of the leader vehicle so as to avoid rear end collisions. Previous studies show that drivers require about 1.5-2.0 seconds under normal conditions and 0.7 to 1.5 seconds under congested conditions (Chakraborty *et al*. 2004; Dey *et al.* 2008; Treiber *et al.* 2010). In this study, a reaction time of 1 s is adopted so as to represent the response time of driver during congested conditions.

4.6.1.2 Sensitivity Factor (α_{ik})

Sensitivity factor (α_{ik}) represents the variability in the gaps maintained by different subject vehicle-leader vehicle type combinations because subject vehicle's longitudinal gap depends on the type of leader vehicle (Brackstone *et al.* 2009). The adopted value of sensitivity factor is 1.

4.6.1.3 Deceleration of Leader Vehicle as Judged by Subject Vehicle ($b_{ik}^{\wedge}$)

Deceleration of leader as judged by subject vehicle ($b_{ik}^{\wedge}$) is defined as deceleration rate of leader estimated by subject vehicle during car following mode. This value is adopted based on the results from the previous study carried out by Ravishankar and Mathew (2011). The value for expected deceleration rate adopted is -1.4 m/s^2.

4.6.2 Vehicle Specific Parameters

A few vehicle-specific parameters are also calibrated using the data collected from the ideal section (ideal_bus) at HAL road, Bangalore city. Acceleration rate (a_k) and deceleration rate (b_{ik}) are the parameters used, where acceleration (+ve) and deceleration (-ve) are the rate of change of speed of a vehicle, expressed in m/s^2.

Table 4.7 Calibrated Parameters used in the Model

Common Parameters	Reaction time, τ (s)		Sensitivity Factor, α_{ik}		Deceleration of LV as judged by SV, $b_{ik}^{\wedge}$(m/s^2)
	1		1		-1.4
Vehicle-Specific Parameters	**TW**	**Cars**	**THW**	**Buses**	**HV**
Acceleration rate (a_k) (m/s^2)	1.6	1.7	1.3	1.4	1.2
Deceleration rate (b_{ik}) (m/s^2)	-1.5	-1.6	-1.4	-1.4	-1.3

4.7 MODEL VALIDATION

Model validation is the process of comparing the model results with the corresponding field observed values to ensure that the simulated results represent the real-world system. It is performed by comparing the results of simulation model and field observed values. In this study, the developed model is validated using both internal and external data sets. Speed is the parameter considered as the measure of effectiveness for mid-block section of urban roads.

4.7.1 Internal Validation

The ideal section data (ideal_bus) collected from HAL road, Bangalore city which is used to develop and calibrate the model is used for internal validation. The comparison of observed and simulated mean speeds, and traffic volume of ideal_bus section for internal validation is shown in Table 4.8. It is found that mean absolute percentage error (MAPE) for mean stream and class-wise speeds, and traffic volume are lesser than 10% which is acceptable (Gowri and Sivanandan 2015). A paired t test is performed to check statistical validity of the simulated and observed mean speeds of vehicles and also, to compare the simulated and observed traffic volumes. The calculated value of t (t_0) for mean speeds is 1.18 against the critical value of 2.57 and it is found that the observed and simulated mean speeds agreed at 5% level of significance. The calculated value of t (t_0) for traffic volume 0.76 against the critical value of 2.57 and it is found that the observed and simulated traffic volume agreed at 5% level of significance.

Table 4.8 Comparison of Observed and Simulated Speeds and Volume

Vehicle Type	Mean Speed Values (m/s)		MAPE (%)	Traffic Volume (veh/h)		MAPE (%)
	Sim.	Obs.		Sim.	Obs.	
Traffic stream	13.4	12.7	5.4	3985	3970	0.38
TW	14.3	13.2	8.5	2112	2080	1.54
Cars	12.7	12.4	2.6	395	391	1.02
THW	11.8	11.6	1.7	1350	1359	0.66
Bus	11.8	11.5	2.5	88	97	9.27
HV	11.2	10.6	5.5	40	43	6.97

4.7.2 External Validation

The ideal section data (ideal_ped) collected from Hosur road, Bangalore city is used for external validation. The comparison of observed and simulated mean speeds, and traffic volume of ideal_ped section used for external validation is shown in Table 4.9. It is found that the mean absolute percentage error (MAPE) for each vehicle type for mean stream and class-wise speeds, and traffic volume are lesser than 10% which gives satisfactory results. A paired t test is performed to check statistical validity of the simulated and observed mean speeds of vehicles and also, to compare the simulated and observed traffic volumes. The calculated value of t (t_0) for mean speeds is 0.57

against the critical value of 2.57 and it is found that the observed and simulated mean speeds agreed at 5% level of significance. The calculated value of t (t_0) for traffic volume -2.23 against the critical value of 2.57 and it is found that the observed and simulated traffic volume agreed at 5% level of significance.

Table 4.9 Comparison of Observed and Simulated Speeds and Volume

Vehicle Type	Mean Speed Values (m/s)		MAPE (%)	Traffic Volume (veh/h)		MAPE (%)
	Sim.	**Obs.**		**Sim.**	**Obs.**	
Traffic stream	12.5	12.7	1.8	3648	3664	0.44
TW	13.1	13.5	3.2	1861	1869	0.43
Cars	12.2	13.1	7.4	328	330	0.61
THW	11.2	10.3	8.4	1095	1099	0.36
Bus	10.5	9.7	8.3	292	293	0.34
HV	10.0	9.1	9.5	72	73	1.37

4.8 SUMMARY

The simulation model for an ideal urban divided mid-block section is developed and implemented in MATLAB using object-oriented programming concepts. The model development includes three major logics: vehicle generation, vehicle placement and vehicle movement. These logics are explained in detail with flow diagrams and algorithms. The object-oriented programming concepts used to write the MATLAB program for developing the model are also explained in detail. The model is developed considering the entire road space as a single unit without lane discipline. Generation of vehicles, identification of vehicle types and assignment of free-flow speeds are done using random numbers. Generated vehicles are placed at the beginning of the simulation road stretch using vehicle placement logic. The movement logic is designed to incorporate vehicle following and lane changing logics for disordered traffic conditions. An overview of inputs and outputs of the model have also been given. The developed model is calibrated using various parameters such as reaction time, sensitivity parameter, deceleration of leader expected by subject vehicle, acceleration and deceleration rate of vehicles. Validation results prove that the developed model replicates the real-world conditions satisfactorily. Traffic stream speed, mean speeds of different vehicle types and traffic volume are the measures of effectiveness used for model calibration and validation.

CHAPTER 5

ESTIMATION OF PASSENGER CAR UNIT VALUES USING EFFECTIVE AREA APPROACH

5.1 GENERAL

As the main objective of the present study is to investigate the impact of roadside frictions on Passenger Car Unit (PCU) and capacity values, accurate determination of dynamic PCU values for different vehicle types is imperative. Also, PCU values for different vehicle types need to be obtained as output from the simulation model and thus, the capacity in veh/h obtained from the model can be converted in terms of PCU/h. Different methods are used to estimate PCU values of vehicle types for different facility types under disordered traffic conditions. For mid-block sections carrying disordered traffic, the widely used method for PCU estimation (Chandra and Kumar 2003) considers the relative speed and projected area (length × width) of the vehicles. However, as a vehicle will be influenced by a larger area than its projected area which is proportionate to the surrounding vehicle types (effective area of a vehicle); it is necessary to deal with the influence of surrounding vehicles while estimating its PCU value. Thus, a new methodology is proposed in this study to estimate PCU values for urban mid-block section in disordered traffic, where vehicles do not follow lanes strictly. PCU values for different vehicle types for an urban arterial road (four-lane divided), are estimated using the proposed method in simulation model and also, the proposed method is validated using manually calculated PCU values. The simulated PCU values are further used to study the impact of roadside frictions on PCU values. This chapter describes the estimation of PCU values using the proposed method in the simulation model and validation of the method.

5.2 ADOPTED METHODOLOGY FOR PCU ESTIMATION

This study suggests a methodology for determining PCU value for each type of vehicle considering speed and effective area of subject and surrounding vehicles which is used by Cao *et al*. (2010) in their study for determining MCUs. In the study, the basic formula developed by Chandra and Kumar (2003) is modified in which projected area (physical size) of a vehicle is better reflected by effective area considering the influence of surrounding vehicles under disordered traffic conditions due to weak lane discipline. Hence, the expression with effective area and speed of subject and surrounding vehicles i.e., effective area approach is incorporated in the validated simulation model to estimate PCU values. The adopted formula for determining PCU is given by:

$$PCU_k = \frac{\left({v_{carm}}/{v_{km}}\right)}{\left({A_{carm}}/{A_{km}}\right)} \tag{5.1}$$

where, PCU_k = PCU for subject vehicle (SV) type 'k'; v_{km}, v_{carm} = mean speeds (m/s) of subject vehicle type 'k' and passenger car 'car', respectively; A_{km}, A_{carm} = mean effective area (m^2) of subject vehicle type 'k' and passenger car 'car', respectively. A subject vehicle is influenced by different combinations of surrounding vehicles, for example, subject vehicle with a leader, subject vehicle surrounded by adjacent vehicles, etc. In this study by taking into account of surrounding vehicles, six different cases (Figure 5.1) such as presence of only subject vehicle (case 1), subject vehicle with an adjacent vehicle (case 2), subject vehicle with two adjacent vehicles one on each side (case 3), subject vehicle following a leader (case 4), subject vehicle with a leader and an adjacent vehicle (case 5), and subject vehicle surrounded by a leader and two adjacent vehicles one on each side (case 6) are considered for estimating PCU values. The closest vehicle in front overlapping with the width of subject vehicle (SV) within a look ahead distance of 30 m (Asaithambi and Joseph, 2018; Anand *et al.*, 2019; PTV VISSIM) is considered as the leader vehicle (LV). The closest vehicle on either side of a subject vehicle overlapping with its length within a lateral gap of 3.5 m (equivalent to one lane width) is considered as the adjacent vehicle (AV).

5.2.1 Estimation of Mean Effective Area of Vehicles

The mean effective area (A_{km}) of a vehicle is assumed to vary based on its speed, traffic condition, driver characteristics (such as age, income or gender) or weather conditions. To reduce the influence of these factors on the mean effective area in this study, the traffic data are collected in peak hour during dry weather conditions. In addition, it is impossible to determine the driver characteristics because the data are collected from each video camera that is set on a high vantage point. Therefore, the influence of driver characteristics is not considered in this study. Thus, it is hypothesized that the mean effective area might vary by the speed of vehicle.

5.2.1.1 Estimation of Effective Area of Vehicles

To determine the mean effective area of a vehicle, a correlation between effective area and speed of each vehicle needs to be plotted. So, it is necessary to estimate the effective area (A_k) of each vehicle which is defined as the area occupied by a vehicle to maintain its current speed. For this purpose, effective area and speed of vehicles are determined manually using the observed field data collected from ideal section (ideal_bus) on HAL road, Bangalore city (Table III.1). Effective area of a subject vehicle also depends on types, physical sizes (length x width) and positions of subject and surrounding vehicles. Thus, considering the influence of surrounding vehicles, effective area for each vehicle type (A_k) is determined for six cases. Effective area in each case is determined using different equations (Table 5.1). The six different cases are as follows:

Case 1: Subject vehicle (SV) with no surrounding vehicle

When a subject vehicle (k) is not surrounded by any vehicle, effective area is equal to projected area of the subject vehicle i.e., the product of length (l_k) and width (w_k) of the vehicle.

Case 2: Subject vehicle with one adjacent vehicle (AV)

When a subject vehicle is surrounded by only one adjacent vehicle, effective area is the product of length (l_k) and effective lateral distance (E_k) of subject vehicle. Effective lateral distance is the lateral distance between subject and adjacent vehicles (based on the ratios of their physical sizes) inclusive of subject vehicle width.

Case 3: Subject vehicle with two adjacent vehicles one on each side

When a subject vehicle has two adjacent vehicles, effective area is the product of length (l_k) and effective lateral distance (E_k) of subject vehicle.

Case 4: Subject vehicle with only leader vehicle.

When a subject vehicle has leader vehicle as the only surrounding vehicle, effective area is the product of effective longitudinal distance (F_k) and width (w_k) of the subject vehicle. Effective longitudinal distance is the longitudinal distance between subject vehicle and leader vehicle inclusive of subject vehicle length.

Case 5: Subject vehicle with a leader and one adjacent vehicle.

When a subject vehicle has leader vehicle and one adjacent vehicle, effective area is the product of effective longitudinal distance (F_k) and effective lateral distance (E_k) of subject vehicle.

Case 6: Subject vehicle with a leader and two adjacent vehicles one on each side.

When a subject vehicle has leader vehicle and two adjacent vehicles, effective area is the product of effective longitudinal distance (F_k) and effective lateral distance (E_k) of subject vehicle.

Effective area of SV is affected by physical sizes of SV and AV on its right (RAV) and left side (LAV). Effective lateral distance of SV (E_k) which is used for determining effective area is assumed to be a function of width of SV (w_k) and lateral distance of SV (D_k). Depending upon the side at the which AV is present, SV lateral distance can be classified as lateral distance at right (D_{kr}) or left (D_{kl}). The lateral distance of SV relies on the ratio of physical sizes of SV and AV (size ratio). Hence, the ratio of physical sizes of SV (Z_k) and AV (Z_{adj}) is considered to calculate the lateral distance of SV (D_k) and that of AV (D_{adj}) as shown in equation 5.2.

$$\frac{D_k}{D_{adj}} = \frac{Z_k}{Z_{adj}} \tag{5.2}$$

The lateral distance of SV 'k' is thus determined as given in the following equation.

$$D_k = \frac{Z_k}{Z_{adj}} \text{ x } D_{adj} \tag{5.3}$$

In figure 5.1 (cases 2, 3, 5 and 6), sum of lateral distance of SV (D_k) and that of AV (D_{adj}) (equation 5.4) is the lateral gap (D) between subject and adjacent vehicle.

$$D = D_k + D_{adj} \tag{5.4}$$

Knowing the value of lateral gap (D) between SV and AV, the following equation is used to determine the lateral distance of AV (D_{adj}) in equation 5.4.

$$D_{adj} = D - D_k \tag{5.5}$$

Equation 5.5 is thus substituted in equation 5.3 to determine lateral distance of SV (D_k). In equations (5.2), (5.3), (5.4) and (5.5), D = lateral gap (m) between subject and adjacent vehicle; D_k = lateral distance (m) of SV 'k' based on size ratio; D_{adj} = lateral distance (m) of AV 'adj' based on size ratio; Z_k = physical size (m^2) of SV 'k'; Z_{adj} = physical size (m^2) of AV 'adj'. In addition to adjacent vehicles, LV also influences SV to a greater extent. Effective longitudinal distance of SV, F_k is calculated to estimate the effective area. Effective longitudinal distance of SV (F_k) is calculated as the sum of longitudinal gap between SV and LV (L), and length of SV (l_k).

Table 5.1 Six Cases and Corresponding Equations for Estimation of Effective Area of Subject Vehicle

Sl. No.	Cases	Equation
1	Only subject vehicle	$A_k = l_k \text{ x } w_k$
2	Subject vehicle - one adjacent vehicle	$A_k = l_k \text{ x } E_k$
3	Subject vehicle - two adjacent vehicles	
4	Subject vehicle - leader vehicle	$A_k = F_k \text{ x } w_k$
5	Subject vehicle – one leader - one adjacent vehicle	$A_k = F_k \text{ x } E_k$
6	Subject vehicle - one leader - two adjacent vehicles	
A_k	= Effective area of subject vehicle type k (m^2)	
l_k	= Length of the subject vehicle (m)	
w_k	= Width of the subject vehicle (m)	
E_k	= Effective lateral distance (m) of subject vehicle with two adjacent vehicles $E_k = D_{k\,r} + D_{k\,l} + w_k$	
E_k	= Effective lateral distance (m) of subject vehicle with one adjacent vehicle $E_k = D_{k\,l} + w_k$ or $E_k = D_{k\,r} + w_k$	
$D_{k\,r}$	= Lateral distance of subject vehicle k, on right side based on size ratio (m)	
$D_{k\,l}$	= Lateral distance of subject vehicle k, on left side based on size ratio (m)	
F_k	= Effective longitudinal distance of subject vehicle (m) $F_k = L + l_k$	
L	= Longitudinal gap between subject vehicle and leader vehicle (m)	

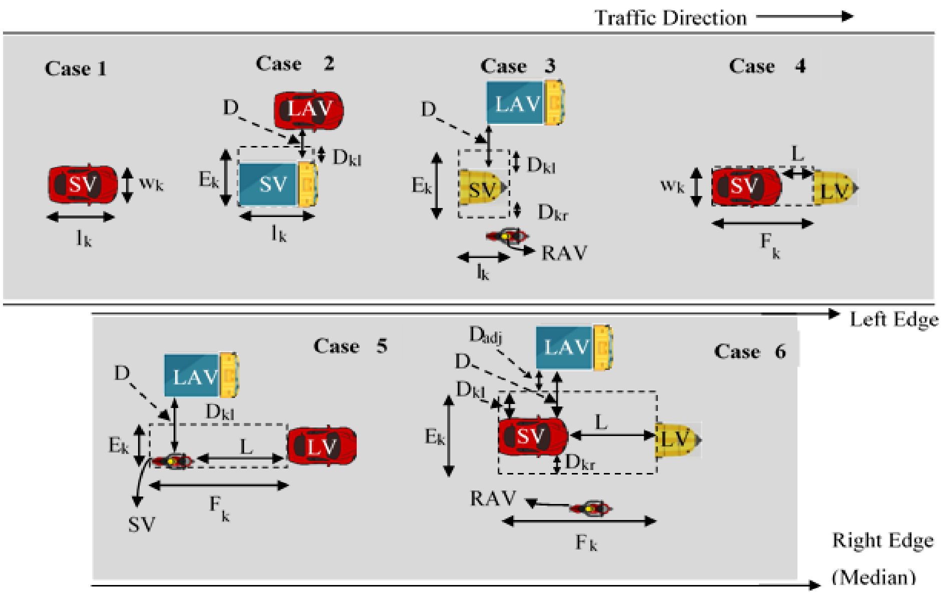

Figure 5.1. Schematic Sketch of Six Different Cases for Estimating Effective Area

5.2.1.2 Relationship Between Effective Area and Speed of Subject Vehicle

After determining the effective area based on physical sizes of vehicles, and corresponding speeds of each vehicle manually from field observed data; equations for determining mean effective area of vehicles are obtained by plotting the relationships between the effective area and speeds. The relationship between effective area and speed are plotted for all types of vehicles for five different cases (Figure 5.2).

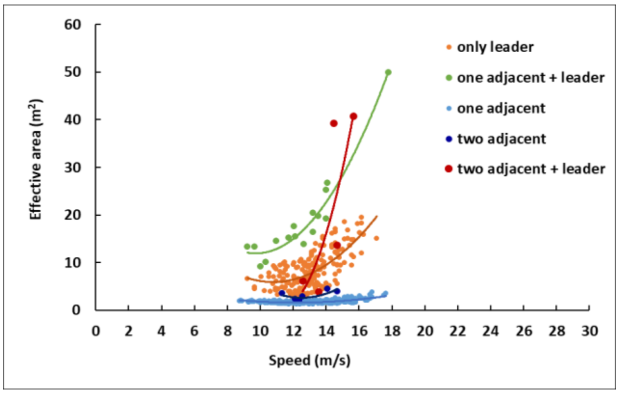

(a)Two-wheelers

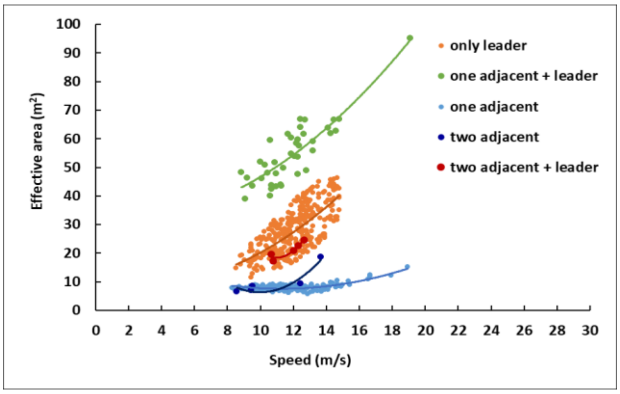

(b) Cars

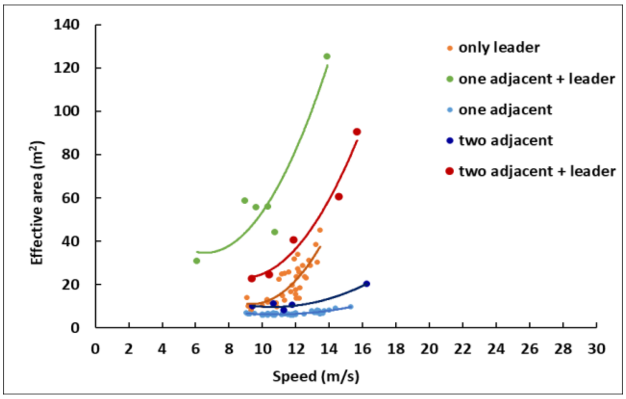

(c)Three-wheelers

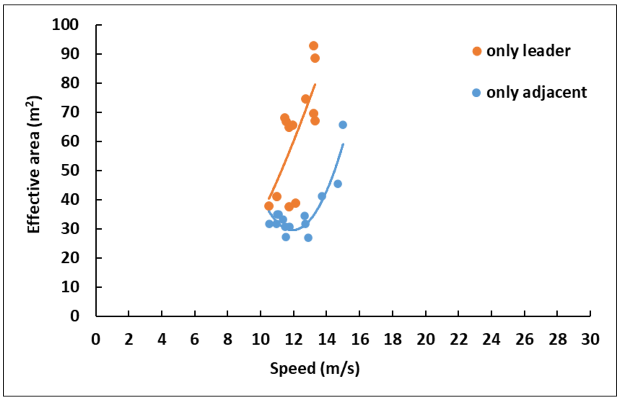

(d) Buses

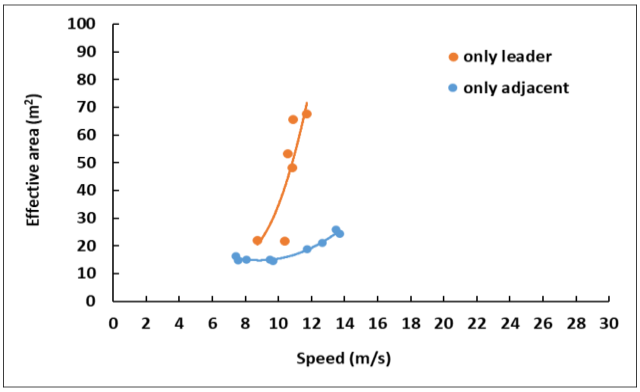

(e) Heavy Vehicles

Figure 5.2 Relationship between Speed and Effective Area of Subject Vehicle

The trend for case 1 is always a straight line since the effective area for case 1 is the projected area (length x width) of the vehicle which does not change with speed. Coefficient of correlation (R^2) is used to determine the goodness of fit of the models. Second degree polynomial relation gives the best R^2 value for all types of vehicles. It indicates that except for case 1, for all the other five cases, the effective area increases with increase in speed providing non-linear equations. As the speed of subject vehicle increases it tend to maintain more gaps with the surrounding vehicles thus resulting in more effective area. Only two cases i.e., only leader case and only one adjacent case along with only subject vehicle case are observed for buses and HV as they occupy most of the road width due to their larger sizes.

Non-linear equations are obtained for all types of vehicles from the effective area vs speed graph. The independent variable is mean speed (v_{km}) and dependant variable is mean effective area (A_{km}). Thus, equation is expressed as follows:

$$A_{km} = a * v_{km}^2 + b * v_{km} + c \tag{5.6}$$

where, A_{km} = mean effective area for vehicle type '*k'* (m^2); v_{km} = mean speed of vehicle type '*k'* (m/s); *a, b, c* = parameters or coefficients of non-linear function. Table 5.2 shows non-linear equations, corresponding R^2 values, mean effective areas, mean speeds, and PCU values for all vehicle types of ideal section (ideal_bus) calculated manually from the field observed data. These non-linear equations obtained from the field data are incorporated in the simulation model to obtain the simulated mean effective area for vehicle types in each case.

5.2.2 Estimation of Weighted PCU Values

Simulated mean effective areas and mean speeds are then used to obtain the PCU values for each case of different vehicle types from the simulation model. A single PCU value for each vehicle type is obtained by calculating the weighted average of PCUs for different cases for each type of vehicle. Weighted PCU values are calculated using the following equation.

$$PCU_k = \frac{\sum_{c=1}^{NC} n_c PCU_c}{\sum_{c=1}^{NC} n_c} \tag{5.7}$$

where, PCU_k = Weighted PCU value for vehicle type '*k*'; *NC* = Total number of cases present; PCU_c = PCU value for case '*c*'; n_c = Number of samples of case '*c*'.

Table 5.2 Non-linear Equations and Observed PCU Values for Vehicle Types of Ideal Section (Ideal_bus)

Veh. Type	Cases	Non-linear equation	R^2	v_{km} (m/s)	A_{km} (m^2)	PCU_c
TW	Case 1			13.24	1.2	0.21
	Case 2	$y = 0.0453x^2 - 1.1001x + 8.2992$	0.65	12.89	1.64	0.20
	Case 3	$y = 0.3846x^2 - 9.6193x + 62.787$	0.61	13.28	2.87	0.16
	Case 4	$y = 0.3474x^2 - 7.4882x + 46.301$	0.85	12.78	7.35	0.25
	Case 5	$y = 0.5848x^2 - 11.362x + 67.135$	0.94	12.49	16.47	0.29
	Case 6	$y =7.0144x^2 - 187.24x + 1251.9$	0.99	13.40	22.39	0.15
THW	Case 1			11.85	4.48	0.91
	Case 2	$y = 0.1676x^2 - 3.6012x + 25.519$	0.68	11.26	6.22	0.87
	Case 3	$y = 0.3378x^2 - 7.1854x + 47.863$	0.94	11.89	10.18	0.84
	Case 4	$y = 1.5764x^2 - 29.509x + 149.1$	0.83	11.55	18.59	0.70
	Case 5	$y = 5.983x^2 - 124x + 692.35$	0.97	10.98	52.17	1.04
	Case 6	$y = 1.3714x^2 - 24.325x + 130.99$	0.97	10.54	64.10	0.88
CAR	Case 1			12.97	5.36	1.00
	Case 2	$y = 0.1209x^2 - 2.7321x + 22.974$	0.55	12.05	7.61	1.00
	Case 3	$y = 0.827x^2 - 16.494x + 88.583$	0.89	10.72	6.81	1.00
	Case 4	$y = 0.2077x^2 - 1.0006x + 9.4259$	0.51	12.03	27.45	1.00
	Case 5	$y = 0.1995x^2 - 0.5411x + 32.144$	0.94	11.92	54.05	1.00
	Case 6	$y = 9.4449x^2 - 208.77x + 1171.2$	0.94	11.67	65.36	1.00
BUS	Case 1			12.40	24.54	4.79
	Case 2	$y= 3.1505x^2 - 75.202x + 478.29$	0.84	10.79	33.61	4.93
	Case 4	$y = 1.686x^2 - 25.577x + 122.13$	0.86	11.96	57.47	3.10
HV	Case 1			10.15	17.62	4.20
	Case 2	$y= 0.4562x^2 - 8.0823x + 50.552$	0.96	10.22	15.60	2.41
	Case 4	$y = 3.4655x^2 - 53.905x + 227.11$	0.86	11.57	67.33	2.55

5.3 VALIDATION OF ADOPTED METHODOLOGY

In order to check the accuracy of PCU values obtained using effective area approach, validation is performed by comparing the simulated and observed (manually calculated) weighted PCU values. Table 5.3 gives the comparison of simulated and observed PCU values for different vehicle types with respect to car having PCU value as 1. MAPE values for PCU values for each vehicle type is found to be less than 7%, thus giving satisfactory results. A paired t-test yielded the calculated value of t-statistic (t_0) as 1.32 against the critical value of 3.18. This implies that there is no significant difference between the observed and simulated PCU values for different vehicle types.

Table 5.3 Comparison of Simulated and Observed PCU Values for Different Vehicle Types- Ideal Section

Vehicle Type	PCU values		MAPE (%)
	Simulated	Observed	
TW	0.24	0.23	4.34
THW	0.82	0.88	6.80
Bus	4.77	4.47	6.71
HV	4.35	4.17	4.32

5.3.1 PCU and Capacity of Ideal Sections

The simulated and observed PCU values are found to be within a reasonable range when compared with PCU values suggested by Indo-HCM (2017) for four-lane divided urban roads. Table 5.4 shows the comparison of simulated PCU values, observed PCU values and PCU values suggested in Indo-HCM for four-lane divided urban roads. The PCU values obtained from the simulation models are further used to convert the capacity of roads in terms of PCU/h. The capacity of ideal section (ideal_bus) using simulated PCU values is found to be 2876 PCU/h (4208 veh/h). The estimated capacity values of ideal_bus section is found to be closer to the capacity of a four-lane divided urban road (2700 PCU /h) suggested by Indian Highway Capacity Manual (Indo-HCM 2017).

Table 5.4 Comparison of PCU Values for Different Vehicle Types for Four-Lane Divided Urban Roads

Vehicle Type	PCU values		Indo-HCM PCU Values - Range
	Simulated	Observed	
TW	0.24	0.23	0.11-0.33
THW	0.82	0.88	0.39-1.66
Bus	4.77	4.47	1.62-5.90
HV	4.35	4.17	2.70-5.68

5.4 SUMMARY

The parameters used in the estimation of PCUs for homogeneous and mixed traffic are different for almost all the facility types. The studies carried out in the countries where homogeneous traffic is present, used single parameter to estimate PCU values.

However, many studies on PCU estimation for disordered traffic used a combination of parameters, i.e., static and dynamic parameters, for estimating the PCU values of vehicles. It may be attributed to the fact that use of both static and dynamic parameters can capture the effects of the variation in dimensions and their manoeuverability. More number of vehicle types, their intra-class variability and weak lane discipline make the disordered traffic more complex to analyse. Hence, the parameters required for PCU estimation under disordered traffic are relatively more complex to measure than that of homogeneous traffic conditions. In case of signalized intersections; headway, queue discharge and travel time are the mainly focused parameters for estimating PCU values. PCU values for highways, expressways and freeways are calculated using parameters such as speed, headway, density, delay, space occupancy etc. On un-signalized intersections and roundabouts, PCU estimation was carried out using headway and time occupancy as the major parameters. For mid-block sections carrying disordered traffic, the widely used method for PCU estimation considers the relative speed and projected area of the vehicles, where the projected area of vehicle does not actually represent the effective area occupied by them due to the influence of surrounding vehicles. To overcome this limitation, a methodology is proposed for PCU estimation for urban mid-block section carrying mixed traffic. This chapter describes the proposed methodology adopted for estimation of PCU values. The estimation of mean effective area and weighted PCU values are explained in detail. This method considers the predominant variations of traffic over time. Therefore, consideration of influence of surrounding vehicles to estimate PCU values for several vehicle types is realistic. In most of the past studies, the speed-flow or speed-density curve which is a macroscopic traffic relationship, is used for validating the PCU values. Such aggregated traffic relationship may not capture effects of individual vehicles. Hence, a systematic procedure for validation of the estimated PCU values becomes imperative. Simulation based validation of PCU values is hence suggested considering the robustness of the simulation tools as they can observe the interactions among the different vehicle types. Validation of the adopted methodology is carried out by comparing the simulated and observed PCU values, and the results obtained are discussed in detail.

CHAPTER 6

SIMULATION MODELS FOR SECTIONS WITH A CURBSIDE BUS STOP AND UNDESIGNATED PEDESTRIAN CROSSINGS

6.1 GENERAL

To study the effect of roadside frictions such as curbside bus stop and undesignated pedestrian crossings on PCU for different vehicle types and capacity of urban roads, the validated base model needs to be modified to simulate the manoeuvers of road users in the presence of these side frictions. As the impact of each side friction is studied separately, two different sets of data (as mentioned in Chapter 4) are provided as inputs to the simulation model for modification. One set of data are collected from bus stop section and ideal_bus section in HAL old airport road to quantify the impact of curbside bus stops on PCU and capacity values. Here, when the base model is modified, the additional data extracted from bus stop section are given as inputs. Similarly, the another set of data used is from pedestrian section and ideal_ped section in Hosur road to examine the influence of undesignated pedestrian crossings on PCU and capacity values. To simulate vehicle-pedestrian interactions, the additional data extracted from pedestrian section are provided as inputs to the base model. This chapter discusses how the base models are modified in order to simulate the vehicular manoeuvers on a section with a curbside bus stop and also, to simulate vehicle-pedestrian interactions on another section with undesignated pedestrian crossings.

6.2 MODIFICATION OF THE BASE MODEL TO SIMULATE A SECTION WITH A CURBSIDE BUS STOP

The base model developed using the input data obtained from ideal section (ideal_bus) is modified to simulate the vehicular manoeuvers linked with a curbside bus stop. PCU and capacity values for a curbside bus stop section is influenced by various factors such as frequency of stopping and non-stopping buses, stopping position of bus, bus dwelling time, acceleration and deceleration rate of stopping buses, the position at which stopping bus starts to decelerate and the position at which stopping bus attains its normal speed and thus, they are incorporated in the base model as additional inputs.

6.2.1 Logics for Simulation of Bus stop Section

Logics for incorporating a curbside bus stop in the base model using object-oriented programming concepts is shown in Figure 6.1. In bus stop section, buses are classified as stopping and non-stopping buses, and they are generated randomly in the traffic stream depending upon their composition using a set of random numbers. The buses are placed and moved along with other vehicles on the simulation stretch based on the logics of base model. However, vehicle movement logic for stopping buses is modified in such a way that when the bus approaches near the bus stop, it tries to decelerate at a position before the bus stop and then stops near the curb randomly within a range of 20 m (length of bus stop) in the simulation stretch. All the buses do not stop at the same point and the stopping position of the bus when it stops depends on many factors such as the driver's attitude and the amount of passenger traffic waiting at the curbside. In this study, the results from the field data shows that stopping position of bus follows normal distribution with mean, μ=41.02 m and standard deviation, σ=5.5 m. At bus stop, the bus halts for a dwell time, which is generated randomly with normal distribution (μ =5 s; σ =3.2 s) and bus speed becomes zero. When the simulation clock time becomes equal to the sum of bus stopped time (the time at which bus stopped at the bus stop) and dwell time, bus accelerates and updates its speed and position. These vehicle movement logics are applicable only for the stopping buses and not for the non-stopping buses such as tourist buses, school buses, etc. that do not stop near the bus stop. When the vehicles such as TW, THW, cars, HV and non-stopping buses approach the bus stop, the type of leader vehicle is checked. If the leader vehicle is a bus which is stopped at the bus stop, the gaps available for lateral shift towards the right side of the leader vehicle is checked. If the lateral and longitudinal gaps are available, then the vehicles laterally shift towards the right side of the stopped bus. Otherwise, the vehicles stop behind the stopped bus. So, whenever a stopping bus approaches the bus stop, the road width gets reduced creating a temporary bottleneck condition where the other vehicles have to either decelerate or shift laterally. Otherwise, the entire width of the road is used by the vehicles based on vehicle movement logics used in base model.

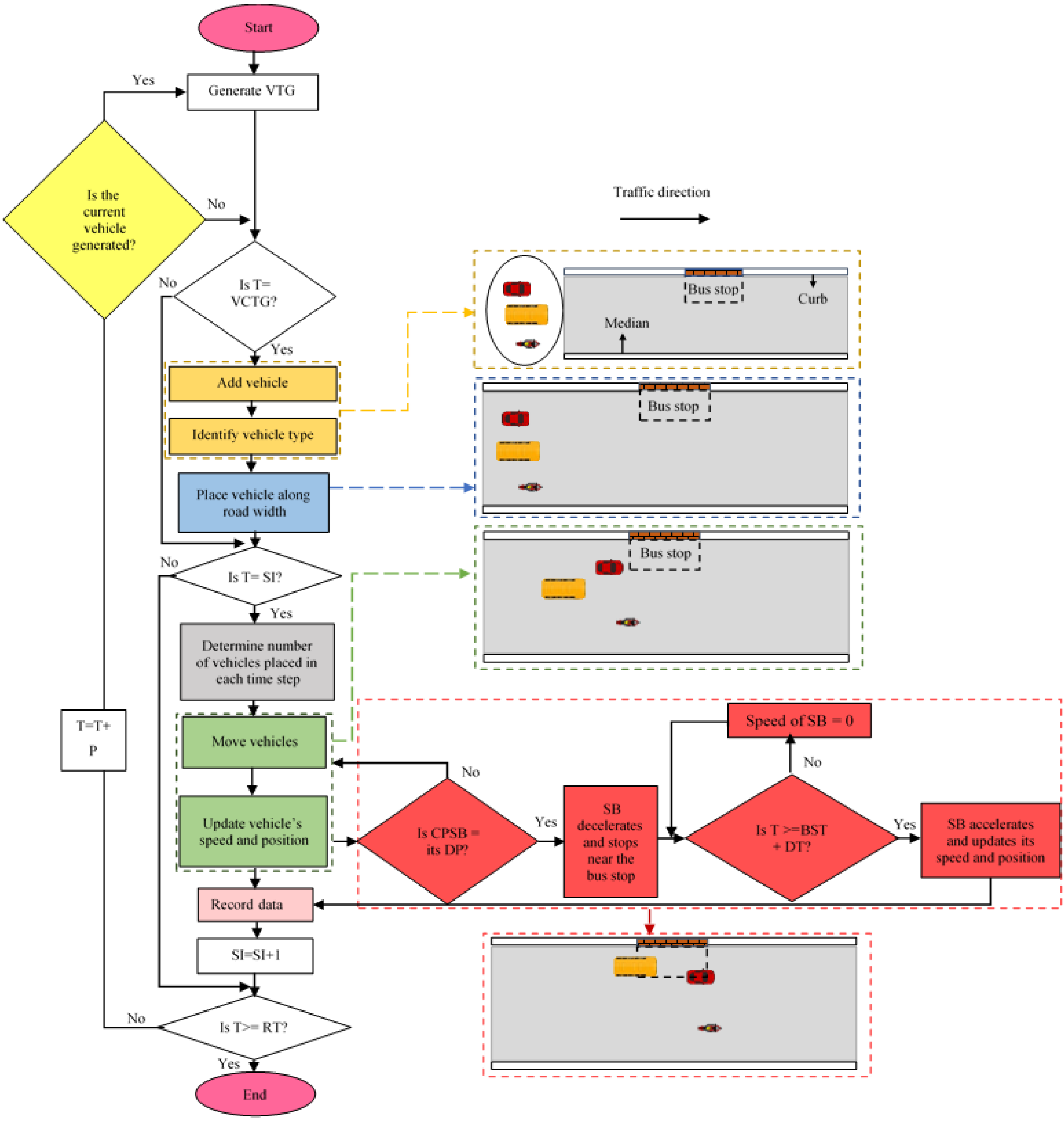

Note: T= Simulation Clock Time; P = Precision Time; SI = Scan Interval; RT =Simulation Run time; VTG = Vehicle Time Gap; = Vehicle Cumulative Time Gap; SB= Stopping Bus; CPSB = Current Position of Stopping Bus; DP =Deceleration position; BST= Bus Stopped Time; DT=Dwell Time.

Figure 6.1 Framework for Simulation of Curbside Bus Stop

6.2.2 Computer Program for Curbside Bus Stop Simulation

The computer program written for simulating ideal section is modified in such a way that the objects such as *TW, car, THW, stopping bus, non-stopping bus and HV* represent different vehicle types. The object *bus* in base model is divided into two different objects i.e., *stopping bus* and *non-stopping bus* in bus stop model (Figure 6.2). The properties of these objects are inherited from the *Vehicle* class. In the *Link* class, the logics of bus stop model are implemented. A new superclass *Busstop* is associated with *Link* class with virtual functions such as *busdwelltime (), busstoppingpos (), decpos ()* and *normalspeed ().* The virtual function, *busdwelltime ()* is used to determine the bus dwelling time, *busstoppingpos ()* is used to estimate the stopping position of bus, *decpos ()* is used to calculate the position at which bus decelerates and *accpos ()* is used to determine the position at which bus attains its normal speed. *Link* class is further associated with *Main Simulator* class to process the entire simulation.

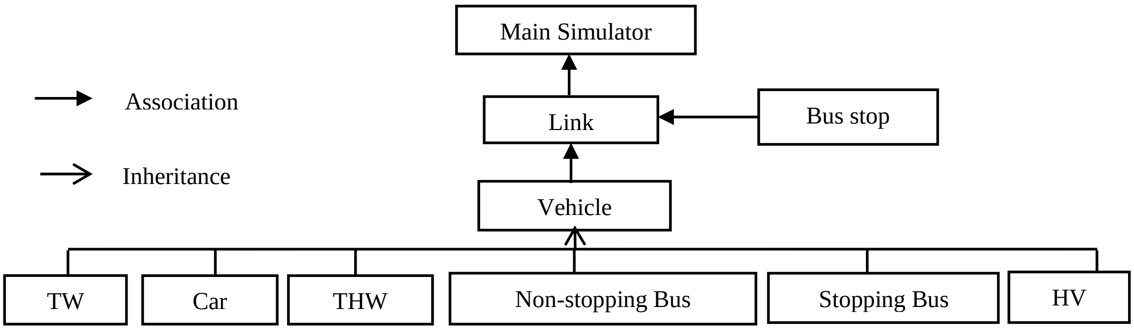

Figure 6.2 Class Diagram for Traffic Simulation of a Section with a Curbside Bus Stop

6.2.3 Validation of Bus stop Model

The bus stop model is validated to compare the vehicular behavior with real world data. Validation of curbside bus stop model is done by comparing observed and simulated average speeds of vehicles from bus stop section (HAL old airport road, Bangalore city). Table 6.1 gives the comparison of simulated and observed mean speed values of vehicles, and traffic volume obtained from bus stop model. Mean Absolute Percentage Error (MAPE) values for mean class-wise speeds and traffic stream speeds are found to be less than 10% which proves that the model is close to real world conditions. A paired t test is performed to check statistical validity of the simulated and observed mean speeds of vehicles and also, to compare the simulated and observed traffic volumes. The calculated value of t (t_0) for mean speeds is 1.44 against the critical value of 2.57 and it is found that the observed and simulated mean speeds agreed at 5% level of significance. The calculated value of t (t_0) for traffic volume is 0.21 against the critical value of 2.57 and it is found that the observed and simulated traffic volume agreed at 5% level of significance.

Table 6.1 Comparison of Simulated and Observed Speeds and Volume of Bus Stop Section

Vehicle Type	Mean Speed values (m/s)		MAPE (%)	Traffic Volume (veh/h)		MAPE (%)
	Simulated	Observed		Simulated	Observed	
Traffic stream	10.3	10.0	3.3	3336	3354	0.53
TW	11.2	10.7	4.9	1769	1778	0.51
Cars	10.2	9.5	6.8	333	335	0.59
THW	9.3	9.2	1.4	1135	1140	0.43
Bus	5.6	6.2	8.6	66	67	1.49
HV	9.5	8.7	9.5	33	34	2.94

6.2.4 Outputs from the Bus Stop Model

Following are the outputs of the simulation model which includes numerical results and animation of traffic flow.

- Traffic flow
- Average traffic stream speed
- Average class-wise speeds of vehicles
- Vehicular time gaps
- Vehicle trajectories at each time step
- Road capacity
- PCU values

Table IV.3 presents the trajectory and speed values of vehicles obtained from the bus stop simulation model. The flow levels are incremented from lower to higher level in the simulation model until a maximum traffic flow is obtained. This maximum traffic flow obtained is considered as the capacity (veh/h). The capacity of bus stop section is obtained as 3448 veh/h from the model. Capacity obtained in veh/h is then converted in terms of PCU/h using the simulated PCU values. As the PCU values are considered as the function of speeds of the vehicles, they change with the variation in vehicular speeds due to the presence of curbside bus stop. Thus, using ideal section PCU values for calculating the capacity of bus stop section may lead to inaccurate estimation. Hence, separate PCU values obtained from the bus stop simulation model for TW, THW, car, bus and HV are 0.25, 0.85,1, 6.11 and 4.02, respectively. These PCU values can be applied to all the urban streets where curbside bus stops (devoid of other side frictions) are present, but only to the influence region of bus stop. The capacity of bus stop section is estimated as 2358 PCU/h using the simulated PCU values. The snapshot of the animated output of vehicles at a random time step is shown in Figure 6.3. The dashed rectangular box in the animated output represents the area of bus stop.

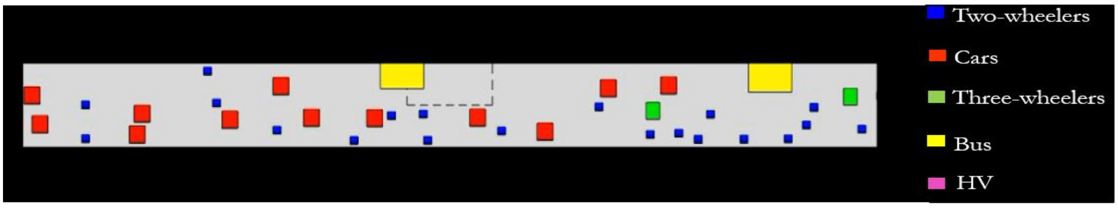

Figure 6.3 Snapshot of Animation of Simulated Traffic Flow in Bus Stop Section

6.3 MODIFICATION OF THE BASE MODEL TO SIMULATE A SECTION WITH UNDESIGNATED PEDESTRIAN CROSSINGS

The base model with the input data from ideal section (ideal_ped) at Hosur road is modified to simulate the real-world interactions between vehicles and pedestrians in disordered traffic. As the selected road stretch is not having proper signalized or designated pedestrian crossings, both vehicles and pedestrians travel simultaneously.

6.3.1 Logics for Simulation of Pedestrian Section

Logics for incorporating undesignated pedestrian crossings in the developed model is shown in Figure 6.4. In the modified model i.e., vehicle-pedestrian interaction model, logics involved in vehicle generation and placement are same as in the base model, and vehicle movement logic is modified only during the vehicle-pedestrian interactions. Here, pedestrians are the additional feature simulated using data such as pedestrian cross flow, pedestrian walking speed, pedestrian entry and exit positions, and pedestrian waiting time. The additional logics involved in the vehicle-pedestrian interaction model are described in the following sections.

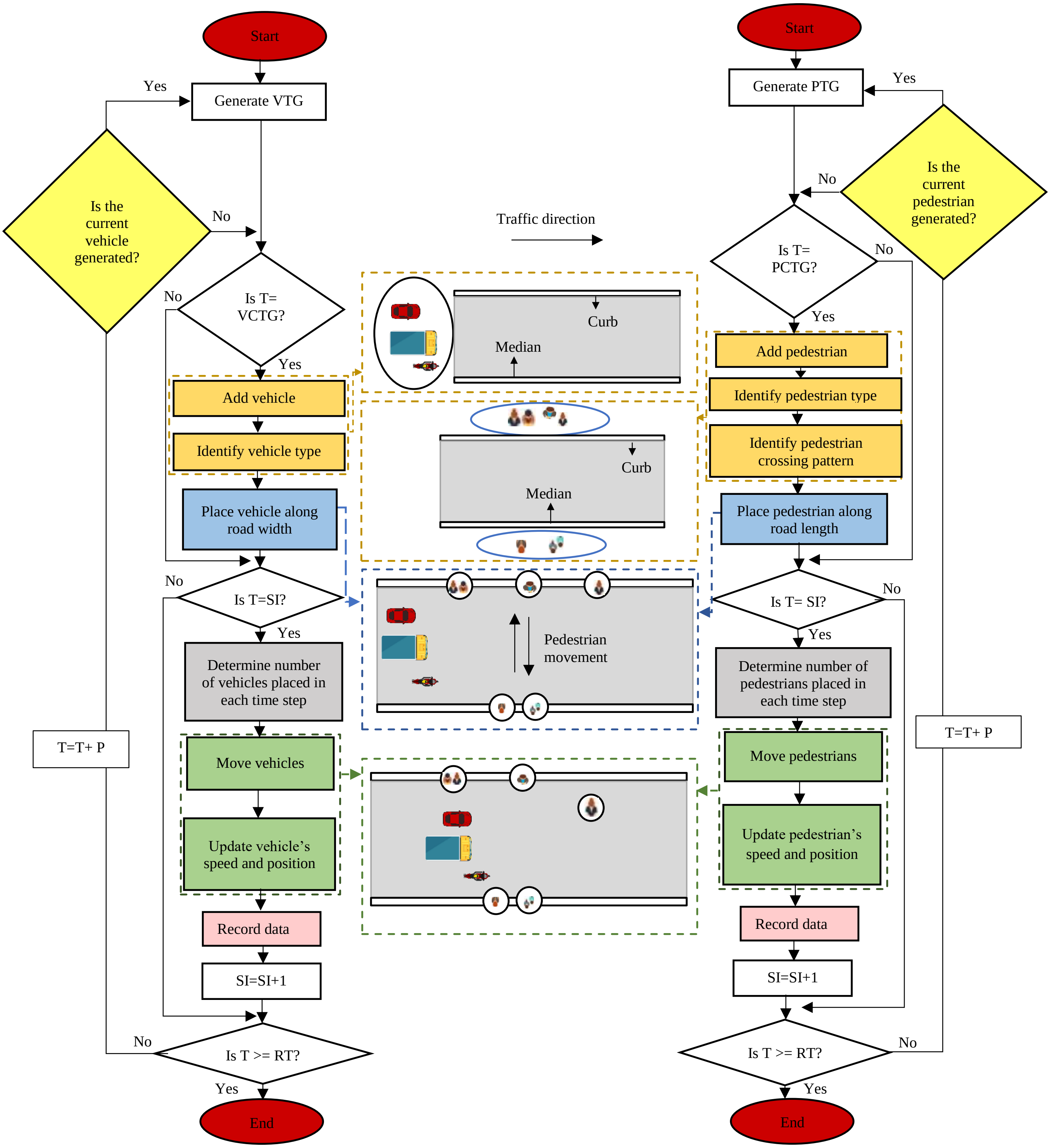

Note: T= Simulation Clock Time; P = Precision Time; SI = Scan Interval; RT =Simulation Run time; VTG and PTG = Vehicle and Pedestrian Time Gaps, respectively; VCTG and PCTG = Vehicle's and Pedestrian's Cumulative Time Gaps, respectively.

Figure 6.4 Framework for Vehicle-Pedestrian Simulation Model

6.3.1.1 Pedestrian Generation

Pedestrians are generated randomly using pedestrian time gap distribution similar to vehicles. Figure 6.5 shows the logics for generation of pedestrians along with vehicles in vehicle-pedestrian interaction model. Time gaps of pedestrians are observed to follow negative exponential distribution based on the field data. Once a pedestrian is generated, its type is identified considering the movement of direction and crossing pattern based on the corresponding cumulative percentage composition.

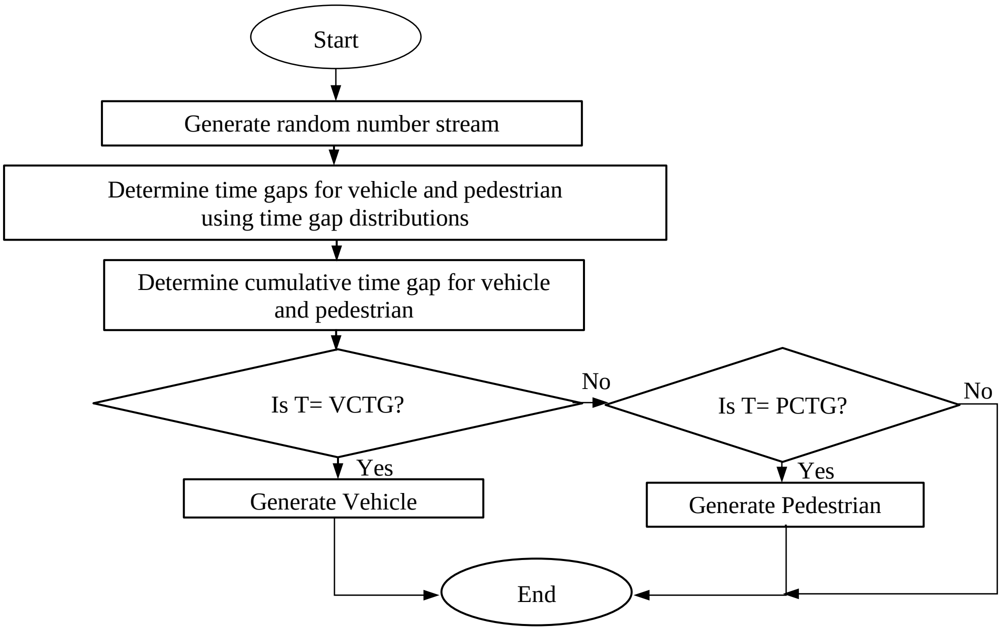

Figure 6.5 Logics for Generation of Pedestrians and Vehicles in Vehicle-Pedestrian Interaction Model

The generated pedestrians are assigned with preferred speed along with static (radii) and dynamic (e.g., maximum speed, relaxation time) characteristics. It is assumed that all the pedestrians enter the simulation stretch with their preferred speed. Moreover, during the simulation process the speeds of the pedestrians are not allowed to exceed their assigned preferred speeds. The simulations assumed that the pedestrian preferred speeds are normally distributed with mean, μ =1.34 m/s and standard deviation, σ = 0.26 m/s (Helbing and Molnar 1995; Helbing *et al.* 2005; Laxman *et al.* 2010). Pedestrian relaxation time is defined as the time a pedestrian takes to adapt his/her motion to his/her preferences. Pedestrian relaxation time is also assumed to follow normal distribution with mean, 0.5 s and standard deviation, 0.05 s (Helbing and Molnar

1995; Moussaid *et al.* 2009; Ningbo *et al.* 2017; Liu *et al.* 2017, Siddharth and Vedagiri, 2018).

6.3.1.2 Pedestrian Placement

When the simulation clock time becomes equal to cumulative time gap of pedestrian generated, the placement logic is invoked. The generated pedestrians are placed simultaneously with the vehicles on the simulation stretch depending upon their cumulative time gap i.e., for example, if the cumulative time gap of a vehicle is around 0.5 s and that of a pedestrian is around 0.9 s, the vehicle gets placed first and then the pedestrian gets placed. If there is another vehicle arriving at 1.1 s, it gets placed only after placing the pedestrian arriving at 0.9 s. Figure 6.6 shows the logics for placement of pedestrians.

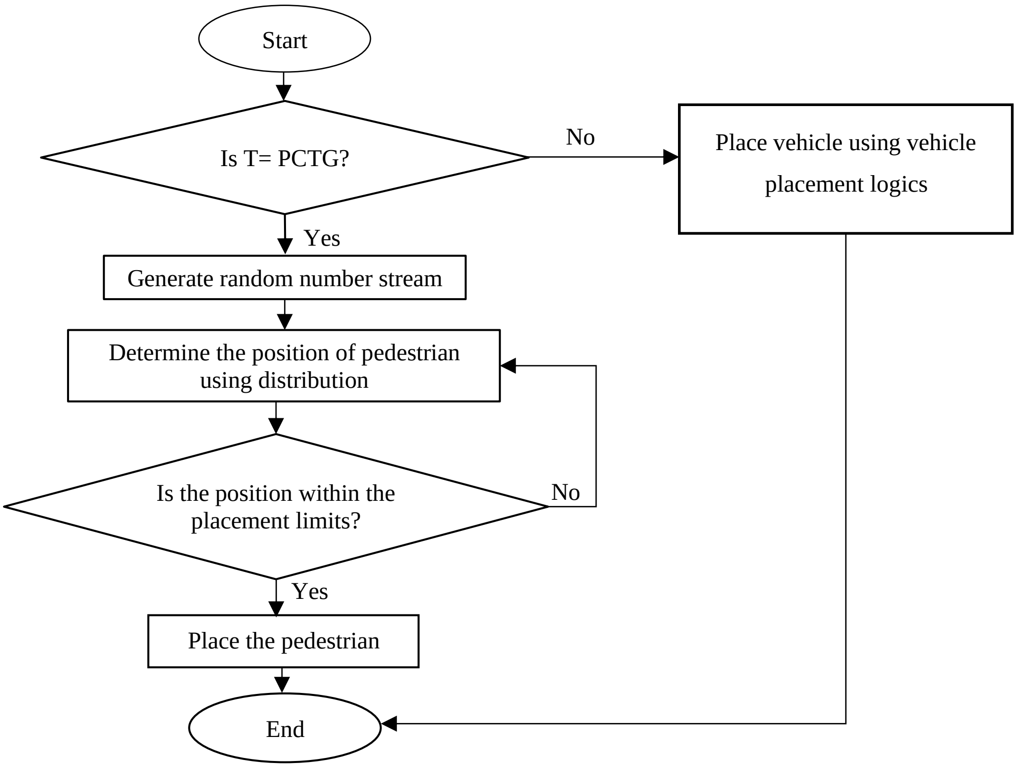

Figure 6.6 Logics for Placement of Pedestrians

Generated pedestrians are placed on the simulation stretch along the road length. The pedestrians generated are placed near the curb or median depending upon the direction of movement i.e., median to curb (MC) and curb to median (CM). Those pedestrians traveling from median to curb (MC) have their entry near the median and those traveling from curb to median (CM) have their entry near the curb. From the field data which covers 70 m length of the selected road stretch in Bangalore city, it is observed that the pedestrian entry positions near the curb or median follows a uniform distribution whose cumulative probability distribution function can be expressed in terms of mean, μ and standard deviation, σ. Based on the distribution, the pedestrians are placed randomly within 70 m (along the road length) in the simulation stretch. To incorporate the randomness in pedestrian placement logic, random numbers are generated. Also, a check is done to ensure that the pedestrians are placed within 70 m (placement limits).

6.3.1.3 Pedestrian Movement and Vehicle-Pedestrian Interaction

When both vehicles and pedestrians are using the road for movement, the pedestrians are made to wait at the positions where they are placed until they find a safe gap between vehicles to cross the road. Once the pedestrian finds a safe gap, the pedestrians are made to walk. Perception of a pedestrian is thus based on the present conditions of the approaching vehicles. Decision-making of a pedestrian, '*j*' is chosen according to a safety judging criterion, i.e., gap acceptance, and performed by checking whether the prevailing gap between vehicles can assure the pedestrian's safe crossing. For this purpose, vehicle's passing time, t_{veh} and pedestrian's crossing time, t_j are estimated. The crossing time (s) of pedestrian, t_j is calculated using the following equation.

$$t_j = \frac{D_j}{v_j} + t_a + t_b \tag{6.1}$$

where, v_j = pedestrian walking speed (m/s), D_j = distance travelled by the pedestrian, '*j*' (m), t_a = reaction time (1 s) of pedestrian when a vehicle approaches (s), and t_b = safe time (1 s) for pedestrians considering the next approaching vehicle (s). Vehicle's passing time (s), t_{veh} is computed using the following equation.

$$t_{veh} = \frac{d_{j\_veh}}{v_{veh}} \tag{6.2}$$

where, v_{veh} = approaching vehicle's current speed (m/s); d_{j_veh} = distance between pedestrian and approaching vehicle (m). The pedestrian is made to cross the road safely only when t_j is less than t_{veh}. Otherwise, the pedestrian needs to wait for the next longer gap between vehicles. Whenever the pedestrians decide to walk, it is assured that they are able to pass through the gaps between the vehicles safely. Pedestrians' speeds and positions are always updated when both pedestrian movement logic and vehicle-pedestrian interaction logic are invoked. When a vehicle comes in contact with a pedestrian, vehicle's speed and position are updated using vehicle-pedestrian interaction logic. Otherwise, vehicle's speed and position are updated sequentially from the exit to the entry of the simulation stretch using vehicle movement logic.

For simulating pedestrian dynamics, most popular models considered are cellular automata model or social force model as they describe most of the self-organization phenomena of large crowd. In simulating pedestrian movements using cellular automata model, pedestrians have to take grid-based motion decisions from a limited set of cells. But, as the pedestrians are flexible and their choice to take the next step is unrestricted, social force model is found to be more robust (Helbing *et al.* 2000; Helbing *et al.* 2005). Hence, in this study to model pedestrian cross flow, Social Force Model (SFM) is used which describes the behavior of individual pedestrian (Helbing *et al.* 2000; Helbing *et al.* 2005) and dynamic pedestrian movement in space. SFM is used to update the position and speed of pedestrians at each time step. The SFM suggests that the movement of a pedestrian, '*j*' is expressed by the sum of 1) a destination force, $\boldsymbol{f}_j^0$ that represents the pedestrian's motivation to travel to their destination, 2) a pedestrian-pedestrian interaction force, $\boldsymbol{f}_j^m$ representing the impact of interactions with other pedestrians '*m*', 3) a repulsive force, $\boldsymbol{f}_j^{obs}$ representing the repulsive effects from obstacles like walls or other static objects and 4) an attractive force, $\boldsymbol{f}_j^a$ representing the force that attracts the pedestrians towards objects like window displays, street performers, etc. In this study, only the destination force and the pedestrian-pedestrian interaction force are considered as the repulsive force (no obstacles like walls found in the selected stretch) and the attractive force (no objects like window displays found in the stretch) are not necessary for a pedestrian to cross the road from his/her origin to his/her destination. Computation of destination force, $\boldsymbol{f}_j^0$ is given in the following equation.

$$\boldsymbol{f}_j^0(t) = \frac{1}{T_j}\left(v_j^0\, \boldsymbol{e}_{d;j}(t) - \boldsymbol{v}_j(t-1)\right) \tag{6.3}$$

$$\boldsymbol{e}_{d;j}(t) = \frac{(\boldsymbol{d}_j(t) - \boldsymbol{p}_j(t))}{|\boldsymbol{d}_j(t) - \boldsymbol{p}_j(t)|} \tag{6.4}$$

where, T_j = relaxation time of pedestrian, '*j*' (s); v_j^0= pedestrian's preferred speed (m/s), $\boldsymbol{v}_j(t-1)$ =pedestrian's walking speed at time (t-1) (m/s), $\boldsymbol{e}_{d:j}(t)$=directional vector from pedestrian, $'j'$ to destination, 'd' at time t, $\boldsymbol{d}_j(t)$= pedestrian's destination position at time t (m), and $\boldsymbol{p}_j(t)$= pedestrian's current position at time t (m). The desired direction of the pedestrian is assumed to be determined by the desired exit (destination) position. The destination position of a pedestrian is obtained from the field by observing the direction to which the pedestrians travel and the final exit point. From the field data, it is observed that destination position follows a normal distribution. Hence, in the simulation model, destination positions are determined randomly using this distribution.

The pedestrian-pedestrian interaction force is used to model the interaction between pedestrians and is implemented to prevent pedestrians from colliding with each other. Pedestrian-pedestrian interaction force, $\boldsymbol{f}_j^m$ is given by:

$$\boldsymbol{f}_j^{\,m}(t)= \boldsymbol{e}_{m;j}(t)U_{m:j}\exp[(\frac{R_{mj}-d_{mj}}{B_{mj}})] \tag{6.5}$$

$$\boldsymbol{e}_{m;j}(t)= \frac{(\boldsymbol{p}_m(t)-\boldsymbol{p}_j(t))}{|\boldsymbol{p}_m(t)-\boldsymbol{p}_j(t)|} \tag{6.6}$$

where, $\boldsymbol{e}_{m:j}$= directional vector from pedestrian, 'j' to pedestrian, 'm'; $U_{m:j}$= interaction strength (m/s^2); $B_{m:j}$= range of interaction (m); d_{mj} = distance (m) between the centers of pedestrians, 'j' and 'm'; R_{mj} = sum of the radii (m) of pedestrians, 'j' and 'm'; $\boldsymbol{p}_j(t)$= current position of pedestrian, 'j' at time t (m); $\boldsymbol{p}_m(t)$= current position of pedestrian, 'm' at time t (m). In addition to the above-mentioned forces, vehicle-pedestrian interaction force, $\boldsymbol{f}_j^{veh}$ is included in SFM to explain the approaching vehicle's (veh) influence on pedestrian. Hence, the total forces (m/s^2) of a pedestrian, 'j' is given by:

$$\boldsymbol{a}_j=\boldsymbol{f}_j^0+\boldsymbol{f}_j^{\,m}+\boldsymbol{f}_j^{veh} \tag{6.7}$$

where,

$$\boldsymbol{f}_j^{veh}=K\,I_p^2\,\boldsymbol{n}_j^{veh} \tag{6.8}$$

where, K = constant value; I_p= intensity of a position stressor; $\boldsymbol{n}_j^{veh}$ = two-dimensional unit vector directing from approaching vehicle to pedestrian 'j'. The approaching vehicle is considered as a position stressor which produces a source of stress for the pedestrian 'j'. The intensity of a stressor I_p is given by:

$$I_p=|p_j-p_{veh}| \tag{6.9}$$

where, p_j and p_{veh} = pedestrian position (m) and vehicle position (m), respectively. It should be noted that, $\boldsymbol{f}_j^{veh}$ is a slightly backward force at the beginning of walking, which causes the pedestrian's slight deceleration behavior. After passing through the vehicle, the pedestrian accelerates based on the forward force, $\boldsymbol{f}_j^{veh}$. After calculating the total forces, walking speed of pedestrian, *'j'* at time *t* is updated using the following equation.

$$\boldsymbol{v}_j(t) = \boldsymbol{v}_j(t\text{-}1) + \boldsymbol{a}_j(t)\,\Delta\, t \tag{6.10}$$

where, $\boldsymbol{v}_j(t)$= pedestrian's walking speed at time t (m/s), $\boldsymbol{v}_j(t\text{-}1)$ = pedestrian's walking speed at time t-1 (m/s); $\boldsymbol{a}_j(t)$= pedestrian's acceleration at time t (m/s^2); and $\Delta\, t$ = time step (s). Pedestrian's position $\boldsymbol{p}_j\,(t)$ at time t is updated using the following equation.

$$\boldsymbol{p}_j(t) = \boldsymbol{p}_j(t\text{-}1) + \boldsymbol{v}_j(t)\,\Delta\, t \tag{6.11}$$

where $\boldsymbol{p}_j\,(t\text{-}1)$ = pedestrian's position (m) at time t-1; $\boldsymbol{v}_j(t)$= pedestrian's walking speed at time t (m/s); and $\Delta\, t$ = time step (s).

If a pedestrian negotiates the gap in between two vehicles safely, Gipps model used to model vehicular flow is not sufficient to evaluate the approaching vehicle's behavior as behavioral patterns between vehicles and pedestrians vary. Hence, pedestrian's information is added to Gipps model to update approaching vehicle's speed during vehicle-pedestrian interactions, which has the following form:

$$v_{veh} = v_{gipps} + b(\,t_{veh}/t_j\,) \tag{6.12}$$

where, v_{veh} = approaching vehicle's speed with respect to the pedestrian's behaviour (m/s); v_{gipps} = approaching vehicle's speed from Gipps model (m/s), b = driver's deceleration (m/s^2); t_{veh} and t_j = vehicle's passing time (s) and pedestrian's crossing time (s), respectively. Figure 6.7 shows the vehicle-pedestrian interactions, and the logic for pedestrian movement and vehicle-pedestrian interaction is illustrated in Figure 6.8.

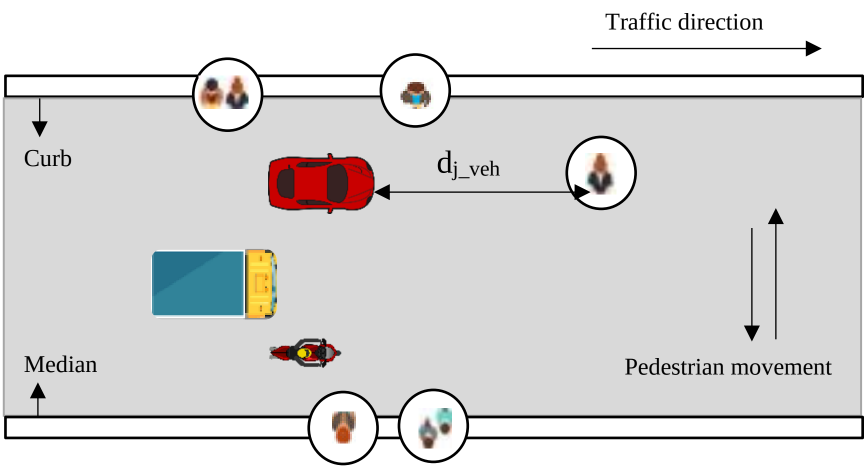

Figure 6.7 Vehicle-Pedestrian Interactions

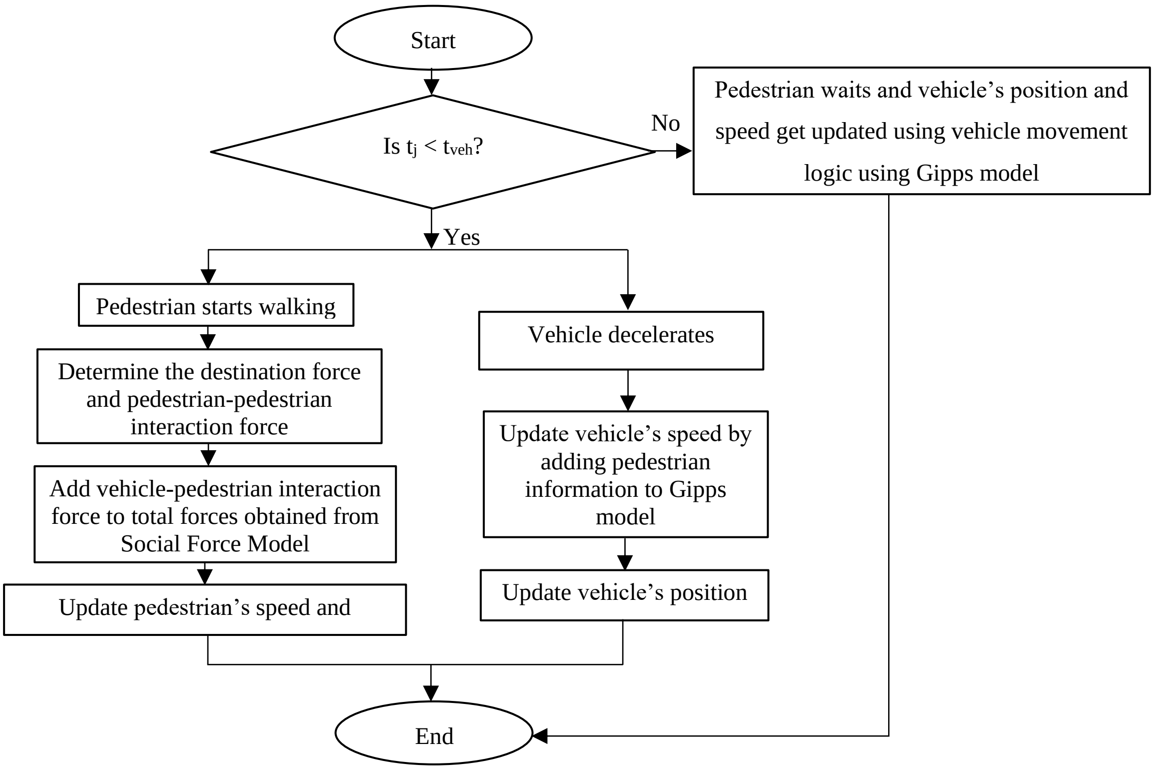

Figure 6.8 Logic for Pedestrian Movement and Vehicle-Pedestrian Interaction

The equation (6.12) is applicable only for the approaching vehicle within 25 m (d_{j_veh}) from the pedestrian and also if the approaching vehicle's speed is greater than 30 km/h (Wang *et al.* 2016). Otherwise, approaching vehicle's speed is updated using Gipps model. Once if the pedestrian starts walking and comes either directly in front or on the front right side of the approaching vehicle, vehicle's position to be updated is checked. If the vehicle's position is less than left hand position of pedestrian, vehicle moves to the updated position. Otherwise, vehicle's speed becomes zero and hence, vehicle remains at the present position. In these cases, pedestrian walks, and his/her position and speed get updated. These cases are applicable only for those pedestrians moving from median to curb, and for those traveling from curb to median the sides are considered vice-versa. Similarly, if the approaching vehicle comes directly in front of the pedestrian, pedestrian walking speed becomes zero and stop at the present position.

6.3.2 Computer Program for Simulating Vehicle-Pedestrian Interactions

The above-mentioned logics for developing the vehicle-pedestrian interaction model for urban roads are implemented in MATLAB programming language using object-oriented programming (OOP) concepts. In this model, along with super class *Vehicle*, another super class *Pedestrian* is included where the pedestrian properties are inherited by two pedestrian objects such as *MC* and *CM*. *MC* is an object of *Pedestrian* class that represents those pedestrians moving from median to curb and *CM* represents those passing from curb to median. *Pedestrian* class encapsulates the properties of a crossing pedestrian. Those properties are defined with a set of values for each type of pedestrian. The properties defined by the *Pedestrian* class build the structure of a pedestrian. This class consists of properties such as pedestrian type, pedestrian radius, pedestrian pattern, pedestrian direction (left or right) based on crossing pattern and maximum speed. Both *Vehicle* class and *Pedestrian* class are associated with *Link* class. *Link* class encapsulates the performance of vehicular and pedestrian flow. The major task of *Link* class is to implement the logics involved in the development of model such as generation, placement and movement of vehicles and pedestrians. The tasks involving pedestrian generation, pedestrian placement and pedestrian movement are performed using virtual functions such as *PedGeneration (), Placeped () and Pedmov ().* The required input includes various parameters such as scan interval, total simulation run time, simulation clock time, precision time, vehicular composition, pedestrian composition, length and width of the road, traffic flow and pedestrian flow. The virtual function, *link* declared in the *Main Simulator* class process the attributes such as length and width of the simulation stretch, traffic flow, pedestrian flow and simulation run time. A class diagram explaining the various classes and their relationship for developing a vehicle-pedestrian interaction model using microscopic simulation is presented in Figure 6.9.

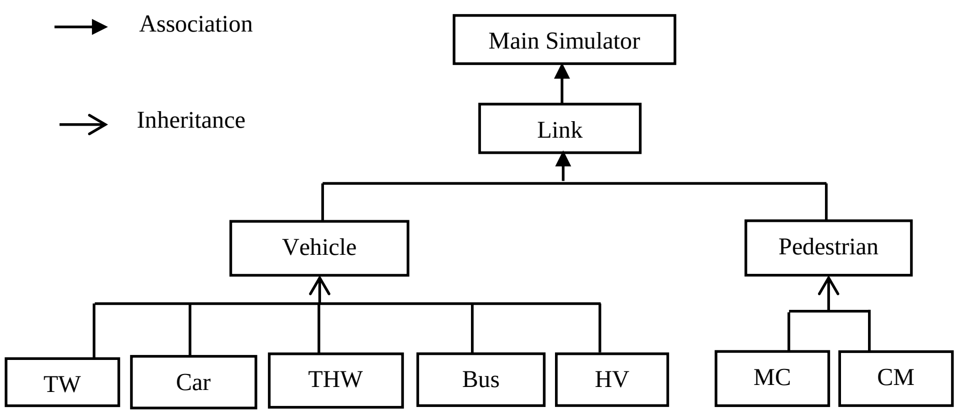

Figure 6.9 Class Diagram for Traffic Simulation of a Section with Undesignated Pedestrian Crossings

6.3.3 Calibration and Validation of Vehicle-Pedestrian Simulation Model

To verify the accuracy and credibility of the vehicle-pedestrian interaction model, calibration and validation are necessary. Although the vehicular parameters in Gipps model are calibrated for base model, the pedestrian parameters in SFM are also calibrated to accurately represent the vehicle-pedestrian interactions in the field. Calibration and validation of the vehicle-pedestrian simulation model are performed using the data collected from Hosur road, Bangalore city. The calibrated parameters of social force model (for simulating pedestrians) are mean preferred speed (v_j^0) (Laxman *et al.*, 2010), mean relaxation time (T_j) (Helbing and Molnar 1995), interaction strength ($U_{m:j}$) (Helbing *et al.*, 2005), range of interaction (B_{mj}) (Helbing *et al.*, 2005), and a constant (K) (used for calculating vehicle-pedestrian interaction force) (Chao *et al.*, 2015) (Table 6.2).

Table 6.2 Calibrated Parameters used in Vehicle-Pedestrian Interaction Model

Calibrated Parameters	**Pedestrian Parameters (Adopted from literature)**				
	Mean preferred speed, v_j^0 (m/s)	Mean relaxation time, T_j (s)	Interaction strength, $U_{m:j}$ (m/s^2)	Range of interaction, B_{mj} (m)	Constant, K
	1.3	0.5	3	0.2	0.012

The vehicle-pedestrian simulation model is then validated to compare vehicular and pedestrian behaviour with real-world data. Tables 6.3 and 6.4 give the comparison of observed and simulated mean speed values of vehicles and pedestrians, respectively and vehicular volume. The results indicate that MAPE values for mean class-wise and traffic stream speeds of vehicles, vehicular volume, and mean speeds of pedestrians is less than 9% which proves that the model is close to the real-world conditions. Independent t-test is also performed for 0.05 significance level to check the statistical validation of the PCU values. It is found that there is no significant difference between the simulated and observed speeds, and volume for different vehicle types. A paired t test is performed to check statistical validity of the simulated and observed mean speeds of vehicles and also, to compare the simulated and observed traffic volumes. The calculated value of t (t_0) for mean speeds is -2.07 against the critical value of 2.57 and it is found that the observed and simulated mean speeds agreed at 5% level of significance. The calculated value of t (t_0) for traffic volume 1.25 against the critical value of 2.57 and it is found that the observed and simulated traffic volume agreed at 5% level of significance.

Table 6.3 Comparison of Simulated and Observed Mean Speeds and Volume of Vehicles

Vehicle Type	Mean Speed Values (m/s)		MAPE (%)	Traffic Volume (veh/h)		MAPE (%)
	Simulated	Observed		Simulated	Observed	
Traffic stream	9.46	8.96	5.6	3299	3276	0.69
TW	8.64	9.29	6.9	1682	1671	0.65
Cars	8.36	9.02	7.3	297	294	1.02
THW	7.44	8.14	8.5	990	984	0.61
Buses	7.71	8.10	4.8	264	262	0.76
HV	7.60	8.00	5.0	66	65	1.53

Table 6.4 Comparison of Simulated and Observed Mean Speeds of Pedestrians

Pedestrian Type	Mean Speed Values (m/s)		MAPE (%)	Pedestrian Volume (ped/h)		MAPE (%)
	Simulated	Observed		Simulated	Observed	
Aggregate	1.00	0.95	5.2	400	404	1.0
Median to Curb	0.97	0.94	3.2	293	296	1.0
Curb to Median	1.02	0.97	5.1	107	108	0.9

6.3.4 Outputs from the Vehicle-Pedestrian Simulation Model

Following are the outputs of the vehicle-pedestrian simulation model which includes numerical results and animation of traffic flow.

- Vehicular and Pedestrian flow
- Mean speeds of all the vehicles and pedestrians
- Mean speeds of class-wise vehicles
- Time gaps of each vehicle and pedestrian
- Vehicle and Pedestrian trajectories
- Road capacity
- PCU values

Table IV.4 presents the trajectory and speed values of vehicles and pedestrians obtained from the vehicle-pedestrian simulation model. The vehicular flow levels are incremented from lower level to higher level until the maximum flow is obtained and this maximum flow is considered as the road capacity (veh/h). As speed values varied due to the presence of pedestrian crossings, PCU values of pedestrian section are determined. Simulated PCU values obtained from pedestrian model for TW, THW, car, bus and HV are 0.25, 0.87, 1, 5.34 and 4.28, respectively. These PCU values can be applied to all the urban streets where undesignated pedestrian crossings (devoid of other side frictions) are present, but only to the influence region of pedestrians (pedestrian section is considered as the influence region in this study). The capacity of pedestrian section is estimated as 3101 PCU/h (3384 veh/h). Vehicles moving on the road are depicted as rectangular blocks with appropriate dimensions (Venkatesan *et al.* 2008) and different colours based on vehicle types. The pedestrians are represented as circles with radii, 0.3 m (Helbing *et al.* 2005) where the pedestrians traveling from median to curb is represented by red circles and from curb to median are represented by blue circles. Figure 6.10 shows the snapshot of animated output of the model for a few continuous time steps.

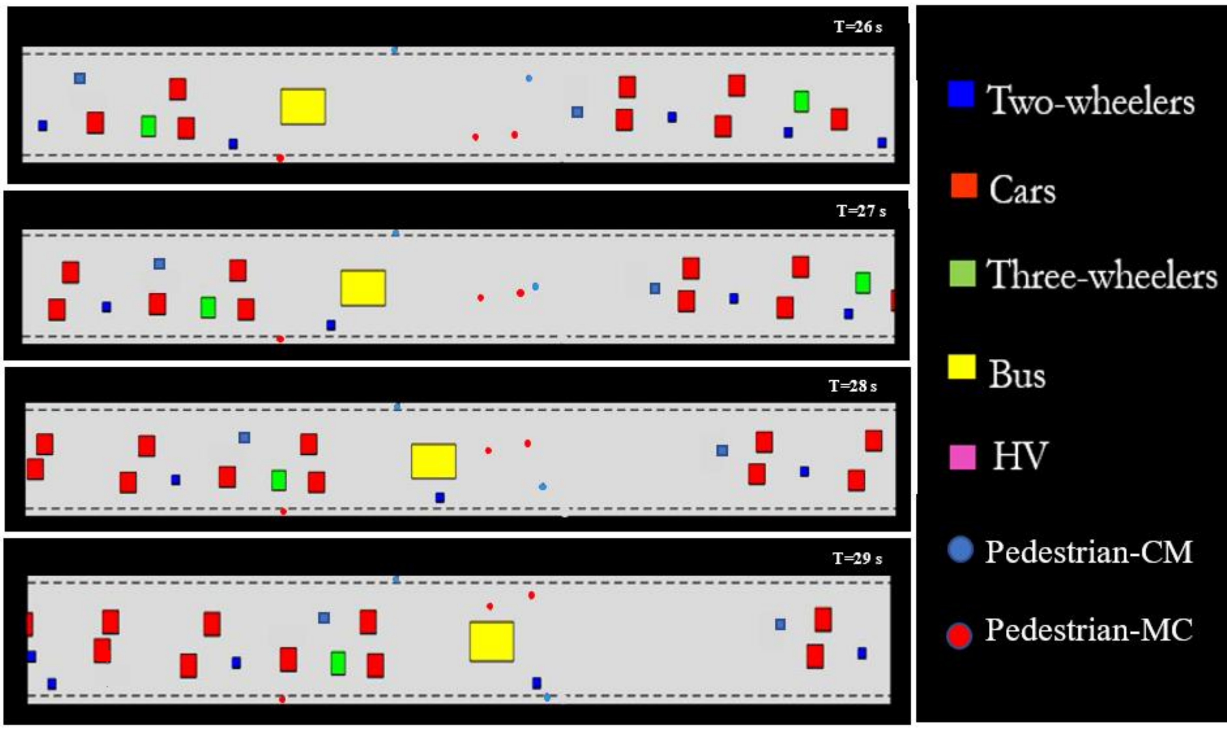

Figure 6.10 Snapshot of Animated Output of the Vehicle-Pedestrian Simulation Model for a Few Continuous Time Steps

6.4 SUMMARY

The modification of base model to incorporate the traffic manoeuvres of bus stop section is discussed in detail. The bus stop model is then validated using vehicular speed as the measure of effectiveness. The traffic data collected from HAL road are used for validation of the bus stop model. Also, the logics involved in modifying the base model to simulate real-world vehicle-pedestrian interactions are described in detail. The vehicle-pedestrian simulation model is calibrated using parameters of social force model for simulating pedestrians such as mean preferred speed, mean relaxation time, interaction strength, range of interaction, and a constant. The vehicle-pedestrian interaction model is then validated considering vehicular and pedestrian speeds as the measures of effectiveness. The vehicular and pedestrian data collected from Hosur road are used for validation of the vehicle-pedestrian simulation model.

CHAPTER 7

INFLUENCE OF CURBSIDE BUS STOP ON PCU AND CAPACITY

7.1 GENERAL

To study the impact of curbside bus stop on PCU and capacity values, simulated PCU and capacity values of ideal_bus section are compared with that of the section with a curbside bus stop. PCU and capacity values depend upon various influencing factors. So, investigation of relative influence of the guiding factors on PCU and capacity in the presence of curbside bus stop is necessary as it has received less attention in disordered traffic. For this purpose, sensitivity analysis is performed, and the comparison of simulated results obtained from base model (ideal_bus model) and modified model (bus stop model) are discussed in this chapter.

7.2 SENSITIVITY ANALYSIS OF PCU AND CAPACITY VALUES WITH AND WITHOUT CURBSIDE BUS STOP

Sensitivity analysis is performed, (1) To study the influence of parameters such as traffic volume, vehicular composition, bus proportion and share of stopping buses on PCU values for vehicle types, and (2) To study the influence of vehicular composition, bus proportion and share of stopping buses on capacity of urban roads.

7.2.1 Influencing Parameters and Values Assumed for Sensitivity Analysis of PCU Values

Following are the influencing factors and values used for sensitivity analysis on PCU.

(i) Case 1: Varying traffic volume

Traffic volume is varied from 1000-4500 veh/h in both sections with an increment of 500 veh/h for the observed vehicular composition (C) and bus proportion (2%).

(ii) Case 2: Varying vehicular composition

Five different vehicular compositions other than the observed composition are assumed from various studies on Indian urban roads (Asaithambi *et al*. 2012, Kotagi, 2019) in such a way that each vehicle type is dominating with respect to the observed composition. The following compositions are used in the study.

- C (observed composition): 53% TW, 34% cars, 10% THW, 2% buses and 1% HV.
- C1: 70% TW, 17% cars, 10% THW, 2% buses and 1% HV. (TW Dominant)
- C2: 50% TW, 14% cars, 34% THW, 1% buses and 1% HV. (THW Dominant)
- C3: 40% TW, 50% cars, 8% THW, 1% buses and 1% HV. (Car Dominant)
- C4: 40% TW, 30% cars, 9% THW, 20% buses and 1% HV. (Bus Dominant)
- C5: 50% TW, 30% cars, 8% THW, 2% buses and 10% HV. (HV Dominant)

In reference to the observed composition, two-wheelers are dominant in case C1, in case C2 three-wheelers contributes to a significant proportion. In contrast, cases C3, C4 and C5 have higher percentages of cars, buses and heavy vehicles, respectively. The traffic volume used in the model for all the compositions is the observed flow of 3970 veh/h and 3354 veh/h for ideal and bus stop sections at HAL road, Bangalore city, respectively.

(iii) Case 3: Varying proportion of buses

Proportion of buses is varied from 2% to 20% in increments of 2% in both ideal and bus stop sections. When the proportion of buses is increased, the proportion of other vehicles are evenly reduced and the share between stopping (70%) and non-stopping buses (30%) are maintained. The traffic volume used in the model for all the bus proportions is the observed flow of 3970 veh/h and 3354 veh/h for ideal and bus stop sections at HAL road, Bangalore city, respectively.

(iv) Case 4: Varying share of stopping buses

Share of stopping buses is varied from 0% to 100% with increments of 10% in bus stop section. Here, the proportion of buses (including stopping and non-stopping buses) is 2% (observed bus proportion). The traffic volume used in the model for all the bus proportions is the observed flow of 3970 veh/h and 3354 veh/h for ideal and bus stop sections at HAL road, Bangalore city, respectively.

(v) Case 5: Varying vehicular composition and traffic volume

For each vehicular composition (C, C1, C2, C3, C4 and C5), the traffic volumes in both the sections are increased from 500 veh/h to 4500 veh/h with an increment of 500 veh/h.

(vi) Case 6: Varying bus proportion and traffic volume

For each bus proportion incremented from 2 % to 20 %, the traffic volumes in both the sections are increased from 500 veh/h to 4500 veh/h with an increment of 500 veh/h.

(vii) Case 7: Varying share of stopping buses and traffic volume

For each share of stopping buses incremented from 0 % to 100 %, the traffic volumes in bus stop section are increased from 500 veh/h to 4500 veh/h with an increment of 500 veh/h.

(viii) Case 8: Varying bus proportion and share of stopping buses

For each share of stopping buses incremented from 0 % to 100 %, the bus proportions in bus stop section are increased from 2 % to 20 % with an increment of 2 %.

(ix) Case 9: Varying vehicular composition and share of stopping buses

For each vehicular composition (C, C1, C2, C3, C4 and C5), share of stopping buses are incremented from 0 % to 100 % with increments of 10%.

In bus stop section, proportion of buses given in cases 1, 2, 3, 5 and 6 are shared by stopping and non-stopping buses with 70% and 30% of total proportion of buses, respectively.

7.2.1.1 Impact of Varying Traffic Volume on PCU Values

When the PCU values for different vehicle types of ideal and bus stop sections are analysed separately, it is observed that increase in traffic flow levels results in a decreasing trend of PCU values for buses and HV. A reduction of 2.3% and 3.8% in PCU values for buses and HV is observed in ideal section, respectively with increase in traffic from 1000 veh/h to 4500 veh/h. PCU values for buses and HV had a reduction of 10.2% and 6.1% in bus stop section, respectively with increase in traffic from 1000 veh/h to 3500 veh/h. The effect of traffic volume caused less change in PCU values for all vehicle types when the flow level is increased after 3500 veh/h in case of bus stop section as the volume approaches the capacity of bus stop section. HV and buses have lower speed ratios at higher flow levels due to their larger sizes resulting in lower PCU values. However, increase in flow levels showed an increase in PCU values for TW and THW in both the sections. This might be due to their smaller sizes and higher manoeuverability compared to cars. But, when comparing the PCU values with and without bus stop, increase in flow levels caused an increase of 4.1% and 6.3% in PCU values for TW from ideal to bus stop section at flow levels of 1000 veh/h and 4500 veh/h, respectively. PCU values for THW increased by 2.5% and 5.2% in bus stop section compared to that of ideal section at flow levels of 1000 veh/h and 4500 veh/h, respectively. This is because TW, THW and cars moving with their normal speed had to reduce their speed to a greater extent as they find a bus stopped near the bus stop. Hence, TW and THW with smaller sizes and higher manoeuverability try to travel in between two vehicles when they reach near the bus stop even in higher flow levels, thereby resulting in higher speed ratios. As HVs are travelling at a lower speed compared to TW and THW, they reduce their speed only to a smaller extent. Hence, speed ratio between car and HV decline causing a reduction in PCU of HV by 7.1% and 8.8% at traffic flow levels of 1000 veh/h and 4500 veh/h, respectively. Speeds of a few buses drop down to zero m/s as they stop near the bus stop. Thus, speed ratio between car and bus increases resulting in higher PCU values of buses in bus stop section compared to that of ideal section (Figure 7.1(a)).

7.2.1.2 Impact of Varying Vehicular Composition on PCU Values

From the analysis, it is observed that in both ideal and bus stop sections, PCU values for all vehicle types in ideal and bus stop sections did not show much change when there is a larger proportion of TW (C1). The larger proportion of TW do not cause much congestion on the road as they provide more space for other vehicles to travel due to their smaller sizes. However, PCU values of TW and THW are found to be higher when the proportion of THW (C2), cars (C3), buses (C4) and HV (C5) are more (Figure 7.1(b)). But, HV and buses move at lower speeds resulting in lower speed ratios and hence their PCU values reduces. Furthermore, it is noticed that when the proportion of TW is dominant (C1), PCU of TW and THW had an increase of 3.2% and 4.3%, respectively from ideal to bus stop section but PCU of HV reduced by 6.6%. Moreover, when the proportions of THW (C2), cars (C3), buses (C4) and HV (C5) are dominant, PCU value of HV in bus stop section reduced by 9.2%, 11.1%, 8.8% and 6.9%, respectively compared to ideal section. This might be due to the reduction in speed of HV even after finding a bus stopping in the bus stop. In contrast, TW and THW had an increase in their PCU values because of their higher relative speed with respect to car. A few buses classified as stopping buses stop near bus stop resulting in the reduction of their speed up to zero m/s. Hence, in all the cases of vehicular composition (C, C1, C2, C3, C4, C5), speed ratio of buses increases leading to an increase in PCU values.

7.2.1.3 Impact of Varying Proportion of Buses on PCU Values

Increase in proportion of buses from 2% (observed bus proportion) to 20% showed an increase in PCU values for TW and THW of both the sections (Figure 7.1(c)). Due to smaller sizes and higher manoeuverability of TW and THW, speeds reduce when there is higher proportion of buses resulting in higher speed ratios. However, as the buses and HV are travelling at lower speeds even at lower proportion of buses, it results in lower speed ratios and hence, their PCU values reduce in both the sections. The results of comparison between PCU values for different vehicles with and without curbside bus stop shows that higher values of PCU are observed for HV (within a range of 3.99 to 4.5) in case of ideal section compared to bus stop section (within a range of 3.02 to 4.13). In this case, speed ratios of HV with respect to car reduces with the increment of bus proportion whereas TW and THW show an increase in PCU values as their speed ratios increases due to the presence of bus stop. PCU values of buses (within a range of 4.2 to 4.9) are found to be lower in ideal section compared to that of bus stop section (within a range of 5.2 to 6.3) with increment of 2 to 20 % as speeds of a few buses reduce up to zero m/s as they stop in the bus stop.

7.2.1.4 Impact of Varying Share of Stopping Buses on PCU Values

The share of stopping buses is varied from 0% to 100% in bus stop section to study its impact on PCU values (Figure 7.2). In ideal section, buses are not categorized as stopping and non-stopping buses and thus, PCU values for all vehicle types do not vary. But in case of bus stop section as the share of stopping buses in total bus proportion increases, the PCU values of buses (including stopping and non-stopping buses) increase drastically by 29%. This is because a greater number of stopping buses in the total proportion of buses causes a higher reduction in speeds of the buses as these stopping buses completely come to rest. Here, when the share of non-stopping buses is increased, PCU values of buses are found to be lower. The PCU values of TW, THW and HV in bus stop section followed the same trend as in case 3 (impact of varying proportion of buses on PCU values) i.e., PCU values for TW and THW increased by 10% and 5.1%, respectively whereas PCU values for HV reduced by 9%.

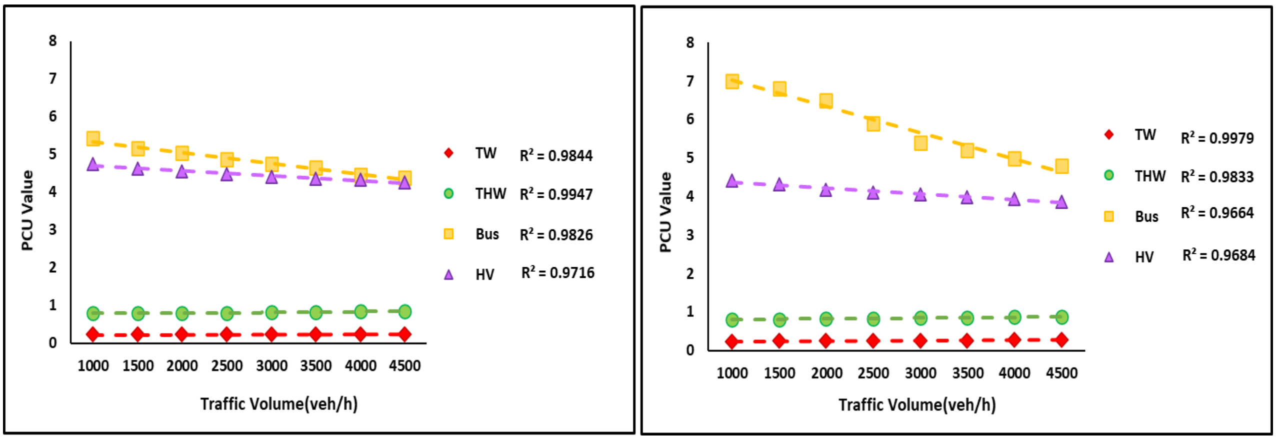

(a) Effect of Traffic Volume

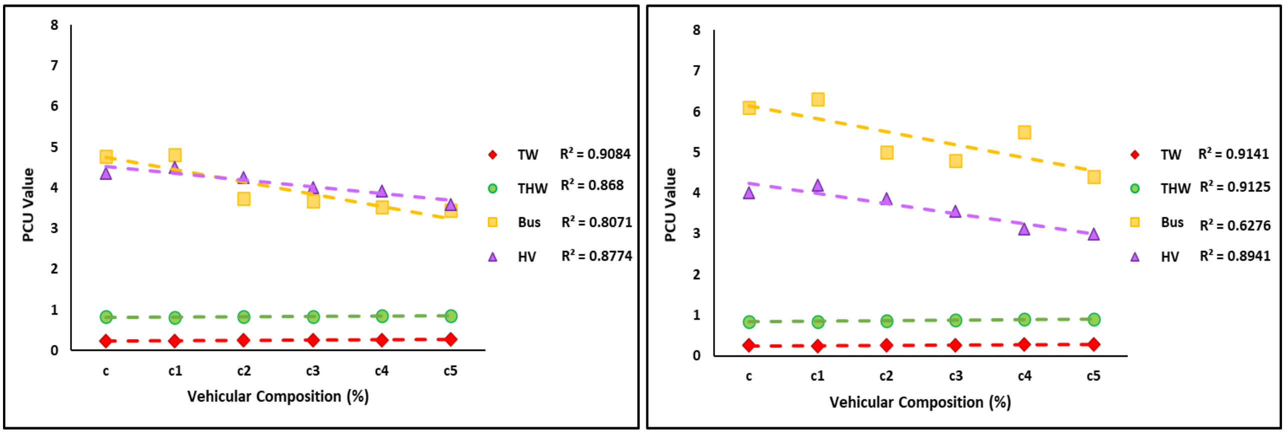

(b) Effect of Vehicular Composition

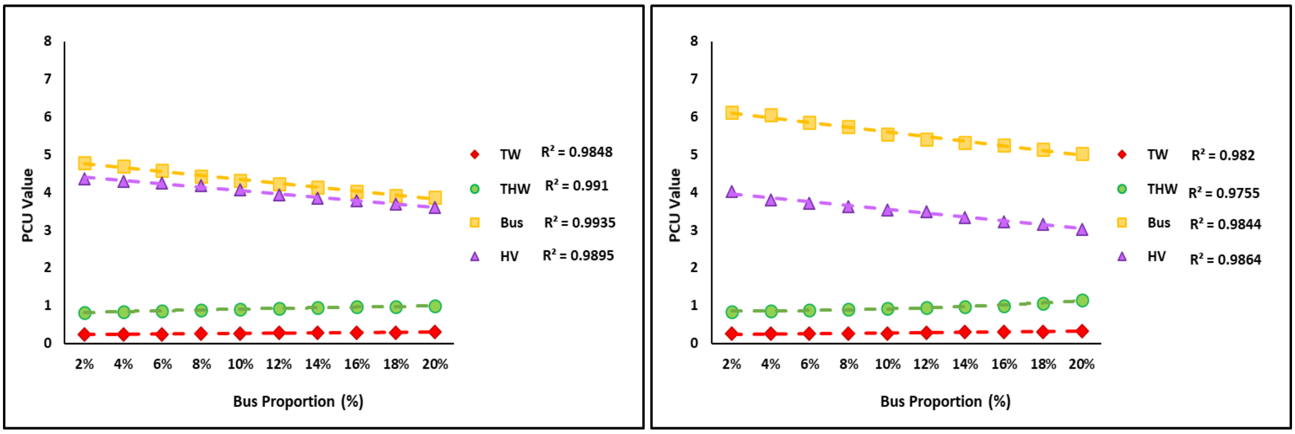

(c) Effect of Bus Proportion

(i) **(ii)**

Figure 7.1 PCU Values for Varying Traffic Volume, Composition and Bus Proportion for (i) Ideal and (ii) Bus Stop Section

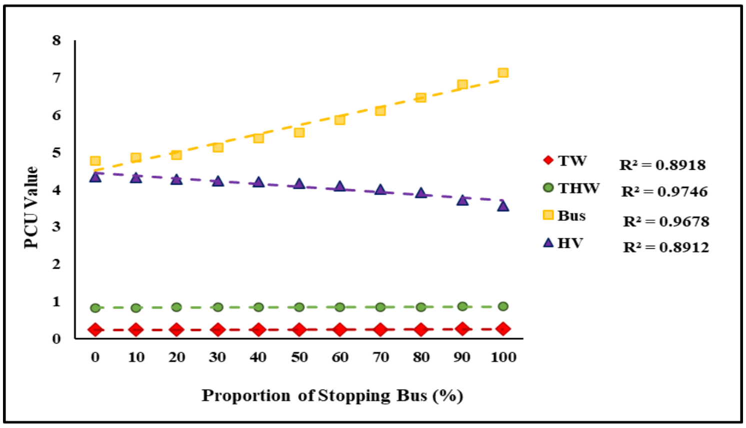

Figure 7.2. PCU Values for Varying Share of Stopping Buses in Bus Stop Section

7.2.1.5 Impact of Varying Traffic Volume and Vehicular Composition on PCU

To analyze the variation in PCU values with varying traffic volume and vehicular composition, the traffic volume is increased from 1000 veh/h to 4500 veh/h for each vehicular composition (C, C1, C2, C3, C4 and C5). Figures 7.3-7.10 illustrate the variations in PCU values for different vehicle types due to the impact of varying traffic volume and vehicular compositions of ideal and bus stop sections. From the figure, it is noticed that irrespective of the vehicular composition when the traffic volume increased, PCU values for TW and THW increased, and PCU values for bus and HV decreased for both the sections when analyzed separately. But, when both the sections are compared with each other, PCU values for TW, THW and bus increased whereas PCU values for HV decreased.

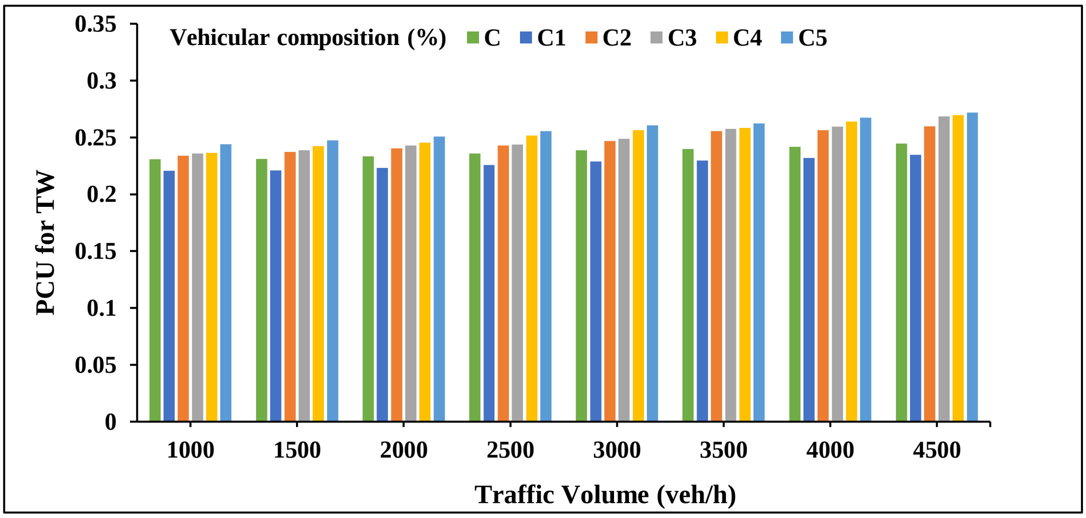

Figure 7.3 Variations in PCU Values for TW with Varying Traffic Volume and Vehicular Composition in Ideal Section

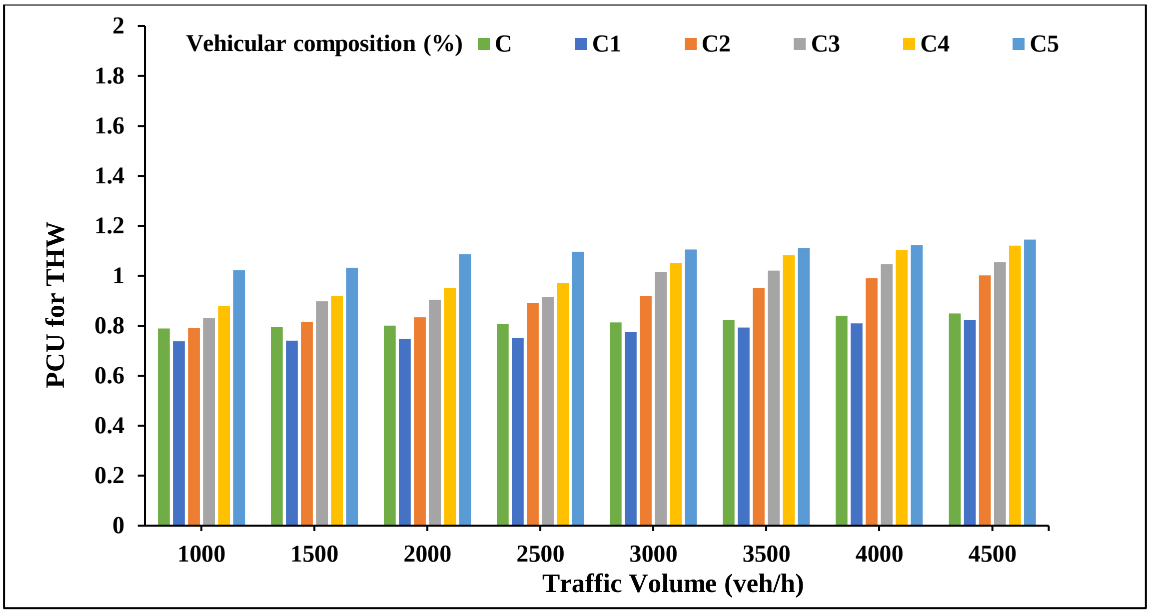

Figure 7.4 Variations in PCU Values for THW with Varying Traffic Volume and Vehicular Compositions in Ideal Section

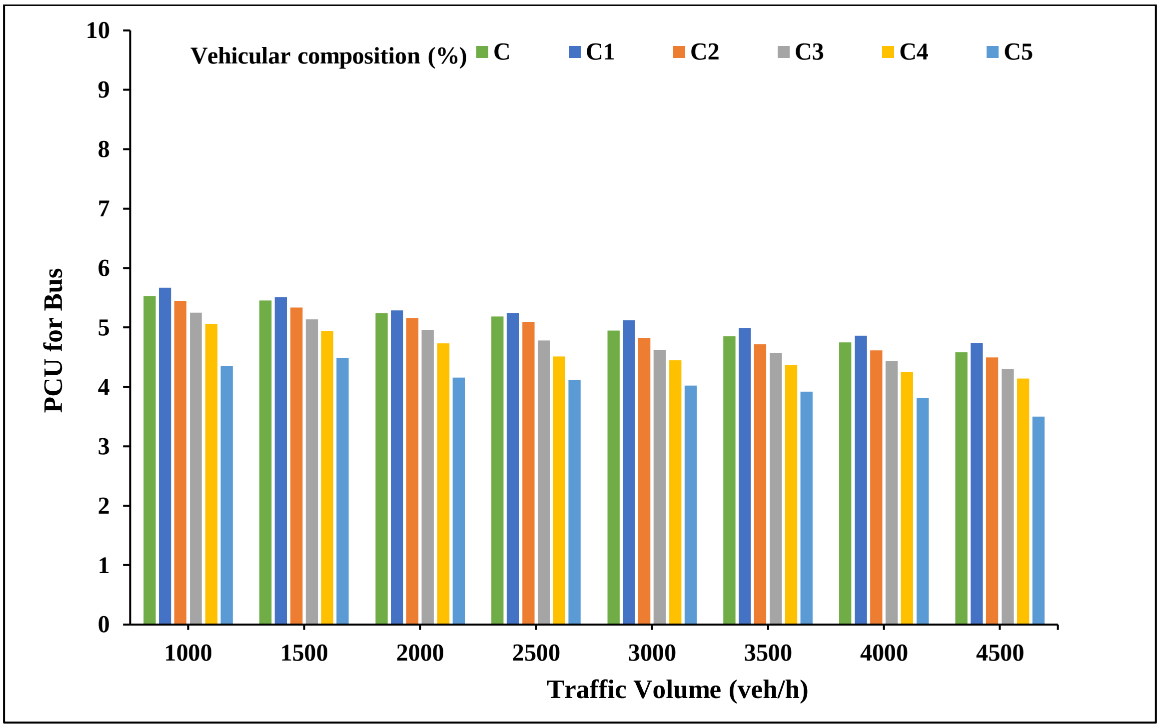

Figure 7.5 Variations in PCU Values for Bus with Varying Traffic Volume and Vehicular Compositions in Ideal Section

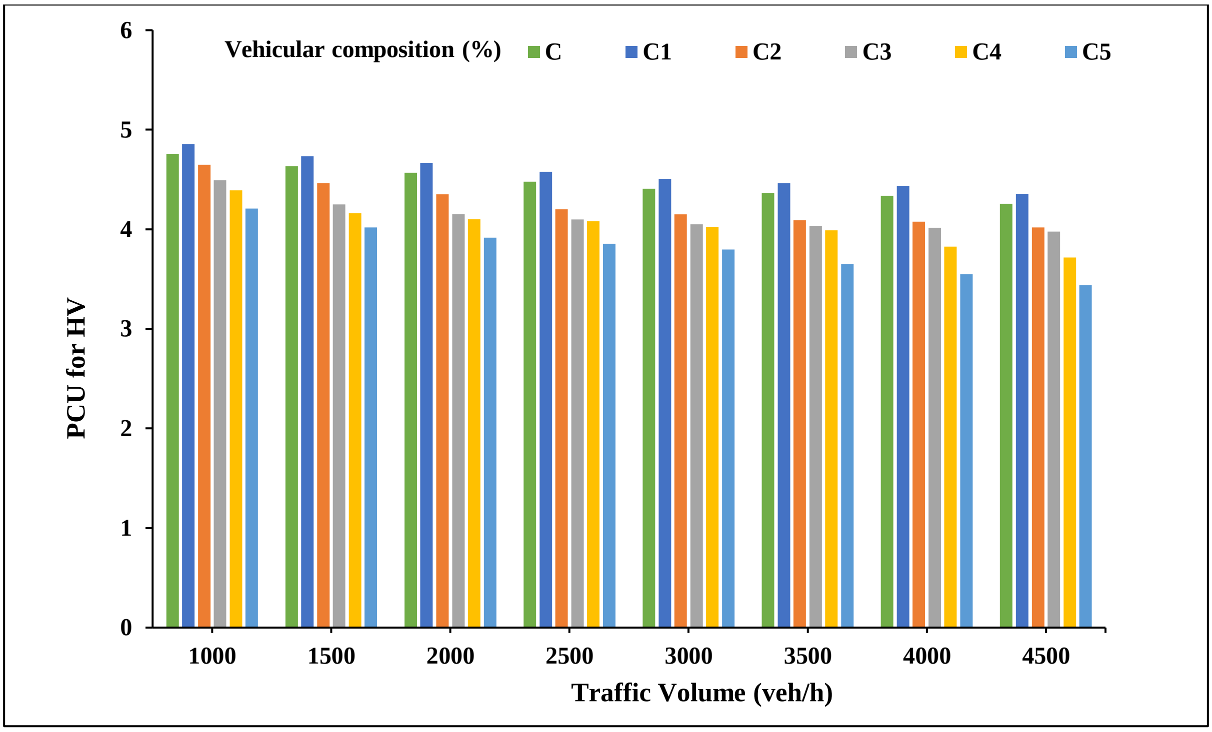

Figure 7.6 Variations in PCU Values for HV with Varying Traffic Volume and Vehicular Compositions in Ideal Section

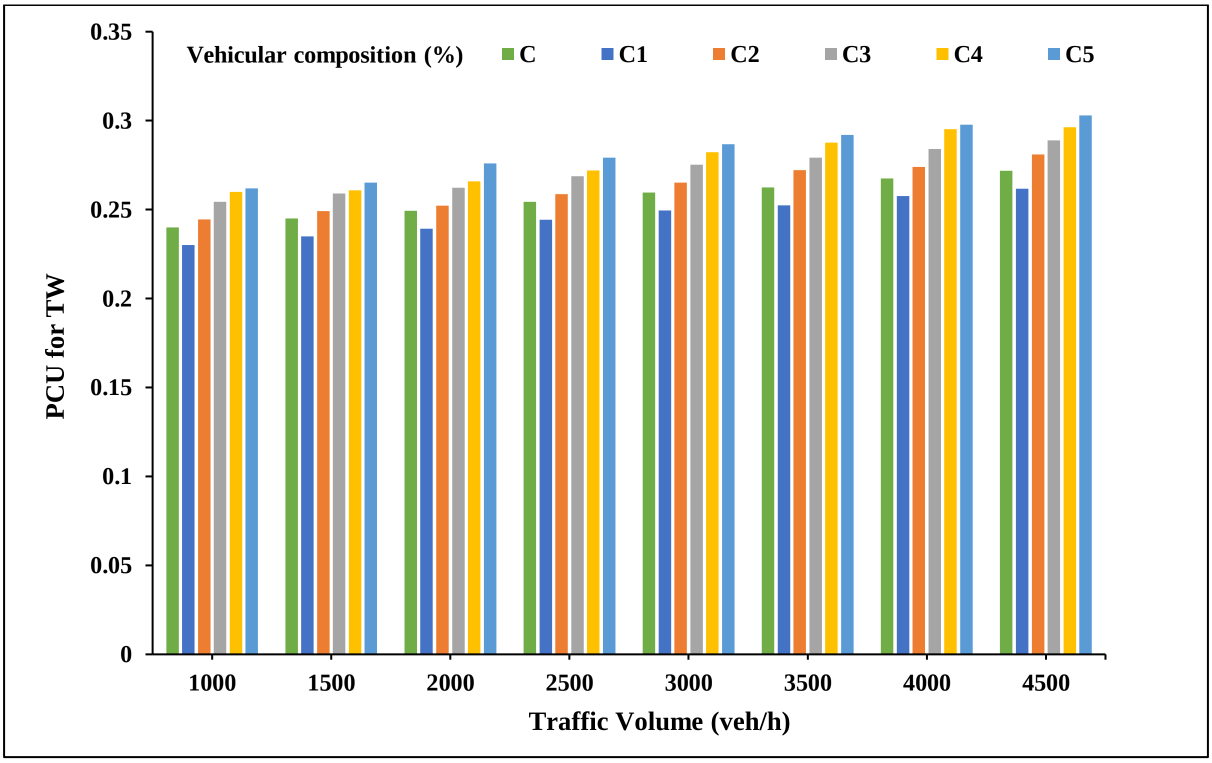

Figure 7.7 Variations in PCU Values for TW with Varying Traffic Volume and Vehicular Compositions in Bus Stop Section

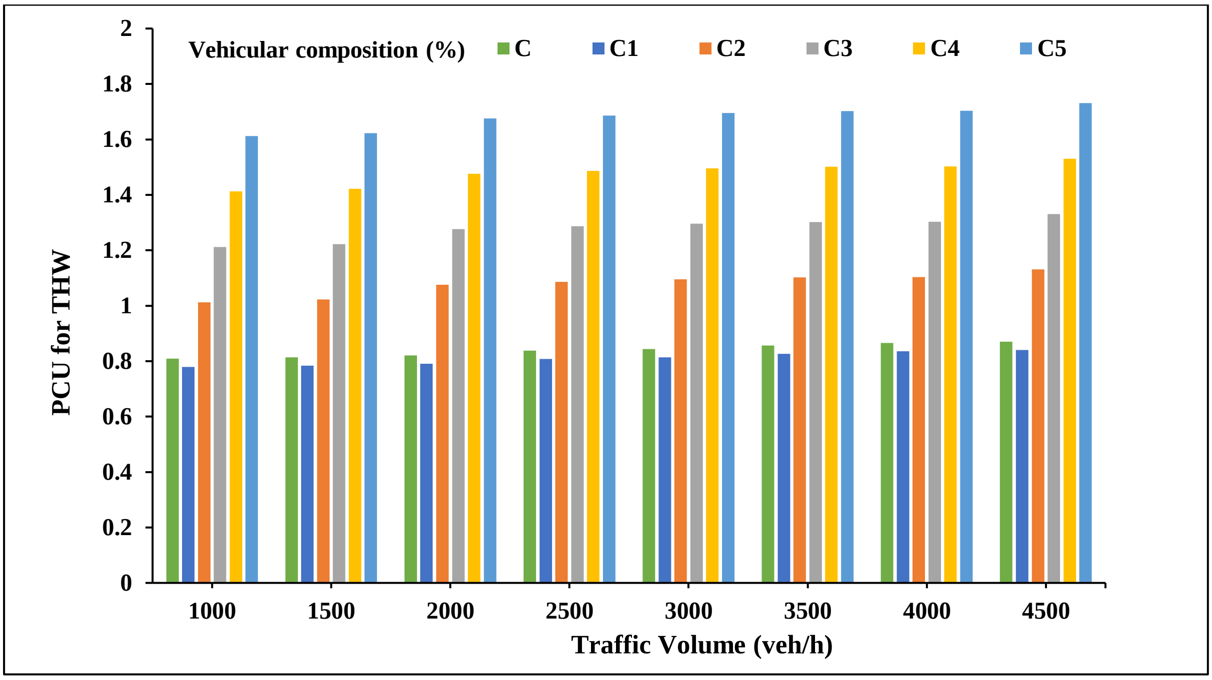

Figure 7.8 Variations in PCU Values for THW with Varying Traffic Volume and Vehicular Compositions in Bus Stop Section

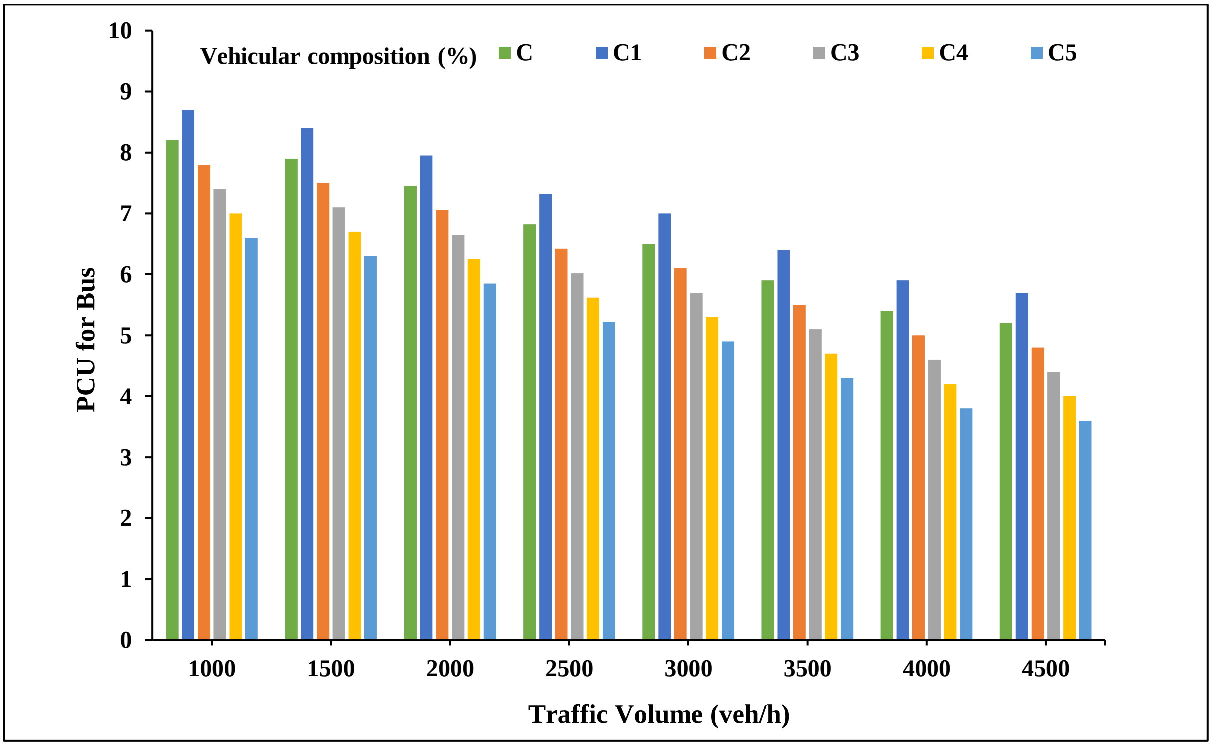

Figure 7.9 Variations in PCU Values for Bus with Varying Traffic Volume and Vehicular Compositions in Bus Stop Section

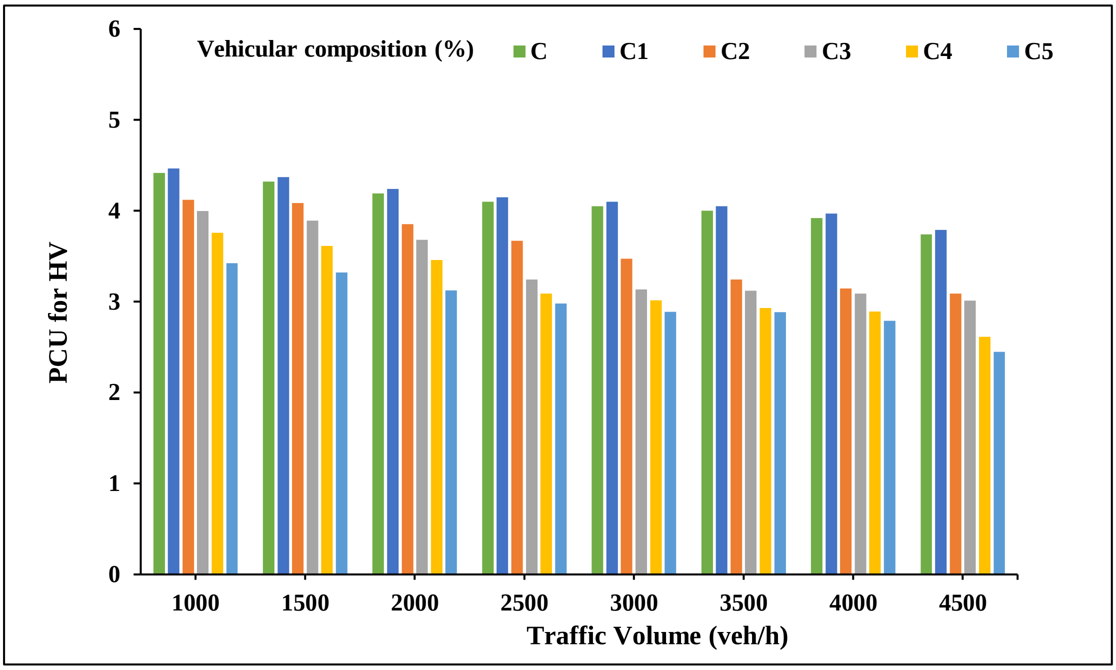

Figure 7.10 Variations in PCU Values for HV with Varying Traffic Volume and Vehicular Compositions in Bus Stop Section

7.2.1.6 Impact of Varying Proportion of Buses and Traffic Volume on PCU Values

For investigating the impact of proportion of buses and traffic volume on PCU values with and without the presence of curbside bus stop, the traffic volume is increased from 1000 veh/h to 4500 veh/h for each bus proportion (incremented from 2 to 20%). Initially PCU values for each type of vehicle are analyzed separately for ideal and bus stop section. Based on the analysis, it is observed that when the traffic volume is increased for each bus proportion; PCU values for TW and THW increased slightly, and PCU values for bus and HV decreased for both the sections. As explained in Section 7.2.1.1, HV and buses have lower speed ratios at higher flow levels due to their larger sizes resulting in lower PCU values. Due to smaller sizes and higher manoeuverability of TW and THW, they have higher speed ratios at higher flow levels resulting in higher PCU values. At higher levels of traffic volume and bus proportion, the section with curbside bus stop will be at its congested stage due to the stoppage of a greater number of buses at the curb. Thus, even with the smaller sizes and higher manoeuverability of TW and THW, they do not get enough space to move which reduces their speed drastically resulting in higher increase in PCU values. Similarly, a higher reduction in PCU values of HV is observed. When comparing the PCU values with and without bus stop, increase in flow levels for each bus proportion caused an increase in PCU values for TW and THW from ideal to bus stop section. This is because TW, THW and cars moving with their normal speed had to reduce their speed more as they approach a stopped bus near the bus stop. Hence, TW and THW having smaller sizes and higher manoeuverability try to travel in between two vehicles when they reach near the bus stop even in higher flow levels, thereby resulting in higher speed ratios. As HVs are travelling at a lower speed compared to TW and THW, they reduce their speed only to a small extent. Hence, speed ratio between car and HV decline causing a reduction in PCU of HV. Speeds of a few buses drop down to zero m/s as they approach near the bus stop. Thus, speed ratio between car and bus increases resulting in higher PCU values of buses in bus stop section compared to that of ideal section. Figures 7.11-7.18 illustrate the variations in PCU values for different vehicle types of ideal and bus stop sections due to the impact of varying traffic volume and bus proportion.

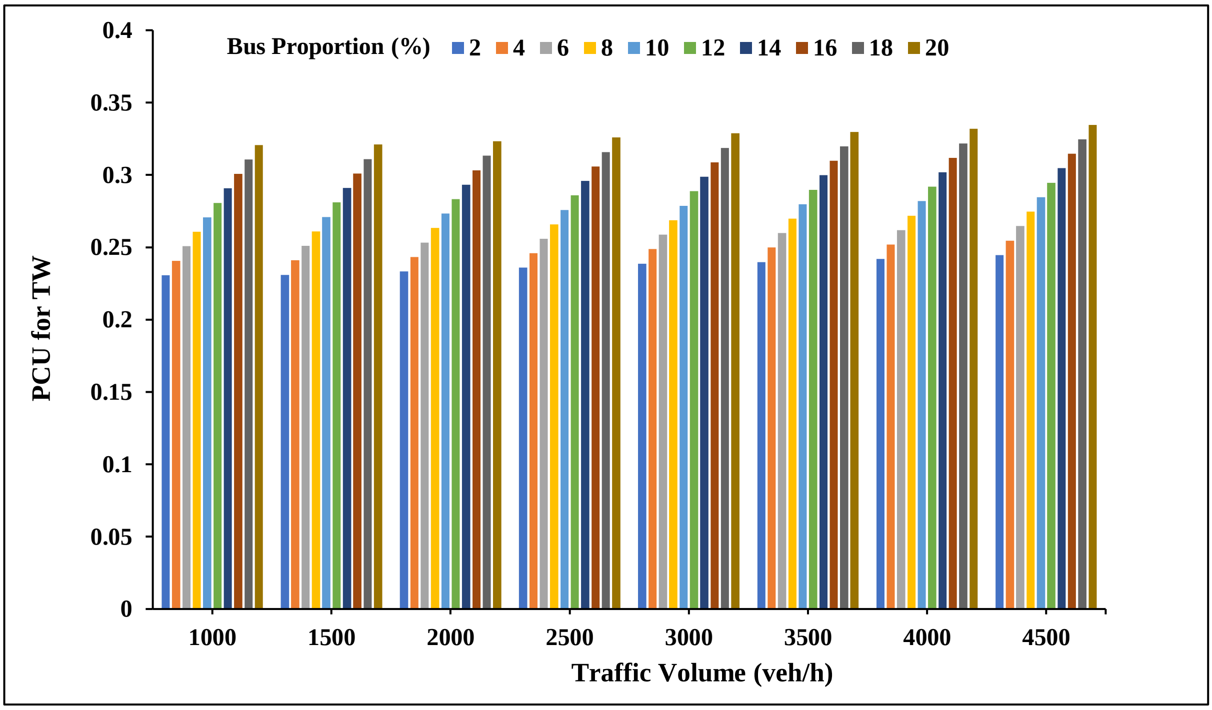

Figure 7.11 PCU Values for TW with Varying Traffic Volume and Bus Proportion in Ideal Section

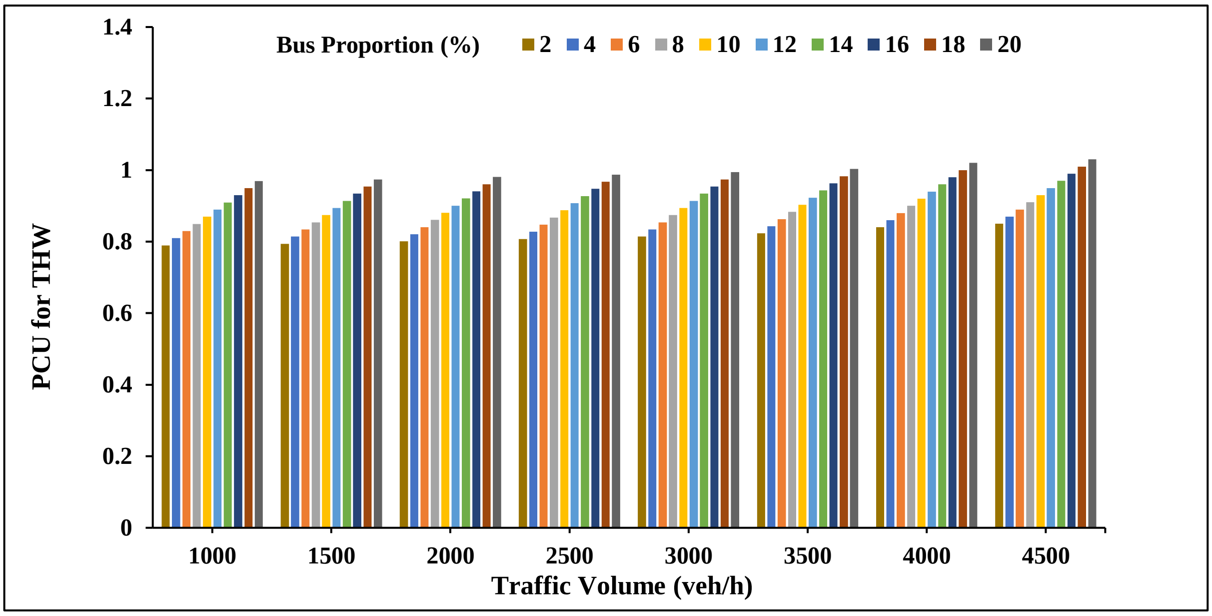

Figure 7.12 Variations in PCU Values for THW with Varying Traffic Volume and Bus Proportion in Ideal Section

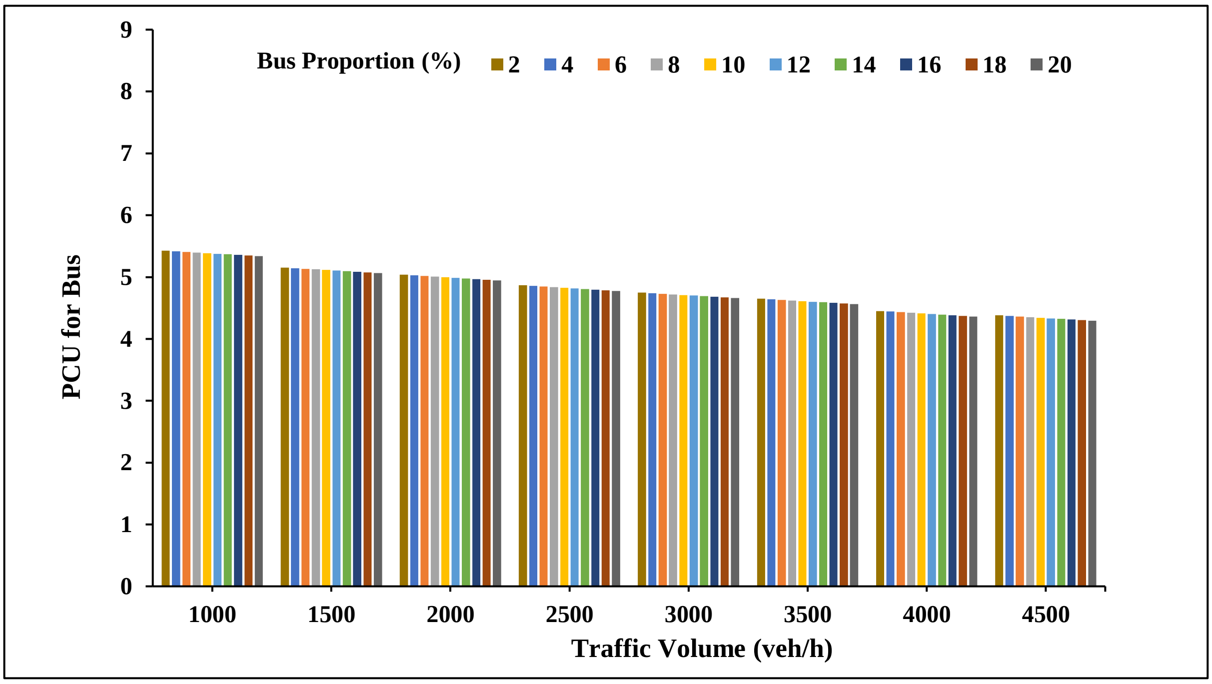

Figure 7.13 Variations in PCU Values for Bus with Varying Traffic Volume and Bus Proportion in Ideal Section

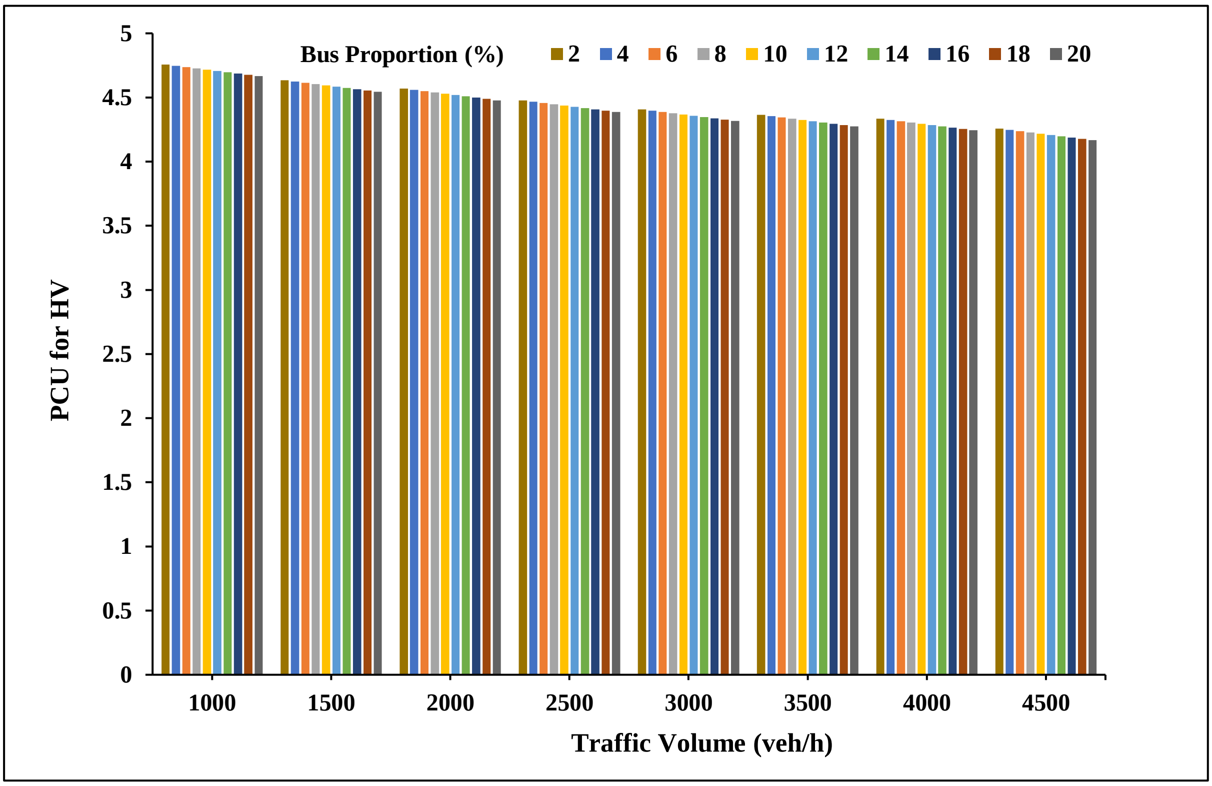

Figure 7.14 Variations in PCU Values for HV with Varying Traffic Volume and Bus Proportion in Ideal Section

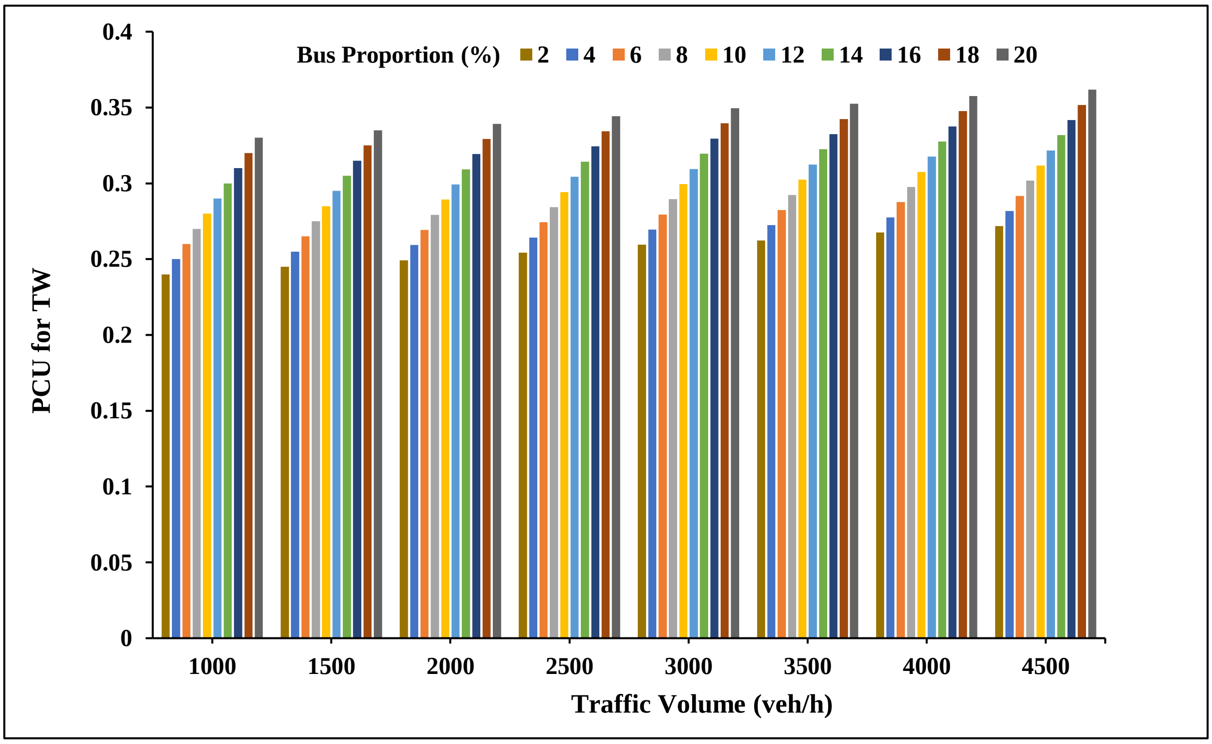

Figure 7.15 Variations in PCU Values for TW with Traffic Volume and Bus Proportion in Bus Stop Section

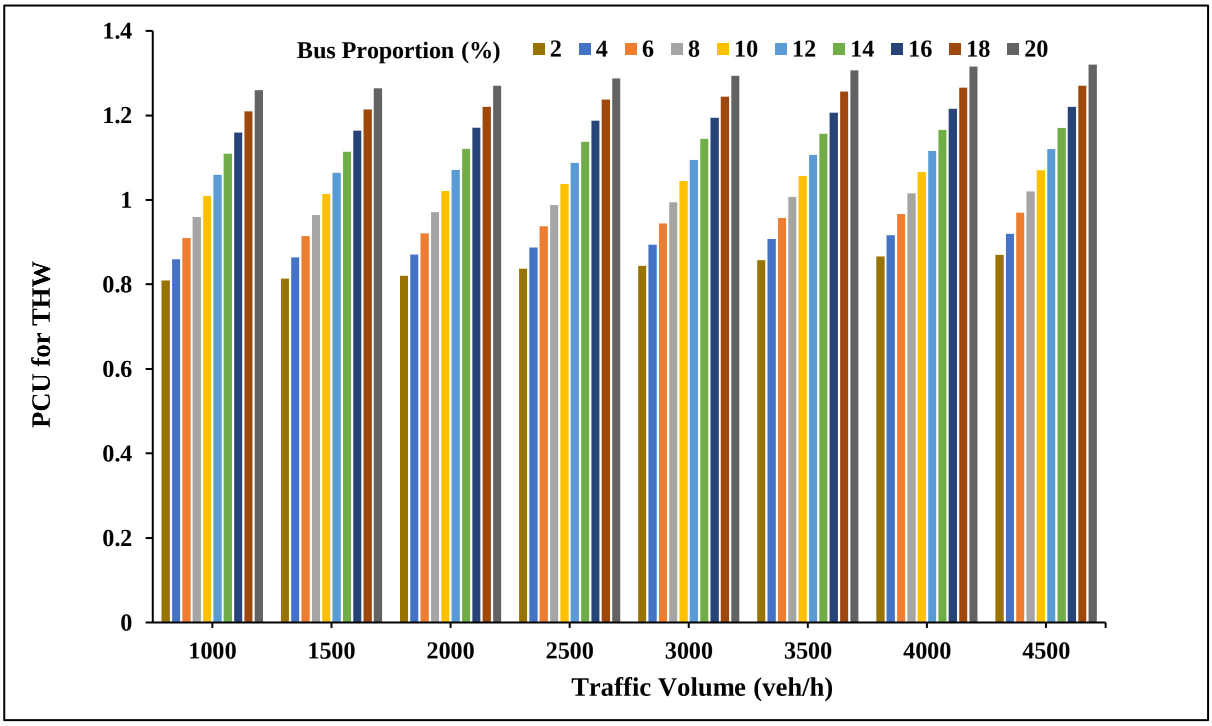

Figure 7.16 Variations in PCU Values for THW with Varying Traffic Volume and Bus Proportion in Bus Stop Section

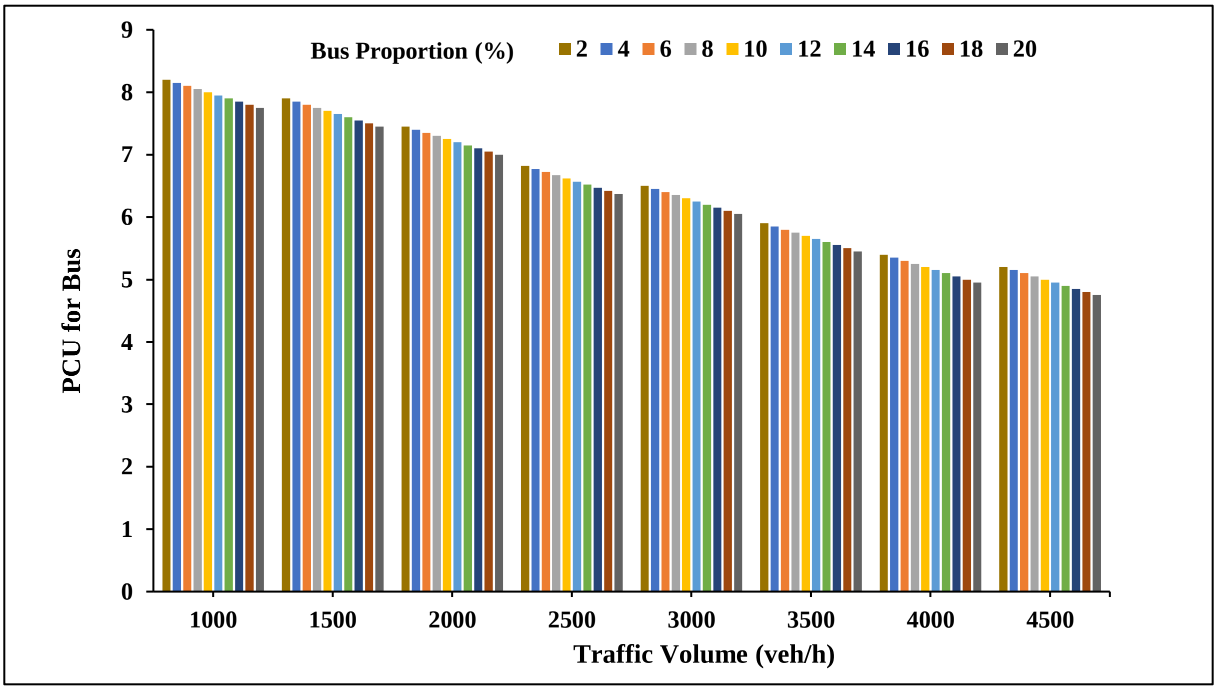

Figure 7.17 Variations in PCU Values for Bus with Varying Traffic Volume and Bus Proportion in Bus Stop Section

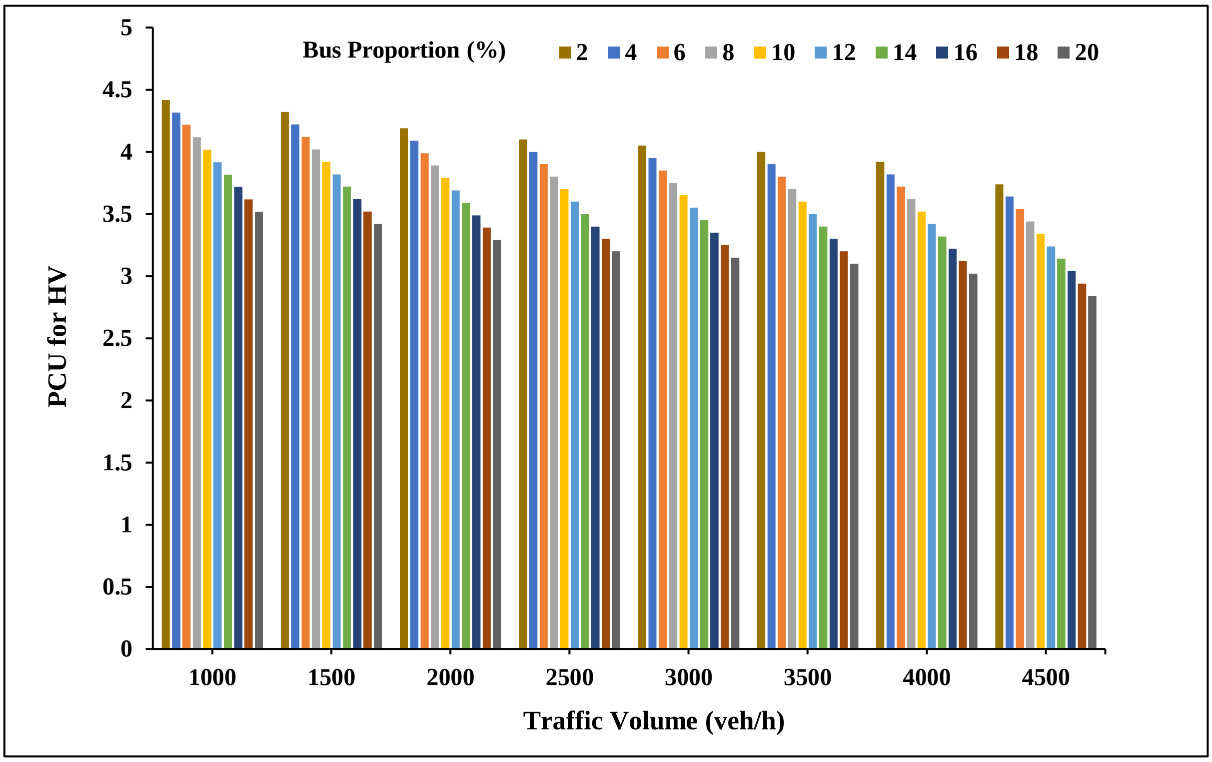

Figure 7.18 Variations in PCU Values for HV with Varying Traffic Volume and Bus Proportion in Bus Stop Section

7.2.1.7 Impact of Varying Share of Stopping Buses and Traffic Volume on PCU Values

To investigate the effect of varying share of stopping buses and traffic volume, the share of stopping buses in bus stop section is increased from 0% to 100% for each traffic volume (1000 veh/h to 4500 veh/h). In ideal section, buses are not categorized as stopping and non-stopping buses and thus, PCU values for all vehicle types in ideal section remains the same. PCU values for TW, THW and HV in bus stop section follow the same trend as in cases 5 (impact of varying vehicular composition and traffic volume on PCU values) and 6 (impact of varying proportion of buses and traffic volume on PCU values) whereas PCU values of bus increases with increase in share of stopping buses for each traffic volume. As the share of stopping buses becomes 100% with higher traffic volume, the speeds of all the buses become zero resulting in higher speed ratios and higher PCU values. Figures 7.19 - 7.22 illustrate the variations in PCU values for different vehicle types for varying traffic volume and share of stopping buses in bus stop section.

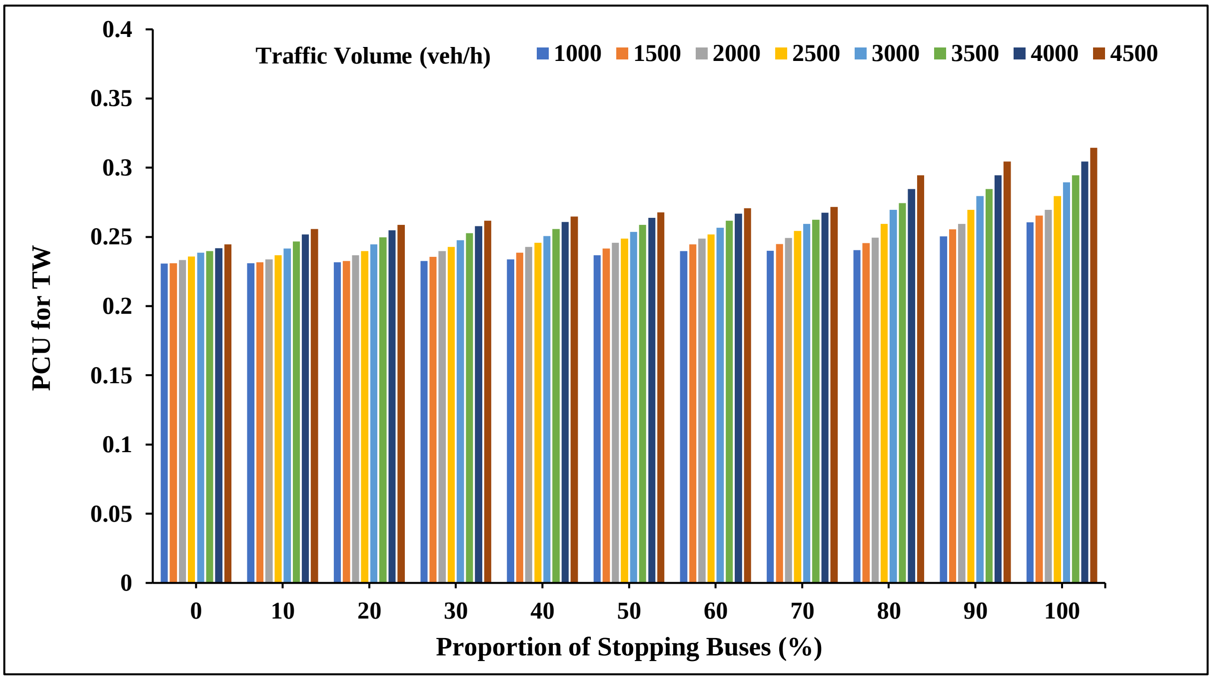

Figure 7.19 Variations in PCU Values for TW with Varying Traffic Volume and Share of Stopping Buses in Bus Stop Section

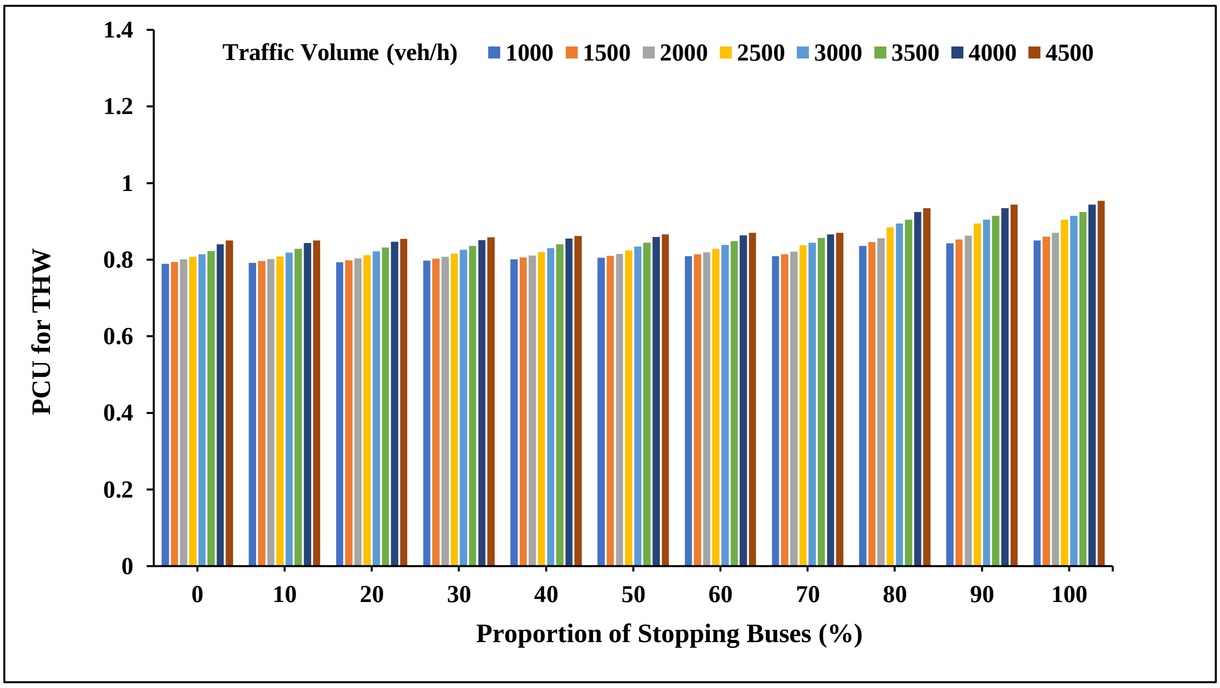

Figure 7.20 Variations in PCU Values for THW with Varying Traffic Volume and Share of Stopping Buses in Bus Stop Section

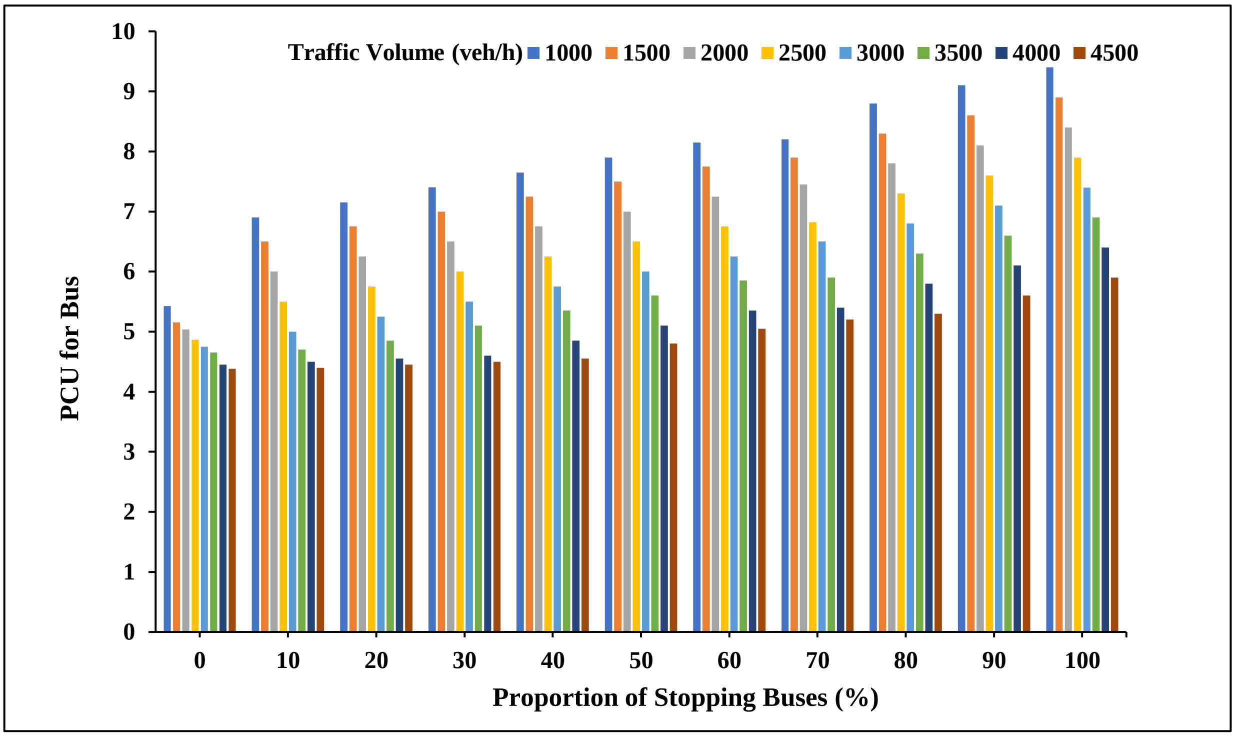

Figure 7.21 Variations in PCU Values for Bus with Varying Traffic Volume and Share of Stopping Buses in Bus Stop Section

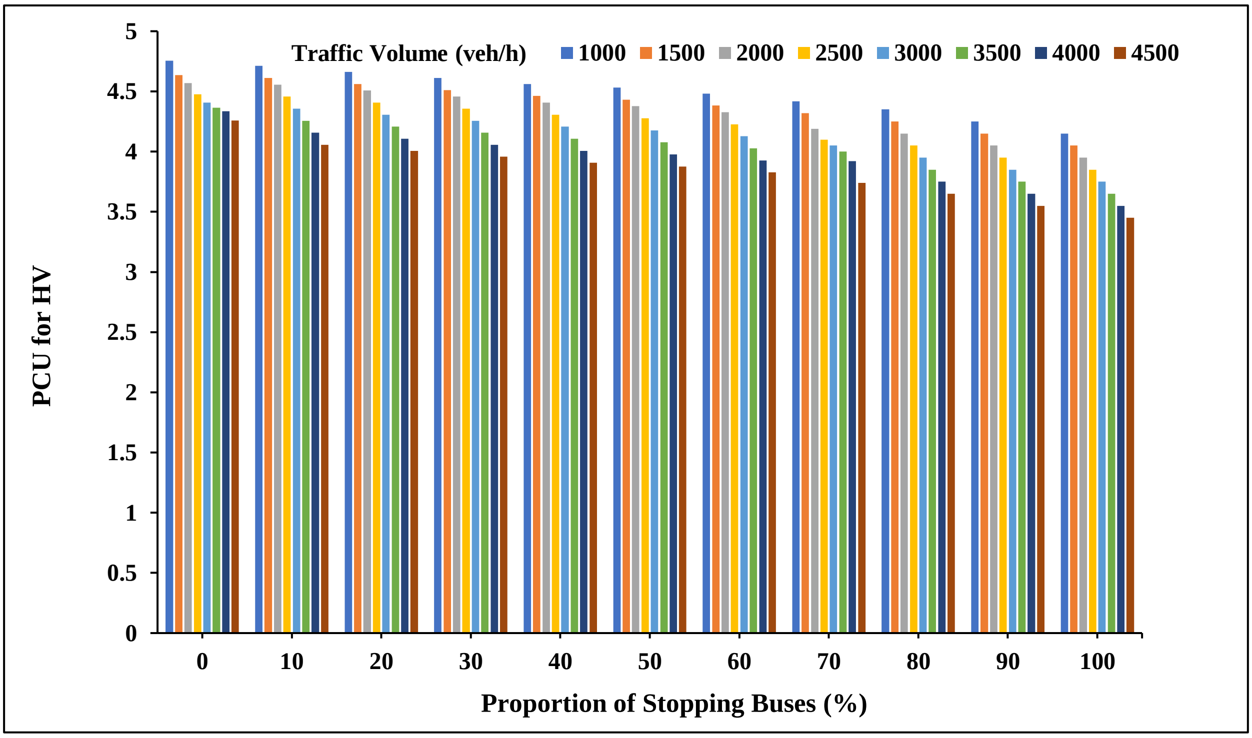

Figure 7.22 Variations in PCU Values for HV with Varying Traffic Volume and Share of Stopping Buses in Bus Stop Section

7.2.1.8 Impact of Varying Bus Proportion and Share of Stopping Buses on PCU Values

For each bus proportion (2% to 20%), share of stopping buses are increased from 0% to 100% to study the influence of varying bus proportion and share of stopping buses on PCU values. Here, similar trend observed in case 7 (impact of varying share of stopping buses and traffic volume on PCU values) is noticed in ideal and bus stop sections. As the bus proportion and stopping bus share increase simultaneously, traffic gets heavily congested leading to drastic decrease in speeds of all vehicle types. Thus, a higher increase in PCU values of TW, THW and buses, and a higher decrease in PCU values of HV are observed when the share of stooping bus is 100% for 20 5 bus proportion. Variations in PCU values for different vehicle types for varying bus proportion and share of stopping buses in bus stop section are illustrated in figures 7.23 - 7.26.

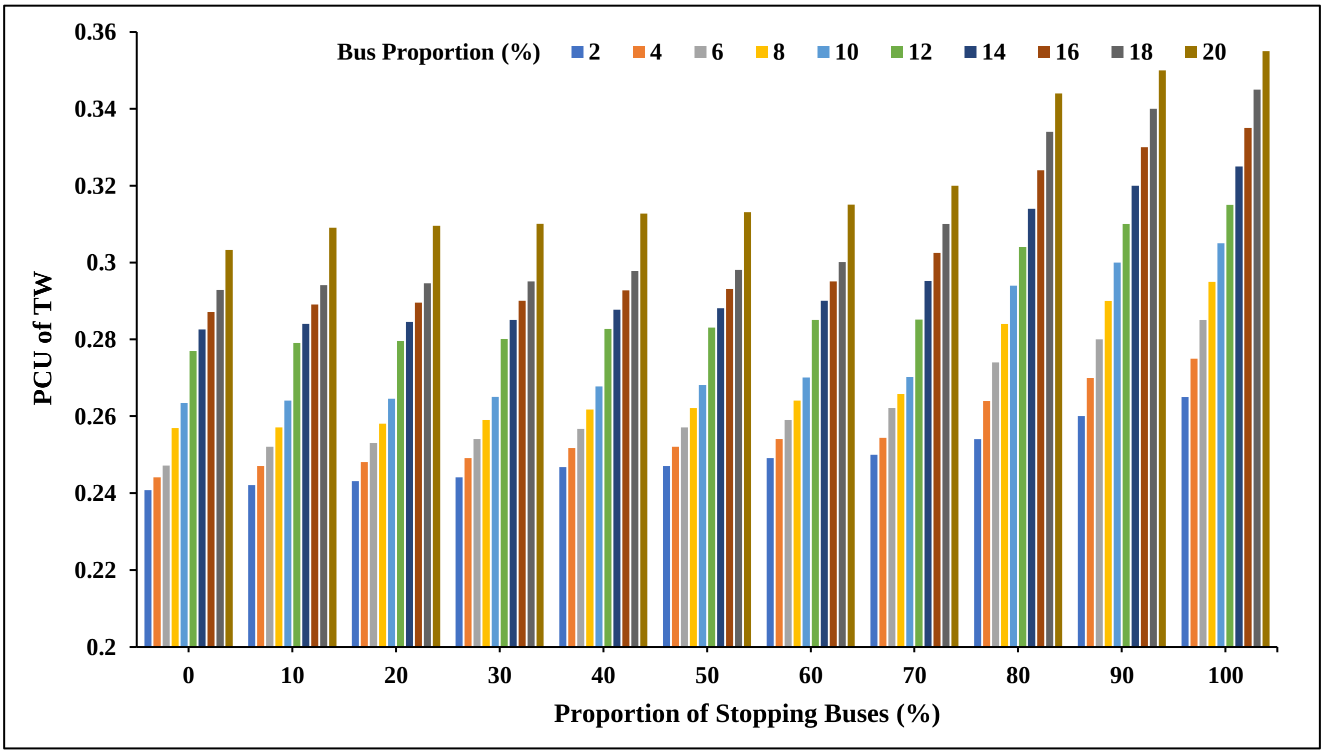

Figure 7.23 Variations in PCU Values for TW with Varying Bus Proportion and Share of Stopping Buses in Bus Stop Section

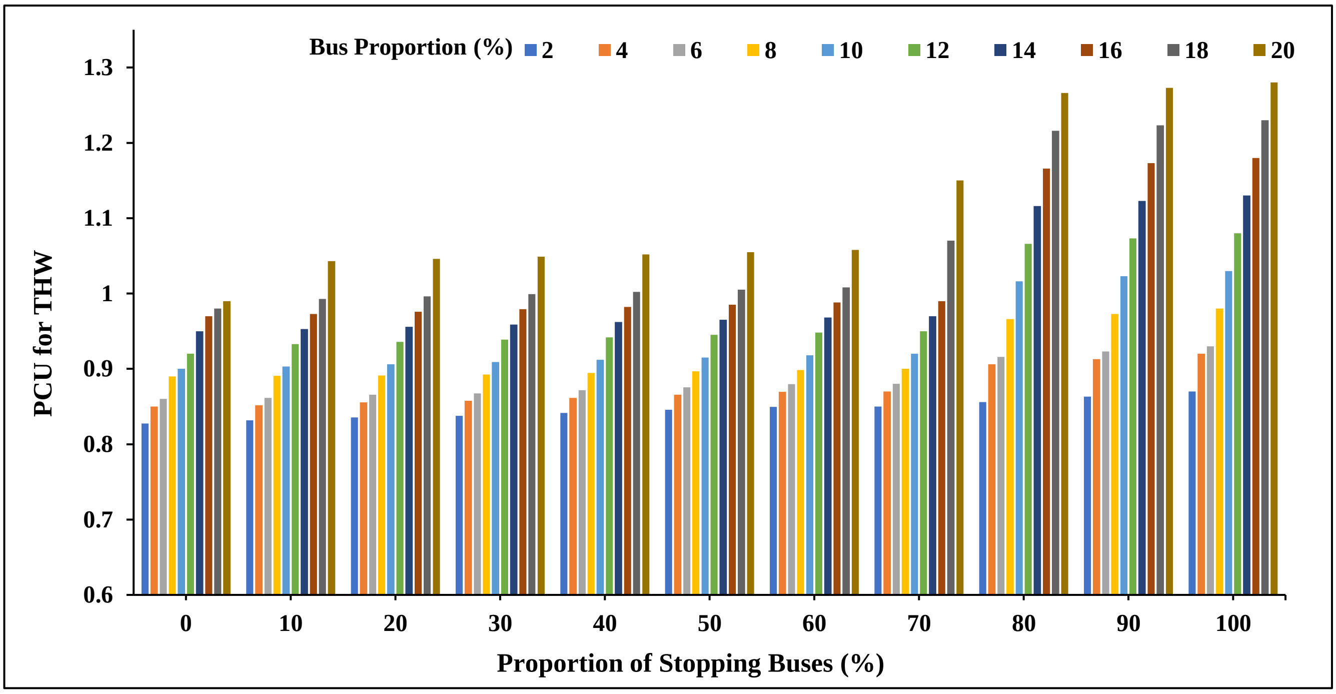

Figure 7.24 Variations in PCU Values for THW with Varying Bus Proportion and Share of Stopping Buses in Bus Stop Section

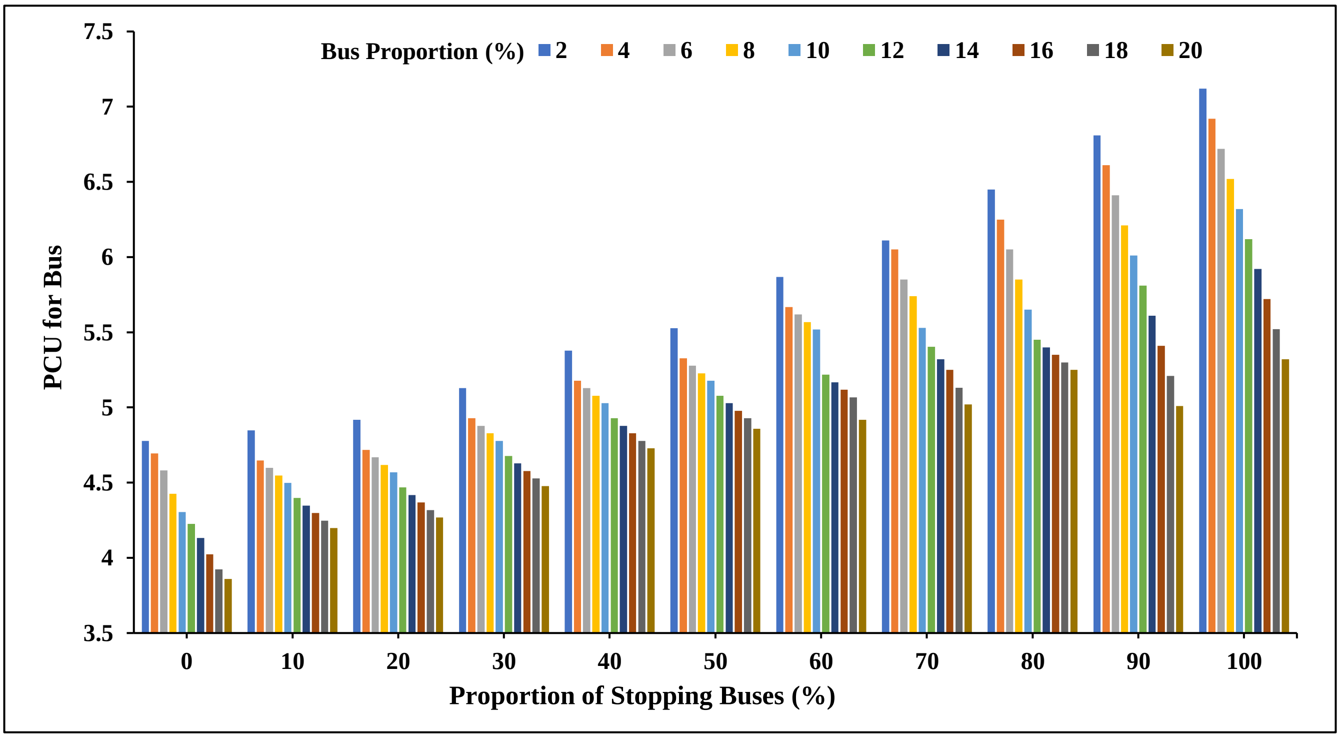

Figure 7.25 Variations in PCU Values for Bus with Varying Bus Proportion and Share of Stopping Buses in Bus Stop Section

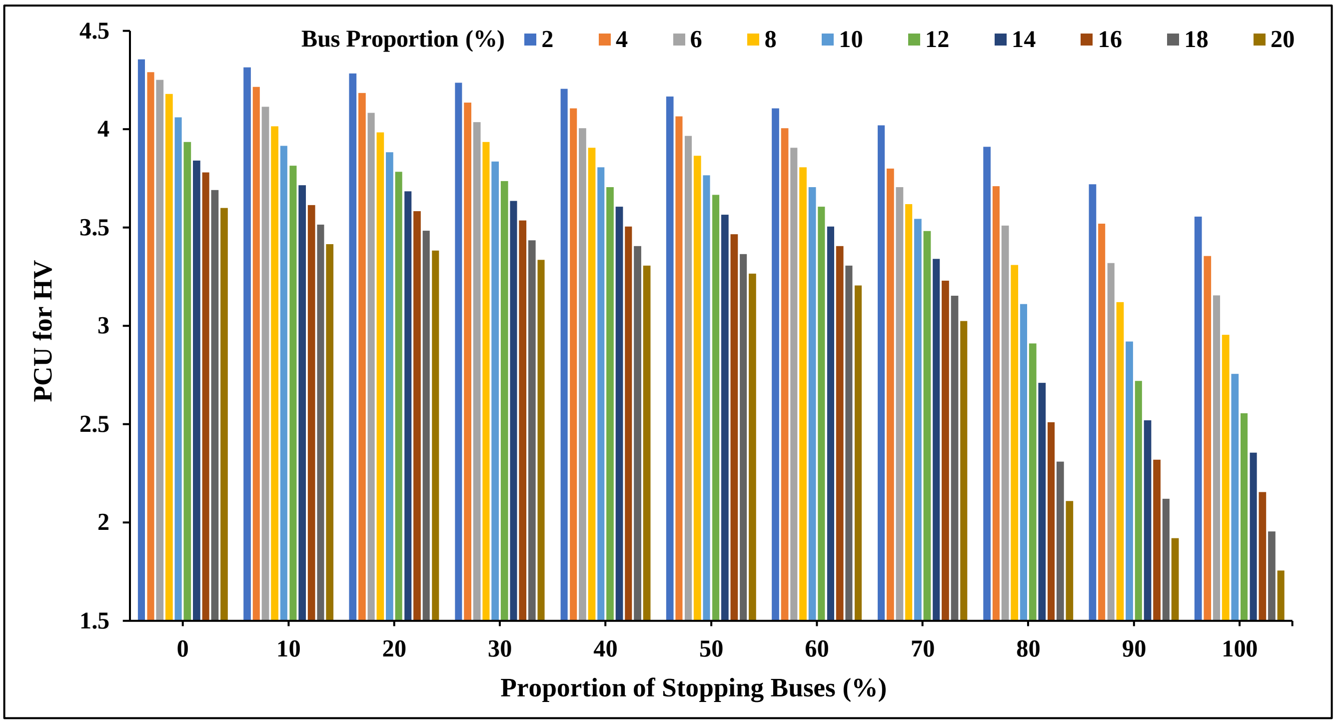

Figure 7.26 Variations in PCU Values for HV with Varying Bus Proportion and Share of Stopping Buses in Bus Stop Section

7.2.1.9 Impact of Varying Vehicular Composition and Share of Stopping Buses on PCU Values

For each vehicular composition (C, C1, C2, C3, C4, C5), share of stopping buses are increased from 0% to 100% to study the influence of varying vehicular composition and share of stopping buses on PCU values. For each vehicular composition, similar trend observed in case 7 (impact of varying share of stopping buses and traffic volume on PCU values) is noticed in ideal and bus stop sections. When the compositions of larger sized vehicles are higher for each share of stopping buses, PCU values of TW and THW increase whereas PCU values of HV decrease. However, PCU values of buses decrease when the proportion of larger sized vehicles such as cars and HV are higher; but when the proportion of buses (including stopping and non-stopping buses) are more for each stopping bus share, PCU values of buses increase. Variations in PCU values for different vehicle types for varying vehicular composition and share of stopping buses in bus stop section are illustrated in figures 7.27 - 7.30.

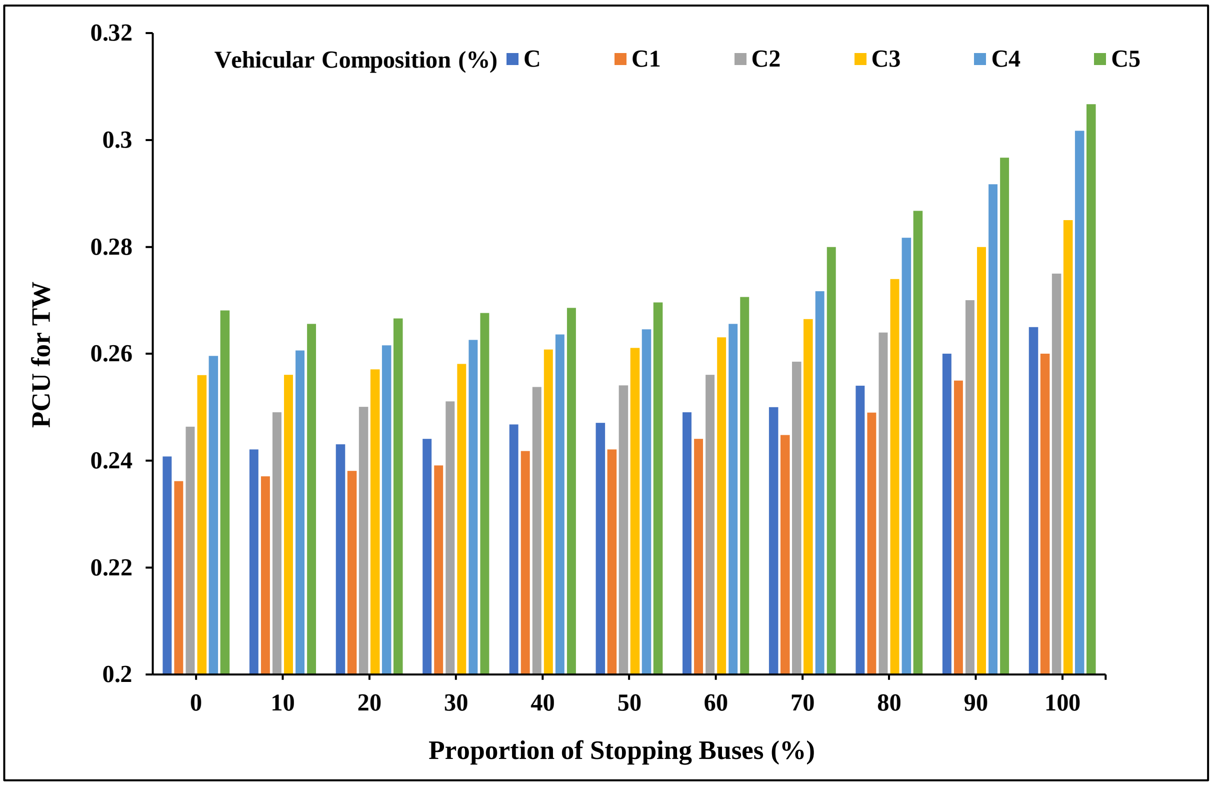

Figure 7.27 Variations in PCU Values for TW with Varying Vehicular Composition and Share of Stopping Buses in Bus Stop Section

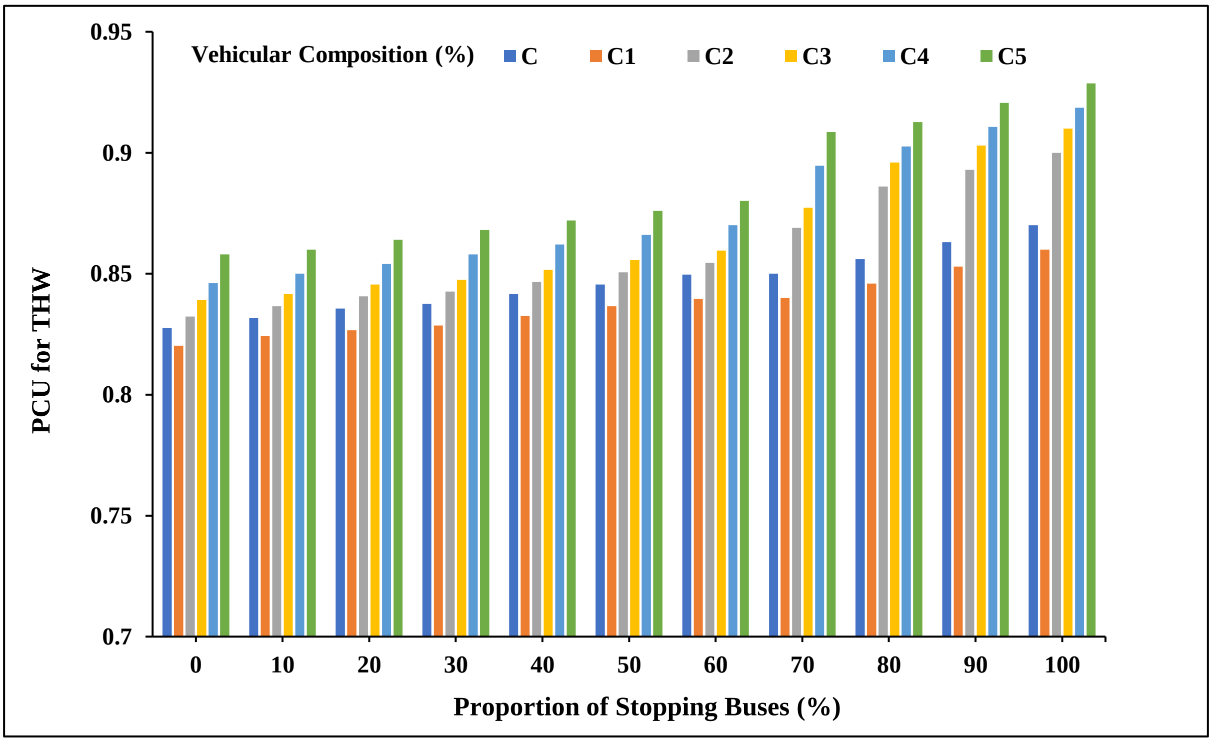

Figure 7.28 Variations in PCU Values for THW with Varying Vehicular Composition and Share of Stopping Buses in Bus Stop Section

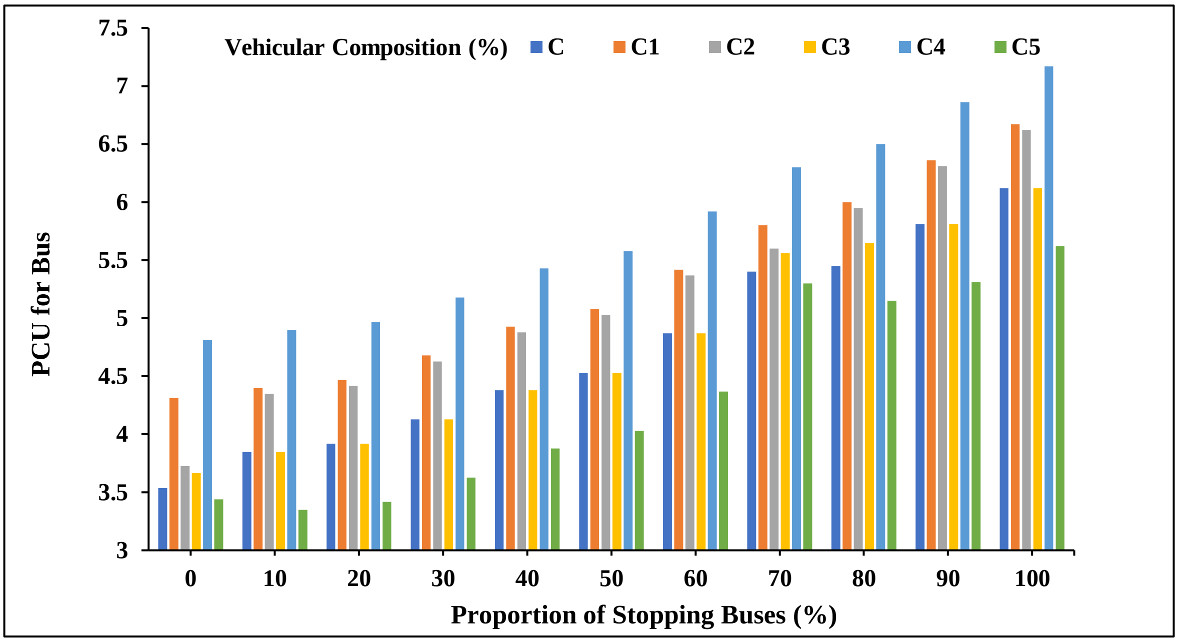

Figure 7.29 Variations in PCU Values for Bus with Varying Vehicular Composition and Share of Stopping Buses in Bus Stop Section

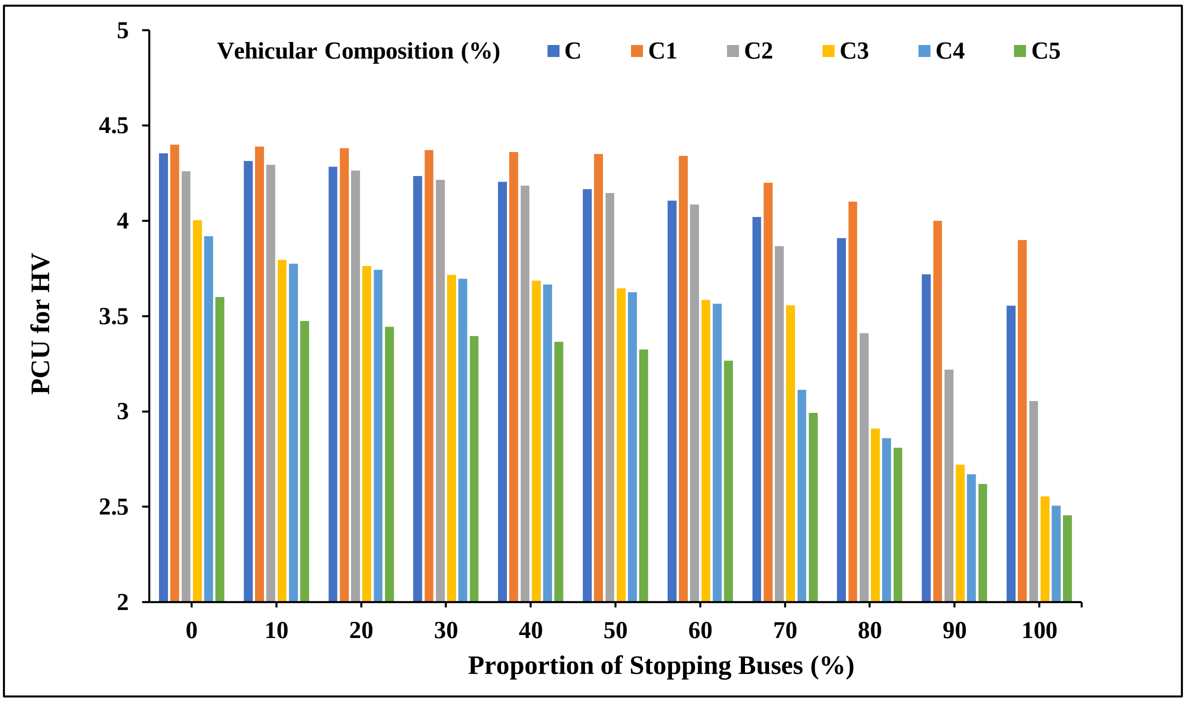

Figure 7.30 Variations in PCU Values for HV with Varying Vehicular Composition and Share of Stopping Buses in Bus Stop Section

7.2.1.10 Multiple Linear Regression Model for Predicting PCU Values

Multiple linear regression (MLR) models are developed to predict the PCU values for different vehicle types with a set of explanatory variables for both ideal and bus stop sections. PCU values of each vehicle type is considered as dependent variable. The variables that significantly influence the PCU values and capacity are determined based on the sensitivity analysis performed using simulation model and those variables are considered as independent variables in the regression models. The best fit regression models for PCU values for each vehicle type for ideal_bus section are given in the following equations.

$$PCU_{TW} = 0.17 + 0.001(P_{TW}) + 0.001(P_{Car}) + 0.001(P_{THW}) + 0.001(P_{Bus}) + 0.002(P_{HV}) + (4.15 \text{ x } 10^{-6})TV \quad (7.1)$$

$$PCU_{THW} = 0.58 + 0.001(P_{TW}) + 0.001(P_{Car}) + 0.003(P_{THW}) + 0.002(P_{Bus}) + 0.004(P_{HV}) + (1.83 \text{ x } 10^{-6})TV \quad (7.2)$$

$$PCU_{BUS} = 7.21 - 0.002(P_{TW}) - 0.019(P_{Car}) - 0.044(P_{THW}) - 0.052(P_{Bus}) - 0.010(P_{HV}) - (1.0 \text{ x } 10^{-7})TV \quad (7.3)$$

$$PCU_{HV} = 5.23 - 0.002(P_{TW}) - 0.001(P_{Car}) - 0.021(P_{THW}) - 0.015(P_{Bus}) - 0.020(P_{HV}) - (6.1 \text{ x } 10^{-5})TV \quad (7.4)$$

The best fit regression models for PCU values for each vehicle type for bus stop section are given in the following equations.

$$PCU_{TW} = 0.19 + 0.001(P_{TW}) + 0.001(P_{Car}) + 0.002(P_{THW}) + 0.001(P_{sBus}) + 0.001(P_{nsBus}) + 0.001(P_{HV}) + (5.03 \text{ x } 10^{-6})TV \quad (7.5)$$

$$PCU_{THW} = 0.66 + 0.001(P_{TW}) + 0.001(P_{Car}) + 0.005(P_{THW}) + 0.003(P_{sBus}) + 0.001(P_{nsBus}) + 0.009(P_{HV}) + (1.26 \text{x } 10^{-6})TV \quad (7.6)$$

$$PCU_{BUS} = 8.54 - 0.003(P_{TW}) - 0.013(P_{Car}) – 0.049(P_{THW}) – 0.046(P_{sBus}) - 0.019(P_{nsBus}) - 0.021(P_{HV}) - (1.1 \text{ x } 10^{-5})TV \quad (7.7)$$

$$PCU_{\mathrm{HV}} = 4.79 - 0.004(P_{TW}) - 0.006(P_{Car}) - 0.031(P_{THW}) - 0.029(P_{sBus}) - 0.015(P_{nsBus}) - 0.016(P_{HV}) - (1 \text{ x } 10^{-5})TV \quad (7.8)$$

In all these equations, PCU_{TW} = PCU of TW, PCU_{THW} = PCU of THW, PCU_{BUS} = PCU of bus, PCU_{HV} = PCU of HV, P_{Car} = percentage of cars (%), P_{THW} = percentage of three-wheelers (%), P_{Bus} = percentage of buses (%), P_{sBus} = percentage of stopping buses (%), P_{nsBus} = percentage of non-stopping buses (%), P_{HV} = percentage of heavy vehicles (%) and *TV* = traffic volume (veh/h). In bus stop section, percentage of stopping and non-stopping buses are considered separately to show the variations in PCU values of vehicle types with varying compositions of stopping and non-stopping buses. The R^2 value (goodness of fit) of the models are obtained within the range of 0.81-0.93 and within the range of 0.78-0.90 for ideal and bus sections, respectively. The models have F–statistics more than the critical value for the sections implying that the models are statistically significant (Table 7.1).

Table 7.1 F-Statistics Value for MLR Equations to Predict PCU Values

Vehicle Type	F-Statistic Values			
	Ideal Section		Bus Stop Section	
	F_{obs}	F_{crit}	F_{obs}	F_{crit}
TW	52.3	2.39	55.9	2.41
THW	50.7	2.37	53.8	2.38
Bus	56.8	2.40	58.0	2.42
HV	60.1	2.37	62.5	2.40

The model results indicate that PCU values of TW and THW increase with increase in percentage of cars, THWs, buses and HVs and with increase in traffic volume in both the sections whereas PCU values of HV and bus decrease. However, from the intercept and coefficient values, it is understood that PCU values of bus in bus stop section are higher compared to that in ideal section. Percentage compositions of cars, THWs, buses and HVs significantly affect the PCU values of all types of vehicles due to their larger sizes and poor dynamic characteristics compared to TW. As two-wheelers try to squeeze in between the vehicles and provide space for other vehicles to travel due to their smaller sizes, their proportion do not affect PCU values of vehicles significantly. Development of the regression model is done using 75% of the simulated results and remaining 25% is used for its validation. The validation results indicate that the model replicates the field conditions reasonably.

7.2.2 Influencing Parameters and Assumed Values for Sensitivity Analysis on Capacity

The influencing factors and values used for performing sensitivity analysis on capacity of ideal (ideal_bus) and bus stop section are the following.

(i) Case 1: Varying vehicular composition.

Five different vehicular compositions other than the observed composition are assumed from various studies on Indian urban roads (Asaithambi *et al*. 2012) in such a way that each vehicle type is dominating with respect to the observed composition. The following compositions are used in the study.

- C (observed composition): 53% TW, 34% cars, 10% THW, 2% buses and 1% HV.
- C1: 70% TW, 17% cars, 10% THW, 2% buses and 1% HV. (TW Dominant)
- C2: 50% TW, 14% cars, 34% THW, 1% buses and 1% HV. (THW Dominant)
- C3: 40% TW, 50% cars, 8% THW, 1% buses and 1% HV. (Car Dominant)

- C4: 40% TW, 30% cars, 9% THW, 20% buses and 1% HV. (Bus Dominant)
- C5: 50% TW, 30% cars, 8% THW, 2% buses and 10% HV. (HV Dominant)

In reference to the observed composition, two-wheelers are dominant in case C1, in case C2 three-wheelers formed a significant component. In contrast, cases C3, C4 and C5 have higher percentages of cars, buses and heavy vehicles, respectively.

(ii) Case 2: Varying proportion of buses.

Proportion of buses are varied in both ideal and bus stop sections from 2% to 20% in increments of 2%. When the composition of buses is increased, the proportion of other vehicles are evenly reduced and the share between stopping (70%) and non-stopping buses (30%) are maintained.

(iii) Case 3: Varying share of stopping buses

Share of stopping buses are varied from 0% to 100% with an increment of 10%. When the share of stopping buses is increased, the total bus proportion (including stopping and non-stopping buses) is 2% (observed bus proportion).

(iv) Case 4: Varying bus proportion and share of stopping buses

For each increment of bus proportion, the share of stopping buses in it is increased from 0% to 100% with an increment of 10%.

(v) Case 5: Varying vehicular composition and share of stopping buses

For each vehicular composition, the share of stopping buses is increased from 0% to 100% with an increment of 10%.

The traffic volume used in the model for all the proportions is the observed flow of 3970 veh/h and 3354 veh/h for ideal and bus stop sections at HAL road, Bangalore city, respectively. In bus stop section, composition of buses given in cases 1 and 2 are shared by stopping and non-stopping buses with 70% and 30% of total composition of buses, respectively.

7.2.2.1 Impact of Varying Vehicular Composition on Capacity

The change in capacities of ideal and bus stop sections with varying vehicular composition is presented in Table 7.2 (a). It is more appropriate to compare capacities in terms of veh/h across all the cases of given compositions when the capacities of ideal and bus stop section are compared separately. A comparison of the capacity values in terms of PCU/h can be misleading when the proportion of larger sized vehicles are more. The simulated results indicate that when the composition of TW is dominant (C1), it provides more space for other vehicles to travel which does not affect traffic stream speeds of both the sections when analysed separately and thus, the capacity is not affected. For compositions C2 (THW dominant), C3 (car dominant), C4 (bus dominant) and C5 (HV dominant), capacities reduced for both the sections. Moreover, when capacities are compared with and without bus stop, a reduction of capacity values from ideal to bus stop section is observed with variation of composition in each case.

7.2.2.2 Impact of Varying Proportion of Buses on Capacity

Increase in the proportion of buses caused a reduction in capacity (veh/h) of both the sections when analysed separately (Table 7.2 (a)). However, when capacity is obtained in terms of PCU/h, capacity increased with increase in bus proportion in both sections due to the increase in PCU values of buses. When capacities are compared with and without bus-stop, capacity is reduced by 18% in bus stop section compared to that of ideal section for 2% buses while a reduction of 19.6% in capacity is observed for 20% of buses. Hence, it is clear that more the number of buses in the traffic stream, capacity reduces as the buses occupy most of the road space especially when stopping near the bus stop making the road width deficient for other vehicles to travel.

7.2.2.3 Impact of Varying Share of Stopping Buses on Capacity

The share of stopping buses are increased only in bus stop section and thus, the capacity of ideal section remains as 4208 veh/h (2876 PCU /h). As the share of stopping buses incremented from 0% to 100% in bus stop section, the capacity of bus stop section reduced (Table 7.2 (b)). When capacities are compared with and without curbside bus stop, it is observed that 0% stopping buses represents an ideal section and thus, percentage reduction in capacity is 0%. But, when the share of stopping buses is increased to 100% in bus stop section, capacity reduction is observed as 20.7%. Therefore, the results indicate that as the share of stopping buses increases, the percentage reduction in capacity also increases.

Table 7.2 Percentage Reduction in Capacity

(a) Impact of Vehicular Composition and Bus Proportion

Variation of Parameters		**Capacity [veh/h (PCU/h)]**		
		Ideal Section	**Bus Stop Section**	**Percentage Reduction**
Composition of Each Vehicle Type (%)	C(observed)	4208(2876)	3448(2358)	18.0
	C1	4854(2844)	3969(2326)	18.2
	C2	4238(2846)	3499(2350)	17.4
	C3	4186(2976)	3452(2455)	17.5
	C4	3904(4171)	3053(3265)	21.7
	C5	3325(3962)	2821(3359)	15.2
Proportion of Buses (%)	2(observed)	4208(2876)	3448(2358)	18.0
	4	4074(3067)	3316(2496)	18.6
	6	3905(3295)	3168(2675)	18.8
	8	3768(3444)	3055(2789)	19.0
	10	3658(3620)	2954(2932)	19.0
	12	3550(3676)	2874(2977)	19.0
	14	3398(3834)	2750(3117)	19.1
	16	3348(3983)	2706(3218)	19.2
	18	3292(4075)	2651(3284)	19.4
	20	3248(4242)	2611(3410)	19.6

(b) Impact of Share of Stopping Bus

Variation of Parameters		**Capacity [veh/h (PCU/h)]**	
		Bus Stop Section	**Percentage Reduction**
Share of Stopping Bus (%)	0	4208 (2876)	0
	10	3926 (2764)	6.7
	20	3852 (2718)	8.4
	30	3738 (2647)	11.1
	40	3565 (2545)	15.2
	50	3539 (2530)	15.8
	60	3479 (2418)	17.3
	70	3448 (2358)	18.0
	80	3385 (2261)	19.5
	90	3354 (2240)	20.2
	100	3336 (2215)	20.7

7.2.2.4 Impact of Varying Bus Proportion and Share of Stopping Buses on Capacity

To analyse the effect of varying bus proportion and share of stopping buses on capacity, the share of stopping buses is increased from 0% to 100% for each bus proportion (2% to 20%) in bus stop section. Figure 7.31 illustrates the reduction in capacity of bus stop section from that of ideal section due to the impact of varying bus proportion and share of stopping buses. From the figure, it is observed that for each bus proportion, when the share of stopping buses increases, the percentage reduction in capacity also increases. For a bus proportion of 20%, when the share of stopping buses is 100%, all the buses stop at the bus stop creating a heavy congestion on the road with a higher percentage reduction in capacity.

7.2.2.5 Impact of Varying Vehicular Composition and Share of Stopping Buses on Capacity

The share of stopping buses is increased from 0% to 100% for each vehicular composition (C, C1, C2, C3, C4 and C5) to investigate the impact of varying vehicular composition and share of stopping buses on capacity. The results from the figure 7.32 indicate that when the proportion of buses are dominant (C4), increase in stopping bus share causes drastic increase in percentage reduction in capacity in bus stop section. For other vehicular compositions (C, C1, C2, C3 and C5), irrespective of the composition, the percentage reduction of capacity increases with increase in share of stopping buses.

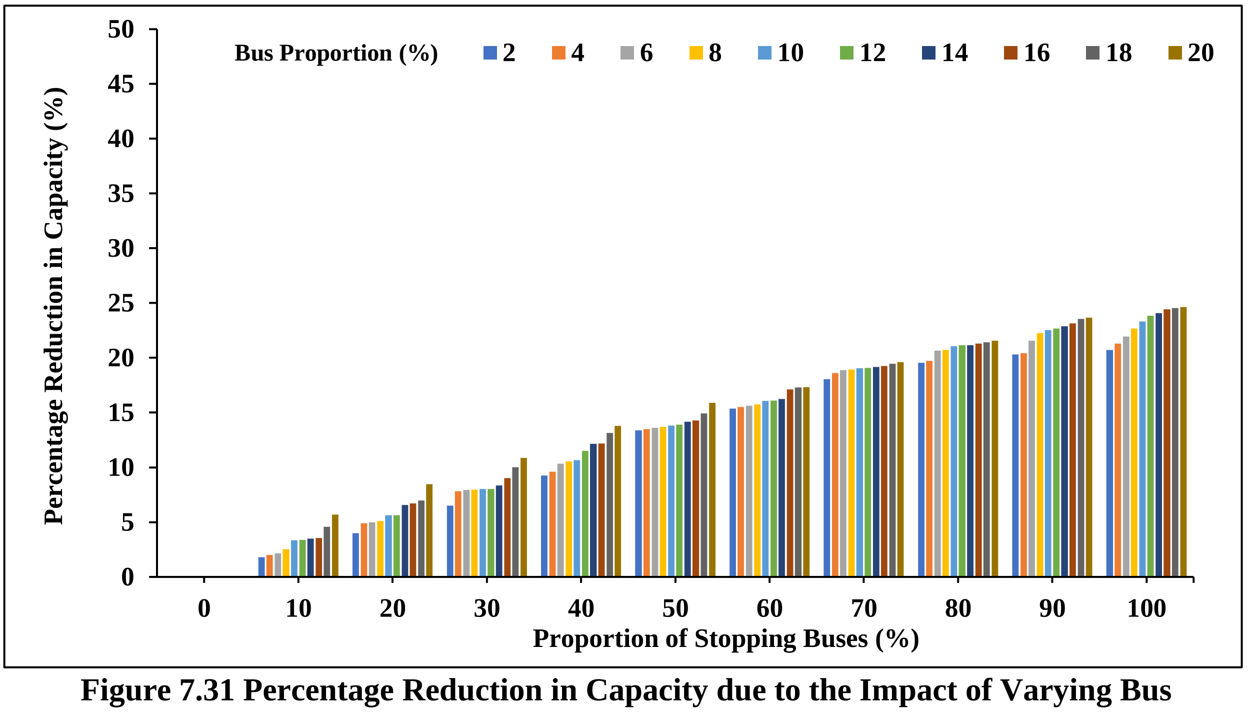

Figure 7.31 Percentage Reduction in Capacity due to the Impact of Varying Bus Proportion and Share of Stopping Buses – Bus Stop Section

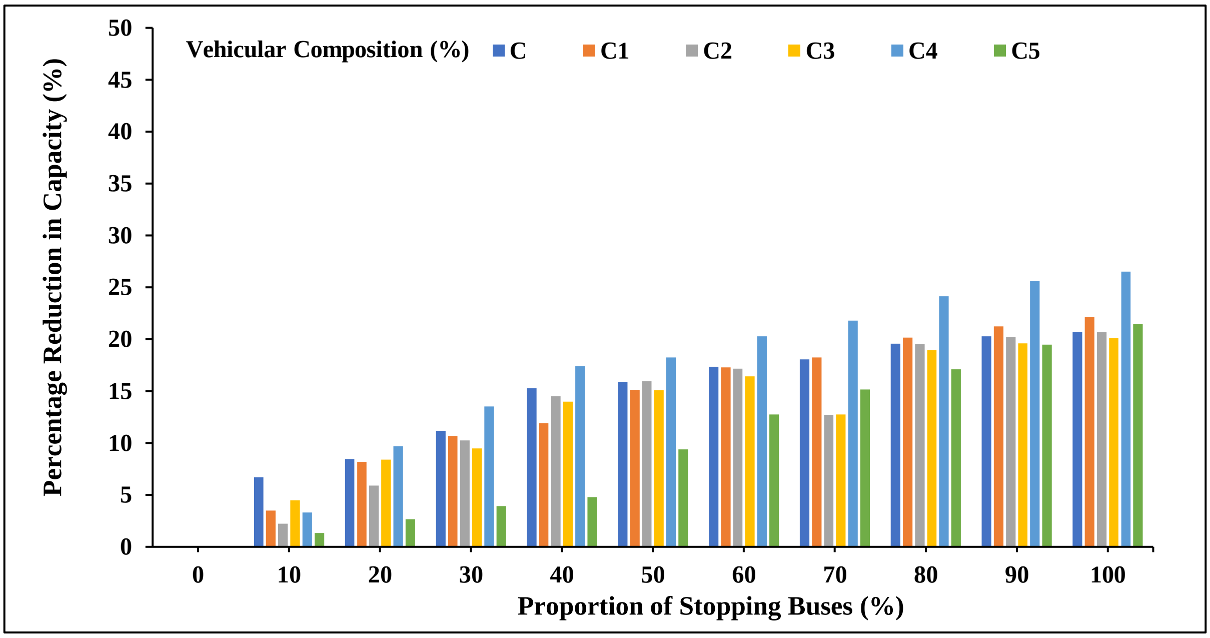

Figure 7.32 Percentage Reduction in Capacity due to the Impact of Varying Vehicular Composition and Share of Stopping Buses – Bus Stop Section

7.2.2.6 Multiple Linear Regression Model for Predicting Capacity

Regression models are developed to predict the capacities of four-lane divided urban roads with and without curbside bus stop using a set of influencing variables. The variables that significantly influence the capacity are determined based on the sensitivity analysis performed using simulation model and those variables are considered as independent variables in the regression models. Multiple linear regression models are developed for both ideal and bus stop sections considering capacity as the dependent variable and percentage composition of different types of vehicles as independent variables. The R^2 value of the models are obtained as 0.95 and 0.96 for ideal and bus stop sections, respectively. The models also have F–statistics more than the critical value (i.e., F_{obs}= 64.2, F_{crit} = 2.42, for ideal section and F_{obs}=50.5, F_{crit}=2.41 for bus stop section) suggesting that model is statistically significant. The best fit regression models to predict capacity of ideal_bus, *Capacity_idealbus* (veh/h) and bus stop sections, *Capacity_busstop* (veh/h) are given as:

$$Capacity\_idealbus = 5523.65 - 21.95(P_{TW}) - 22.94\ (P_{Car}) - 22.15(P_{THW}) - 76.23(P_{Bus}) - 23.12(P_{HV}) \quad (7.9)$$

$$Capacity\_busstop = 4459.36 - 20.15(P_{TW}) - 21.34(P_{Car}) - 19.56(P_{THW}) - 43.91(P_{sBus}) - 23.13(P_{nsBus}) - 21.06(P_{HV}) \quad (7.10)$$

where, P_{Car}= percentage of cars (%), P_{THW}= percentage of three-wheelers (%), (%), P_{Bus} = percentage of buses (%), P_{sBus}=percentage of stopping buses (%), P_{nsBus} = percentage of non-stopping buses (%), and P_{HV}= percentage of heavy vehicles (%). The model results indicate that as the proportion of cars, THW, buses and heavy vehicles increases, capacity decreases considerably for both the sections. In case of bus stop section, the proportions of stopping and non-stopping buses are considered separately instead of bus category as a whole (including stopping and non-stopping buses) in order to show the difference in capacity with varying compositions of stopping and non-stopping buses. The regression equations obtained to predict capacity are validated and it is found that the model replicates the field conditions reasonably. Regression model development is carried out using 75% of the simulated results and remaining 25% is used for its validation.

7.3 SUMMARY

The validated base (ideal_bus) and bus stop models are used to study the variations in PCU values and capacity with and without a curbside bus stop. Sensitivity of PCU and capacity values are analysed with the change in various influencing factors in the presence of curbside bus stops. The results of regression models show that PCU values for TW and THW increase with the increase in proportion of cars, THWs, buses and HVs, and traffic volume in both ideal and bus stop sections whereas PCU values of HV and bus decrease. However, the PCU values of buses are higher in case of bus stop section as the speeds of the buses drastically get reduced when few buses stop near the bus stop. Also, capacity decreases considerably with increase in proportion of cars, THW, buses and HVs.

CHAPTER 8

INFLUENCE OF UNDESIGNATED PEDESTRIAN CROSSINGS ON PCU VALUES AND CAPACITY

8.1 GENERAL

Simulated PCU and capacity values of ideal section (ideal_ped) are compared with that of a section with undesignated pedestrian crossings to investigate the influence of crossing pedestrians on PCU values and capacity. To address this, quantification of relative impact of various influencing factors on PCU values and capacity with and without crossing pedestrians is essential. This chapter mainly discusses the simulated results obtained by performing sensitivity analysis using various guiding factors to study the variations in PCU and capacity values with and without undesignated pedestrian crossings.

8.2 SENSITIVITY ANALYSIS OF PCU VALUES AND CAPACITY WITH AND WITHOUT UNDESIGNATED PEDESTRIAN CROSSINGS

Sensitivity analysis is performed, (1) To study the impact of parameters such as traffic volume, vehicular composition and pedestrian volume on PCU values for vehicle types, and (2) To study the impact of pedestrian volume and vehicular composition on capacity of urban roads. The developed base model (ideal_ped) and the vehicle-pedestrian simulation model are used for performing sensitivity analysis.

8.2.1 Influencing Parameters and Assumed Values for Sensitivity Analysis of PCU Values

Following are the guiding parameters and values assumed for sensitivity analysis of PCU values.

(i) Case 1: Varying traffic volume

Traffic volume is varied from 1000-4500 veh/h in ideal and pedestrian crossing sections with an increment of 500 veh/h for the observed vehicular composition (C). When the vehicular flow is increased, pedestrian volume in the pedestrian section remains as 404 ped/h (observed volume of pedestrians).

(ii) Case 2: Varying vehicular composition

Five different vehicular compositions other than the observed composition are assumed from various studies on Indian urban roads (Asaithambi *et al.* 2012) in such a way that each vehicle type is dominating with respect to the observed composition. The following compositions are used for the sensitivity analysis:

- C (observed composition): 51% TW, 30% cars, 9% THW, 8% buses and 2% HV.
- C1: 70% TW, 17% cars, 10% THW, 2% buses and 1% HV (TW Dominant)
- C2: 50% TW, 14% cars, 34% THW, 1% buses and 1% HV (THW Dominant)
- C3: 40% TW, 50% cars, 8% THW, 1% buses and 1% HV (Cars Dominant)
- C4: 40% TW, 30% cars, 9% THW, 20% buses and 1% HV (Buses Dominant)
- C5: 50% TW, 30% cars, 8% THW, 2% buses and 10% HV (HV Dominant)

The observed pedestrian volume of 404 ped/h for the pedestrian section is used for all the compositions. Also, the observed vehicular flow of 3664 veh/h and 3276 veh/h for ideal and pedestrian sections at Hosur road, Bangalore city, respectively are used for all the composition.

(iii) Case 3: Varying pedestrian volume

The pedestrian volume in the pedestrian section is increased from 500 ped/h to 4500 ped/h with an increment of 500 ped/h for the observed vehicular composition (C). The observed vehicular flow of 3276 veh/h for pedestrian section is used for all the pedestrian volume.

(iv) Case 4: Varying traffic volume and varying vehicular composition

For each vehicular composition (C, C1, C2, C3, C4 and C5), the traffic volumes in both the sections are increased from 1000 veh/h to 4500 veh/h with an increment of 500 veh/h. The observed pedestrian volume of 404 ped/h for the pedestrian section is used for all the vehicular compositions and traffic volumes.

(v) Case 5: Varying traffic volume and pedestrian volume

For each pedestrian volume (500 ped/h -4500 ped/h with an increment of 500 ped/h), the traffic volume in the pedestrian section is increased from 1000 veh/h to 4500 veh/h with an increment of 500 veh/h for the observed vehicular composition (C).

(vi) Case 6: Varying pedestrian volume and varying vehicular composition

For each vehicular composition (C, C1, C2, C3, C4 and C5), the pedestrian volume in the pedestrian section is increased from 500 ped/h to 4500 ped/h with an increment of 500 ped/h. The observed vehicular flow of 3276 veh/h for pedestrian section is used for all the pedestrian volume and composition.

In all the above cases, pedestrian crossings are absent in the ideal section and hence, the pedestrian volume is taken as zero ped/h.

8.2.1.1 Impact of Varying Traffic Volume on PCU Values

When the PCU values for different vehicle types of ideal (ideal_ped) and pedestrian sections are analysed separately, it is observed that increase in traffic flow levels results in a decreasing trend of PCU values for buses and HV, and an increasing trend of PCU values for TW and THW. In case of ideal section, increase in traffic volume from 1000 veh/h to 4500 veh/h caused a reduction of 15% and 17% in PCU values for buses and HV, respectively and caused an increase in PCU values for TW and THW by 2.5% and 3%, respectively. Similar trend is observed in pedestrian section. In this section, PCU values for buses and HV had a reduction of 20% and 24%, respectively, and PCU values for TW and THW had an increase of 2.9% and 3.6%, respectively, with an increase in traffic volume from 1000 veh/h to 3500 veh/h. The reason for this trend in both the sections is that HV and buses have lower speed ratios at higher flow levels due to their larger sizes resulting in decrease in PCU values. Increase in PCU values for TW and THW in both the sections may be due to their smaller sizes and higher manoeuverability compared to cars. When the traffic flow approaches the capacity in pedestrian section, the effect of traffic flow caused less change in PCU values for all vehicle types.

When the PCU values of ideal and pedestrian sections are compared with each other, PCU values for TW are increased by 3.7% and 10.2% from ideal to pedestrian section for flow levels of 1000 veh/h and 4500 veh/h, respectively. PCU values for THW are increased by 6.6% and 12.2% for flow levels of 1000 veh/h and 4500 veh/h, respectively. The reason may be, TW and THW have to reduce their speed to a greater extent in pedestrian section whenever pedestrians are crossing the road. But, buses and HV reduce their speed only to a smaller extent in pedestrian section even if they find a crossing pedestrian due to their larger size and lower operating characteristics compared to TW and THW. Moreover, if pedestrians find a larger sized vehicle approaching them, they will cross the road unless otherwise the current available gap is large enough. Hence, a reduction in PCU values for HV by 2.9% and 6.9% for traffic flow levels of 1000 veh/h and 4500 veh/h, respectively and a reduction in PCU for bus by 5% and 10.7% for traffic flow levels of 1000 veh/h and 4500 veh/h, respectively are obtained (Figure 8.1(a)).

8.2.1.2 Impact of Varying Vehicular Composition on PCU Values

From the simulated results, it is observed that PCU values for all vehicle types in ideal and pedestrian sections did not show much change when there is a larger proportion of TW (C1) because they provide more space for other vehicles to travel due to their smaller sizes and higher manoeuverability. However, the significant proportion of medium and larger sized vehicles such as THW (C2), cars (C3), buses (C4) and HV (C5) cause deficiency in road space, and thus, PCU values for HV and buses reduce. But, PCU values for TW and THW are found to be higher as they try to travel in between the vehicles due to their higher maneuverability (Figure 8.1(b)).

When the PCU values are compared with and without undesignated pedestrian crossings with varying vehicular composition, it is noticed that when the proportion of TW is dominant (C1), PCU values for TW and THW are increased by 9.6% and 12%, respectively from ideal to pedestrian section. This is because in pedestrian section, pedestrians try to cross the road even though the chances for collision is high when they find more smaller sized vehicles. Moreover, TW and THW squeeze through gaps between vehicles and pedestrians due to their higher manoeuverability. But PCU values for buses and HV are reduced by 4% and 5.8%, respectively. Furthermore, when the proportion of THW (C2), cars (C3), buses (C4) and HV (C5) are dominant, PCU value for buses in pedestrian section are decreased by 4.3%, 6.9%, 10.2%, and 9.1%, respectively and PCU values for HV in pedestrian section are reduced by 7.5%, 8.1%, 8.8% and 6.9%, respectively compared to ideal section. This may be because when these vehicles travel on the pedestrian section, pedestrians try to wait for the next available gap to cross the road as when they find a large sized approaching vehicle close to them. However, when the pedestrians find a larger available gap, they try to cross the road which make the approaching vehicles reduce their speed in pedestrian section compared to that of ideal section. In contrast, TW and THW had an increase in their PCU values because of their higher relative speed with respect to car.

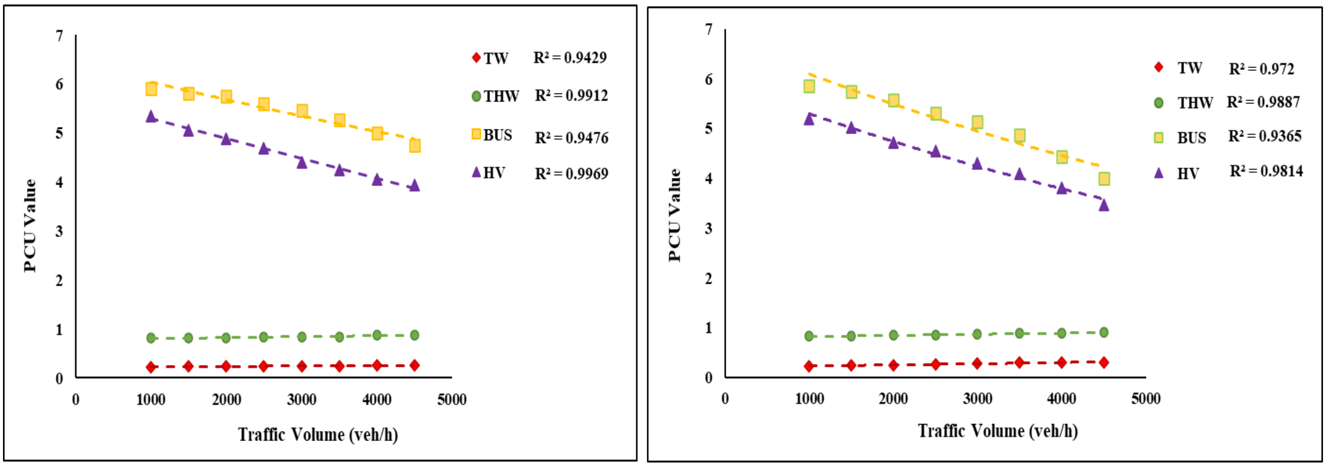

(a) Impact of Traffic Volume

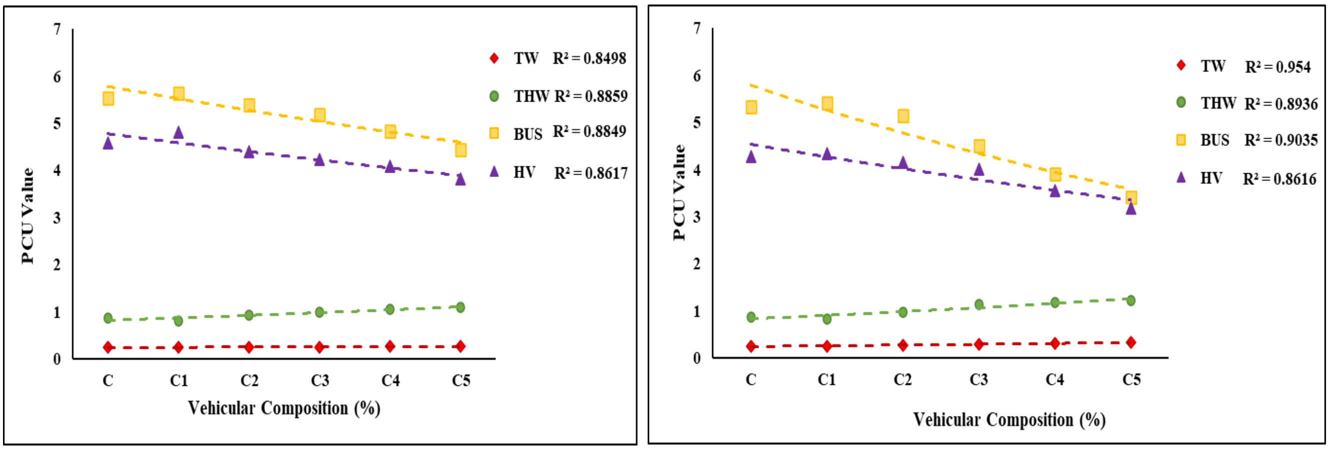

(b) Impact of Vehicular Composition

(i) **(ii)**

Figure 8.1 PCU Values for Varying Traffic Volume and Vehicular Composition for (i) Ideal Section and (ii) Pedestrian Section

8.2.1.3 Impact of Varying Pedestrian Volume on PCU Values

In this analysis, for the observed vehicular composition (C), the observed vehicular flow of 3664 veh/h and 3276 veh/h are considered for ideal and pedestrian sections, respectively while the pedestrian volume in the pedestrian section is incremented from the 500 ped/h to 4500 ped/h. As pedestrian volume in pedestrian section increases, PCU values for TW and THW had an increment by 12.6% and 11.9%, respectively whereas

PCU values for bus and HV reduced by 7.8% and 8.7%, respectively. In the ideal_ped section, the pedestrian volume remains zero ped/h and hence, PCU values for all vehicle types do not vary. Figure 8.2 represents the trend for variations in PCU values for different vehicle types of pedestrian section compared to that of the ideal section with varying pedestrian volume. PCU values for TW and THW increased and PCU values for bus and HV decreased in pedestrian section when compared to that of ideal section with increase in the pedestrian volume.

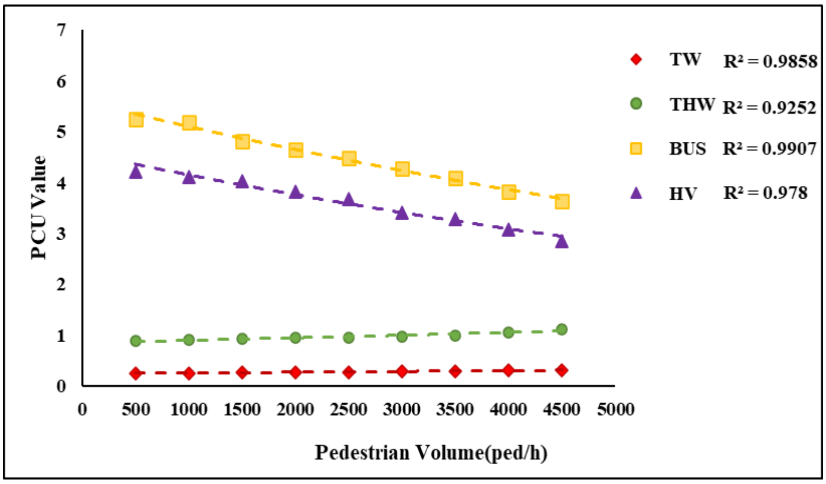

Figure 8.2 Variations in PCU Values with Pedestrian Volume-Pedestrian Section

8.2.1.4 Impact of Varying Traffic Volume and Vehicular Composition on PCU Values

When the traffic volume is increased from 1000 veh/h to 4500 veh/h for each vehicular composition (C, C1, C2, C3, C4 and C5), the PCU values for TW and THW increase but PCU values for bus and HV reduce for both ideal and pedestrian section when analysed separately. Similarly, when the PCU values of ideal and pedestrian sections are compared with each other, higher PCU values are obtained for TW and THW whereas lower PCU values are obtained for bus and HV in pedestrian section. Trends are similar to that observed in cases 1(impact of varying traffic volume on PCU values) and 2 (impact of varying vehicular composition on PCU values). Figures 8.3-8.10

illustrate the variations in PCU values for different vehicle types of ideal and pedestrian sections due to the impact of varying traffic volume and vehicular composition.

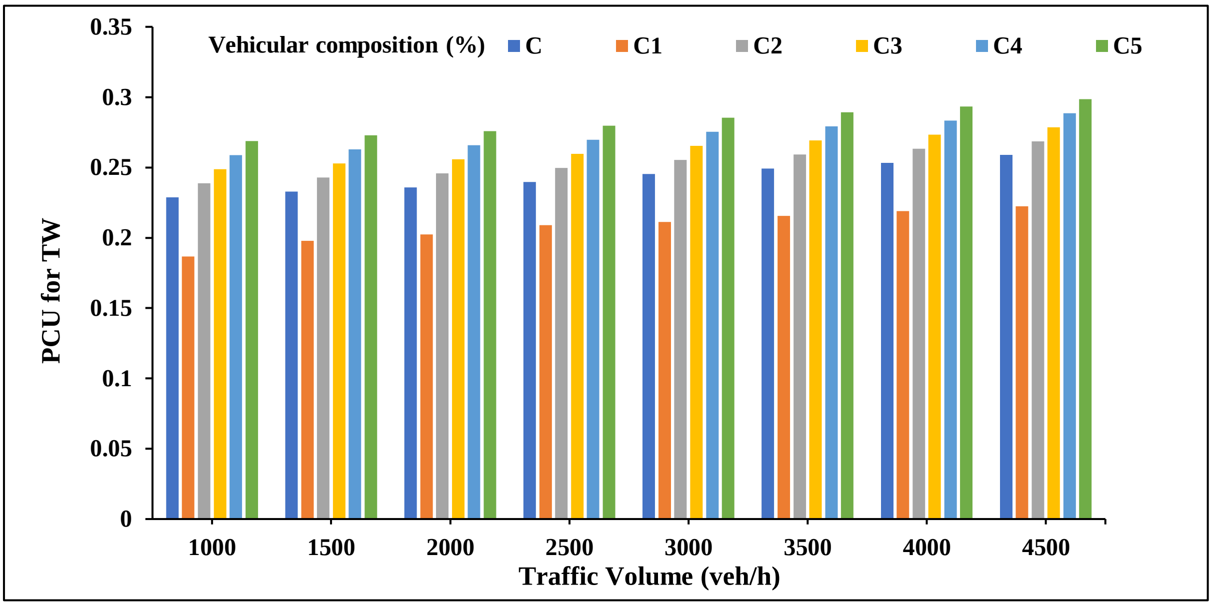

Figure 8.3 PCU Values for TW with Varying Traffic Volume and Vehicular Composition - Ideal Section

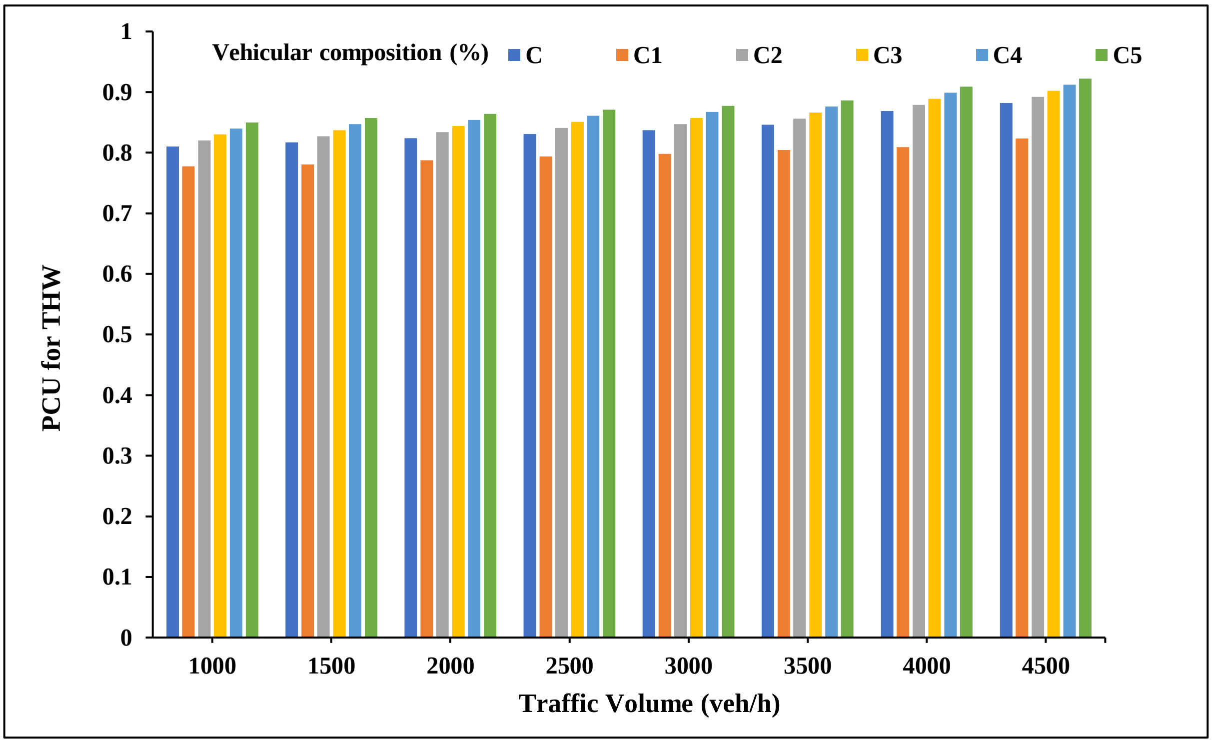

Figure 8.4 PCU Values for THW with Varying Traffic Volume and Vehicular Composition -Ideal Section

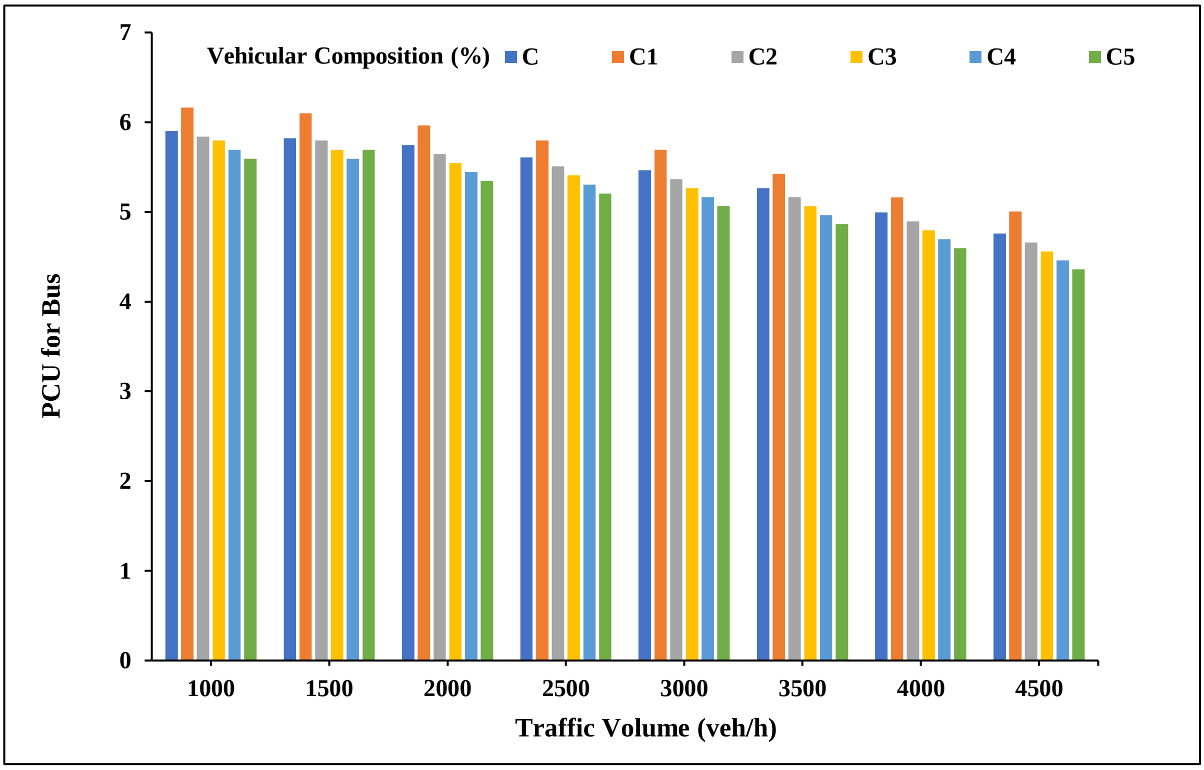

Figure 8.5 PCU Values for Bus with Varying Traffic Volume and Vehicular Composition - Ideal Section

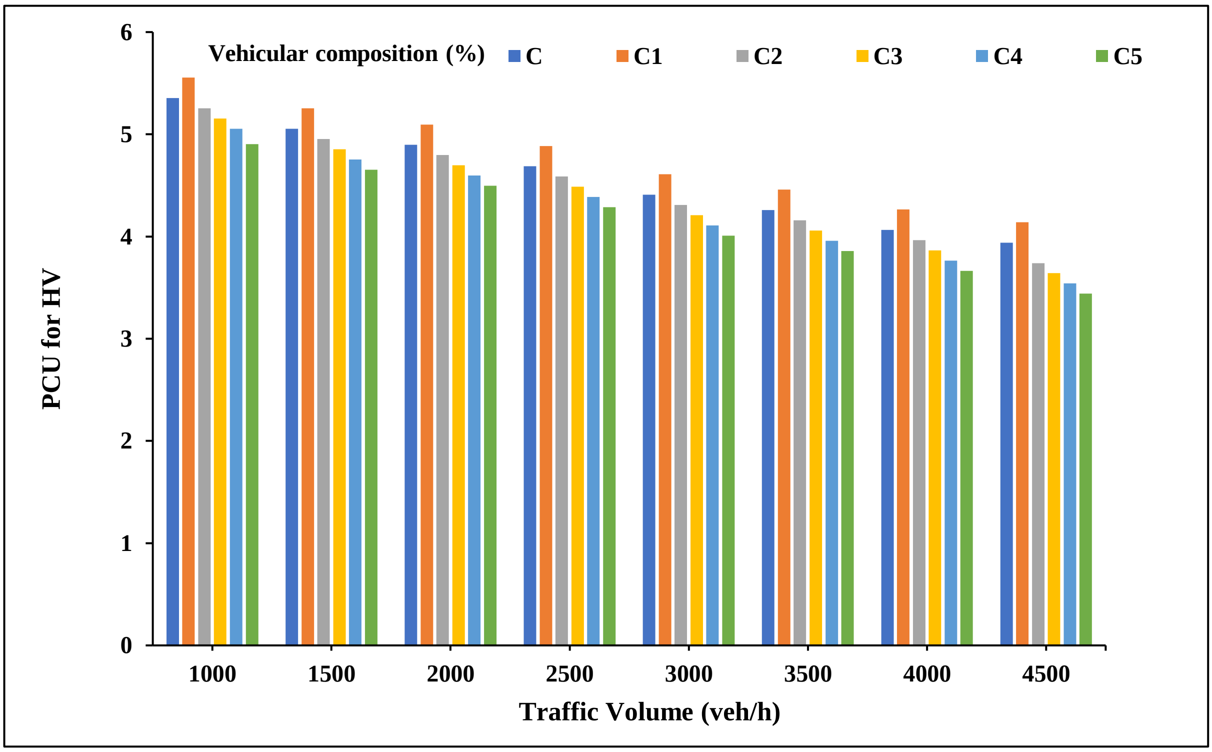

Figure 8.6 PCU Values for HV with Varying Traffic Volume and Vehicular Composition -Ideal Section

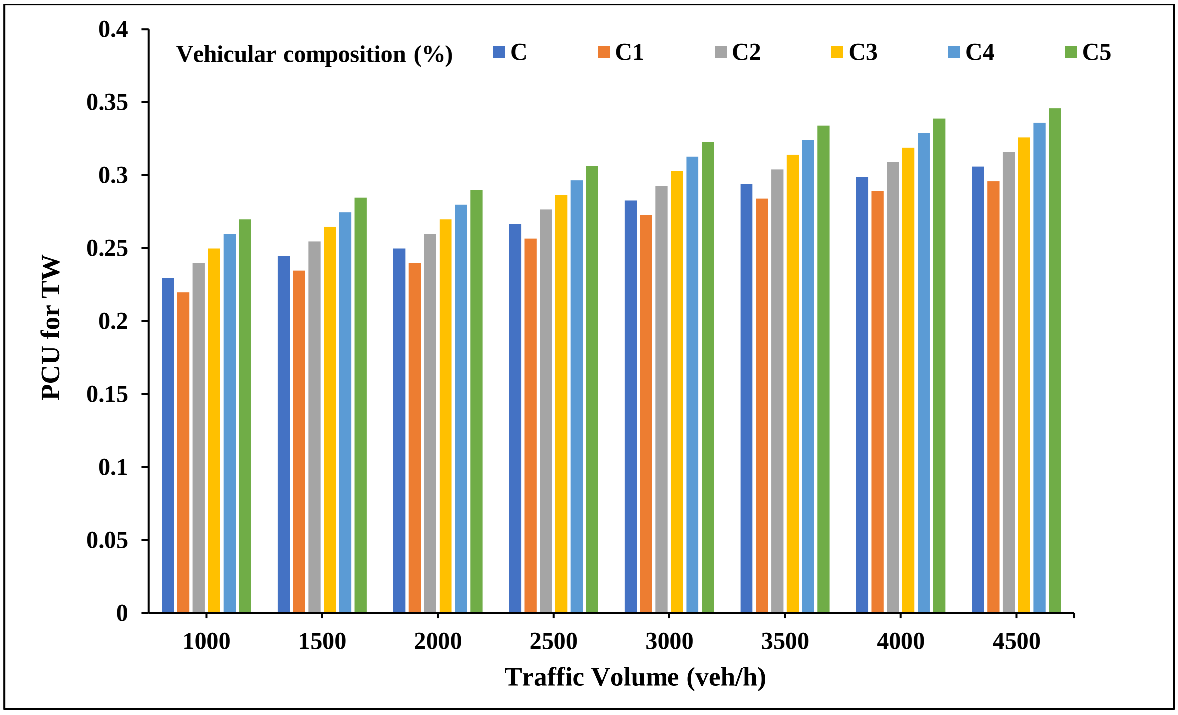

Figure 8.7 PCU Values for TW with Varying Traffic Volume and Vehicular Composition - Pedestrian Section

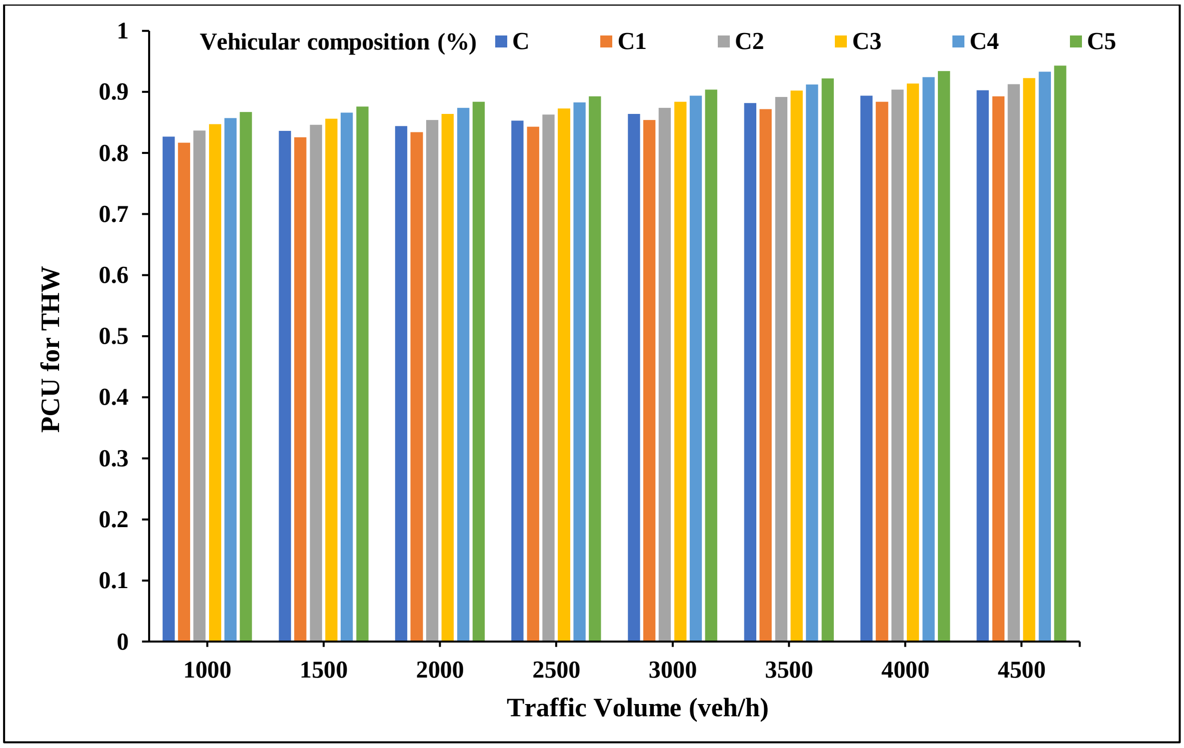

Figure 8.8 PCU Values for THW with Varying Traffic Volume and Vehicular Composition - Pedestrian Section

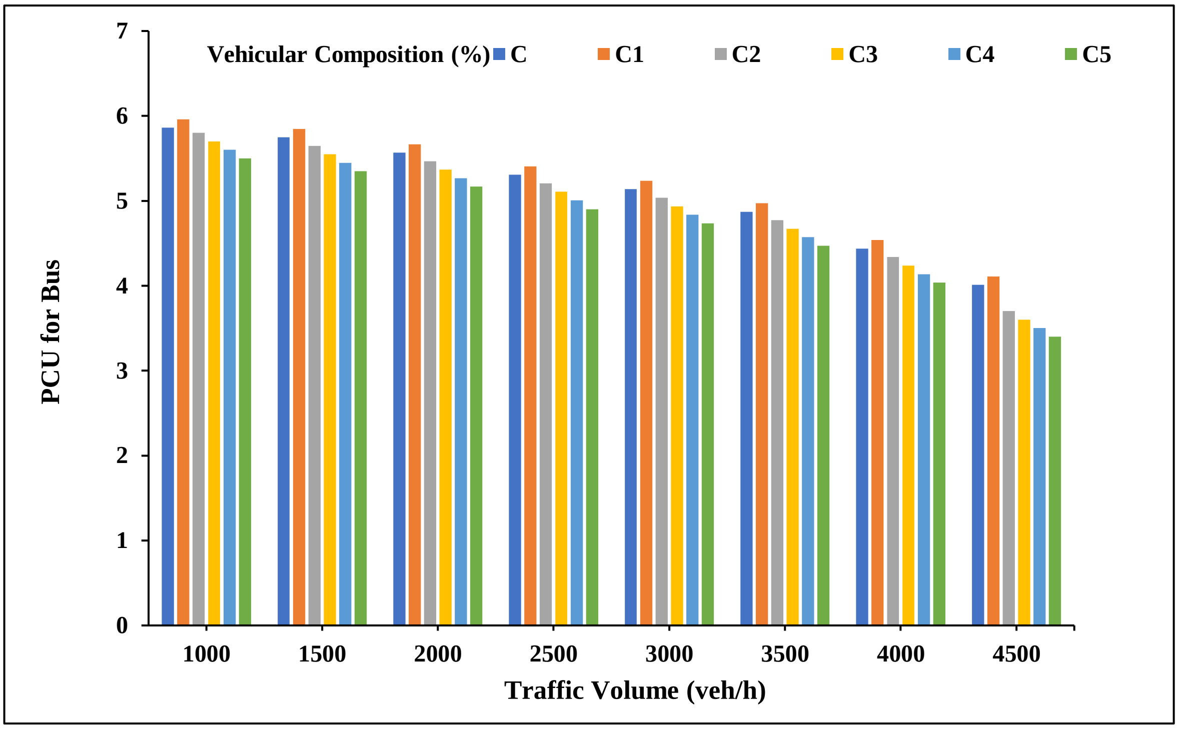

Figure 8.9 PCU Values for Bus with Varying Traffic Volume and Vehicular Composition - Pedestrian Section

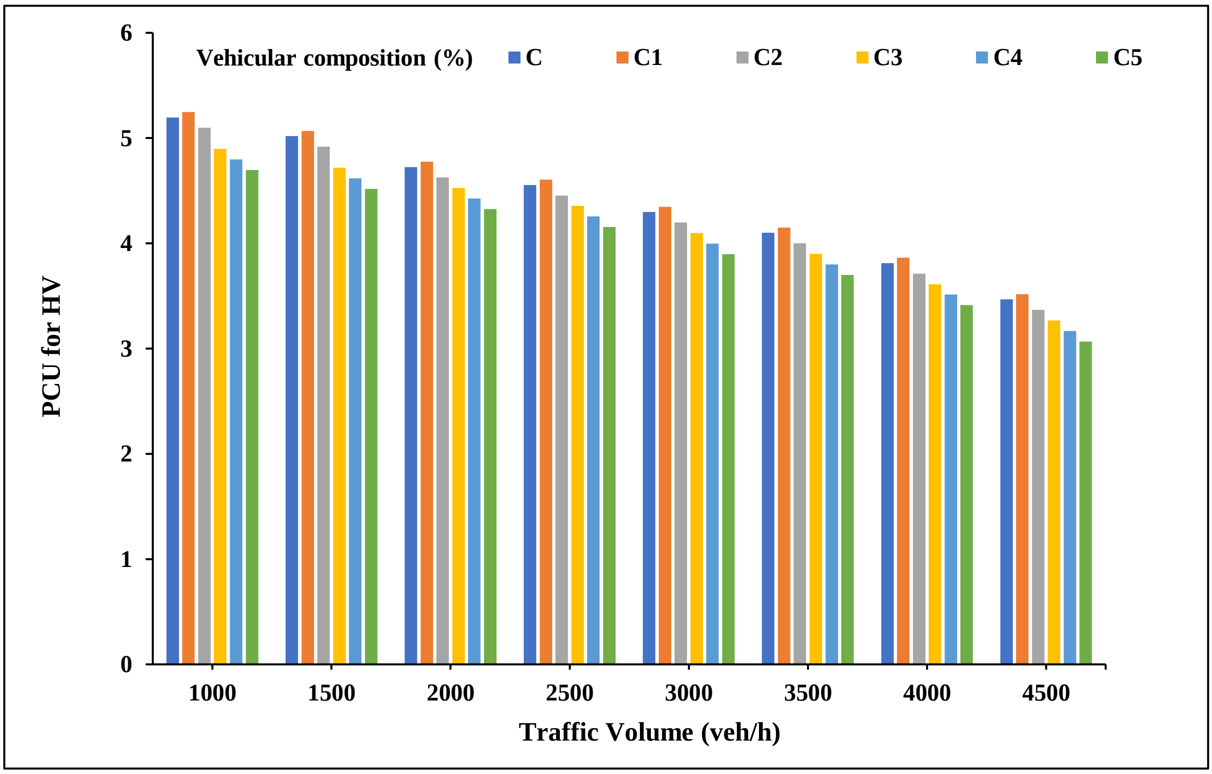

Figure 8.10 PCU Values for HV with Varying Traffic Volume and Vehicular Composition - Pedestrian Section

8.2.1.5 Impact of Varying Traffic Volume and Pedestrian Volume on PCU Values

For the observed vehicular composition (C), only the traffic volume is incremented from 1000 veh/h to 4500 veh/h in ideal section as the pedestrian volume is zero ped/h. Hence, the PCU values for all vehicle types in ideal section followed the same trend as observed in section 8.2.1.1. But, in pedestrian section, traffic volume is incremented from 1000 veh/h to 4500 veh/h for each pedestrian volume (500 ped/h to 4500 ped/h). As the traffic volume in pedestrian section increases with increase in pedestrian volume, PCU values for TW and THW had an increment whereas PCU values for bus and HV reduced (Figures 8.11-8.14). It can be observed that as a greater number of pedestrians start crossing the road with increase in traffic volume, the percentage increase in PCU values for TW and THW, and percentage reduction in PCU values for HV and buses are higher. When the PCU values of ideal and pedestrian sections are compared with each other, similar trend in results is observed i.e., PCU values for TW and THW increased, and PCU values for bus and HV decreased in pedestrian section when compared to that of ideal section with varying vehicular and pedestrian volume.

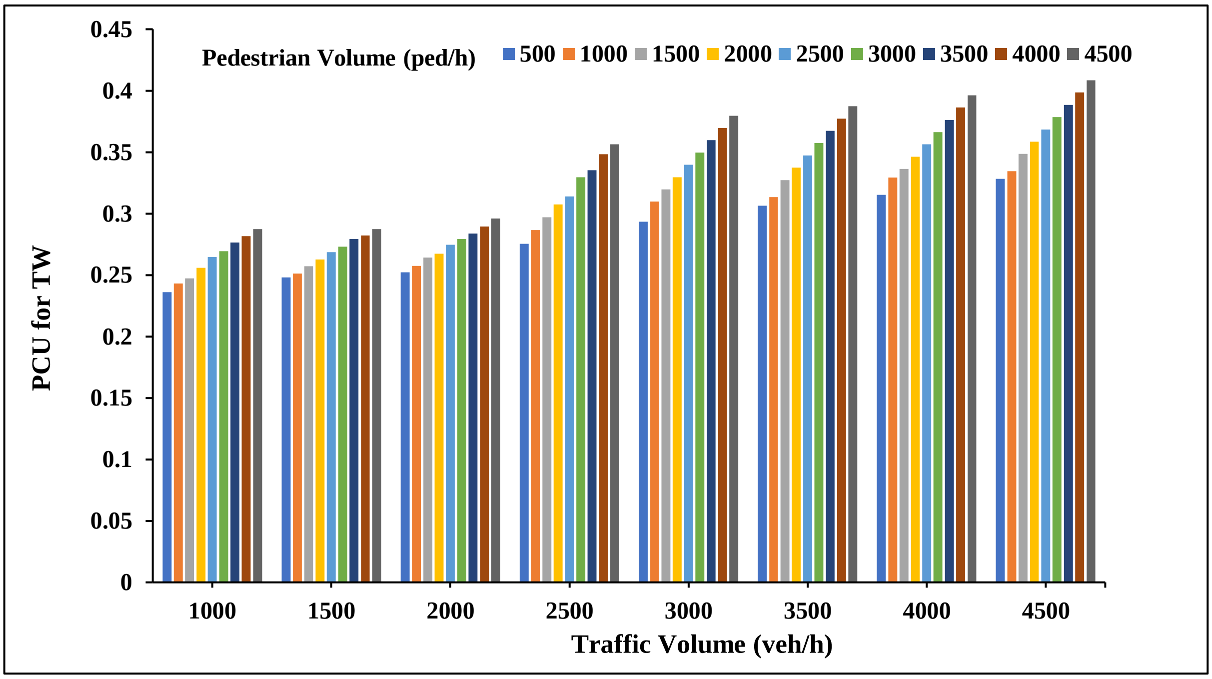

Figure 8.11 PCU Values for TW with Varying Traffic Volume and Pedestrian Volume - Pedestrian Section

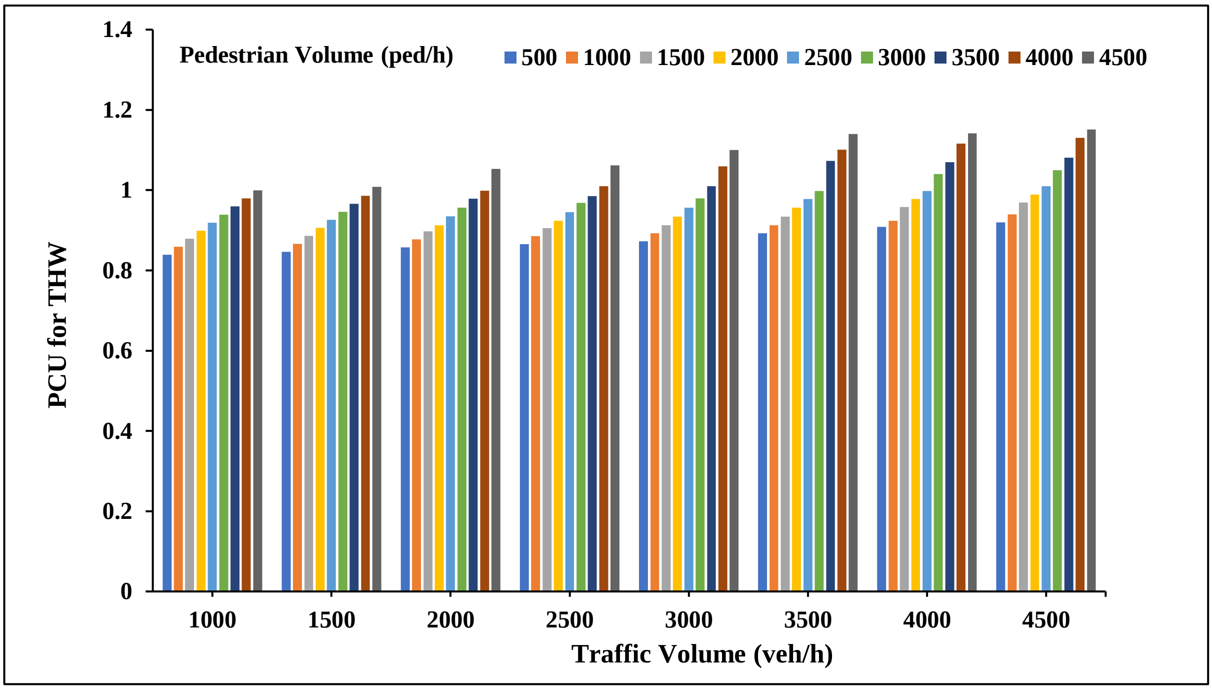

Figure 8.12 PCU Values for THW with Varying Traffic Volume and Pedestrian Volume - Pedestrian Section

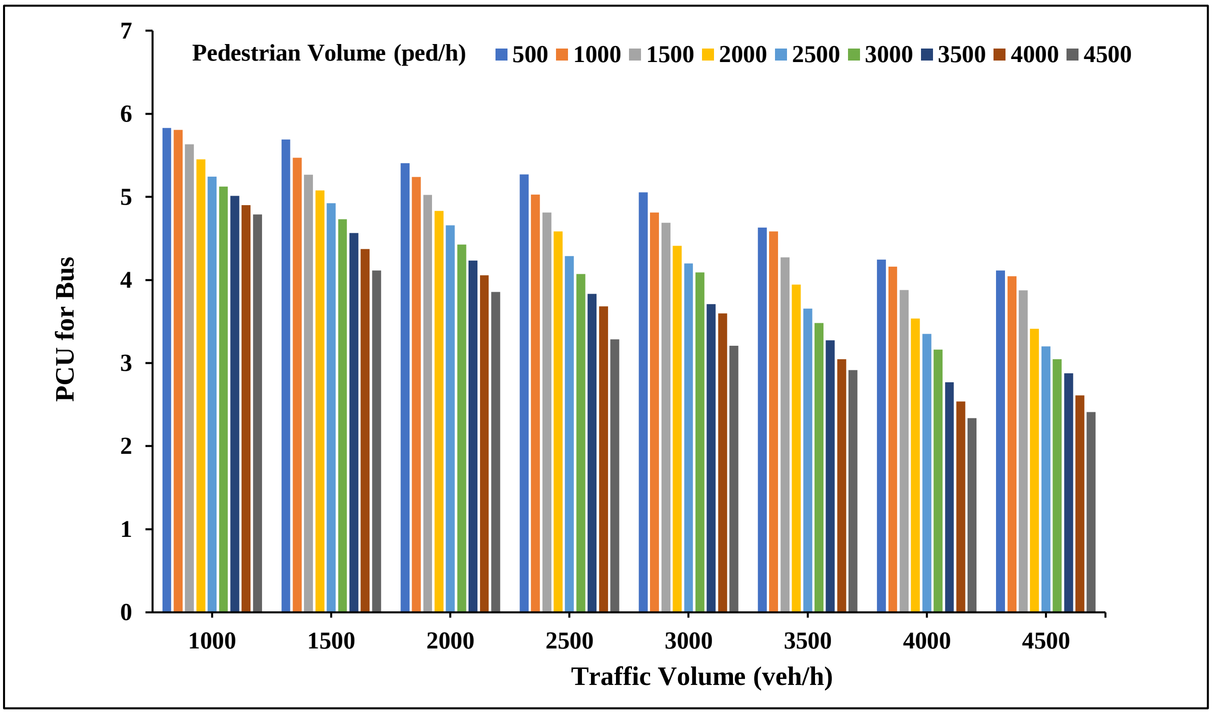

Figure 8.13 PCU Values for Bus with Varying Traffic Volume and Pedestrian Volume -Pedestrian Section

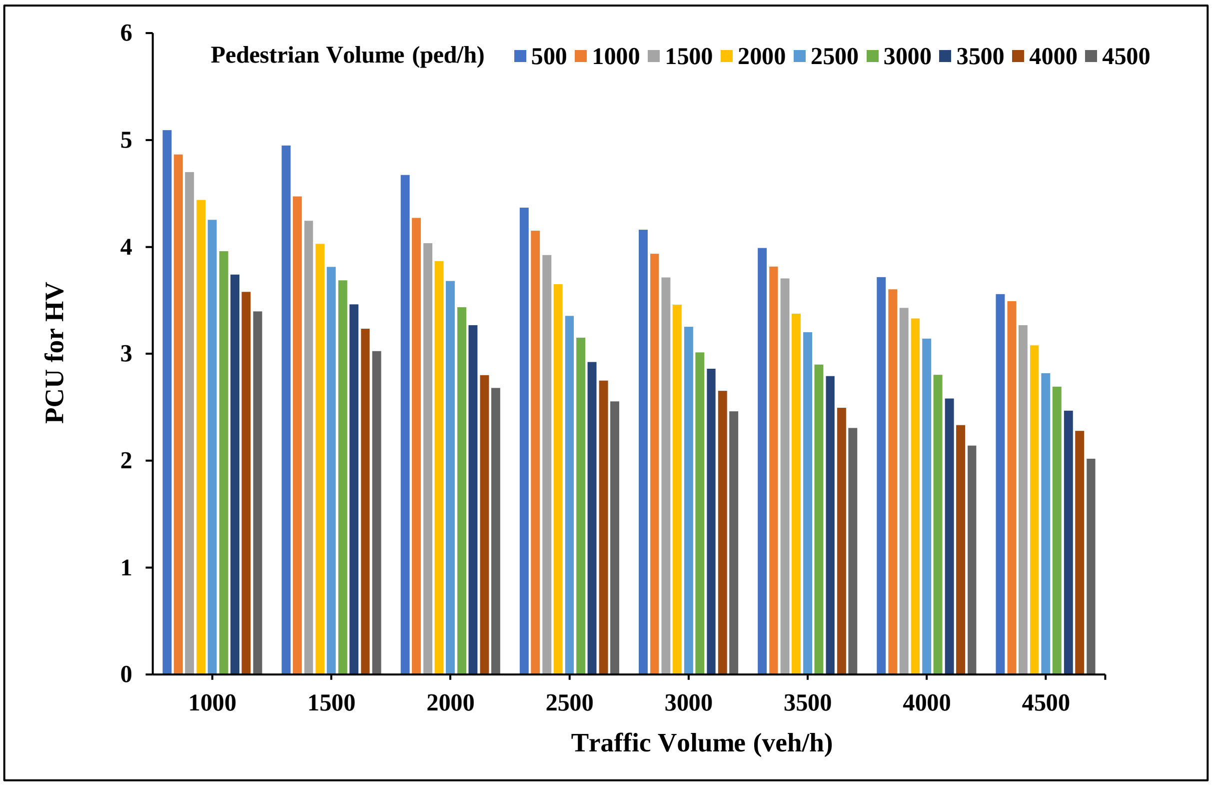

Figure 8.14 PCU Values for HV with Varying Traffic Volume and Pedestrian Volume -Pedestrian Section

8.2.1.6 Impact of Varying Vehicular Composition and Pedestrian Volume on PCU Values

To analyse the variations in PCU values with increase in pedestrian volume for varying vehicular composition, the pedestrian volume is increased from observed 500 ped/h to 4500 ped/h for each vehicular composition (C, C1, C2, C3, C4 and C5). When the PCU values are analysed for pedestrian section, as the pedestrian volume increases for each vehicular composition, the same trend observed in case 5 (impact of varying traffic volume and pedestrian volume on PCU values) is noticed. Similar trend is also observed when PCU values are compared with and without undesignated pedestrian crossings. When the pedestrian volumes are higher, pedestrians tend to move in a group. Hence, even when they find larger sized vehicles closer to them, they cross the road. Figures 8.15-8.18 represents the PCU values for different vehicle types of ideal and pedestrian sections for varying vehicular composition and pedestrian volume.

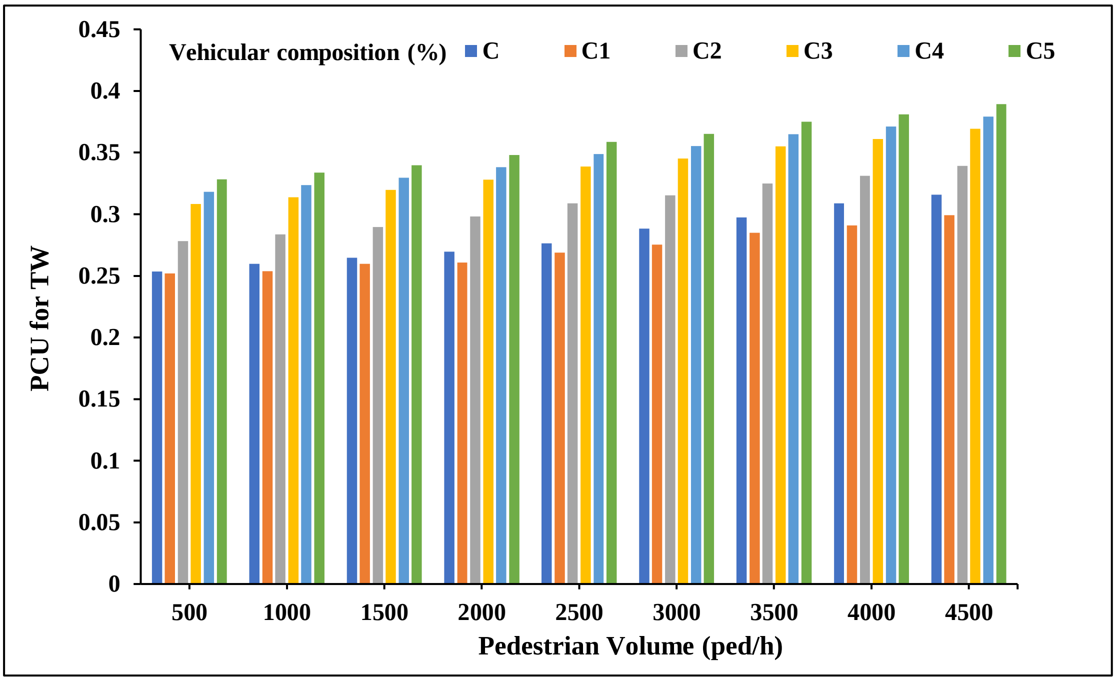

Figure 8.15 PCU Values for TW with Varying Vehicular Composition and Pedestrian Volume - Pedestrian Section

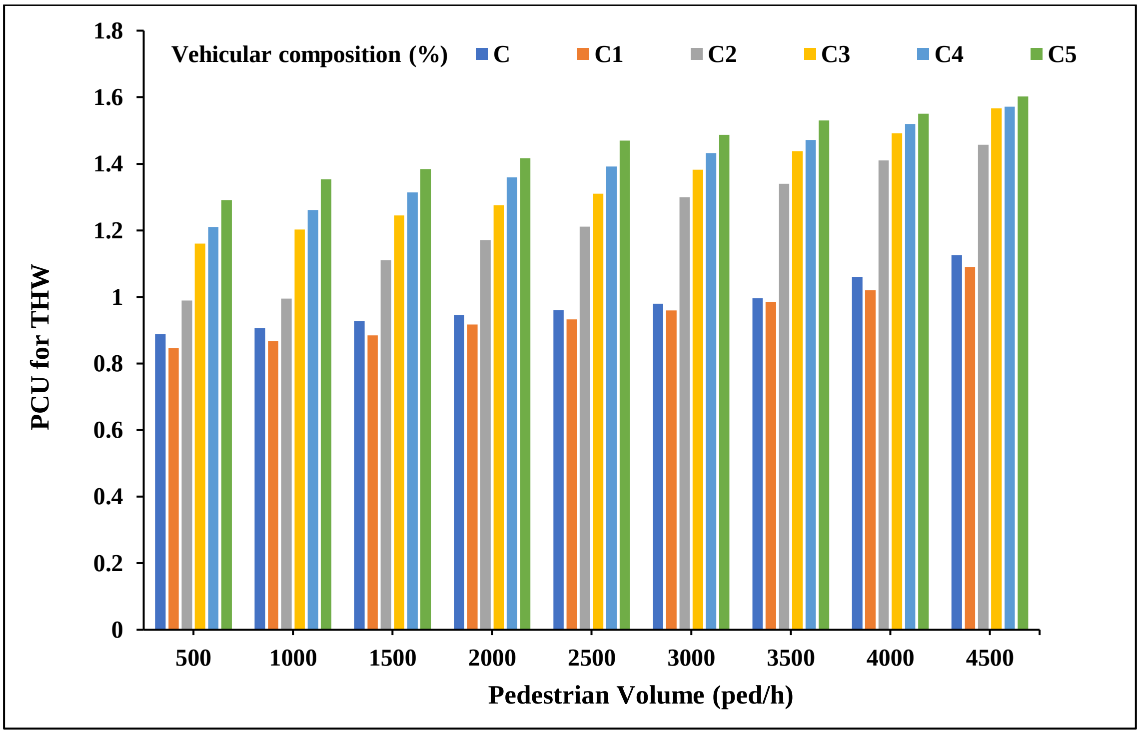

Figure 8.16 PCU Values for THW with Varying Vehicular Composition and Pedestrian Volume - Pedestrian Section

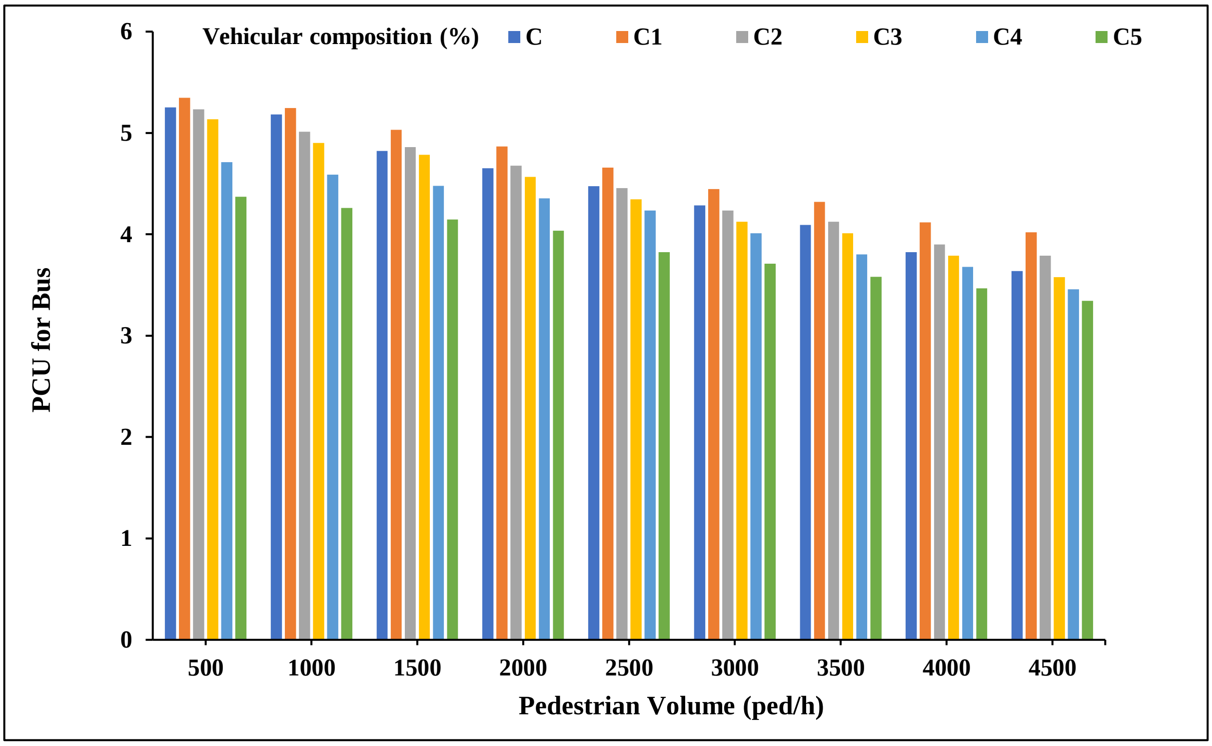

Figure 8.17 PCU Values for Bus with Varying Vehicular Composition and Pedestrian Volume - Pedestrian Section

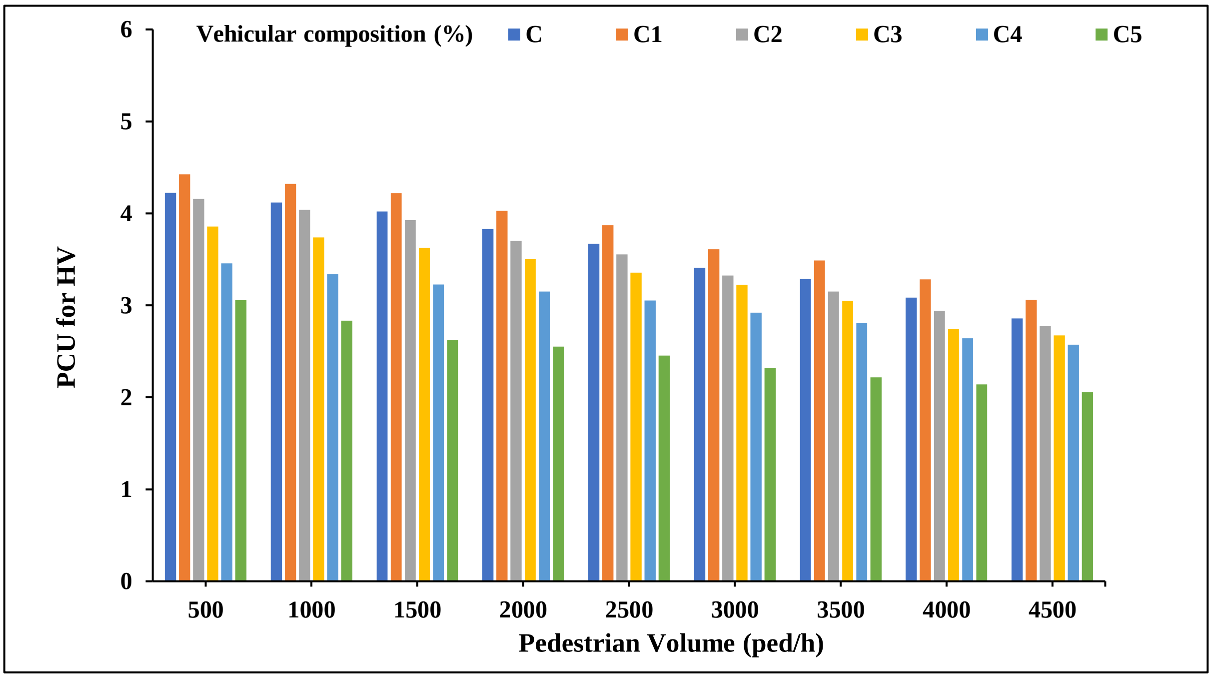

Figure 8.18 PCU Values for HV with Varying Vehicular Composition and Pedestrian Volume - Pedestrian Section

8.2.1.7 Multiple Linear Regression Model for Predicting PCU

Considering the simulated results, regression models are developed to predict the PCU values for different vehicle types with and without undesignated pedestrian crossings using a set of influencing variables such as traffic volume, pedestrian volume, and proportion of cars, THW, buses and HV. Multiple linear regression models are developed for both the sections considering PCU for each vehicle type as dependent variable, and proportion of vehicle types, pedestrian volume and traffic volume as independent variables. The best fit regression models to predict PCU values for each vehicle type for ideal_ped section are given below:

$$PCU_{TW} = 0.18 + 0.001(P_{TW}) + 0.002(P_{Car}) + 0.001(P_{THW}) + 0.002(P_{Bus}) + 0.003(P_{HV}) + \left(4.12 \text{ x } 10^{-6}\right)TV \tag{8.1}$$

$$PCU_{THW} = 0.60 + 0.001(P_{TW}) + 0.001(P_{Car}) + 0.004(P_{THW}) + 0.003(P_{Bus}) + 0.003(P_{HV}) + \left(1.86 \text{ x } 10^{-6}\right)TV \tag{8.2}$$

$$PCU_{BUS} = 7.12- 0.002(P_{TW}) - 0.015(P_{Car}) - 0.040(P_{THW}) - 0.055(P_{Bus}) - 0.011(P_{HV}) - \left(1.0 \text{ x } 10^{-7}\right)TV \tag{8.3}$$

$$PCU_{HV} = 5.20 - 0.002(P_{TW}) - 0.002(P_{Car}) - 0.025(P_{THW}) - 0.014(P_{Bus}) - 0.023(P_{HV}) - \left(5.9 \text{ x } 10^{-5}\right)TV \tag{8.4}$$

The best fit regression models for PCU values for each vehicle type for pedestrian section are given in the following equations:

$$PCU_{TW} = 0.23+ 0.001(P_{TW}) + 0.001(P_{Car}) + 0.004(P_{THW}) + 0.004(P_{Bus})+ 0.003(P_{HV}) + \left(6.11 \text{ x } 10^{-6}\right) TV+ 24.56(ped\_vol) \tag{8.5}$$

$$PCU_{THW} = 1.09+ 0.002(P_{TW})+ 0.002(P_{Car}) + 0.003(P_{THW}) + 0.005(P_{Bus}) + 0.007(P_{HV}) + \left(1.34\text{x } 10^{-6}\right) TV+ 19.99(ped\_vol) \tag{8.6}$$

$$PCU_{BUS} = 6.05- 0.015(P_{TW}) - 0.015(P_{Car}) - 0.064(P_{THW}) - 0.034(P_{Bus}) - 0.025(P_{HV}) - \left(1.5 \text{ x } 10^{-5}\right) TV- 26.64(ped\_vol) \tag{8.7}$$

$$PCU_{\mathrm{HV}} = 4.87- 0.003(P_{TW}) - 0.005(P_{Car}) - 0.042(P_{THW}) - 0.024(P_{Bus})- 0.014(P_{HV}) - \left(1 \text{ x } 10^{-5}\right) TV- 29.24(ped\_vol) \tag{8.8}$$

In these equations, P_{Car}= percentage of cars (%), P_{THW}= percentage of three-wheelers (%), P_{Bus} = percentage of buses (%), P_{HV} = percentage of heavy vehicles (%), TV = traffic volume (veh/h), and *ped_vol* = pedestrian volume (ped/h). The R^2 value of the models are obtained within the range of 0.80-0.94 and within the range of 0.79-0.92 for ideal_ped and pedestrian sections, respectively. The models also have F–statistics more than the critical value both for ideal section and pedestrian section suggesting that the models are statistically significant (Table 8.1). The model results indicate that as the traffic volume, and proportion of cars, THW, buses and heavy vehicles increases; PCU values for TW and THW increase whereas PCU values for of HV and bus reduce in both the sections. As the pedestrian volume remains zero (ped/h) in ideal section, PCU values doesn't get affected whereas in pedestrian section, PCU values for TW and THW increase, and PCU values for HV and bus reduce with increase in pedestrian volume. The regression equations obtained to predict PCU values are validated and it is found that the model replicates the field conditions reasonably. Development of the regression model is done using 75% of the simulated results and remaining 25% is used for its validation.

Table 8.1 F-Statistics Value for MLR Equations to Predict PCU Values

Vehicle Type	F-Statistics Values			
	Ideal Section		Pedestrian Section	
	F_{obs}	F_{crit}	F_{obs}	F_{crit}
TW	63.2	2.35	50.6	2.37
THW	54.9	2.34	45.1	2.36
Car	61.5	2.36	52.4	2.35
Bus	45.9	2.34	41.3	2.35
HV	41.9	2.34	38.2	2.36

8.2.2 Influencing Parameters and Assumed Values for Sensitivity Analysis of Capacity

The influencing factors and values used for performing sensitivity analysis of capacity of ideal (ideal_ped) and pedestrian sections are as follows:

(i) Case 1: Varying vehicular composition

Five different vehicular composition other than the observed composition are assumed from various studies on Indian urban roads (Asaithambi *et al.* 2012) in such a way that each vehicle type is dominating with respect to the observed composition. The following compositions are used in the study.

- C (observed composition): 51% TW, 30% cars, 9% THW, 8% buses and 2% HV
- C1: 70% TW, 17% cars, 10% THW, 2% buses and 1% HV (TW Dominant)
- C2: 50% TW, 14% cars, 34% THW, 1% buses and 1% HV (THW Dominant)
- C3: 40% TW, 50% cars, 8% THW, 1% buses and 1% HV (Cars Dominant)
- C4: 40% TW, 30% cars, 9% THW, 20% buses and 1% HV (Buses Dominant)
- C5: 50% TW, 30% cars, 8% THW, 2% buses and 10% HV (HV Dominant)

The observed pedestrian volume of 404 ped/h for the pedestrian section is used for all the composition.

(ii) Case 2: Varying pedestrian volume

The pedestrian volume in the pedestrian section is increased from 500 ped/h to 4500 ped/h with an increment of 500 ped/h for the observed vehicular composition (C) and traffic volume.

(iii) Case 3: Varying pedestrian volume and varying vehicular composition

For each vehicular composition (C, C1, C2, C3, C4 and C5), the pedestrian volume in the pedestrian section is increased from 500 ped/h to 4500 ped/h with an increment of 500 ped/h.

In all the above cases as the pedestrian crossings are absent in the ideal section, the pedestrian volume is taken as zero ped/h. Also, the observed traffic volume of 3664 veh/h and 3276 veh/h for ideal and pedestrian sections, respectively are used for all the composition and pedestrian volume.

8.2.2.1 Impact of Varying Vehicular Composition on Capacity

Comparing the capacities of ideal and pedestrian section separately in terms of vehicles per hour will be more appropriate to study the impact of varying vehicular composition on capacity as the comparison in terms of PCUs per hour can be misleading when the proportion of larger sized vehicles are significant. The capacity values for ideal and pedestrian sections with varying vehicular composition are presented in Table 8.2. The simulated results indicate that when the composition of TW is dominant (C1), it provides more space for other vehicles to travel which does not affect traffic stream speeds of both the sections when analysed separately and thus, the capacity is not affected. However, the capacity reduces in both the sections when the proportion of larger sized vehicles (THW dominant, car dominant, HV (includes LCV and trucks) dominant and buses dominant) increases due to the deficient space for movement.

Reduction in capacity values is observed with varying vehicular composition when the capacity of pedestrian section is compared with that of ideal section. In case of observed composition (C), the capacity of pedestrian section is reduced by 19.1% when compared to that of ideal section. Moreover, when the proportion of TW is dominant (C1), capacity of pedestrian section had a reduction of 19.7% from that of ideal section. This is because in pedestrian section, pedestrians try to cross the road besides the possibility of accidents when they find more smaller sized vehicles like TWs. But in ideal section, TWs provide more space for other vehicles to travel. Hence, those vehicles traveling at higher speeds in ideal section have to reduce their speed in the pedestrian section. For composition C2 (THW dominant), C3 (cars dominant), C4 (buses dominant) and C5 (HV dominant), capacity of pedestrian section declined by 18.9%, 18.8%, 18.1% and 18.4%, respectively as the proportion of medium and larger sized vehicles are higher. The higher proportion of medium and larger sized vehicles provides lesser road space for all the vehicles to travel which results in speed reduction in both ideal and pedestrian sections. Moreover, when these vehicles travel to the pedestrian section, pedestrians try to wait for the next available gap to cross the road as they find a large sized approaching vehicle close to them. However, when the pedestrians find a larger gap, they try to cross the road which make the approaching vehicles reduce their speed resulting in reduction in capacity of pedestrian section compared to that of ideal section.

Table 8.2. Variation in Capacity of Ideal and Pedestrian Section With Change in Vehicular Composition

Variation of Parameters		Capacity [veh/h (PCU/h)]		
		Ideal Section	**Pedestrian Section**	**Percentage Reduction (%)**
Composition of Each Vehicle Type (%)	C(observed)	4184 (3834)	3384 (3101)	19.1
	C1	4267 (2217)	3424 (1779)	19.7
	C2	4160 (2479)	3372 (2009)	18.9
	C3	4126 (3003)	3348 (2436)	18.8
	C4	3931 (5527)	3217 (4523)	18.1
	C5	4056 (3795)	3308 (3095)	18.4

8.2.2.2 Impact of Varying Pedestrian Volume on Capacity

For the observed vehicular composition, when the pedestrian volume in the pedestrian section is incremented from the observed volume (404 ped/h) to 4000 ped/h, the road capacity of the pedestrian section gets reduced by 47%, and further increase in the pedestrian volume from 4000 ped/h to 4500 ped/h doesn't affect the road capacity. Increase in pedestrian volume tends pedestrians to move in a group thus causing higher reduction in capacity. In the ideal section, the pedestrian volume remains zero (ped/h) and hence, the ideal section capacity (3834 PCU/h [4184 veh/h]) doesn't vary. Table 8.3 presents the impact of pedestrian volume on capacity of pedestrian section compared to that of the ideal section. From the table, it is observed that the percentage reduction in the road capacity of pedestrian section from that of the ideal section increases with increase in the pedestrian volume.

Table 8.3. Reduction in Capacity of Pedestrian Section with Varying Pedestrian Volume

Pedestrian Volume[ped/h]	Pedestrian Section Capacity [veh/h (PCU/h)]	Percentage Reduction (%)
404	3384 (3101)	19.1
500	3149 (2886)	24.7
1000	2985 (2735)	28.6
1500	2856 (2617)	31.7
2000	2748 (2518)	34.3
2500	2320 (2126)	44.5
3000	2099 (1924)	49.8
3500	2004 (1836)	52.1
4000	1790 (1640)	57.2
4500	1784 (1635)	57.3

8.2.2.3 Impact of Varying Pedestrian Volume and Varying Vehicular Composition on Capacity

In order to analyse the variation in capacity with varying pedestrian volume and varying vehicular composition, the pedestrian volume is increased from 500 ped/h to 4500 ped/h for each vehicular composition (C, C1, C2, C3, C4 and C5). Figure 8.19 illustrates the reduction in capacity of pedestrian section from that of ideal section due to the impact of varying pedestrian volume and varying vehicular compositions. From the figure, it is noticed that irrespective of the composition, the percentage reduction of capacity increases with increase in pedestrian volume. However, when the vehicular composition is varied for each pedestrian volume, the same trend observed in section 8.2.2.1 is noticed for pedestrian volume from 500 ped/h to 1500 ped/h. But the trend varies for pedestrian volume from 2000 ped/h to 4500 ped/h. This is because when the pedestrian volume is higher, pedestrians tend to move in a group. Hence, even when they find larger sized vehicles closer to them, they cross the road, leading to a higher percentage reduction in capacity of roads with the presence of higher proportion of larger sized vehicles.

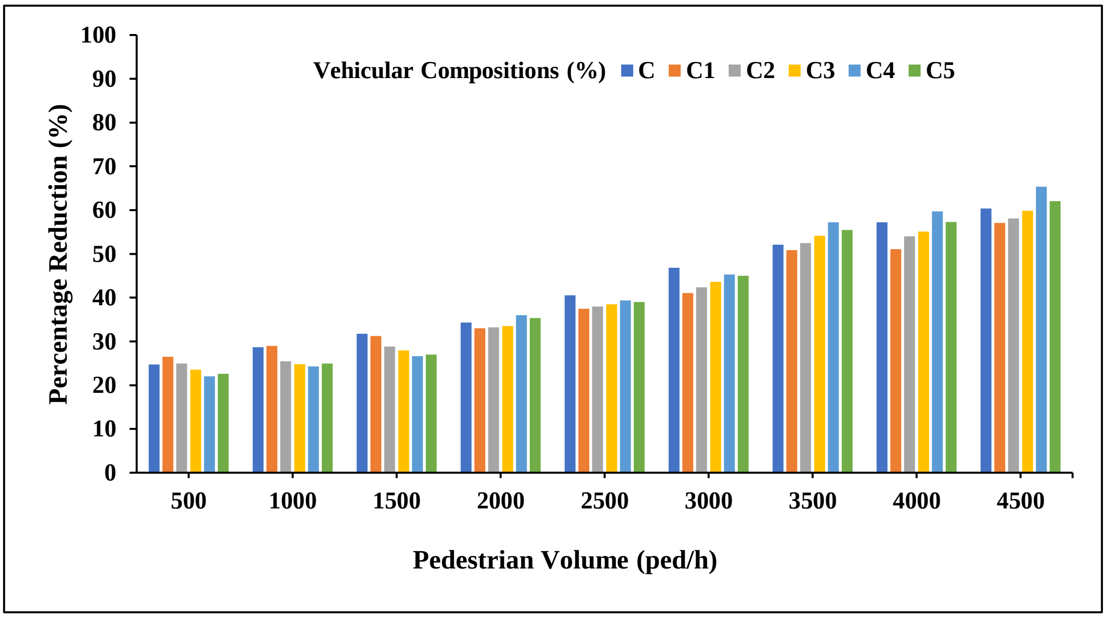

Figure 8.19 Reduction in Capacity due to the Impact of Varying Pedestrian Volume and Varying Vehicular Composition- Pedestrian Section

8.2.2.4 Multiple Linear Regression Model for Predicting Capacity

Considering the simulated results, regression models are developed to predict the capacities of four-lane divided urban roads with and without undesignated pedestrian crossings using a set of influencing variables such as pedestrian volume, and proportion of cars, THW, buses and HV. Multiple linear regression models are developed for both the sections with capacity as the dependent variable, and proportion of vehicle types and pedestrian volume as independent variables. The best fit regression models to predict capacity of ideal_ped, *Capacity_idealped* (veh/h) and pedestrian sections, *Capacity_ped* (veh/h) are given as:

$$Capacity\_idealped = 5489.17 - 20.56(P_{TW}) - 21.84\,(P_{Car}) - 22.65(P_{THW}) - 79.03(P_{Bus}) - 22.72(P_{HV}) \quad (8.9)$$

$$Capacity\_ped = 4138.73 - 17.31(P_{TW}) - 17.25(P_{Car}) - 17.19(P_{THW}) - 18.41(P_{Bus}) - 17.66(P_{HV}) - 22.69(ped\_vol) \quad (8.10)$$

where, P_{Car}= percentage of cars (%), P_{THW}= percentage of three-wheelers (%), (%), P_{Bus} = percentage of buses (%), P_{HV}= percentage of heavy vehicles (%) and *ped_vol* = pedestrian volume (ped/h). The R^2 value of the models are obtained as 0.96 and 0.94 for ideal and pedestrian sections, respectively. The models also have F–statistics more than the critical value both for ideal section (F_{obs} = 56.3, F_{crit} = 2.37) and pedestrian section (F_{obs} = 47.6, F_{crit} = 2.39) suggesting that the models are statistically significant. The model results indicate that as the proportion of cars, THW, buses and heavy vehicles increases, capacity decreases considerably for both the sections. As the pedestrian volume remains zero (ped/h) in ideal section, its capacity doesn't get affected whereas the capacity of pedestrian section reduces with increase in pedestrian volume. The regression equations obtained to predict capacity are validated and it is found that the model replicates the field conditions reasonably. Regression model development is carried out using 75% of the simulated results and remaining 25% is used for its validation.

8.3 SUMMARY

The quantification of PCU and capacity values with and without undesignated pedestrian crossings is performed using the validated base model (ideal_ped) and vehicle-pedestrian interaction model, respectively. Sensitivity analysis of PCU and capacity values in the presence of undesignated pedestrian crossings is performed by varying several influencing factors such as pedestrian volume, vehicular composition and traffic volume. The results indicate significant differences in PCU (with varying vehicular composition, traffic volume and pedestrian volume) and capacity values (with varying vehicular composition and pedestrian volume) due to the presence of pedestrians.

CHAPTER 9

CONCLUSIONS AND FUTURE SCOPE

9.1 SUMMARY AND CONCLUSIONS

Indian roads have disordered traffic with vehicles of widely varying static and dynamic characteristics occupying any available position on the road space without complying to any lane discipline. Therefore, the complex vehicular manoeuvers in disordered traffic make it complicated to estimate capacity. Also, expressing capacity as the maximum number of vehicles passing a given section of road per unit time is inappropriate. To overcome this, traffic flow is analysed by converting different vehicle types into a uniform measure of vehicles called Passenger Car Unit (PCU)and thus, capacity can be expressed in terms of PCU/h. These PCU values depend on various factors such as traffic flow conditions, geometric conditions, roadside frictions, etc. However, in urban roads of developing countries, roadside frictions such as curbside bus stops, undesignated pedestrian crossings, roadside parking, etc. considerably influence the PCU values of vehicles. Out of the existing roadside frictions, curbside bus stops and undesignated pedestrian crossings which are commonly observed in urban roads lead to significant deterioration of traffic flow thereby affecting the PCU as well as capacity values. Thus, the present study focuses on assessing the impact of these roadside frictions on PCU and capacity of urban roads under disordered traffic conditions. For this purpose, a microscopic traffic simulation model (base model) is developed for an ideal urban divided mid-block section in disordered traffic. Logics involved in model development are formulated and implemented in MATLAB using object-oriented programming concepts. The logics involved in the base model development are generation, placement and movement of vehicles. Gipps car following model is used to model the vehicular movements. The developed model is calibrated and validated using the data collected from Bangalore city, India. Validation is performed using internal and external data sets. To estimate the PCU values for different vehicles, a new methodology considering the influence of surrounding vehicles is proposed and incorporated in the validated base model, and the proposed methodology is then validated by comparing the simulated and manually calculated PCU values. The validated base model is further modified to simulate the traffic behaviour in sections with side frictions such as curbside bus stop and undesignated pedestrian crossings in order to investigate the impact of these side frictions on PCU values for several vehicle types and capacity. The relative influences of various parameters such as traffic volume, vehicular composition, bus proportion (applicable only for bus stop section), proportion of stopping buses (applicable only for bus stop section), and pedestrian volume (applicable only for pedestrian section) in the presence of side frictions are investigated by carrying out sensitivity analysis. With simulated results of sensitivity analysis, multiple linear regression models are developed to predict the PCU and capacity values for ideal, bus stop and pedestrian sections.

9.1.1 Significant Contributions of the Research

The major contributions in this research compared to the previous studies are:

a) A methodology is proposed to estimate PCU values for different vehicle types considering the influence of surrounding vehicles (effective area approach), and the logics for estimating PCU values using this approach are implemented in the simulation model.
b) The base simulation model is modified to simulate the vehicular movements on sections with side frictions such as curbside bus stop and undesignated pedestrian crossings to study the impact of these side frictions on PCU values and capacity.
c) Modification of base model to simulate bus stop section

- The vehicle movement logic in the base model is modified in such a way that when the bus approaches the bus stop, it tries to decelerate at a position before the bus stop and then stops near the bus stop randomly in the simulation stretch.

d) Modification of base model to simulate vehicle-pedestrain interaction

- The base model is modified to study the real-world vehicle-pedestrian interactions in disordered traffic having wide variety of vehicles traveling without lane discipline. The movement logics of vehicles and pedestrians engages the interaction between vehicles and pedestrians. During the interaction process, both vehicles and pedestrians are affected mutually.

- To explain the approaching vehicle's influence on pedestrian, an additional force, i.e., vehicle-pedestrian interaction force is added along with the other forces (destination force and pedestrian-pedestrian interaction force) in the Social Force Model (SFM) used for modelling pedestrian movements. When there is no interaction between vehicles and pedestrians on the road, vehicular movements are modelled using Gipps car following model. If a pedestrian negotiates the gap between two vehicles successfully, the Gipps model which is used to model vehicular flow is not sufficient to evaluate the behaviour of approaching vehicle. Hence, pedestrian information is added to the Gipps model to update the speeds of approaching vehicles during interactions.
- A simple gap-acceptance criterion based on pedestrian's crossing time and approaching vehicle's passing time are considered in pedestrian decision-making for crossing the road.
- The unique pedestrian crossing patterns observed in disordered traffic such as moving in perpendicular pattern and oblique pattern are also introduced in model.

9.1.2 Key Findings of the Research

The key findings arising out of this research based on the application of the base and modified simulation models are:

(i) Influence of curbside bus stop on PCU values and capacity

a) At flow levels of 1000 veh/h and 4500 veh/h, it is observed that

- There is an increase in PCU values for TW by 4.1% and 6.3%, respectively and an increase in PCU values for THW by 2.5% and 5.2%, respectively from ideal to bus stop section.
- There is a reduction in PCU for HV by 7.1% and 8.8%, respectively in bus stop section compared to that of ideal section.
- Speeds of a few buses drop down to zero m/s when they stop near the bus stop, the speed ratio between car and bus increases resulting in higher PCU values.

b) The results of variation in vehicular composition shows that,

- When the proportion of TW is dominant (C1), PCU for TW and THW had an increase of 3.2% and 4.3%, respectively from ideal to bus stop section but HV's PCU reduced by 6.6%.
- For compositions C2, C3, C4 and C5, PCU for HV in bus stop section reduced by 9.2%, 11.1%, 8.8% and 6.9%, respectively compared to that of ideal section but PCU for TW and THW incremented due to their higher relative speed with respect to car.
- PCU for buses had an increase in all the cases (C1, C2, C3, C4, C5).

c) Increase in bus proportion from 2 to 20% results in:

- Lower values of PCU for HV in case of bus stop section compared to that of ideal section whereas TW, THW and bus showed an increase in PCU values.

d) When the proportion of stopping buses is 100%,

- PCU values for TW, THW and bus increased by 10%, 5.1% and 29%, respectively whereas PCU values for HV reduced by 9%. In ideal section, buses are not categorized as stopping and non-stopping buses and thus, PCU values for vehicle types do not change.

e) Similar trend is observed for PCU values for all vehicle types with varying proportion of buses, traffic volume, proportion of stopping buses and vehicular composition.

f) A reduction in capacity values from ideal to bus stop section is observed with variation of vehicular compositions (C1, C2, C3, C4, C5) with observed traffic volume.

g) Capacity is reduced by 18% in bus stop section compared to that of ideal section for 2% buses while a reduction of 19.6% in capacity is observed for 20% of buses.

h) Bus stop section capacity is reduced by 20.7% when proportion of stopping buses is 100%.

i) Also, when the vehicular composition, bus proportion and proportion of stopping vehicles are varied simultaneously, the same trend is observed for capacity.

(ii) Influence of undesignated pedestrian crossings on PCU values and capacity

a) At flow levels of 1000 veh/h and 4500 veh/h, it is observed that

- There is an increase in PCU values for TW by 3.7% and 10.2%, respectively and an increase in PCU values for THW by 6.6% and 12.2%, respectively from ideal to pedestrian section.
- PCU for HV reduced by 2.9% and 6.9%, respectively and PCU values for bus reduced by 5% and 10.7%, respectively from ideal to pedestrian section.

b) When PCU values are compared for varying vehicular compositions, it is noticed that:

- PCU values for TW and THW had an increase of 9.6% and 12%, respectively from ideal to pedestrian sections for TW dominant (C1) proportion. PCU for bus and HV reduced by 4% and 5.8%, respectively.
- For proportions C2, C3, C4 and C5, PCU for bus in pedestrian section decreased by 4.3%, 6.9%, 10.2%, and 9.1%, respectively and PCU for HV in pedestrian section reduced by 7.5%, 8.1%, 8.8% and 6.9%, respectively compared to that of ideal section.

c) As pedestrian volume in pedestrian section increases:

- PCU values for TW and THW had an increment by 12.6% and 11.9%, respectively whereas PCU values for bus and HV reduced by 7.8% and 8.7%, respectively.

d) The same trend in PCU values is followed when traffic volume, pedestrian volume, and vehicular composition are varied simultaneously.

e) The capacity reduced by 19.1 % and 19.7 % compared to that of ideal section for the observed composition (C) and TW dominant proportion (C1).

f) For compositions C2, C3, C4 and C5, capacities declined by 18.9%, 18.8%, 18.1% and 18.4%, respectively.

g) When the pedestrian volume is incremented from the observed volume to 4000 ped/h, the road capacity reduced by 47%.

h) When pedestrian volume is increased with vehicular composition, it is found that irrespective of composition, reduction in capacity increases with increase in pedestrian volume.

The present study finds interesting applications in developing and updating standards related to PCU as well as capacity estimation in the presence of side frictions such as curbside bus stops and undesignated pedestrian crossings on urban roads in disordered traffic. The study findings and results can be used by traffic engineers and planners to predict realistic PCU and capacity values for planning and designing of new facilities with side frictions instead of directly adopting the values available in the existing manuals.

Furthermore, it is possible to implement the study results and findings for improving the existing policies in India. Based on the study findings, it is clearly observed that the side frictions such as curbside bus stops and pedestrians affects the performance of traffic flow. Thus, to overcome the congestion causing due the side frictions, certain strategies can be implemented. Exclusive bus lanes help to reduce delays due to traffic congestion. Exclusive lanes can be time-based, i.e., they can be exclusive during peak periods and reverting to mixed-flow or parking lanes at other times. Frequent number of safe pedestrian facilities like pedestrian over bridge or underpass considering their demand needs to be provided. Designing a walkable side walk can be considered as another strategy. Thin sidewalks force pedestrians to compete for space with cars and auto-rickshaws, making it uncomfortable and unsafe for those who use the sidewalks.

9.2 LIMITATIONS AND FURTHER SCOPE OF THE STUDY

Due to limited field of view of camera, data for the present study are collected from urban divided roads considering only 70 m length of the road, which can be considered as one of the limitations of the study. Moreover, the effect of change in driver characteristics, road width, road type, dwell times of buses, length of curbside bus stops, behavior of pedestrians considering their gender, age, disability, etc. on PCU values and capacity of roads with curbside bus stops and undesignated pedestrian crossings may be considered for better results. In future, this research can be extended to study the impact of other roadside frictions (e.g. parking, encroachments) on PCU values and capacity by modifying the logics in the simulation model. Furthermore, this research can be also extended to study the impact of side frictions on a greater number of test sections on different facility types (e.g. urban undivided roads, rural roads, intersections) by modifying the developed base model. The developed simulation models can be modified for other urban roads by providing the vehicular composition, distributions of time gap, desired speeds of vehicles, pedestrian volume, frequency of stopping buses, bus stop position, etc. as inputs. Also, if an additional vehicle such as tractor or a horse cart is plying on the same road section, the composition, static and dynamic characteristics of the respective vehicle type can be added in to the simulation model and their respective PCU values can be calculated. The bus stop model can be further modified to simulate the traffic manoeuvers in the sections with bus bays and exclusive bus lanes. The model describing vehicle-pedestrian interactions can be modified to determine surrogate safety measures (e.g. time-to-collision between vehicles and pedestrians) that reflect safety of urban roads where the presence of pedestrians is significant. Also, the Gipps model and Social Force Model used to simuate vehicle and pedestrian movements in this study can be replaced by other microscopic behaviour control models.

APPENDIX I

SAMPLE CALCULATION OF CORRECTION FACTOR

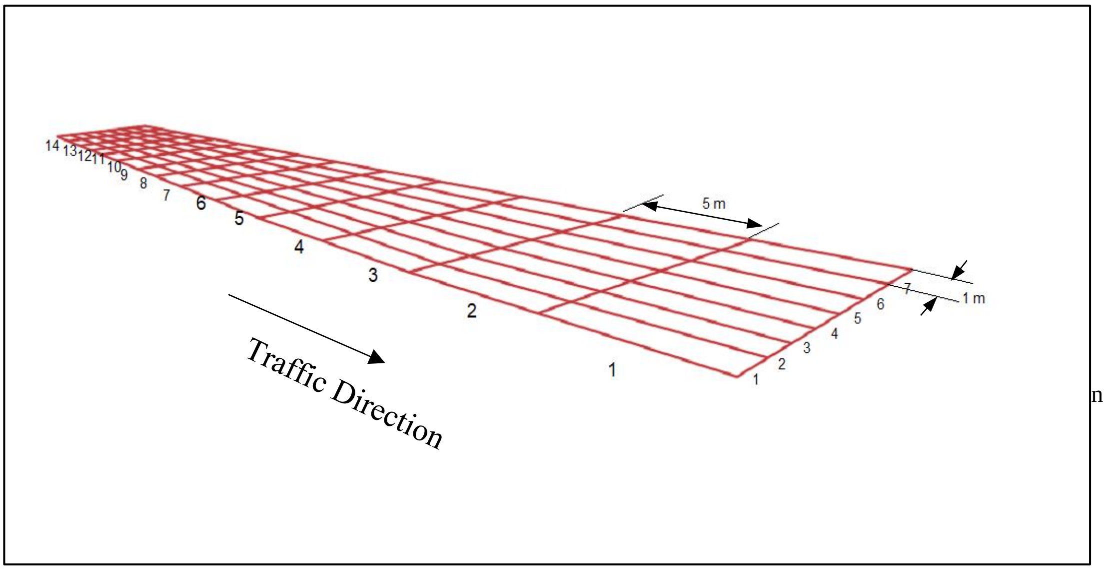

Figure I.1 Gridline Image of Ideal section located on HAL Road, Bangalore City

The sample calculations for the above image are shown below for block 14, 1 (longitudinal grid line number, lateral grid line number).

(112, 411) A D (132, 409)

14

(123, 416) B C (144, 413)

1

Distance between two points = $\sqrt{(x_2 - x_1)^2 + (y_2 - y_1)^2}$ (I.1)

From above, distance AB = $\sqrt{(123 - 112)^2 + (416 - 411)^2}$

= 12.08 pixels

Similarly, BC = 21.21 pixels,

CD = 12.64 pixels,

DA = 20.09 pixels.

Longitudinal distance = Mean of AB, CD

= (12.08 +12.64)/2

= 12.36 pixels

Lateral distance = Mean of BC, DA

= (21.21 +20.09)/2

= 20.65 pixels

Actually 12.36 pixels = 500 cm

So, 1 pixel = 40.43 cm

Actually 20.65 pixels = 100 cm

so, 1 pixel = 4.84 cm

For block 14, 1 correction factor in longitudinal direction is 40.43 cm, and correction factor in lateral direction is 4.84 cm

Table I.1 Sample Correction Factors for Longitudinal and Lateral Blocks of Gridline Image -Ideal_bus Section

Block No.		Distance in cm for one pixel		Block No.		Distance in cm for one pixel	
Longitudinal	**Lateral**	**Longitudinal**	**Lateral**	**Longitudinal**	**Lateral**	**Longitudinal**	**Lateral**
1	1	1.40	2.57	5	1	3.39	2.85
1	2	1.46	2.99	5	2	3.39	3.09
1	3	1.54	2.88	5	3	3.41	2.95
1	4	1.63	3.10	5	4	3.46	2.85
1	5	1.72	2.98	5	5	3.50	2.95
1	6	1.83	2.86	5	6	3.51	2.89
1	7	1.97	3.11	5	7	3.51	3.06
2	1	1.27	3.21	6	1	5.06	3.05
2	2	1.36	3.80	6	2	5.06	3.08
2	3	1.45	3.76	6	3	4.95	3.09
2	4	1.55	3.86	6	4	4.83	2.93
2	5	1.66	3.83	6	5	4.76	2.99
2	6	1.80	3.77	6	6	4.71	3.05
2	7	1.95	4.05	6	7	4.59	3.33
3	1	1.59	3.26	7	1	7.07	3.06
3	2	1.68	3.65	7	2	6.82	3.50
3	3	1.76	3.65	7	3	6.55	3.44
3	4	1.86	3.60	7	4	6.30	3.28
3	5	1.97	3.65	7	5	5.99	3.32
3	6	2.10	3.66	7	6	5.76	3.26
3	7	2.23	3.91	7	7	5.62	3.83
4	1	2.25	2.70	8	1	9.81	3.33
4	2	2.30	3.16	8	2	9.51	3.86
4	3	2.39	3.17	8	3	9.22	3.86
4	4	2.47	3.04	8	4	8.77	3.73
4	5	2.55	3.19	8	5	8.58	3.63
4	6	2.66	3.03	8	6	8.41	3.58
4	7	2.77	3.29	8	7	8.28	3.99

APPENDIX II

SAMPLE DATA USED FOR EXTRACTION

Table II.1 Sample Data Sheet used for Extraction of Free-flow Speed of Vehicles-Ideal_bus Section

Sl. No.	Subject Vehicle Type	Entry Frame No.	Exit Frame No.	Free-flow Speed (m/s)	Free-flow Speed (km/h)
1	TW	6	90	25	90
2	CAR	14	119	20	72
3	CAR	23	170	14.28	51.42
4	TW	31	157	16.7	60
5	THW	39	354	6.7	24
6	CAR	47	236	11.11	40
7	CAR	55	181	16.7	60
8	CAR	63	189	16.7	60
9	TW	71	197	16.7	60
10	CAR	80	206	16.7	60
11	HV	88	256	12.5	45
12	CAR	96	243	14.28	51.42
13	CAR	104	230	16.7	60
14	CAR	114	303	11.11	40
15	CAR	122	290	12.5	45
16	TW	131	257	16.7	60
17	TW	139	286	14.28	51.42
18	CAR	147	273	16.7	60
19	TW	158	305	14.28	51.42
20	CAR	166	313	14.28	51.42
21	CAR	174	300	16.7	60
22	CAR	184	331	14.28	51.42
23	TW	192	276	25	90
24	CAR	202	307	20	72
25	CAR	314	461	14.28	51.42

Table II.2 Sample Data Sheet used for Extraction of Speed, Time Gap, Acceleration and Deceleration Rate of Vehicles – Ideal_bus Section

Sl. No.	Subject Vehicle Type	Speed		Speed (m/s)	Time Gap (s)	Speed (m/s)		Time to travel from Stretch 1 to stretch 2 (s)	Acceleration /Deceleration Rate (m/s^2)
		Entry Frame No.	Exit Frame No.			Stretch 1	Stretch 2		
1	TW	7223	7372	14.09	0.76	16.28	12.28	3.54	1.50
2	TW	7243	7403	13.12	0.66	16.5	14.28	3.57	-1.15
3	TW	7253	7428	12	0.33	13.63	13.04	3.87	-1.12
4	TW	7278	7452	12.06	0.83	12.5	12	4.14	-1.12
5	TW	7332	7510	11.79	1.8	12.5	12	4.17	-1.22
6	CAR	7332	7502	12.35	0	12.5	11.53	4.2	1.34
7	TW	7415	7593	11.79	2.76	11.11	12.5	4.04	-1.85
8	TW	7416	7571	13.54	0.03	11.5	7.89	4.27	1.54
9	CAR	7429	7578	14.09	0.43	11.5	13.63	3.87	-1.37
10	HV	7463	7658	10.76	1.13	15	13.63	3.6	1.29
11	CAR	7490	7638	14.18	0.9	9.67	11.11	4.84	1.39
12	CAR	7535	7717	11.53	1.5	13.63	15	3.44	1.21
13	CAR	7567	7715	14.18	1.06	11.11	12	4.2	1.63
14	CAR	7583	7740	13.37	0.53	11.11	16.66	3.4	-1.44
15	TW	7604	7807	10.34	0.7	13.63	12	3.7	0.8
16	TW	7609	7748	15.10	0.16	10.71	11.11	4.74	-1.22
17	CAR	7622	7801	11.73	0.13	15	14.28	3.17	0.62
18	TW	7636	7828	10.93	0.46	14.28	14.28	3.64	-0.9
19	THW	7697	7903	10.19	2.03	10.34	13.04	4.34	-1.16
20	CAR	7729	7923	10.82	0.96	16.28	12.28	3.54	-1.17

Table II.3 Sample Data Sheet used for Extraction of Lateral Gaps of Vehicles - Ideal_bus Section

Sl. No.	Subject Vehicle				Left Adjacent Vehicle					Right Adjacent Vehicle				
	Vehicle Type	X	Y	Speed (m/s)	Vehicle Type	X	Y	Lateral Gap (m) with Subject Vehicle	Speed (m/s)	Vehicle Type	X	Y	Lateral Gap (m) with Subject Vehicle	Speed (m/s)
6	TW	811	512	11.79	CAR	758	533	1.73	12.35					
7	CAR	758	533	12.35	TW	811	512	1.73	11.75					
12	CAR	673	495	14.18	HV	643	506	0.95	10.73					
19	CAR	831	527	11.73	THW	847	518	0.54	10.34					
21	THW	912	548	10.19	THW	857	590	2.01	10.60					
22	THW	857	590	10.60	THW	912	548	2.01	10.19					
32	CAR	748	552	12.06	TW	811	515	2.13	12.06					
33	TW	811	515	11.61						CAR	748	552	2.13	12.06
34	CAR	632	513	10.44	CAR	663	504	1.02	10.93					
35	CAR	663	504	10.93						CAR	632	513	1.022	10.93
36	CAR	715	536	10.55	THW	748	520	1.10	10.34					
37	THW	748	520	10.34						CAR	715	536	1.10	10.55

Table II.4 Sample Data Sheet used for Extraction of Longitudinal Gaps of Vehicles - Ideal_bus Section

Sl. No.	Subject Vehicle				Leader Vehicle				
	Vehicle Type	X	Y	Speed (m/s)	Vehicle Type	X	Y	Longitudinal Gap (m) with Subject Vehicle	Speed (m/s)
42	CAR	662	524	10.24	CAR	1463	692	24.23	11.29
43	CAR	736	556	9.37	CAR	941	600	7.06	10.24
45	THW	688	512	9.17	THW	810	532	3.79	9.63
46	CAR	743	561	9.05	CAR	1557	729	25.31	9.37
47	CAR	656	537	8.78	CAR	942	606	9.61	9.05
48	THW	856	528	8.97	THW	1155	581	22.01	9.17
49	CAR	998	574	9.21	CAR	1054	581	2.10	8.78
50	TW	892	514	12.80	THW	1283	584	26.64	6.93
51	TW	761	542	9.33	CAR	805	550	1.35	8.78
52	CAR	583	476	8.78	CAR	823	519	7.47	9.21
53	CAR	510	504	10	CAR	1040	625	18.35	8.78
55	CAR	715	523	8.89	CAR	1008	556	9.73	8.78
57	TW	904	534	10.24	CAR	1040	557	4.58	8.78
58	CAR	579	518	10.29	CAR	1158	651	21.73	10
59	CAR	869	531	9.45	CAR	1097	569	7.69	8.89

Table II.5 Sample Data Sheet used for Extraction of Lateral Position of Vehicles - Ideal_bus Section

Sl. No.	Subject Vehicle Type	Left Edge Coordinate of Vehicle				Edge Coordinate of Median				Lateral Position (m) with Applied Correction Factors
		X	Y	Longitudinal Block No.	Lateral Block No.	X	Y	Longitudinal Block No.	Lateral Block No.	
1	TW	188	405	14	6	112	411	14	1	4.48
2	TW	166	407	14	4	112	411	14	1	3.37
3	TW	140	407	14	2	112	411	14	1	2.26
4	TW	209	398	14	7	112	411	14	1	6.85
5	TW	181	404	14	5	112	411	14	1	4.34
6	TW	186	404	14	6	112	411	14	1	4.55
7	CAR	162	405	14	3	112	411	14	1	3.55
8	TW	188	405	14	6	112	411	14	1	4.48
9	TW	166	406	14	4	112	411	14	1	3.54
10	CAR	182	403	14	5	112	411	14	1	4.60
11	HV	167	405	14	4	112	411	14	1	3.79
12	CAR	211	400	14	6	112	411	14	1	6.40
13	CAR	155	407	14	3	112	411	14	1	2.80
14	CAR	188	403	14	5	112	411	14	1	4.84
15	CAR	152	407	14	3	112	411	14	1	2.66
16	THW	205	407	14	6	112	411	14	1	5.06
17	TW	132	410	14	2	112	411	14	1	1.24
18	CAR	137	407	14	2	112	411	14	1	2.13

Table II.6 Sample Data Sheet used for Extraction of Bus Dwelling Time and Stopping Position of Bus at Bus Stop

Sl. No.	Subject Vehicle Type	Bus Dwelling Time (s)			Stopping Position of Bus (m)				
					Front Coordinates of Bus when Stopped		Entry Line Coordinates		Bus Stopping Position
		Entry Frame No.	Exit Frame No.	Dwelling Time	X	Y	X	Y	
25	Stopping Bus	5029	5244	7.1	862	426	297	523	40.7
58	Stopping Bus	6269	6335	2.2	897	420	297	524	48.9
164	Stopping Bus	14611	14887	9.2	890	421	297	524	48.3
181	Stopping Bus	15270	15312	1.4	870	426	297	524	41.3
220	Stopping Bus	19434	19440	1.2	898	425	304	537	43.8
64	Stopping Bus	5418	5678	8.6	899	418	299	518	48.9
128	Stopping Bus	10138	10255	3.9	900	420	296	523	49.1
199	Stopping Bus	15287	15323	1.2	905	422	303	535	37.5
317	Stopping Bus	1638	1735	3.2	873	426	298	525	41.5
403	Stopping Bus	6782	7012	7.6	887	422	297	523	48.0
507	Stopping Bus	14830	15000	5.6	867	427	299	525	41.0
641	Stopping Bus	1370	1427	1.9	881	429	306	539	39.2
651	Stopping Bus	1886	1910	1.8	849	435	304	535	33.9

Table II.7 Sample Data Sheet used for Extraction of Pedestrian Data

Sl. No.	Pedestrian's Direction of Movement		Pedestrian Walking Speed			Pedestrian Time Gap (s)	Pedestrian Coordinates		Edge Coordinates		Position of Pedestrian (m)	Pedestrian Waiting Time		
	Median to Curb	Curb to Median	Entry Frame No.	Exit Frame No.	Speed (m/s)		X	Y	X	Y		Entry Frame No.	Exit Frame No.	Waiting Time
1	1		393	675	0.74	9.4	1017	297	641	527	49.68	1	393	13.06
2	1		393	675	0.74	0	1020	297	641	527	49.72	1	393	13.06
3		1	412	619	1.01	0.63	1243	295	809	588	67.13	412	412	0
4		1	440	651	0.99	0.93	1111	405	809	588	41.66	1	435	14.46
5		1	465	651	1.12	0.83	1114	405	809	588	41.70	1	435	14.46
6		1	484	651	1.25	0.63	867	455	809	588	24.21	1	436	14.5
7		1	484	651	1.2	0	873	448	809	588	26.83	1	436	14.5
8		1	484	651	1.25	0	880	442	809	588	29.45	1	436	14.5
9		1	534	629	2.21	1.66	1087	425	809	588	36.79	537	537	0
10	1		751	893	1.47	7.23	849	406	641	527	23.53	751	751	0
11		1	1228	1433	1.02	15.9	1244	295	809	588	67.15	1226	1266	1.33
12	1		1369	1595	0.92	4.7	1056	286	641	527	57.26	1351	1351	0
13	1		1385	1595	1	0.53	1067	280	641	527	59.41	1376	1376	0
14		1	2419	2608	1.11	34.46	906	375	641	527	31.00	2420	2420	0
15	1		3470	3737	0.78	35.03	849	406	641	527	23.53	2978	3470	16.4

APPENDIX III

PROCEDURE FOR CALCULATING THE EFFECTIVE AREA

Table III.1 Vehicle Types and Coordinates of Subject Vehicle and Surrounding Vehicles

Subject Vehicle							Left Adjacent Vehicle			Right Adjacent Vehicle			Leader		
Vehicle Type	Front Coordinates		Left Coordinates		Right Coordinates		Vehicle Type	Right Coordinates		Vehicle Type	Left Coordinates		Vehicle Type	Back Coordinates	
	X	Y	X	Y	X	Y		X	Y		X	Y		X	Y
THW	215	409	222	399	200	411	TW	230	399	CAR	177	414	CAR	231	413

Longitudinal gap = 1.10 m

Left lateral gap = 0.47 m

Right lateral gap = 1.48 m

The left lateral gap and right lateral gap are then divided based on size ratio of the subject vehicle and adjacent vehicle.

D_k = lateral distance of subject vehicle type k (m);

Z_k = physical size of subject vehicle type k (m^2);

Z_{adj} = physical size of adjacent vehicle type adj (m^2).

$$D_k = \frac{Z_k}{(Z_k + Z_{adj})} * \text{lateral gap} \quad \text{(III.1)}$$

Here, the subject vehicle is three-wheeler. The left adjacent vehicle is a two-wheeler and right adjacent vehicle is car

$$\text{Left } D_{THW} = \frac{4.48}{(4.48+1.2)} * 0.47 \text{ m} = 0.37 \text{ m}$$

$$\text{Right } D_{THW} = \frac{4.48}{(4.48+5.36)} * 1.48 \text{ m} = 0.67 \text{ m}$$

Effective area of subject vehicle = (Length of subject vehicle + Longitudinal gap) ×

(Width of subject vehicle + Left D_{tw} + Right D_{tw}) (III.2)

= (3.2 + 1.10) * (1.4 + 0.37 +0.67) = 10.5 m^2

The effective areas of all the vehicles are calculated as shown in the above example.

APPENDIX IV

OUTPUTS OBTAINED FROM SIMULATION MODELS

Table IV.1 Time Gaps of Vehicles obtained from the Base Simulation Model

Vehicle ID	Time gap (s)	Vehicle Type
1	0.14	CAR
2	1.75	BUS
3	4.5	THW
4	6	CAR
5	8	CAR
6	10	CAR
7	11	CAR
8	12	BUS
9	12	TW
10	13	TW
11	14	BUS
12	17	CAR
13	18	CAR
14	18	TW
15	20	CAR
16	22	CAR
17	22	TW
18	23	TW
19	24	CAR
20	24	TW
21	25	BUS
22	27	TW
23	28	CAR
24	29	BUS
25	32	CAR
26	32	CAR
27	33	TW
28	33	TW
29	34	TW
30	35	CAR

Table IV.2 Trajectory and Speed Values of Vehicles obtained from the Base Simulation Model

Time Step	Vehicle ID	Vehicle Type	x (m)	y (m)	Speed (m/s)
10	1	TW	179.19	2.08	15.05
10	2	CAR	140.81	2.71	14.06
10	3	TW	152.02	4.65	15.16
10	4	TW	110.75	1.66	13.78
10	5	THW	73.45	4.13	9.71
10	6	CAR	50.78	2.83	9.57
10	7	CAR	9.26	2.55	11.11
11	1	TW	184.19	2.08	15.16
11	2	CAR	146.81	2.71	14.22
11	3	TW	157.02	4.65	15.26
11	4	TW	115.75	1.66	14.01
11	5	THW	75.45	4.13	9.87
11	6	CAR	56.78	2.83	9.99
11	7	CAR	15.26	2.55	11.45
12	1	TW	189.19	2.08	15.26
12	2	CAR	152.81	2.71	14.37
12	3	TW	162.02	4.65	15.35
12	4	TW	120.75	1.66	14.21
12	5	THW	77.45	4.13	10.02
12	6	CAR	62.78	2.83	9.88
12	7	CAR	21.26	2.55	11.77
13	1	TW	194.19	2.08	15.35
13	2	CAR	158.81	2.71	14.50
13	3	TW	167.02	4.65	15.43
13	4	TW	125.75	1.66	14.40
13	5	THW	79.45	4.13	10.16
13	6	CAR	68.78	2.83	10.28
13	7	CAR	27.26	2.55	12.08
13	8	BUS	11.50	3.51	11.79
14	1	TW	199.19	2.08	15.43
14	2	CAR	164.81	2.71	14.63
14	3	TW	172.02	4.65	15.51
14	4	TW	130.75	1.66	14.57

Table IV.3 Trajectory and Speed Values of Vehicles obtained from the Bus Stop Simulation Model

Time Step	Vehicle ID	Vehicle Type	x (m)	y (m)	Speed (m/s)
43	7	CAR	521.48	5.20	11.72
43	8	Stopping Bus	483.60	4.51	11.86
44	7	CAR	529.48	5.20	11.73
44	8	Stopping Bus	487.21	4.51	9.07
45	7	CAR	537.48	5.20	11.74
45	8	Stopping Bus	490.93	5.53	8.95
46	7	CAR	545.48	5.20	11.75
46	8	Stopping Bus	490.93	5.53	0
47	7	CAR	553.48	5.20	11.75
47	8	Stopping Bus	490.93	5.53	0
48	7	CAR	561.48	5.20	11.76
48	8	Stopping Bus	490.93	5.53	0
49	7	CAR	569.48	5.20	11.77
49	8	Stopping Bus	490.93	5.53	0
50	7	CAR	577.48	5.20	11.77
50	8	Stopping Bus	490.93	5.53	0
51	7	CAR	585.48	5.20	11.77
51	8	Stopping Bus	490.93	5.53	0
52	7	CAR	593.48	5.20	11.78
52	8	Stopping Bus	490.93	5.53	0
53	7	CAR	601.48	5.20	11.78
53	8	Stopping Bus	490.93	5.53	0
54	7	CAR	609.48	5.20	11.79
54	8	Stopping Bus	490.93	5.53	0
55	7	CAR	617.48	5.20	11.79
55	8	Stopping Bus	490.93	5.53	0
56	7	CAR	625.48	5.20	11.79
56	8	Stopping Bus	490.93	5.53	0
57	7	CAR	633.48	5.20	11.79
57	8	Stopping Bus	490.93	5.53	0
58	7	CAR	641.48	5.20	11.80
58	8	Stopping Bus	493.16	5.53	1.359
59	7	CAR	649.48	5.20	11.80
59	8	Stopping Bus	496.97	5.53	6.87
60	7	CAR	521.48	5.20	11.72
60	8	Stopping Bus	483.60	4.45	11.86
61	7	CAR	529.48	5.20	11.73
61	8	Stopping Bus	487.21	4.45	9.07

Table IV.4 Trajectory and Speed Values of Vehicles and Pedestrians obtained from the Vehicle-Pedestrian Simulation Model

Time Step	Vehicle ID	Vehicle Type	Vehicular Position		Vehicular Speed (m/s)	Pedestrian ID	Pedestrian Type	Pedestrian's Position		Pedestrian's Speed (m/s)
			x (m)	y (m)				x (m)	y (m)	
152	132	TW	460.93	1.49	10.57	18	MC	486.78	0	0
152	133	CAR	449.75	2.72	11.64	19	CM	485.32	6.50	0.89
153	132	TW	468.39	1.49	8.65	18	MC	486.78	1.37	1.37
153	133	CAR	455.15	5.31	12.05	19	CM	486.84	5.35	1.04
154	132	TW	471.10	1.49	11.25	18	MC	486.78	2.95	1.17
154	133	CAR	461.07	5.31	12.44	19	CM	488.36	4.17	0.98
155	132	TW	479.10	1.49	12.16	18	MC	486.78	4.15	1.19
155	133	CAR	470.49	5.31	12.81	19	CM	489.88	3.40	0.97

REFERENCES

Aerde, V. M. and Yagar, S. (1984). "Capacity, speed, and platooning vehicle equivalents for two-lane rural highways." *Transportation Research Record,* 971, *Transportation Research Board,* Washington, D.C., USA.

Ahmed, U. (2010). "Passenger car equivalent factors for level freeway segments operating under moderate and congested conditions." Master's Thesis, Marquette University.

Akcelik, R. and Besley, M. (2001). "Micro-simulation and analytical methods for modelling urban traffic." *Proceedings of Conference on Advance Modelling Techniques and Quality of Service in Highway Capacity Analysis*, California, USA, 1-18.

Al-Kaisy, A. F., Hall, F. L. and Reisman, E. S. (2002). "Developing passenger car equivalents for heavy vehicles on freeways during queue discharge flow." *Transportation Research Part A: Policy and Practice*, 36(8), 725-742.

Al-Kaisy, A., Jung, Y. and Rakha, H. (2005). "Developing passenger car equivalency factors for heavy vehicles during congestion." *Journal of Transportation Engineering, ASCE,* 131(7), 514-523.

Al-zerjawi, A. K. (2016). "Estimation of free-flow speeds and passenger car equivalent factors for multilane highways." *International Journal Scientific and Engineering Research*, 7 (6), 721-727.

Amini, S. and Tilg, G. (2018). "Estimating the effects of temporary bottlenecks on the capacity of urban arterial: An MFD-approach." *Proceedings of 7th Symposium of the European Association for Research in Transportation* (*EART 2018*).

Anand, P. A., Atmakuri, P., Anne, V. S. R., Asaithambi, G., Srinivasan, K. K., Sivanandan, R., and Chilukuri, B. R. (2019). "Calibration of vehicle-following model parameters using mixed traffic trajectory data." *Transportation in Developing Economies*, 5(2), 1-11.

Arasan, V. T., and Kashani, S. H. (2003). “Modeling platoon dispersal pattern of heterogeneous road traffic.” *Transportation Research Record*, 1852(1), 175-182.

Arasan, V. T., and Vedagiri, P. (2010). “Study of the impact of exclusive bus lane under highly heterogeneous traffic condition.” *Public Transport*, 2(1), 135-155.

Arasan, V. T. and Koshy, R. Z. (2005). “Methodology for modelling highly heterogeneous traffic flow.” *Journal of Transportation Engineering, ASCE,* 131(7), 544-551.

Arasan, V. T. and Vedagiri, P. (2008). “Bus priority on roads carrying heterogeneous traffic: a study using computer simulation.” *European Journal of Transport and Infrastructure Research*, 8 (1): 45–64.

Arasan, V. T. and Arkatkar, S. S. (2010). “Micro-simulation study of effect of volume and road width on PCU of vehicles under heterogeneous traffic.” *Journal of Transportation Engineering, ASCE*, 136 (12), 1110-1119.

Arasan, V. T. and Krishnamurthy, K. (2008). “Study of the effect of traffic volume and road width on PCU value of vehicles using microscopic simulation.” *Journal of the Indian Roads Congress*, 69 (2): 130–150.

Arasan, V. T., and Vedagiri, P. (2010). “Microsimulation study of the effect of exclusive bus lanes on heterogeneous traffic flow.” *Journal of Urban Planning and Development*, 136(1), 50-58.

Arasan, V. T., and Dhivya, G. (2010). “Simulation of highly heterogeneous traffic flow characteristics.” *Proceedings of 24th European Conference on Modelling and Simulation*, 81-87.

Arkatkar, S. S., and Arasan, V. T. (2010). “Effect of gradient and its length on performance of vehicles under heterogeneous traffic conditions.” *Journal of Transportation Engineering, ASCE,* 136(12), 1120-1136.

Aronsson, K.F.M., and Bang, K.L. (2005). "Factors influencing speed profiles on urban streets." *3rd International Symposium on Highway Geometric Design*, Illinois, Chicago.

Arun, A., Velmurugan, S., Kannan, S., Chakraborty, S. and Roy, S. K. (2016). "Effect of road geometry and roughness on free-flow speeds and roadway capacity for Indian multilane interurban highways." *Proceedings of the 12th Transportation Planning and Implementation Methodologies for Developing Countries,* IIT Bombay, India, December 2016.

Asaithambi, G., Kanagaraj, V., Srinivasan, K. K., and Sivanandan, R. (2012). "Characteristics of mixed traffic on urban arterials with significant volumes of motorized two-wheelers: role of composition, intra-class variability and lack of lane discipline." *Transportation Research Record*, 2317, Washington, D.C., USA, 51-59.

Asaithambi, G. and Mahesh, A. (2016). "Estimation of motorcycle unit for motorcycle dominated mixed traffic on urban roads in India." *Proceedings of the 95th Transportation Research Board Annual Meeting,* Washington D.C., USA.

Asaithambi, G., Kuttan, M. O. and Chandra, S. (2016). "Pedestrian road crossing behaviour under mixed traffic conditions: a comparative study of an intersection before and after implementing control measures." *Transportation in Developing Economies*, 2(2): 14.

Asaithambi, G., Hayjy, S. M., and Sivanandan, R. (2017). "Passenger car unit estimation at signalized intersection for non-lane based mixed traffic using microscopic simulation model." *Periodica Polytechnica Transportation Engineering*, 45(1), 12-20.

Asaithambi, G., Kanagaraj, V., Srinivasan, K.K. and Sivanandan, R. (2018). "Study of traffic flow characteristics using different vehicle-following models under mixed traffic conditions." *Transportation Letters,* 10(2), 92-103.

Asaithambi, G., and Joseph, J. (2018). "Modelling duration of lateral shifts in mixed traffic conditions." *Journal of Transportation Engineering, Part A: Systems, ASCE,* 144(9), 04018055.

Astarita, V., Florian, M., and Musolino, G. (2001). "A microscopic traffic simulation model for the evaluation of toll station systems." *Proceedings of IEEE Intelligent Transportation Systems, IEEE,* 692-697.

Aycin, M. F., and Benekohal, R. F. (2001). "Stability and performance of car following models in congested traffic." *Journal of Transportation Engineering, ASCE,* 127(1), 2-12.

Bahrami, A. (1999). "Object Oriented Systems Development using Unified Modeling Language." Irwin/ McGraw-Hill, Singapore.

Ballari, S. O. (2020). "Passenger car equivalent estimation methods of trucks in traffic stream." *International Journal of Recent Technology and Engineering (IJRTE),* 8(5), 710-716

Bang, K. L. (1995). "Impact of side friction on speed-flow relationships for rural and urban highways." *SWEROAD,* Indonesia.

Bansal, P., Agrawal, R. and Tiwari, G. (2014). "Impacts of bus-stops on the speed of motorized vehicles under heterogeneous traffic conditions: a case-study of Delhi, India." *International Journal of Transportation Science and Technology,* 3(2): 167–178.

Bains, M. S., Ponnu, B. and Arkatkar, S. S. (2012). "Modelling of traffic flow on Indian expressways using simulation technique." *Procedia-Social and Behavioral Science,* 43, 475–493.

Benekohal, R. F., and Zhao, W. (1999). "Delay-based passenger car equivalents for heavy vehicles at signalized intersections." *Transportation Research Part A,* 34, 437-457.

Ben-Dor, G., Ben-Elia, E. and Benenson, I. (2018). "Assessing the impacts of dedicated bus lanes on urban traffic congestion and modal split with an agent-based model." *Procedia Computer Science*, 130, 824-829.

Bergman, A., Olstam, J., and Allström, A. (2011). "Analytical traffic models for roundabouts with pedestrian crossings." *Procedia-Social and Behavioural Sciences*, 16, 697-708.

Bharadwaj, N., Mathew, S., Pani, A., Arkatkar, S., Joshi, G., and Ravinder, K. (2018). "Effect of traffic composition and emergency lane on capacity: a case study of intercity expressway in India." *Transportation letters*, 10(6), 316-332.

Biswas, S., Chandra, S., and Ghosh, I. (2020). "Side friction parameters and their influences on capacity of urban streets." *International Journal of Transportation Science and Technology*. https://doi.org/10.1016/j.ijtst.2020.03.007.

Booch, G. (1994). "Object Oriented Analysis and Design." Addison-Wesley, Reading, MA.

Bowman, C. N., and Miller, J. A. (2016). "Modeling traffic flow using simulation and big data analytics." Proceedings of 2016 Winter Simulation Conference (WSC), IEEE, 1206-1217.

Brackstone, M., and McDonald, M. (1999). "Car-following: a historical review." *Transportation Research Part F: Traffic Psychology and Behaviour,* 2(4), 181-196.

Brackstone, M., Waterson, B. and McDonald, M. (2009). "Determinants of following headway in congested traffic." *Transportation Research Part F: Traffic Psychology and Behaviour*. 12(2): 131-142.

Brilon, W., Geistefeldt, J., and Zurlinden, H. (2007). "Implementing the concept of reliability for highway capacity analysis." *Transportation Research Record,* 2027(1), 1-8.

Budhkar, A. K., and Maurya, A. K. (2014). "Modeling of bidirectional mixed traffic stream with weak lane discipline." *Proceedings of 93rd Annual Meeting of the Transportation Research Board*, Washington, DC.

Cao, N.Y., Sano, K., Tu, V. T. and Tan, D T. (2010). “Estimating capacity and vehicle equivalent unit by motorcycles at road segments in urban road.” *Proceedings of the 89th Annual Meeting of the Transportation Research Board,* Washington, D.C., USA.

Cao, N. Y., and Sano, K. (2012). “Estimating capacity and motorcycle equivalent units on urban roads in Hanoi, Vietnam.” *Journal of Transportation Engineering, ASCE,* 138(6), 776-785.

Casas, J., Ferrer, J. L., Garcia, D., Perarnau, J., and Torday, A. (2010). “Traffic simulation with AIMSUN.” *In Fundamentals of Traffic Simulation,* Springer, New York, NY, 173-232.

Castrillon, F., and Laval, J. (2018). “Impact of buses on the macroscopic fundamental diagram of homogeneous arterial corridors.” *Transportmetrica B: Transport Dynamics*, 6(4), 286-301.

Chakroborty, P., Agrawal, S., and Vasishtha, K. (2004). “Microscopic modelling of driver behaviour in uninterrupted traffic flow.” *Journal of Transportation Engineering,* 130(4), 438-451.

Chand, S., Chandra, S., and Dhamaniya, A. (2014). “Capacity drop of urban arterial due to a curb side bus stop.” *Proceedings of International Conference on Sustainable Civil Infrastructure,* Hyderabad, October 17-18.

Chandra, S., Gangopadhyay, S., Velmurugan, S., and Ravinder, K. (2018). “Indian Highway Capacity Manual (Indo-HCM).” *CSIR- Central Road Research Institute (CRRI)*, New Delhi, India.

Chandra, S., Kumar, V and Sikdar, P.K. (1995). “Dynamic PCU and estimation of capacity of urban roads.” *Indian Highways,* 23 (4), 17-28.

Chandler, R.E., Herman, R., and Montroll, E.W. (1958). “Traffic dynamics: studies in car following.” *Operations Research Society of America*, 6(2), 165-184.

Chandra, S. and Sikdar, P.K. (2000). “Factors affecting PCU in mixed traffic situation in urban roads.” *Road and Transport Research*, 9(3), 40-50.

Chandra, S. and Kumar, U. (2003). “Effect of lane width on capacity under mixed traffic condition in India.” *Journal of Transportation Engineering, ASCE,* 129(2), 155-160.

Chandra, S. (2004). “Effect of road roughness on capacity of two-lane roads.” *Journal of Transportation Engineering, ASCE,* 130(3), 360-364.

Chandra, S., Mehar, A. and Velmurugan, S. (2015). “Effect of traffic composition on capacity of multilane highways.” *KSCE Journal of Civil Engineering,* 20(5), 2033-2040.

Chao, Q., Deng, Z., and Jin, X. (2015). “Vehicle–pedestrian interaction for mixed traffic simulation.” *Computer Animation and Virtual Worlds*, 26(3-4), 405-412.

Chauhan, D., Pitroda, R., Gore, N., Dave, S., and Joshi, G. J. (2020). “Comparative study of legal and illegal on-street parking behaviour in CBD area—a case study of Surat city.” *In Transportation Research,* Springer, Singapore, 125-136.

Chen, X., Yu, L., Zhu, L., Guo, J. and Sun, M. (2010). “Microscopic traffic simulation approach to the capacity impact analysis of weaving sections for the exclusive bus lanes on an urban expressway.” *Journal of Transportation Engineering, ASCE*, 136 (10): 895–902.

Chen, Y., Chen, G. and Wu, K. (2016). “Evaluation of performance of bus lanes on urban expressway using paramics micro-simulation model.” *Procedia Engineering,* 137: 523–530.

Cherry, C., Donlon, B., Yan, X., Moore, S. E. and Xiong, J. (2012). “Illegal mid-block pedestrian crossings in china: gap acceptance, conflict and crossing path analysis.” *International Journal of Injury Control and Safety Promotion*, 19(4): 320-330.

Chiguma, M. L. (2007). “Analysis of side friction impacts on urban roads: case study Dar-Es-Salaam.” *Doctoral dissertation,* KTH University, Sweden.

Chodur, J. (2005). “Capacity models and parameters for un-signalized urban intersections in Poland.” *Journal of Transportation Engineering, ASCE*, 131, 924-930.

Craus, J., Polus, A., and Grinberg, I. (1980). “A revised method for the determination of passenger car equivalencies.” *Transportation Research Part A: General*, 14(4), 241-246.

Cunagin, W. D., and Messer, C. J. (1983). “Passenger-car equivalents for rural highways.” *Transportation Research Record*, 905, Washington, D.C., USA.

Dahl, J., and Lee, C. (2012). “Empirical estimation of capacity for roundabouts using adjusted gap-acceptance parameters for trucks.” *Transportation Research Record: Journal of the Transportation Research Board*, (2312), 34-45.

Das, A. K., Biswal, M. K., and Chattaraj, U. (2020). “Development of a Model for Heterogeneous Traffic Simulation.” *In Transportation Research*, Springer, Singapore, 699-706.

Dayyabu, A., Amuda, A. G., Mambo, A. D., and Mohammed, A. (2019). “Estimation of three-wheeler passenger unit (PCU) using headway method case study of Abuja Nigeria.” *Proceedings of 15th International Conference on Electronics, Computer and Computation (ICECCO), IEEE*, 1-7.

Dea, Z. P., Reddy, R. R. and Abera, G. (2019). “Evaluation of the impact of kerb side bus stop on traffic speed under mixed traffic conditions-a case study in Addis-Ababa city.” *International Journal of Multidisciplinary Research and Publications*, 2 (1): 29–34.

Demarchi, S. H., and Setti, J. R. (2003). “Limitations of passenger-car equivalent derivation for traffic streams with more than one truck type.” *Transportation Research Record*, 1852(1), 96-104.

Deshmukh, M., Dhamaniya, A. and Khode, B. (2019). “Estimation of capacity, passenger car unit and level of service of an urban arterial using micro-simulation technique.” *International Journal of Scientific Research and Review*, 7 (2): 132–148.

Dey, P. P., Chandra, S., and Gangopadhyay, S. (2008). “Simulation of mixed traffic flow on two-lane roads.” *Journal of Transportation Engineering, ASCE,* 134(9), 361-369.

Dhamaniya, A., and Chandra, S. (2013). “Speed prediction models for urban arterials under mixed traffic conditions.” *Procedia-Social and Behavioral Sciences*, 104, 342-351.

Dhamaniya, A., and Chandra, S. (2014). “Influence of undesignated pedestrian crossings on mid-block capacity of urban roads.” *Transportation Research Record: Journal of the Transportation Research Board,* 2461, *Transportation Research Board of the National Academies*, Washington, D.C., 137–144.

Elefteriadou, L., Torbic, D., and Webster, N. (1997). “Development of passenger car equivalents for freeways, two-lane highways, and arterials.” *Transportation Research Record*, 1572, 51–58.

Fan, H. S. (1989). “Passenger car equivalents for vehicles on Singapore expressways.” *Transportation Research Part A: General,* 24(5), 391-396.

Fitzpatrick, K. and Nowlin, R. L. (1997). “Effects of bus stop design on suburban arterial operations.” *Transportation Research Record*, 1571(1), 31-41.

Fritzsche, T. (1994). “A model for traffic simulation.” *Traffic Engineering Control,* 35(5), 317-321.

Galatioto, F. and Bell, M. C. (2007). “Simulation of illegal double parking: quantifying the traffic and pollutant impacts.” *Proceedings of 4th International SIIV Congress*, Palermo, Italy, 12-14.

Gaur, P., and Sachdeva, S. N. (2020). “Capacity analysis of a 4-lane intercity road with varying shoulders.” *International Journal of Applied Engineering Research*, 15(2), 144-48.

Gayah, V. V., Ilgin Guler, S. and Gu, W. (2016). “On the impact of obstructions on the capacity of nearby signalised intersections.” *Transportmetrica B: Transport Dynamics*, 4(1), 48-67.

Gazis, D.C., Herman, R., and Rothrey, R.W. (1961). “Non-linear follow the leader models of traffic flow.” *Operations Research,* 9(4), 545-567.

Gipps, P.G. (1981). “A behavioural car following model for computer simulation.” *Transportation Research B,* 15, 105-111.

Giuffre, O., Grana, A., Mauro, R., Silva, A. B., and Chiappone, S. (2015). “Developing passenger car equivalents for freeways by micro-simulation.” *Transportation Research Procedia,* 10, 93-102.

Golakiya, H. D. and Dhamaniya, A. (2019). “Modelling speed and capacity estimation at urban mid-block sections under the influence of crossing pedestrians.” *Journal of Transportation Engineering, ASCE,* 145(9): 04019036.

Golakiya, H. D., Patkar, M. and Dhamaniya, A. (2020). “Analysis of vehicular pedestrian interaction at urban undesignated mid-block sections.” *In Transportation Research,* Springer, Singapore, 389-407.

Gowri, A., Venkatesan, K. and Sivanandan, R. (2009). “Object-oriented methodology for intersection simulation model under heterogeneous traffic conditions.” *Advances in Engineering Software,* 40(10), 1000-1010.

Gowri, A. (2011). “Evaluation of turn lanes at signalized intersection in heterogeneous traffic using microscopic simulation model.” Ph.D. Thesis, IIT Madras.

Gowri, A. and R. Sivanandan. (2015). “Evaluation of right-turn lanes at signalized intersection in non-lane-based heterogeneous traffic using microscopic simulation model.” *Transportation Letters,* 7(2): 61-72.

“Guidelines for capacity of urban roads in plain areas.” (1990). *Indian Roads Congress,* 106 (IRC 106), Indian Code of Practice, New Delhi, India.

Gunay, B. (2007). “Car-following theory with lateral discomfort.” *Transportation Research Part B,* 41, 722-735.

Hagring, O., Rouphail, N. M., and Sørensen, H. A. (2003). “Comparison of capacity models for two-lane roundabouts.” *Transportation Research Record*, 1852(1), 114-123.

Harison, A., Bellal, A. and Suryavanshi, S. (2016). “Side friction problems in state highways - a case study.” *International Journal of Innovative Research in Science, Engineering and Technology,* 5(6), 9652-9656.

Helbing, D. and Molnar, P. (1995). “Social force model for pedestrian dynamics.” *Physical Review E,* 51(5): 4282.

Helbing, D., Farkas, I. and Vicsek, T. (2000) “Simulating dynamical features of escape panic.” *Nature*, 407(6803): 487–490.

Helbing, D., Buzna, L., Johansson, A. and Werner, T. (2005). “Self-organized pedestrian crowd dynamics: Experiments, simulations, and design solutions.” *Transportation Science,* 39(1): 1–24.

“Highway capacity manual.” (2010). *Transportation Research Board*, National Research Council, Washington, D.C., USA.

Hidas, P. (1998). “A car following model for urban traffic simulation.” T*raffic Engineering Control*, 39(5), 300-305.

Hidayati, N., Liu, R., and Montgomery, F. (2012). “The impact of school safety zone and roadside activities on speed behavior: the Indonesian case.” *Procedia-Social and Behavioral Sciences*, 54, 1339-1349.

Huber, M. J. (1982). “Estimation of passenger-car equivalents of trucks in traffic stream.” *Transportation Research Record,* 869.

Iin, I. (2015). “Delay evaluation as the impact of side friction on heterogeneous traffic towards road performance with Vissim microsimulation.” *International Journal of Engineering Research and Technology (IJERT),* 4(2).

"Indonesian highway capacity manual." (1997). *Directorate General of Highways*, Republic Indonesia, Jakarta.

Irawati, I. (2015). "Delay evaluation as the impact of side friction on heterogeneous traffic towards road performance with VISSIM microsimulation." *International Journal of Engineering Research and Technology,* 4(2).

Irfanview 4.38 software, http://www.irfanview.com.

Jabeena, M., Joshi, G., Arkatkar S. and Ravinder K. (2015). "Study of flow characteristics and traffic stream modelling on Indian expressway: a case study of Mahatma Gandhi expressway." *Proceedings of the Eastern Asia Society for Transportation Studies,* 10.

Jianrong, H. and Hua, C. (2007). "Influence of public transit bus stopping on traffic flow." *Urban Roads Bridges and Flood Control,* 8.

Jin, H., Yu, J. and Yang, X. (2019). "Impact of curbside bus stop locations on mixed traffic dynamics: a bus route perspective." *Transportmetrica A: Transport Science,* 15 (2): 1419–1439.

Kadali, B. R., Chiranjeevi, T. and Rajesh, R. (2015). "Effect of pedestrians un-signalized mid-block crossing on vehicular speed." *International Journal for Traffic and Transport Engineering*, 5(2), 170 – 183.

Kanagaraj, V., Asaithambi, G., Kumar, C. N., Srinivasan, K. K., and Sivanandan, R. (2013). "Evaluation of different vehicle following models under mixed traffic conditions." *Procedia-Social and Behavioural Sciences*, 104, 390-401.

Kanagaraj, V. and Treiber, M. (2018). "Self-driven particle model for mixed traffic and other disordered flows." *Physica A: Statistical Mechanics and its Applications*, 509, 1-11.

Keller, E. L., and Saklas, J. G. (1984). "Passenger car equivalents from network simulation". *Journal of Transportation Engineering, ASCE,* 110(4), 397-411.

Khanorkar, A. R., Ghodmare, S. D., and Khode, B. V. (2014). “Impact of lane width of road on passenger car unit capacity under mix traffic condition in cities on congested highways.” *International Journal of Engineering Research and Application*, 4(5), 180-184.

Koshy, R. Z. and Arasan, V.T. (2005). “Influence of bus stops on flow characteristics of mixed traffic.” *Journal of Transportation Engineering, ASCE*, 131(8): 640-643.

Kotagi, P. B., Asaithambi, G., and Gurumurthy, K. M. (2018). “Development of microscopic simulation model for bidirectional mixed traffic on urban roads.” *Proceedings of 97th Annual Meeting of Transportation Research Board,* Washington DC, U.S.A, 18-04818.

Kotagi, P. B. (2019). “Development of bidirectional mixed traffic simulation model for urban roads.” Doctoral Dissertation, National Institute of Technology Karnataka, Surathkal.

Krammes, R. A., and Crowley, K. W. (1986). “Passenger car equivalents for trucks on level freeway segments.” *Transportation Research Record: Journal of Transportation Research Board,* 1091.

Krishna, B.V., Ramesh, A. and Kumar, M. (2019). ‘Estimation of passenger car units for heterogeneous traffic condition using vehicular speed and composition at mid–block section.” *International Journal for Traffic and Transport Engineering,* 9(4).

Kumar, P., Arkatkar, S. S., Joshi, G. and Dhamaniya, A. (2017). “New methodology for estimating PCU on multi-lane urban roads under mixed traffic scenario based on area occupancy.” *Transportation Research Board,* 17-03248.

Kuttan, M. O., Babu, S., and Asaithambi, G. (2017). “Impact of pedestrian road crossing on capacity and level of service of urban undivided roads in Indian traffic conditions.” *Proceedings of 96th Annual Meeting of Transportation Research Board,* Washington DC, U.S.A, 17-04900.

Laxman, K. K., Rastogi, R. and Chandra, S. (2010) “Pedestrian flow characteristics in mixed traffic conditions.” *Journal of Urban Planning and Development,* 136(1), 23-33.

Lee, C. (2015). “Developing passenger-car equivalents for heavy vehicles in entry flow at roundabouts.” *Journal of Transportation Engineering, ASCE,* 04015013.

Lee, J.T., Kweon, Y.J., Dittberner, R. and Horodyskyj, I.M. (2014). “Drivers’ lane-changing behaviour at bus stops on three-lane roadways.” *Institute of Transportation Engineers Journal,* 84(11), 37-39.

Leutzbach, W. and Wiedemann, R. (1986). “Development and application of traffic simulation models at Karlsruhe institute.” *Traffic Engineering and Control,* 27(5), 270-278.

Lint, J. W. C.V. and Calvert, S. C. (2018). “A generic multi-level framework for microscopic traffic simulation—Theory and an example case in modelling driver distraction.” *Transportation Research Part B: Methodological*, 117, 63-86.

Liu, M., Zeng, W., Chen, P. and Wu, X. (2017). “A microscopic simulation model for pedestrian-pedestrian and pedestrian-vehicle interactions at crosswalks.” *PLoS One*, 12(7).

Loder, A., Ambühl, L., Menendez, M. and Axhausen, K. W. (2019). “Understanding traffic capacity of urban networks.” *Scientific Reports*, 9(1), 1-10.

Lu, L., Ren, G., Wang, W., Chan, C. Y. and Wang, J. (2016). “A cellular automaton simulation model for pedestrian and vehicle interaction behaviours at unsignalized mid-block crosswalks.” *Accident Analysis and Prevention*, 95: 425-437.

Lu, P., Zheng, Z., Tolliver, D. and Pan, D. (2020). “Measuring passenger car equivalents (PCE) for heavy vehicle on two lane highway segments operating under various traffic conditions.” *Journal of Advanced Transportation*, 2020.

Luo, Z., Liu, Y. and Guo, C. (2014). “Operational characteristics of mixed traffic flow under bi-directional environment using cellular automaton.” *Journal of Traffic and Transportation Engineering*, 1(6), 383-392.

Macioszek, E. (2019). “The passenger car equivalent factors for heavy vehicles on turbo roundabouts.” *Frontiers in Built Environment*, 5, 68.

Madhu, E. and Velmurugan, S. (2011). “Estimation of roadway capacity of eight-lane divided urban expressways under heterogeneous traffic through microscopic simulation models.” *International Journal of Science and Technology Education Research*, 2 (9): 146-162.

Mahidadiya, A. N. and Juremalani, J. (2016). “Estimation of passenger car unit value at signalized intersection.” *IJSRSET*, 2(2), 1317-1324.

Mallikarjuna, C. and Rao, K. R. (2006). “Modelling of passenger car equivalency under heterogeneous traffic conditions.” *Proceedings of 22nd Australian Road Research Board Conference*, Canberra, Australia, 7.

Mankar, P. U. and Khode, B. V. (2016). “Capacity estimation of urban roads under mixed traffic condition.” *International Research Journal of Engineering and Technology*, 3(4), 2750-2755.

Mathew, T. V., Gundaliya, P. and Dhingra, S. L. (2006). “Heterogeneous traffic flow modelling and simulation using cellular automata.” *Proceeding of Applications of Advanced Technology in Transportation*, 492-497.

Mathew, V. T. and Radhakrishnan, P. (2010). “Calibration of micro-simulation models for non-lane based heterogeneous traffic at signalized intersections.” *Journal of Urban Planning and Development, ASCE,* 136, 59-66.

Mathew, V. T. and Ravishankar K.V.R. (2011). “Car-following behaviour in traffic having mixed vehicle-types.” *Transportation Letters: The International Journal of Transportation Research,* 3, 113-126.

Mehar, A., Chandra, S. and Velmurugan, S. (2013). “Passenger car units at different levels-of-service for capacity analysis of multilane divided highways.” *Journal of Transportation Engineering, ASCE,* 140 (1), 81-88.

Mehar, A., Chandra, S. and Velmurugan, S. (2014). “Highway capacity through VISSIM calibrated for mixed traffic conditions.” *KSCE Journal of Civil Engineering*, 18(2), 639-645.

Mei, Z. Y., Chen, J. and Wang, W. (2009). “A model of road traffic delay caused by curb parking.” *Journal of Harbin Institute of Technology*, 41, 164-168.

Meneguzzer, C. and Rossia, R. (2011). “Evaluating the impact of pedestrian crossings on roundabout entry capacity.” *Procedia-Social and Behavioural Sciences,* 20, 69-78.

Metkari, M., Budhkar, A. and Maurya, A. K. (2013). “Development of simulation model for heterogeneous traffic with no lane discipline.” *Procedia - Social and Behavioral Sciences,* 104, 360 – 369.

Minh, C. C., Sano, K. and Matsumoto, S. (2005). “The speed, flow and headway analyses of motorcycle traffic.” *Journal of the Eastern Asia Society for Transportation Studies,* 6, 1496-1508.

“Ministry of road transport and highways” (2020). *Annual Report: 2019-20,* New Delhi.

Mishra, R., Kumar, P., Arkatkar, S.S., Sarkar, A.K. and Joshi, G.J. (2017). “Novel area occupancy–based method for passenger car unit estimation on multilane urban roads under heterogeneous traffic scenario.” *Transportation Research Record*, 2615(1), 82-94.

Mohan, M., and Chandra, S. (2016). “Three methods of PCU estimation at un-signalized intersections.” *Transportation Letters*, 1-7.

Mohan, M. and Chandra, S. (2017). “Queue clearance rate method for estimating passenger car equivalents at signalized intersections.” *Journal of Traffic and Transportation Engineering,* 4(5), 487-495.

Mondal, S., Chakraborty, S., Roy, S. K., and Gupta, A. (2017). “Estimation of passenger car unit for heterogeneous traffic stream of urban arterials: case study of Kolkata.” *Transportation Letters*, 1-13.

Mondal, S., and Gupta, A. (2020). "Microsimulation-based framework to analyse urban signalised intersection in mixed traffic." *Proceedings of Institution of Civil Engineers-Transport,* 1-13.

Moussaid, M., Helbing, D., Garnier, S., Johansson, A., Combe, M. and Theraulaz, G. (2009). "Experimental study of the behavioural mechanisms underlying self-organization in human crowds." *Proceedings of the Royal Society B: Biological Sciences,* 276(1668), 2755-2762.

Munawar, A. (2011). "Speed and capacity for urban roads, Indonesian experience." *Procedia Social and Behavioural Sciences,* 16, 382-387.

Naidu, P.S., Navya, G., Deepika, C. and Yamala, M. (2015). "Capacity of road with vehicle characteristics and road geometrics interface modeling." *SSRG International Journal of Civil Engineering,* 2(10), 27-33.

Ningbo, C., Wei, W., Zhaowei, Q., Liying, Z. and Qiaowen, B. (2017). "Simulation of pedestrian crossing behaviours at unmarked roadways based on social force model." *Discrete Dynamics in Nature and Society,* 2017, 1-15.

Obiri-Yeboah, A. A., Tuffour, Y. A., and Salifu, M. (2014). "Passenger car equivalents for vehicles at signalized intersections within the Kumasi metropolis in Ghana." *IOSR Journal of Engineering,* 4(4), 24-9.

Pajecki, R., Ahmed, F., Qu, X., Zheng, X., Yang, Y., and Easa, S. (2019). "Estimating passenger car equivalent of heavy vehicles at roundabout entry using micro-traffic simulation." *Frontiers in Built Environment,* 5, 77.

Palaniswamy, S.P. (1983). "A generalized simulation model for vehicular behavior under heterogeneous traffic conditions." *Ido-Swedish Traffic Simulation Research Project,* IIT, Kanpur, India.

Pal, S., and Roy, S. K. (2016). "Impact of roadside friction on travel speed and LOS of rural highways in India." *Transportation in Developing Economies,* 2(2), 9.

Pal, S. and Roy, S. K. (2017). "Effect of side friction on travel speed and road user cost in rural roads in India." *International Journal of Innovative Research in Science, Engineering and Technology*, 6 (12).

Pallavi, G., Mehar, A. and Neeraja, D. (2016). "Effect of side friction on the traffic flow behaviour of multilane divided urban road at mid-block sections." *Proceedings of 12th Transportation Planning and Implementation Methodologies for Developing Countries*, IIT Bombay, December 2016.

Parmar, R., Maru, A., and Chhabra, R. S. (2016). "Macroscopic analysis of side friction impact on speed of urban roads-case study of Jawahar Marg, Indore." *Proceedings of 12th Transportation Planning and Implementation Methodologies for Developing Countries*, IIT Bombay, December 2016.

Parmar, N. P., P. N. Patel, and L. B. Zala. 2018. "Effect of traffic characteristics on the dynamic PCU under mixed traffic condition at urban signalized intersection." *International Research Journal of Engineering and Technology*, 5 (5), 3614–3624.

Patel, C. R. and Joshi, G. J. (2014). "Mixed traffic speed–flow behaviour under influence of road side friction and non-motorized vehicles: a comparative study of arterial roads in India." *International Journal of Civil, Environmental, Structural, Construction and Architectural Engineering*, 8(11), 1144-1150.

Patel, M. R., Shukla, R. N. and Golakiya, H. D. (2018). "Study of interaction between pedestrian and vehicle at undesignated urban mid-block section." *International Research Journal Engineering and Technology (IRJET)*, 5(2), 1109-1112.

Patel, P. and Dhamaniya, A. (2019). "Stream equivalency factor for mixed traffic at urban signalized intersections." *Transportation Research Procedia*, 37, 362-368.

Patkar, M. and Dhamaniya, A. (2020). "Developing capacity reduction factors for curbside bus stops under heterogeneous traffic conditions." *Arabian Journal for Science and Engineering*, 45, 1–15.

Patnaik, A. K., Krishna, Y., Rao, S., and Bhuyan, P. K. (2017). “Development of roundabout entry capacity model using INAGA method for heterogeneous traffic flow conditions.” *Arabian Journal for Science and Engineering*, 42(9), 4181-4199.

Patnaik, A. K., Agarwal, L. A., Panda, M. and Bhuyan, P. K. (2020). “Entry capacity modelling of signalized roundabouts under heterogeneous traffic conditions.” *Transportation Letters*, 12(2), 100-112.

Paul, P. K., and Sarkar, P. K. (2013). “Determination of dynamic PCUs of different types of passenger vehicles on urban roads: a case study, Delhi urban area.” *Indian Highways*, 41(4), 37-47.

Pei, Y.L. and Wu, S.M. (2004). “Study on the bus-stops' impact on capacity of unsignal-controlled intersections.” *Journal of Harbin Institute of Technology*, 36(11), 1524-1526.

Prasetijo, J. (2005). “Development of a new method of capacity analysis at unsignalized intersections under mixed traffic flow (preliminary design for Indonesia)”. *Proceedings of Eastern Asia Society for Transportation Studies*, 5, 967-983).

Praveen, P. S. and Arasan, V. T. (2013). “Influence of traffic mix on PCU value of vehicles under heterogeneous traffic conditions.” *International Journal of Traffic and Transport Engineering*, 3(3).

Praveen, P.S. and Ashalatha, R. (2019). “Passenger car equivalency factors under platooning conditions.” *Transportation in Developing Economies*, 5(2), pp.8.

PTV VISSIM 5.20 User Manual, Karlsluhe, Germany.

Puvvala, R., Ponnu, B., Arkatkar, S. and Velmurugan, S. (2013). “Estimating capacity for eight-lane divided urban expressway under mixed-traffic conditions using computer simulation.” *International Journal of Advances in Engineering Sciences and Applied Mathematics*, 5 (2–3): 177–194.

Rahman, M. M., Okura, I. and Nakamura, F. (2003) "Measuring passenger car equivalents (PCE) for large vehicles at signalized intersections." *Journal of EASTS*, 5, 1223-1233.

Rao, A. and Rao, K. R. (2015). "Free speed modelling for urban arterials – a case study on Delhi." *Periodica Polytechnica Transportation Engineering*, 43(3), 111-119.

Rao, A. M., Velmurugan, S. and Lakshmi, K. M. V. N. (2017). "Evaluation of influence of roadside frictions on the capacity of roads in Delhi, India." *Transportation Research Procedia*, 25, 4771–4782.

Ravishankar, K.V.R. and Mathew, V. T. (2011). "Vehicle-type dependent car-following model for heterogeneous traffic conditions." *Journal of Transportation Engineering, ASCE*, 137(11), 775-781.

Reddy, R., Rao, S.N. and Rao, C.R. (2008). "Modelling and evaluation patterns on the impact of on-street parking in reference to traffic mobility." *Journal of Indian Roads Congress*, 69, 101-109.

Saha, P., Hossain, Q.S., Mahmud, H.M.I. and Islam, M. Z. (2009). "Passenger car equivalent (PCE) of through vehicles at signalized intersections in Dhaka metropolitan city, Bangladesh." *Journal of International Association of Traffic and Safety Sciences*, 33 (2), 99-104.

Salini, S., George, S. and Ashalatha, R. (2016). "Effect of side frictions on traffic characteristics of urban arterials." *Transportation Research Procedia*, 17, 636-643.

Shah, B.B. and Raval, N.G. (2016). "Estimation of capacity for arterial road of urban area." *International Journal of Innovative Research in Technology*, 2(12), 63-64.

Sarraj, Y. and Jadili, I. (2012). "Estimating passenger car unit factors for buses and animal driven carts in Gaza city, Palestine." *IUG Journal of Natural Studies*, 20(2).

Satyanarayana, P. V. H., Rani, D. K. and Raju, S. G. (2012). "Development of PCU factors and capacity norms at mid blocks of rural highways in Visakhapatnam." *Indian Journal of Education and Information Management*, 1(5), 197-202.

Shalkamy, A., Said, D. and Radwan, L. (2015). “Influence of carriageway width and horizontal curve radius on passenger car unit values of two-lane two-way rural roads.” *Civil and Environmental Research,* 7(3), 157-166.

Siddharth, S. M. P., and Vedagiri, P. (2018). “Modelling the gender effects of pedestrians and calibration of the modified social force model.” *Transportation Research Record*, 2672(31), 1-9.

Silva, P. C. M. (2000). “Simulating bus stops in mixed traffic.” *Proceedings of UTSG 32nd Annual Conference,* Liverpool, U.K.

Sonu, M., Dhamaniya, A., Arkatkar, S. and Joshi, G. (2016). “Time occupancy as measure of PCU at four legged roundabouts.” *Transportation Letters,* 1-12.

Sugiarto, S., Apriandy, F., Faisal, R. and Saleh, S. M. (2018). “Measuring passenger car unit at four-legged roundabout using time occupancy data collected from drone.” *Aceh International Journal of Science and Technology,* 7(2), 77-84.

Sun, J., Liu, H. and Ma, Z. (2019). “Modelling and simulation of highly mixed traffic flow on two-lane two-way urban streets.” Simulation Modelling Practice and Theory, 95, 16-35.

Swamy, C. R. M. and Anjaneyulu, M.V.L.R (2016). “Passenger car unit based on influence area.” *Proceedings of the 12th Transportation Planning and Implementation Methodologies for Developing Countries*, IIT Bombay, December 2016.

Tan, D. T., Tu, T. V. and Sano, K. (2018). “Estimation of Motorcycle Equivalent Units on Urban Streets.” *Asian Transport Studies,* 5(2), 243-255.

Tiwari G., Fazio J. and Pavitravas S. (2000). “Passenger car units for heterogeneous traffic using a modified density method.” *Proceedings of 4th International Symposium on Highway Capacity,* 246-257.

Tiwari G., Fazio J. and Gaurav, S. (2007). “Traffic planning for non-homogeneous traffic.” *Sadhana,* 32(4), 309-328.

Toledo, T. (2002). “Integrated driving behaviour modelling.” *Ph.D. Thesis*, Department of Civil and Environmental Engineering, MIT, USA.

“Transportation road and research laboratory” (1965). *TRRL,* Research on Road Traffic, H.M.S.O., London, UK.

“Transport for London”. (2010). *Traffic Modelling Guidelines: TfL Traffic Manager and Network Performance Best Practice Version 3.0*.

Treiber, M., Kesting, A., and Helbing, D. (2010). “Three-phase traffic theory and two-phase models with a fundamental diagram in the light of empirical stylized facts.” *Transportation Research Part B: Methodological*, 44(8-9), 983-1000.

Tu, T. V., Tai, N. H. T., Dac, H. S. and Nishiuchi, H. (2020). “A study on motorcycle equivalent unit of container truck in motorcycle dominated cities.” *Proceedings of International Conference on Green Technology and Sustainable Development*, Springer, Cham, 580-589.

Velmurugan, S., Errampalli, M., Ravinder, K., Sitaramanjaneyulu, K., and Gangopadhyay, S. (2010). “Critical evaluation of roadway capacity of multi-lane high speed corridors under heterogeneous traffic conditions through traditional and microscopic simulation models.” *Journal of Indian Roads Congress*, 71(3), 235-264.

Venkatesan, K., Asaithambi, G., and Sivanandan R. (2008). “Development of microscopic simulation model for heterogeneous traffic using object-oriented approach.” *Transportmetrica*, 4(3), 227-247.

Wang, T., Wu, J. and McDonald, M. (2012). “A micro-simulation model of pedestrian-vehicle interaction behaviour at unsignalized mid-block locations.” *Proceedings of 15th International IEEE Conference on Intelligent Transportation Systems*, 1827-1833.

Wang, T., Jiang, X., Wang, W. and Cheng, Q. (2016). “Analysis of vehicle speed change at non-signalized crosswalks based on driving behaviour.” *Procedia Engineering*, 2016 (137), 547-53.

Wang, Y., Peng, Z. and Chen, Q. (2018). "Simulated interactions of pedestrian crossings and motorized vehicles in residential areas." *Physica A: Statistical Mechanics and its Applications*, 490, 1046-1060.

Widanapathiranage, R., Bunker, J.M. and Bhaskar, A. (2013). "A microscopic simulation model to estimate bus rapid transit station bus capacity." *Proceedings of Australasian Transport Research Forum*, October, 2013.

Xiong, C., Zhu, Z., He, X., Chen, X., Zhu, S., Mahapatra, S., Chang, G. and Zhang, L. (2015). "Developing a 24-hour large-scale microscopic traffic simulation model for the before-and-after study of a new tolled freeway in the Washington, DC–Baltimore Region." *Journal of Transportation Engineering*, 141(6), 05015001.

Xue, X. J., Shi, F. and Chen, Q. (2014). "Capacity estimation for on-ramp merging section of urban expressway based on time headway loss." *Discrete Dynamics in Nature and Society*, 1-9.

Yang, Q. and Koutsopoulos, H. N. (1996). "A microscopic traffic simulator for evaluation of dynamic traffic management systems." *Transportation Research Part C: Emerging Technologies*, 4(3), 113-129.

Yang, Z., Zhang, Y., Zhu, R., Ye, X. and Jiang, X. (2015). "Impacts of pedestrians on capacity and delay of major street through traffic at two-way stop-controlled intersections." *Mathematical Problems in Engineering*, 2015.

Zhang, H. M. and Jin, W. L. (2002). "Kinematic wave traffic flow model for mixed traffic." *Transportation Research Record*, 1802(1), 197-204.

Zhao, J., Li, P. and Zhou, X. (2016). "Capacity estimation model for signalized intersections under the impact of access point." *PloS one*, 11(1).

Zheng, C. J., He, R., Wan, X. and Wang, C. (2016). "The study on in-city capacity affected by pedestrian crossing." *Mathematical Problems in Engineering,* 2016.

Zhenga, J., Suzuki, K. and Fujita, M. (2012). “Evaluation of car-following models using trajectory data from real traffic.” *Procedia - Social and Behavioral Sciences*, 43, 356-366.

LIST OF PUBLICATIONS

Sl. No.	Title of the paper	Authors (in the same order as in the paper. Underline the Research Scholar's name)	Name of the Journal/ Conference/ Symposium, Vol., No., Pages	Month & Year of Publication	Category *
1	Modelling and Simulation of Vehicle-Pedestrian Interactions on Urban Roads in Disordered Traffic.	**Pooja Raj**, Gowri Asaithambi, and A. U. Ravi Shankar	Transportation Research Record: Journal of Transportation Research Board	Under Second Revision	2
2	Effect of Curbside Bus Stops on Passenger Car Units and Capacity in Disordered Traffic using Simulation Model.	**Pooja Raj**, Gowri Asaithambi, and A. U. Ravi Shankar	Transportation Letters, 1-10	September 2020	1
3	Assessment of Impact of Roadside Bus-Stops on Capacity of Urban Divided Roads using Microscopic Simulation Model.	**Pooja Raj**, Gowri Asaithambi, and A. U. Ravi Shankar	5th Conference of Transportation Research Group of India, December 2019, Bhopal.	Presented in December 2019	3
4	Review of Methods for Estimation of Passenger Car Unit Values of Vehicles.	**Pooja Raj**, Kalaanidhi Sivagnanasundaram, Gowri Asaithambi, and A. U. Ravi Shankar	Journal of Transportation Engineering, Part A: Systems, ASCE, 145(6), 04019019.	March 2019	1
5	An Approach for Estimation of Passenger Car Unit Values of Vehicles based on Influence of Neighboring Vehicles.	**Pooja Raj**, Shahana, A., Gowri Asaithambi, and A. U. Ravi Shankar	Proceedings of 97th Transportation Research Board Annual Meeting, Washington D.C., USA, 18-03860, 1-20.	January 2018	3

Category: 1: Journal paper, full paper reviewed, 2: Journal paper, Abstract reviewed, 3: Conference/Symposium paper, full paper reviewed, 4: Conference/Symposium paper, abstract reviewed, 5: others (including papers in Workshops, NITK Research Bulletins, Short notes etc.). (If the paper has been accepted for publication but yet to be published, the supporting documents must be attached.)

Pooja Raj
Research Scholar

Prof. A. U. Ravi Shankar
Research Guide

CURRICULUM VITAE

Name : Pooja Raj

Guardian's Name : L. J. Dileep

Mother's Name : Anitha Das K M

Date of Birth : 8th August 1992

Nationality : Indian

Contact Address : Chithrakoodam, CC-63,
Chinmaya Colony,
Vidyanagar, Kasaragod
Kerala, 671123

E-mail : poojarajhere@gmail.com

Mobile Number : +91-8547811375, +91-6282170017

Educational Qualification:

Discipline	University/ Institution	Year	% Marks/ C.G.P. A
Ph.D. (Transportation Engineering)	National Institute of Technology Karnataka, Surathkal	2016 - present	8.75
M.Tech. (Research) (Transportation Engineering)	National Institute of Technology Karnataka, Surathkal	2014 - 2016	8.86
B.Tech.(Civil Engineering)	Cochin University of Science and Technology	2010 - 2014	80.46%
12th	Kendriya Vidyalaya No.2, Kasaragod	2010	92.4%
10th	Kendriya Vidyalaya No.2, Kasaragod	2008	90.6%